

DE GRUYTER

# CHEMICAL SCIENCES IN THE FOCUS

VOLUME 1: PHARMACEUTICAL APPLICATIONS

*Edited by Ponnadurai Ramasami*

Copyright 2021. De Gruyter. All rights reserved. May not be reproduced in any form without permission from the publisher, except fair uses permitted under U.S. or applicable copyright law.



Ponnadurai Ramasami (Ed.)  
**Chemical Sciences in the Focus**

## Also of interest



*Chemical Sciences in the Focus*  
*Volume 2: Green and Sustainable Processing*  
Ponnadurai Ramasami (Ed.), 2021  
ISBN 978-3-11-072659-6, e-ISBN 978-3-11-072614-5



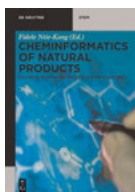
*Chemical Sciences in the Focus*  
*Volume 3: Theoretical and Computational Chemistry Aspects*  
Ponnadurai Ramasami (Ed.), 2021  
ISBN 978-3-11-073974-9, e-ISBN 978-3-11-073976-3



*Computational Chemistry Methods.*  
*Applications*  
Ponnadurai Ramasami (Ed.), 2020  
ISBN 978-3-11-062906-4, e-ISBN 978-3-11-063162-3



*Chemoinformatics of Natural Products*  
*Volume 1: Fundamental Concepts*  
Fidele Ntie-Kang (Ed.), 2020  
ISBN 978-3-11-057933-8, e-ISBN 978-3-11-057935-2



*Chemoinformatics of Natural Products*  
*Volume 2: Advanced Concepts and Applications*  
Fidele Ntie-Kang (Ed.), 2021  
ISBN 978-3-11-066888-9, e-ISBN 978-3-11-066889-6



*Physical Sciences Reviews.*  
e-ISSN 2365-659X

# Chemical Sciences in the Focus

---

Volume 1: Pharmaceutical Applications

Edited by  
Ponnadurai Ramasami

**DE GRUYTER**

**Editor**

Prof. Dr. Ponnadurai Ramasami  
Computational Chemistry Group,  
Department of Chemistry, Faculty of Science,  
University of Mauritius,  
Reduit 80837,  
Mauritius

Department of Chemistry,  
College of Science, Engineering and Technology,  
University of South Africa,  
P.O. Box 392, Pretoria 0003,  
South Africa  
E-mail address: p.ramasami@uom.ac.mu

ISBN 978-3-11-071072-4  
e-ISBN (PDF) 978-3-11-071082-3  
e-ISBN (EPUB) 978-3-11-071087-8

**Library of Congress Control Number: 2021940583**

**Bibliographic information published by the Deutsche Nationalbibliothek**

The Deutsche Nationalbibliothek lists this publication in the Deutsche Nationalbibliografie;  
detailed bibliographic data are available on the Internet at <http://dnb.dnb.de>.

© 2021 Walter de Gruyter GmbH, Berlin/Boston  
Cover image: BlackJack3D/E+/Getty Images  
Typesetting: TNQ Technologies Pvt. Ltd.  
Printing and binding: CPI books GmbH, Leck

[www.degruyter.com](http://www.degruyter.com)

# Preface of the Book of Proceedings of the Virtual Conference on Chemistry and its Applications (VCCA-2020)

A virtual conference on chemistry and its applications (VCCA-2020) was organized online from 1<sup>st</sup> to 31<sup>st</sup> August 2020. The theme of the virtual conference was “Research and Innovations in Chemical Sciences: Paving the Way Forward”.

There were 190 presentations for the virtual conference with 300 participants from 50 countries. A secured platform was used for virtual interactions of the participants. After the virtual conference, there was a call for full papers to be considered for publication in the conference proceedings. Manuscripts were received and they were processed and reviewed as per the policy of De Gruyter.

This book, volume 1, is a collection of the ten accepted manuscripts having pharmaceutical applications.

Ojo and Derek reviewed the traditional uses, biological activities and phytochemicals of *Lecaniodiscus cupanioides*. Mshelia et al studied the phytochemical and antioxidant activity of *Cadaba farinosa* stem bark extracts. Binang and Takuwa applied reverse phase high performance liquid chromatography for the determination of selected antihypertensive active flavonoids (rutin, myricetin, quercetin and kaempferol) in medicinal plants used to manage hypertension by herbalists in Botswana. Fotsing et al reviewed the synthesis of biologically active heterocyclic compounds by the Michael addition and the double Michael addition of various amines and diamines on allenic nitriles, acetylenic nitriles, hydroxyacetylenic nitriles, acetylenic acids and acetylenic aldehydes. Djellouli et al applied differential scanning calorimetry, Fourier transformed infrared spectroscopy, scanning electron microscopy and X-ray powder diffractometry techniques to evaluate the interaction between diclofenac sodium with excipients commonly used in solid dosage forms: microcrystalline cellulose as diluent and stearic acid acid. Lukhele et al provided an overview of the traditional uses *Rapanea melanophloeos* bark, fruit and leaf extracts and compared the phytochemicals and antibacterial activities of various crude extracts validate their uses. Omobolanle et al evaluated the extracts and isolated compounds from *Alternanthera brasiliensis* plant for their activity against Methicillin-resistant *Staphylococcus aureus*. Kafeelah et al evaluated the raw, treated and effluent water quality from selected water treatment plants from Lagos Water Corporation. Attah et al extracted the peptide -rich aqueous portion of *Tragia benthamii* and subjected this to pre -purification via solid phase extraction to yield an optimized crude peptide mixture whose biophysical properties, nature and individual masses were determined by a combination of reversed phase liquid chromatography, chemical derivatization and Matrix assisted laser desorption time of flight mass spectrometry. Maria et al reported on combinatorial library

<https://doi.org/10.1515/9783110710823-201>

designing and virtual screening of cryptolepine derivatives against Topoisomerase IIA by molecular docking.

I hope that these chapters of this volume 1 will add to literature and they will be useful references for researchers.

To conclude, VCCA-2020 was a successful event and I would like to thank all those who have contributed. I would also like to thank the Organising and International Advisory committee members, the participants and the reviewers.

Prof. Ponnadurai Ramasami

# Contents

Preface — V

List of contributing authors — XIII

Olusesan Ojo and Derek T. Ndinteh

## **1 Traditional uses, biological activities, and phytochemicals of *Lecaniodiscus cupanioides*: a review — 1**

- 1.1 Introduction — 1
- 1.2 Botanical description of *L. cupanioides* — 2
- 1.3 Ethnomedicinal uses of *L. cupanioides* — 3
- 1.4 Biological activities of *L. cupanioides* — 4
  - 1.4.1 Antibacterial activity — 4
  - 1.4.2 Analgesic and ameliorative effects — 6
  - 1.4.3 Antioxidant activity — 6
  - 1.4.4 Anti-protozoal activity — 8
  - 1.4.5 Anti-CNS depressant activity — 9
  - 1.4.6 Antifungal activity — 9
  - 1.4.7 Anticancer activity — 9
  - 1.4.8 Toxicity activity — 10
  - 1.4.9 Anti-diabetic activity — 10
  - 1.4.10 Aphrodisiac effect — 11
  - 1.4.11 Nutritional composition and values — 11
  - 1.4.12 Other activity — 12
- 1.5 Phytochemicals reported from *L. cupanioides* — 12
- 1.6 Conclusion — 13
- References — 14

Emmanuel M. Halilu, Abdullahi M. Abdurrahman, Sylvester N. Mathias,  
Chinenye J. Ugwah-Oguejiofor, Muntaka Abdulrahman and Saadu Abubakar

## **2 Phytochemical and antioxidant activity of *Cadaba farinosa* Forssk stem bark extracts — 19**

- 2.1 Introduction — 20
- 2.2 Methodology — 21
  - 2.2.1 Location, identification, collection, and preparation of plant sample — 21
  - 2.2.2 Extraction of plant material — 21
  - 2.2.3 Preliminary phytochemical screening of the extracts of *C. farinosa* — 22
  - 2.2.4 Thin layer chromatographic studies chromatographic studies — 22
  - 2.2.5 Determination of total phenolic content — 22
  - 2.2.6 Qualitative TLC screening of antioxidant compounds — 22
  - 2.2.7 Quantitative antioxidant studies — 23



2.2.8	Data analysis —	23
2.3	Results and discussion —	23
2.3.1	Extraction of plant material —	23
2.3.2	Preliminary phytochemical screening —	24
2.3.3	Thin layer chromatography —	24
2.3.4	Total phenolic content —	25
2.3.5	Qualitative and quantitative antioxidant studies —	26
2.4	Conclusion —	28
	References —	29

Katso Binang and David T. Takuwa

**3 Development of reverse phase-high performance liquid chromatography (RP-HPLC) method for determination of selected antihypertensive active flavonoids (rutin, myricetin, quercetin, and kaempferol) in medicinal plants found in Botswana — 31**

3.1	Introduction —	31
3.2	Experimental —	33
3.2.1	Instruments and apparatus —	33
3.2.2	Chemicals and reagents —	33
3.2.3	Preparation of flavonoid standards —	33
3.2.4	Preparation of medicinal plant samples —	34
3.2.5	HPLC-DAD-UV-Vis separation of flavonoid standards —	34
3.2.6	Statistical analysis —	34
3.3	Results and discussion —	34
3.3.1	Development of RP-HPLC method —	34
3.3.2	Fitness for purpose —	36
3.3.3	Application of the optimized method on the selected medicinal plants —	38
3.4	Conclusion —	41
	References —	42

Marthe Carine Djuidje Fotsing, Dieudonné Njamén, Zacharias Taneé Fomum and Derek Tantoh Ndinteh

**4 Synthesis of biologically active heterocyclic compounds from allenic and acetylenic nitriles and related compounds — 45**

4.1	Introduction —	45
4.2	Usefulness of heterocycles —	46
4.3	Heterocycles synthesis —	47
4.3.1	Double Michael addition —	47
4.3.2	Heterocyclic compounds by Michael addition to allenic nitriles —	47
4.3.3	Synthesis of heterocycles from acetylenic nitriles —	66

- 4.3.4 Synthesis of heterocycles from acetylenic acids — 73
- 4.3.5 Synthesis of heterocycles from acetylenic aldehydes — 73
- 4.4 Biological applications of heterocycles — 75
- 4.4.1 Pyrimidopyrimidines — 75
- 4.4.2 Pyrazolopyrimidines — 76
- 4.4.3 Aminopyridylpyrazoles — 76
- 4.4.4 Pyrimido(1,2a)benzimidazoles — 76
- 4.4.5 Oxazoles — 76
- 4.4.6 Pyrimidobenzothiazolones — 76
- 4.5 Current biological relevance of heterocycles — 76
- 4.6 Conclusion — 77
- References — 78

Djellouli Fayrouz, Dahmani Abdallah and Hassani Aicha

## **5 Experimental investigation of ternary mixture of diclofenac sodium with pharmaceutical excipients — 85**

- 5.1 Introduction — 85
- 5.2 Materials and methods — 88
- 5.2.1 Materials — 88
- 5.2.2 Sample preparation — 88
- 5.2.3 Infrared spectroscopy — 88
- 5.2.4 Differential scanning calorimetry — 88
- 5.2.5 X-ray powder diffraction — 89
- 5.2.6 Scanning electron microscopy — 89
- 5.3 Discussion of experimental results — 89
- 5.3.1 DSC — 89
- 5.3.2 SEM — 93
- 5.4 Conclusions — 93
- References — 95

Thabile Lukhele, Denise Olivier, Marthe C. D. Fotsing, Charlotte M. Tata, Monisola I. Ikhile, Rui W. M. Krause, Sandy Van Vuuren and Derek Tantoh Ndinteh

## **6 Ethnobotanical survey, phytoconstituents and antibacterial investigation of *Rapanea melanophloeos* (L.) Mez. bark, fruit and leaf extracts — 97**

- 6.1 Introduction — 98
- 6.2 Materials and methods — 99
- 6.2.1 Ethnobotanical survey — 99
- 6.2.2 Plant material — 99
- 6.2.3 Preparation of plant extracts and alcohol precipitable solids (APS) — 99
- 6.2.4 TLC variation study — 101
- 6.2.5 GC-MS analyses of PE extract — 101

- 6.2.6 Amino acid extraction and analyses — **101**
- 6.2.7 Antibacterial activity by microdilution assay — **102**
- 6.3 Results and discussion — **104**
- 6.3.1 Ethnobotanical knowledge — **104**
- 6.3.2 Extract yields, APS content and TLC profiles — **105**
- 6.3.3 Results of petroleum ether extract analysed by GC-MS — **107**
- 6.3.4 Amino acid analysis by means of GC-MS — **109**
- 6.3.5 Antibacterial properties by means of MIC determination — **111**
- 6.4 Conclusions — **117**
- References — **118**

Enitan Omobolanle Adesanya, Mubo Adeola Sonibare, Edith Oriabure Ajaiyeoba and Samuel Ayodele Egieyeh

**7 Compounds isolated from hexane fraction of *Alternanthera brasiliensis* show synergistic activity against methicillin resistant *Staphylococcus aureus* — 123**

- 7.1 Introduction — **124**
- 7.2 Materials and methods — **124**
- 7.2.1 Plant material — **124**
- 7.2.2 Plant extraction and fractionation — **124**
- 7.2.3 Isolation of compounds from the *A. brasiliensis* — **125**
- 7.2.4 High performance liquid chromatography (HPLC) analysis — **125**
- 7.2.5 Gas Chromatography-Mass Spectrometry (GCMS) analysis — **125**
- 7.2.6 Nuclear Magnetic Resonance (NMR) analysis — **126**
- 7.2.7 Antibacterial assay — **126**
- 7.2.8 Statistical analysis — **127**
- 7.3 Results and discussion — **127**
- 7.3.1 Identification of potential compounds in *A. brasiliensis* hexane fraction — **127**
- 7.3.2 Isolation and structural elucidation of compounds from *A. brasiliensis* hexane fraction — **128**
- 7.3.3 Antibacterial assay — **130**
- 7.4 Conclusion — **134**
- 7 Appendix — **135**
- References — **144**

Kafeelah Yusuf, Abdulrafiu Majolagbe and Sherifat Balogun

**8 Evaluation of raw, treated and effluent water quality from selected water treatment plants: a case study of Lagos Water Corporation — 147**

- 8.1 Introduction — **147**
- 8.2 Materials and methods — **148**

8.2.1	Sampling and sample preparation —	<b>148</b>
8.2.2	Description of the study area —	<b>148</b>
8.2.3	Analytical procedure —	<b>149</b>
8.3	Statistical analysis —	<b>149</b>
8.3.1	Correlation analysis (CA) —	<b>149</b>
8.3.2	Principal component analysis —	<b>150</b>
8.3.3	Water quality index —	<b>150</b>
8.3.4	Health risk assessment —	<b>150</b>
8.3.5	Non-carcinogenic risk assessment —	<b>152</b>
8.4	Results and discussion —	<b>152</b>
8.4.1	WQI analysis —	<b>158</b>
8.4.2	Principal component analysis —	<b>159</b>
8.4.3	Health risk assessment —	<b>161</b>
8.4.4	Correlation analysis of water quality parameters —	<b>162</b>
8.5	Conclusion —	<b>166</b>
	References —	<b>166</b>

Alfred F. Attah, Abobarin I. Omobola, Jones O. Moody, Mubo A. Sonibare,  
Olubori M. Adebukola and Samuel A. Onasanwo

<b>9</b>	<b>Detection of cysteine-rich peptides in <i>Tragia benthamii</i> Baker (Euphorbia- ceae) and <i>in vivo</i> antiinflammatory effect in a chick model —</b>	<b>169</b>
9.1	Introduction —	<b>170</b>
9.2	Materials and method —	<b>171</b>
9.2.1	Plant material —	<b>171</b>
9.2.2	Extraction, SPE pre purification and preliminary MALDI TOF/TOF analysis —	<b>172</b>
9.2.3	RP-HPLC fractionation of C <sub>18</sub> peptide positive fraction —	<b>172</b>
9.2.4	Reduction/alkylation of peptides and MALDI-MS analysis —	<b>172</b>
9.2.5	Derivatization of peptides and MALDI TOF/TOF analysis —	<b>172</b>
9.2.6	<i>In vivo</i> anti-inflammatory assay using the chick model —	<b>173</b>
9.2.7	Brine shrimp cytotoxicity (lethality assay) —	<b>173</b>
9.3	Results —	<b>173</b>
9.3.1	Extraction of cysteine-rich peptides and mass spectrometry experiment —	<b>173</b>
9.3.2	Effect of extract on carrageenan-induced foot edema in chicks and brine shrimp cytotoxicity —	<b>174</b>
9.4	Discussion —	<b>176</b>
9.5	Conclusions —	<b>182</b>
	References —	<b>183</b>

Maria, Zahid Khan and Aleksey E. Kuznetsov

**10 Combinatorial library design and virtual screening of cryptolepine derivatives against topoisomerase IIA by molecular docking and DFT studies — 187**

- 10.1 Introduction — **188**
- 10.2 Computational methods — **189**
  - 10.2.1 Retrieval and refinement of crystal structure — **189**
  - 10.2.2 Combinatorial library designing — **189**
  - 10.2.3 Docking and virtual screening — **190**
  - 10.2.4 Docking protocol applied by MOE — **190**
  - 10.2.5 Docking analysis — **191**
  - 10.2.6 DFT studies — **191**
- 10.3 Results and discussion — **195**
  - 10.3.1 Combinatorial library design and docking analysis — **195**
  - 10.3.2 Detailed interaction analysis of the docked ligands in the binding pocket of receptor TOP2A — **197**
  - 10.3.3 DFT studies — **203**
- 10.4 Conclusions — **208**
- 10.5 Supporting information — **209**
  - References — **210**

**Index — 213**

## List of contributing authors

Enitan Omobolanle Adesanya  
University of Ibadan Faculty of Pharmacy  
PHARMACOGNOSY  
Ibadan, Oyo  
Nigeria  
enitadesanya@gmail.com

Edith Ajaiyeoba  
University of Ibadan Faculty of Pharmacy  
PHARMACOGNOSY  
Ibadan, Oyo  
Nigeria  
Edajaiye@gmail.com

Francis Alfred Attah  
University of Ilorin  
Pharmacognosy and Drug Development  
Ilorin, West Africa  
Nigeria  
attah.fau@unilorin.edu.ng

Sherifat Bola Balogun  
Lagos State Government  
Lagos State Ministry of Commerce, industry and  
cooperatives  
Ikeja, Lagos  
Nigeria  
sheribalogun@yahoo.com

Katso Binang  
University of Botswana  
Faculty of Science  
Gaborone  
Botswana  
binangkatso@gmail.com

Abdallah Dahmani  
Universite des Sciences et de la Technologie  
Houari Boumediene  
chimie physique et theorique  
Bp32 El Alia  
16111Bab Ezzouar  
Alger Algerie 16111  
abdahmani@yahoo.fr

Samuel Ayodele Egieyeh  
University of the Western Cape  
Pharmacology and Clinical Pharmacy  
Bellville, CAPE TOWN  
South Africa  
segieyeh@gmail.com

Djellouli Fayrouz  
Universite des Sciences et de la Technologie  
Houari Boumediene  
chimie physique et theorique  
Bp32 El Alia  
16111Bab Ezzouar  
Alger Algerie 16111  
alafa2006@yahoo.fr

Zacharias Tanee Fomum  
University of Yaounde  
Faculty of Sciences  
Department of Animal Biology and Physiology  
Yaounde  
Cameroon  
tantohtantoh@gmail.com

Marthe C. D. Fotsing  
University of Johannesburg  
Auckland Park  
Gauteng  
South Africa  
carinemarthe@gmail.com

Emmanuel Mshelia Halilu  
Usmanu Danfodiyo University  
Pharmacognosy and Ethnopharmacy  
Sokoto  
Nigeria  
emshelia2002@gmail.com

<https://doi.org/10.1515/9783110710823-202>

## XIV — List of contributing authors

Aicha Hassani  
Universite des Sciences et de la Technologie  
Houari Boumediene  
chimie physique et theorique  
Bp32 El Alia  
16111Bab Ezzouar  
Alger Algeria 16111  
aicha\_hassani2@yahoo.f

Monisola Ikhile  
Johannesburg  
South Africa  
mikhile@uj.ac.za

Zahid Khan  
Institute of Chemical Sciences  
Peshawar  
Pakistan  
zahidkhansup1122@gmail.com

R. Krause  
Grahamstown  
South Africa  
r.krause@ru.ac.za

Aleksey E. Kuznetsov  
Universidad Tecnica Federico Santa Maria  
Chemistry  
Av. Santa Maria 6400, Vitacura, Santiago  
7660251  
Chile  
aleksey.kuznetsov@usm.cl

Thabile Lukhele  
Johannesburg  
South Africa  
thabilemhlanti@gmail.com

Abdulrafii Olaiwola Majolagbe  
Lagos State University  
Chemistry  
Lagos, Lagos State  
Nigeria  
abdulrafii.majolagbe@lasu.edu.ng

Maria  
Institute of Chemical Sciences  
Peshawar  
Pakistan  
mariabiochemist1@gmail.com

Derek Tantoh Ndinteh  
University of Johannesburg  
Auckland Park  
Gauteng  
South Africa  
dndinteh@uj.ac.za

Dieudonne Njamen  
University of Yaounde  
Faculty of Sciences  
Department of Animal Biology and Physiology  
Yaounde  
Cameroon  
dnjamen@gmail.com

Denise Olivier  
Johannesburg  
South Africa  
denise@seobi.co.za

Ojo Olusesan  
University of Johannesburg  
Auckland Park  
Gauteng  
South Africa  
Ojoolusesan33@gmail.com

Mubo Adeola Sonibare  
University of Ibadan Faculty of Pharmacy  
PHARMACOGNOSY  
Ibadan, Oyo  
Nigeria  
sonibaredeola@yahoo.com

Charlotte Mungo Tata  
University of Johannesburg  
Doornfontein Campus, Chemical Sciences  
Gauteng 2094  
South Africa  
ttcharlym@yahoo.com

Sandy van Vuuren  
Johannesburg  
South Africa  
sandy.vanvuuren@wit.ac.za

Kafeelah Yusuf  
Lagos State University  
Chemistry  
Lagos, Lagos State  
Nigeria  
kafyusuf@yahoo.co.uk

Olusesan Ojo and Derek T. Ndinteh\*

# 1 Traditional uses, biological activities, and phytochemicals of *Lecaniodiscus cupanioides*: a review

**Abstract:** Medicinal plants are indispensable source of therapeutic agents, and have proved to be “warehouse” of lead drug candidates. *Lecaniodiscus cupanioides* Planch. ex Benth is a medicinal tree plant that is extensively distributed in both Asia and Africa. The species has many ethnomedicinal uses in the treatment of fever, cough, typhoid, wound, skin infection, measles, jaundice, diabetes, sexual dysfunction, cancer, bone fracture, and as galactogogues. In the recent decades, the extracts and phytochemicals of *L. cupanioides* have been investigated to possess antibacterial, anticancer, aphrodisiac, antifungal, cytotoxic, antidiabetic, antiprotozoal, antioxidant, antidiarrhoeal, analgesic and ameliorative properties. However, triterpenoids which have been linked to its anticancer and antifungal actions, are the only isolated active constituents identified from the species despite the results of the phytochemical screenings and reported biological activities. Moreover, the mechanisms of action of the extracts and active components are yet to be fully elucidated. This paper provides a general review on the ethnomedicinal, phytochemicals, and biological activities of *L. cupanioides*, and lays a solid foundation for future investigations on the plant.

**Keywords:** biological activity; ethnomedicine; *Lecaniodiscus cupanioides*; medicinal plants; phytochemicals.

## 1.1 Introduction

There have been arousing interests nowadays in the utilization of medicinal plants. This is partly due to continuous and alarming rise in the prices of synthetic drugs as well as partly due to associated side effects, such as human toxicity of these synthetic drugs [1]. Medicinal plants and/or plant-derived medicines are currently used globally to treat various forms of ailments. Plant-based medicines have shown their potential over synthetic drugs by mostly having fewer or no side effects, and lower or no toxicity. Moreover, they serve as templates or models structurally and pharmacologically for synthetic drugs, and sometimes they are used directly as therapeutics [2, 3]. The World Health Organization (WHO) opined that up to 80% of the people living in developing

---

\*Corresponding author: **Derek T. Ndinteh**, Department of Chemical Sciences, University of Johannesburg, Doornfontein, Johannesburg 2028, South Africa, E-mail: dndinteh@uj.ac.za  
**Olusesan Ojo**, Department of Chemical Sciences, University of Johannesburg, Doornfontein, Johannesburg 2028, South Africa

This article has previously been published in the journal *Physical Sciences Reviews*. Please cite as: O. Ojo and D. T. Ndinteh. “Traditional uses, biological activities, and phytochemicals of *Lecaniodiscus cupanioides*: a review” *Physical Sciences Reviews* [Online] 2021, 5. DOI: 10.1515/psr-2020-0207 | <https://doi.org/10.1515/9783110710823-001>



countries currently utilize medicinal plants as remedies for one disease or the other [4]. Plants have been used for treating diverse diseases from the time immemorial by the traditional herbal healers or rural dwellers. For several decades, plants have been employed in medicine, nutrition and cosmetics, with little or no harmful effects [5]. It has been reported that medicinal plants possess several bioactive phytochemicals with pharmacological properties, including antibacterial, anticancer, antioxidant, anti-fungal, antiviral, analgesic, and anti-inflammatory [6–10]. These bioactive phytochemicals include alkaloids, terpenoids, coumarins, steroids, tannins, saponins, flavonoids, phenolic acids, lignin, and quinines to mention a few [11].

Our nature environment provides us with variety of chemical compounds that are diverse in structure, and naturally-derived compounds are well-known for unique pharmacological properties. Natural products possess structurally diverse chemical compounds that are “optimized” by the evolutionary changes as drug-like molecules [12]. It is well reported in the literature that natural products provide a matchless resource for the discovery of novel drug candidates. A synthetic review of natural products (NPs) from 1981 to 2014 showed that approximately 40% of the therapeutics licenced by the U.S. Food and Drug Administration (FDA) were mainly NPs, derivatives of NPs, or synthetic mimetic products related to NPs [13]. Literature is replete with examples of phytochemicals or drugs derived from natural products or medicinal plants. This includes morphine (from the opium poppy *Papaver somniferum*), anti-carcinogenic agent Taxol (from *Taxus brevifolia*), and the artemisinin, an antimalarial drug, from a Chinese plant, *Artemisia annua* [14–16].

Medicinal plants, undoubtedly, have become a focal point for meeting or improving the health needs of man [17]. Nature is endowed with amazing medicinal plants to handle every human disease as well as health challenges, and to serve as alternative bio-resources to synthetic drugs. Unfortunately, many of these medicinal plants have been underutilized to enhance quality of human health because of lack of adequate information on their pharmacological potential. One of such medicinal plants is *Lecaniodiscus cupanioides* Planch. ex Benth. This plant is chosen because of its numerous medicinal values, and lacks of review literature on its medicinal potential. Therefore, the present study is designed to review previously published and original data on the traditional uses, biological properties, and phytochemistry of *L. cupanioides* as a potential source of new bioactive molecules.

## 1.2 Botanical description of *L. cupanioides*

The plant *L. cupanioides* belongs to the family Sapindaceae (Table 1.1). It is an elegant, tropical tree widely common in Asia and Africa. It is known by several local names. For instance, it is named “Akika” among the Yoruba tribe, “Ukpo” among the Igbos, and “Kafi-nama-zaki” among the Hausa in Nigeria; in Sierra Leone as Bulati (Limba), Babwi (Loko), and in Ivory Coast as Bue (Akye) and Klima (Baule). The plant is about 6–12 m

**Table 1.1:** Taxonomical classification of *Lecaniodiscus cupanioides*.

Taxonomy	
Kingdom	Plantae
Phylum	Tricheophyta
Class	Magnoliopsida
Order	Sapindales
Family	Sapindaceae
Genus	<i>Lecaniodiscus</i>
Species	<i>Lecaniodiscus cupanioides</i>

high or more, with a low-branching, spreading crown. It is planted as shade tree in some towns. The tree is evergreen, semi-deciduous, and often found in seasonally flooded forest, on rocky riverside, and sometimes on the forest outliers in Savanna regions. It extends from Senegal to West Cameroons and across Africa to Sudan, Uganda, and Southern Angola. The tree has alternate compound leaves. The leaflets have a petiolule which is swollen at the bottom (Figure 1.1). The flowers have unusual disc which surrounds the stamens. Hence, the name “*Lecaniodiscus*”, meaning saucer-shaped disc [18, 19].

### 1.3 Ethnomedicinal uses of *L. cupanioides*

*L. cupanioides* has been used in the traditional clinical practices of many cultures worldwide, including those of the African and Asian to treat a number of diseases and



**Figure 1.1:** *L. cupanioides* plant, showing fruiting branches (Photograph by: International Institute of Tropical Agriculture (IITA), Oyo State, Nigeria).

sickness. The leaves, stems, roots, and barks of *L. cupanioides* have been documented in the existing literature for use in the treatment of infections among the traditional healers. The plant has enormous potential for medicinal uses, especially in the treatment of infertility and sex-related challenges and malaria [20]. The leaves and the roots are used to treat malaria, a deadly infectious disease, by the rural dwellers in Benin [21]. The ethnomedicinal uses of *L. cupanioides* in traditional medicine have been detailed in Table 1.2. Various parts of the plant are used for the treatment of oral hygiene, wounds, burns, wound, fever, and abdominal swelling [20].

## 1.4 Biological activities of *L. cupanioides*

Different pharmacological activities have been reported for *L. cupanioides* by various researchers. The extracts and chemical constituents isolated from *L. cupanioides* have been shown to exhibit varying biological activities which include, but not limited to, antibacterial, analgesic, ameliorative, antioxidant, antiprotozoal, antifungal, anti-CNS depressant, and anticancer activities (Figure 1.2).

### 1.4.1 Antibacterial activity

It has been documented in the literature that *L. cupanioides* exhibited antibacterial activity against a number of human pathogens [33, 34]. Sofidiya et al. [33] screened

**Table 1.2:** Ethnomedicinal uses of *L. cupanioides*.

Category of use	Part(s) used	Reference
Malaria fever	Leaves, roots	[21]
Sexual dysfunction	Roots	[20–22]
Typhoid	Leaves, roots, stem	[23, 24]
Jaundice	Leaves, stem, roots	[23, 24]
Cough	Stem, bark	[23, 24]
Skin infection	Bark	[25]
Cancer, tumour	Bark, roots	[26]
Pain	–	[27]
Scalp infection	Roots, bark	[28]
Diabetes	Stem-bark	[29]
Wound and sore	Leaves, stem, bark	[30]
Abdominal swelling	Leaves, bark, stem	[30]
Measles	Leaves, bark, stem	[30]
Boils and burns	Leaves	[30]
Galactogogues	Roots	[31]
Bone fracture	Leaves	[32]

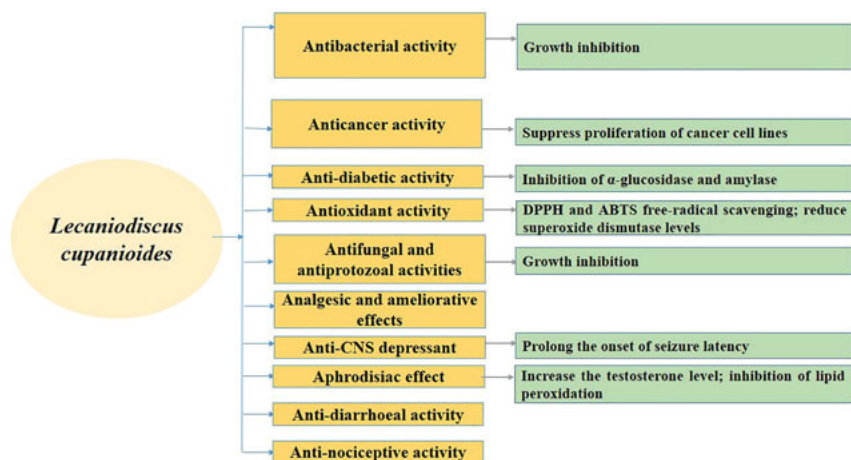


**Figure 1.2:** Schematic representation of the biological activities of *L. cupanioides* extracts and active constituents, showing some of their mechanisms of actions.

methanolic leaves extract of *L. cupanioides* against 10 bacteria. The authors revealed that six of the tested organisms were inhibited. They found that *Bacillus cereus*, *Streptococcus pyrogens*, *Micrococcus kristinae*, and *Staphylococcus aureus* were more inhibited by the extract, with minimum inhibitory concentration (MIC) value  $<1.0$  mg/mL. Similarly, *Pseudomonas aeruginosa* and *Salmonella pooni* were inhibited at MIC value of 2.0 mg/mL. However, *Staphylococcus epidermidis*, *Escherichia coli*, *Serratia marcescens*, and *Klebsiella pneumoniae* were not inhibited at the highest concentration of the extract. Ethanolic and hexane root extracts of *L. cupanioides* were tested against six pathogens, including *E. coli*, *S. aureus*, *Streptococcus pneumonia*, *Shigella flexneri*, *Pseudomonas aeruginosa*, and *Salmonella typhi*. It was revealed that ethanol extract of *L. cupanioides* showed the highest zone of inhibition of 30 mm at 125  $\mu$ g/mL against *S. aureus*, which is comparatively as active as the ceftriaxone sodium used as the standard. Similarly, *L. cupanioides* was singly active against *S. aureus*, with a zone of inhibition of 8 mm at 7.8125  $\mu$ g/mL for the hexane extract [35]. Thus, it can be inferred that the phytochemicals that are responsible for the antibacterial efficacy were more present or soluble in ethanolic extract than hexane extract of *L. cupanioides*, because it had the same inhibitory potency as the standard (ceftriaxone sodium) against *S. aureus*. Kazeem and his co-author [36] reported the antimicrobial activities of *L. cupanioides* leaf extract against some typed cultures and locally isolated pathogens. The authors assessed the antimicrobial efficacy by using agar-well diffusion as well as by determining the minimum bacteriostatic and bactericidal concentrations. The findings revealed that the extract exhibited zones of inhibition, ranging from  $20 \pm 0.00$  to  $23 \pm 0.58$  mm at 20 mg/mL. The MICs were between 1.25 and 2.50 mg/mL, and the minimum bactericidal concentrations (MBCs) ranged from 2.50 to 5.00 mg/mL.

The ethanol and the aqueous extracts of *L. cupanioides* leaves were comparatively assessed for their antibacterial activities. The clinical isolates of *S. aureus*, *E. coli*, *P. aeruginosa*, *Klebsiella pneumoniae*, and *Bacillus subtilis* along with a standard strain of *S. aureus* were used for the study. The MICs of the extracts were reportedly varied from 2.5 to 6.25 mg/mL. Comparatively, the ethanol extract showed more potency than the aqueous extract against all the pathogens, with the exception of the clinical isolates of *S. aureus* [37]. Research carried out by Okore et al. [38] on the aqueous pods extract against standard strains of *E. coli*, *S. aureus*, *P. aeruginosa*, and the untyped strains of *K. pneumoniae*, *B. subtilis*, and *Salmonella paratyphi* using agar-cup diffusion method showed no inhibitory action against all the tested bacteria strains. Differences in these test results when compared with the previous findings may be due to various parameters, such as plant parts, places and time of plant collection, soil composition, solvents, season, climate and difference in bioassay method used [39]. However, further studies need to be conducted using the same parameters with the previous findings to either validate or invalidate the above assertions.

Pharmacologically, *L. cupanioides* may be a promising source of new antibacterial drugs based on the reported MIC values, though some authors are of the opinion that only extracts having the MIC value of <0.1 mg/mL could have promising antimicrobial activity. Gibbons [40] opined that a plant extract or its isolated pure constituent is of little or no relevance clinically when its MIC value is greater than 1.0 mg/mL. However, there is tendency it may have some inert substances having good antibacterial activities at higher concentrations. Thus, the minimum inhibitory zone displayed by *L. cupanioides* extracts against different bacteria strains indicates that the plant has clinical value in the search for new drugs, especially as it inhibited bacteria strains that are already resistant to the orthodox drugs [41, 42]. Table 1.3 summarizes the antibacterial activities of different extracts of *L. cupanioides* against different strains of bacteria.

### 1.4.2 Analgesic and ameliorative effects

Adeyemi et al. [43] reported analgesic activities of *L. cupanioides* aqueous root extract. In the study, the authors revealed that the extract (400 mg/kg) had comparable effects ( $P < 0.05$ ) to the reference drug, morphine or aspirin. In another separate study carried out on the *L. cupanioides* using loperamide-induced Wistar rats, it was reported that the aqueous root extract (250 mg/kg) significantly normalized ( $P < 0.05$ ) the body weight gain (8.15 g) as well as the gastrointestinal ratio (87.75) of the rats compared to the control [44].

### 1.4.3 Antioxidant activity

Ogbunugafor et al. [45] investigated ethanol leaves extract of *L. cupanioides* on the serum antioxidant system and lipid profile of Albino rats. The findings revealed that

**Table 1.3:** Summary of in vitro antibacterial activities of *L. cupanioides* different extracts.

Extract	Antibacterial testing model	Bacteria tested <sup>a</sup>	Results	MIC	Reference
Methanol	Agar diffusion	Bc	Sensitive	<1.0 mg/mL	[34]
		Se	Resistant	No activity	[34]
		Sa	Sensitive	<1.0 mg/mL	[34]
		Mk	Sensitive	<1.0 mg/mL	[34]
		Sp	Sensitive	<1.0 mg/mL	[34]
		Ec	Resistant	No activity	[34]
		Sp*	Sensitive	2.0 mg/mL	[34]
		Sm	Resistant	No activity	[34]
		Pa	Sensitive	2.0 mg/mL	[34]
		Ethanol	Microdilution	Ec	Resistant
Sa	Sensitive			16 µg/mL	[35]
Sp**	Resistant			No activity	[35]
Sf	Resistant			No activity	[35]
Pa	Resistant			No activity	[35]
St	Resistant			No activity	[35]
Hexane	Microdilution	Ec	Resistant	No activity	[35]
		Sa	Sensitive	Not stated	[35]
		Sp**	Resistant	No activity	[35]
		Sf	Resistant	No activity	[35]
		Pa	Resistant	No activity	[35]
		St	Resistant	No activity	[35]
Methanol-water	Agar diffusion	Ah	Sensitive	2.50 mg/mL	[36]
		Ac	Sensitive	1.25 mg/mL	[36]
		Bp	Sensitive	1.25 mg/mL	[36]
		Ec	Sensitive	2.50 mg/mL	[36]
		Ef	Sensitive	1.25 mg/mL	[36]
		Ef *	Sensitive	2.50 mg/mL	[36]
		Kp	Sensitive	2.50 mg/mL	[36]
		Ls	Sensitive	1.25 mg/mL	[36]
		Ss	Sensitive	1.25 mg/mL	[36]
		Sf	Sensitive	2.50 mg/mL	[36]
		St*	Sensitive	2.50 mg/mL	[36]
		St	Sensitive	1.25 mg/mL	[36]
		Sa	Sensitive	1.25 mg/mL	[36]
		Ps	Sensitive	1.25 mg/mL	[36]
		Pv	Sensitive	1.25 mg/mL	[36]
		Pa	Sensitive	1.25 mg/mL	[36]
Water	Agar diffusion	Sa	Sensitive	2.50 mg/mL	[37]
		Bs	Sensitive	2.50 mg/mL	[37]
		Ec	Sensitive	2.50 mg/mL	[37]
		Pa	Sensitive	6.25 mg/mL	[37]
Ethanol	Agar diffusion	Kp	Sensitive	5.00 mg/mL	[37]
		Sa	Sensitive	2.50 mg/mL	[37]
		Bs	Sensitive	2.50 mg/mL	[37]
		Ec	Sensitive	2.50 mg/mL	[37]

Table 1.3: (continued)

Extract	Antibacterial testing model	Bacteria tested <sup>a</sup>	Results	MIC	Reference
Water	Agar diffusion	Pa	Sensitive	5.00 mg/mL	[37]
		Kp	Sensitive	2.50 mg/mL	[37]
		Ec	Resistant	No activity	[38]
		Sa	Resistant	No activity	[38]
		Pa	Resistant	No activity	[38]
		Kp	Resistant	No activity	[38]
		Bs	Resistant	No activity	[38]
		Sp***	Resistant	No activity	[38]

<sup>a</sup>Bc—*Bacillus cereus*; Se—*Staphylococcus epidermidis*; Sa—*Staphylococcus aureus*; Mk—*Micrococcus kristinae*; Sp—*Streptococcus pyrogenes*; Ec—*Escherichia coli*; Sp\*—*Salmonella pooni*; Sm—*Serratia marcescens*; Pa—*Pseudomonas aeruginosa*; Kp—*Klebsiella pneumoniae*; Sp\*\*—*Streptococcus pneumoniae*; Sf—*Shigella flexineri*; St—*Salmonella typhi*; Ah—*Aeromonas hydrophilla*; Ac—*Acinetobacter calcoaceticus anitratus*; Bp—*Bacillus pumilis*; Ef—*Enterobacter faecalis*; Ef\*—*Enterococcus faecalis*; Ls—*Listeria sp.*; Ss—*Shigella soonei*; St\*—*Salmonella typhimurium*; Ps—*Plesiomonas shigelloides*; Pv—*Proteus vulgaris*; Bs—*Bacillus subtilis*; Sp\*\*\*—*Salmonella paratyphi*.

the extract significantly exhibited lower ( $P < 0.05$ ) catalase and superoxide dismutase activities in the treated rats when compared with the control and vitamin E-treated rats. The malondialdehyde which was employed as the index for lipid peroxidation was significantly higher ( $P < 0.05$ ) in animals treated with *L. cupanioides* extract ( $4.20 \pm 0.35$  mmol/L) compared to the control rats ( $2.87 \pm 0.23$  mmol/L). Lipid profile estimation showed that the levels of triacylglycerides were significantly reduced ( $P < 0.05$ ) in all the rats treated. Sofidiya and his co-authors [33] reported that methanol extract of *L. cupanioides* leaves possesses radical scavenging activity against 2, 2-diphenyl-1-picrylhydrazyl (DPPH) and 2, 2'-azino-bis(3-ethylbenzothiazoline-6-sulphonic acid) (ABTS). It was revealed that 0.1 mg/mL of the crude methanol extract displayed DPPH and ABTS radicals scavenging activity up to 99.4 and 98.5%, respectively. Quantitatively, the flavonoid and the proanthocyanidin contents of the leaves extract were  $4.142 \pm 0.06$  and  $2.548 \pm 0.32$  mg/g, respectively. Owing to the relatively high proportion of flavonoids in *L. cupanioides*, the species could be a rich and natural source of antioxidants against oxidative stress diseases, including Alzheimer and Parkinson. The toxic effects of ethanol leaves extract of the species on antioxidant enzymes in Albino rats have been reported. The authors revealed that at the extract concentrations of 800 and 1600 mg/kg there was significant ( $P < 0.05$ ) increased in the sizes of liver, brain and kidney compared to the control [46].

#### 1.4.4 Anti-protozoal activity

Studies have shown that *L. cupanioides* extracts possess anti-protozoal activities. In a study, aqueous root extract of the plant was reported to exhibit antimalarial activity against a chloroquine-sensitive strain of *Plasmodium berghei* (NK 65) in Albino mice

model [47]. Meanwhile, the methanol leaves extract of *L. cupanioides* was screened against chloroquine-sensitive strains, including *Plasmodium falciparum*, *Trypanosoma brucei brucei* and *Leishmania donovani*. The extract exhibited no significant antiplasmodial activity against *P. falciparum*, with inhibitory activity lesser than 47%. However, it displayed more than 90% inhibition against *T. brucei brucei* [33]. The excellent inhibitory activity of *L. cupanioides* against *T. brucei brucei* is an indicative that it would be a novel source of drugs against *T. brucei brucei*, a parasitic protozoan, of the genus *Trypanosoma*. In man, it causes trypanosomiasis (also called sleeping sickness) [48]. It is a neglected, and potentially fatal disease in Africa, especially if left untreated immediately.

#### 1.4.5 Anti-CNS depressant activity

According to the existing literature, the aqueous root extract has been investigated for central nervous system (CNS) anti-depressant activity in Swiss mice. The extract reportedly showed anti-CNS depressant activity which is comparable to the effects produced by the standard, chlorpromazine (4 mg/kg). Similarly, the extract significantly prolonged the onset of seizure latency at concentrations of 400 mg/kg p.o. and 100 mg/kg i.p. for both the strychnine-induced seizure and the picrotoxin-induced seizure [30].

#### 1.4.6 Antifungal activity

*L. cupanioides* aqueous pod extract was screened against the clinical isolate of *Candida albicans*. The extract exhibited selective inhibitory activity against *C. albicans*, without showing any inhibition on other fungi or bacteria strains [37]. Adesegun et al. [49] reported that triterpenoid saponins isolated from ethanolic stem extract exhibited antifungal activity against three fungi, including *C. albicans*, *Candida neoformans* and *Aspergillus fumigates*. Straadt et al. [50] identified fungal plasma membrane H<sup>+</sup>-ATPase inhibitors from the ethyl acetate stem-bark extract of the species. In a study carried out by Ugorji et al. [51], clotrimazole creams formulated with saponin obtained from the seeds of *Lecaniodiscus cupanioides* were found to possess anti-candidal activity. The anti-candidal activity of the creams was evaluated against the clinical isolates of *C. albicans*. It was reported that the saponin exhibited dual functions when used in combination with clotrimazole—as an emulsifier in creams as well as a potent anti-candidal drug.

#### 1.4.7 Anticancer activity

Phytochemicals from *L. cupanioides* have been reported to exhibit anti-tumour and anti-cancer activity. Two triterpenoid saponins from the plant have been linked with the ability



to inhibit cancerous cells growth. First, the constituent 3-O-[ $\alpha$ -L-arabinofuranosyl-(1 $\rightarrow$ 3)- $\alpha$ -L-rhamnopyranosyl-(1 $\rightarrow$ 2)- $\alpha$ -L-arabinopyranosyl]-hederagenin was reportedly active against human cancer cell lines, including colon carcinoma (H-116), lung carcinoma (A-549) and lung carcinoma (HT-29), with IC<sub>50</sub> of 5.0, 2.5 and 2.5  $\mu$ g/mL, respectively. Second, the compound 3-O-[ $\alpha$ -L-arabinopyranosyl-(1 $\rightarrow$ 3)- $\alpha$ -L-rhamnopyranosyl-(1 $\rightarrow$ 2)- $\alpha$ -L-arabinopyranosyl]-hederagenin showed anticancer activity, with IC<sub>50</sub> of 5.0, 5.0 and 2.5  $\mu$ g/mL respectively [52]. Ogbole and his colleagues [53] reported that methanol leaves extract of *L. cupanioides* exhibited cytotoxic activity (CC<sub>50</sub> = 17.23  $\pm$  1.98  $\mu$ g/mL) against Rhabdomyosarcoma (RD) cell line. This finding is significant in the search of new anti-cancer drugs from medicinal plants as the cytotoxic activity of the methanol leaves extract falls within the range of CC<sub>50</sub> < 30  $\mu$ g/mL which is the criterion of cytotoxicity for crude extracts in a preliminary anticancer assay as stipulated by the American National Cancer Institute (NCI) [54].

### 1.4.8 Toxicity activity

Toxicity of the *L. cupanioides* aqueous root extract was investigated in Albino rats model by Joshua et al. [55]. The root extract produced any serious toxicity or mortality at 200 mg/kg dose within two weeks of treatment. In another study, the aqueous root extract was administered orally to fasted mice at doses up to 20 g/kg, or at doses up to 800 mg/kg intraperitoneally. The study revealed that the extract produced no signs of toxicity up to 14 days after oral administration. However, acute (24 h) i.p toxicity was noticed at a dose of 455.2 mg/kg [30]. The cytotoxic effect of the leaf extract against the larvae of *Artemia salina* has also been reported. The lethality doses at LD<sub>50</sub> and LC<sub>90</sub> were 4.255 and 36.766  $\mu$ g/mL, respectively [36].

### 1.4.9 Anti-diabetic activity

Ayokun-nun et al. [56] investigated inhibitory activity of ethyl acetate fraction of the leaves on  $\alpha$ -amylase and  $\alpha$ -glucosidase enzymes, which have been implicated for the role they play in blood glucose levels. The fraction displayed significant and mild inhibitory effects on  $\alpha$ -amylase and glucosidase (IC<sub>50</sub> = 0.73 and 0.58 mg/mL respectively). The study showed that ethyl acetate leaf fraction of *L. cupanioides* displayed anti-diabetic potential. In another separate study, aqueous leaves extract of *L. cupanioides* was investigated for anti-diabetic activity *in vitro*. It was revealed that aqueous leaves extract of *L. cupanioides* inhibited  $\alpha$ -amylase (12.5–75.0%) and  $\alpha$ -glucosidase (33.3–75.0%) from 0.001 to 0.004 mg/mL in a concentration dependent manner [57]. Considering these results, *L. cupanioides* is arguably an important species for fighting diabetes because of the roles it plays in inhibiting  $\alpha$ -amylase and  $\alpha$ -glucosidase enzymes.

### 1.4.10 Aphrodisiac effect

Ajiboye et al. [22] reported the aphrodisiac effects of the *L. cupanioides* aqueous root extract on paroxetine-induced sexual dysfunction male rats. In another studies, aqueous root extract of the species was reported to restore testicular dysfunction parameters and nitric oxide/cyclic guanosine monophosphate pathway by reversing the decrease in the physiology of enzymes gamma-glutamyl transferase, lactate dehydrogenase, acid and alkaline phosphatases, and testosterone level of paroxetine-induced sexually impaired rats [58, 59]. The authors are of the opinion that the mode of action of the extract is to improve the sexual activity of the sexually impaired rats by increasing the testosterone level. Muanya et al. [60] assessed inhibition of lipid peroxidation by *L. cupanioides* extract as index of male fertility. The extract significantly inhibited extent of lipid peroxidation. The above findings show that *L. cupanioides* may be a promising plant species to explore for new aphrodisiac drugs, however more investigations should be carried out to substantiate this activity.

### 1.4.11 Nutritional composition and values

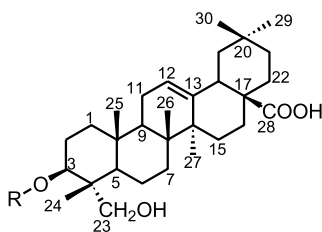
Olujobi [61] investigated nutritional composition of samples of the leaves of *L. cupanioides*. The proximate analysis showed that the species contains the highest proportion of fat (6.49%), carbohydrate (42.83%), and energy value content (1228.30%). Mineral contents of the leaves were sodium (74.60 mg/kg), potassium (445.89 mg/kg), calcium (70.23 mg/kg), magnesium (17.38 mg/kg) and iron (2.78 mg/kg). Vitamins contents contained vitamin A (545.77 mg/100 g), vitamin B1 (0.75 mg/100 g), vitamin B2 (0.64 mg/100 g), vitamin B3 (0.55 mg/100 g), vitamin C (223.86 mg/100 g), vitamin D (0.63 mg/100 g) and vitamin E (0.21 mg/100 g). Anti-nutrient contents showed that *L. cupanioides* leaves contain saponins (60.04 mg/100 g), oxalates (19.41 mg/100 g), phytates (1.27 mg/100 g), and tannin (0.14 mg/100 g). Proximate, phytochemical and nutrient compositions of leaves of *L. cupanioides* were reported by Dike [62]. Proximate compositions consisted of moisture content (5.28%), fat (3.94%), crude protein (14.69%), fibre (4.84%), ash (8.26%), and carbohydrates (68.27%). Phytochemical compositions revealed saponins (0.07%), alkaloids (4.14%), flavonoids (1.98%), anthocyanins (0.02%), sterols (0.02%), and tannins (0.95%). Mineral contents are calcium (19.0 mg/mg), magnesium (5.50 mg/mg), potassium (112.5 mg/g), sodium (5.3 mg/g), phosphorus (133 mg/g), iron (10.20 mg/kg), zinc (15.78 mg/kg), lead (0.55 mg/kg), copper (15.0 mg/kg), cadmium (0.01 mg/kg), and chromium (0.01 mg/kg). Undoubtedly, vegetable fat and oil are relatively lower in cholesterol. The significant level of fat content in *L. cupanioides* may be employed as a cheap and readily available source of natural supplement in the meal of people suffering from coronary artery diseases, thereby help in reducing blood lipids. Moreover, fats are a major source of energy, and they are fundamental for the development of brain as well as growing foetus.

### 1.4.12 Other activity

Abe et al. [63] reported anti-nociceptive activity of the plant. Oritsegbemi and Uwu-marongie [64] reported antidiarrhoeal efficacy of the hexane and the methanol leaves extracts of the plant on mice gastrointestinal tract. The findings suggested that the extracts possess, in a dose-dependent manner, laxative activity, and could be used in the treatment of constipation. Joseph et al. [65] reported that *L. cupanioides* had the ability to inhibit the onset of corrosion on normalized and annealed mild steels in 0.5 M hydrochloric acid.

## 1.5 Phytochemicals reported from *L. cupanioides*

Few phytochemicals have been reported from *L. cupanioides* based on the existing literature. Triterpenoid saponins, 3-O-[ $\alpha$ -L-arabinopyranosyl-(1 $\rightarrow$ 3)- $\alpha$ -L-rhamnopyranosyl-(1 $\rightarrow$ 2)- $\alpha$ -L-arabinopyranosyl]-hederagenin (**1**) and 3-O-[ $\alpha$ -L-arabinofuranosyl-(1 $\rightarrow$ 3)- $\alpha$ -L-rhamnopyranosyl-(1 $\rightarrow$ 2)- $\alpha$ -L-arabinopyranosyl]-hederagenin (**2**), have been isolated from the ethanolic stem of *L. cupanioides*, and they have been shown to be responsible for the anticancer [52] and antifungal activities [49] of the plant. These two saponins in addition to 3-O-[ $\beta$ -D-xylopyranosyl-(1 $\rightarrow$ 3)- $\alpha$ -L-rhamnopyranosyl-(1 $\rightarrow$ 2)- $\alpha$ -L-arabinopyranosyl]-hederagenin (**3**) and 3-O-[ $\alpha$ -L-rhamnopyranosyl-(1 $\rightarrow$ 2)- $\alpha$ -L-arabinopyranosyl]-hederagenin (**4**) have also been reported from the stem-bark of the plant collected in Sembe, northern Congo/Brazzaville [66] (Figure 1.3). Family Sapindaceae is well reputed for saponins having hederagenin as the aglycone. For instance, 3-O-[ $\alpha$ -L-arabinopyranosyl-(1 $\rightarrow$ 3)- $\alpha$ -L-rhamnopyranosyl-(1 $\rightarrow$ 2)- $\alpha$ -L-arabinopyranosyl]-hederagenin has also been isolated



R = 3-O-[ $\alpha$ -L-arabinopyranosyl-(1 $\rightarrow$ 3)- $\alpha$ -L-rhamnopyranosyl-(1 $\rightarrow$ 2)- $\alpha$ -L-arabinopyranosyl]-hederagenin (**1**)

R = 3-O-[ $\alpha$ -L-arabinofuranosyl-(1 $\rightarrow$ 3)- $\alpha$ -L-rhamnopyranosyl-(1 $\rightarrow$ 2)- $\alpha$ -L-arabinopyranosyl]-hederagenin (**2**)

R = 3-O-[ $\beta$ -D-xylopyranosyl-(1 $\rightarrow$ 3)- $\alpha$ -L-rhamnopyranosyl-(1 $\rightarrow$ 2)- $\alpha$ -L-arabinopyranosyl]-hederagenin (**3**)

R = 3-O-[ $\alpha$ -L-rhamnopyranosyl-(1 $\rightarrow$ 2)- $\alpha$ -L-arabinopyranosyl]-hederagenin (**4**)

**Figure 1.3:** Structures of triterpenoid saponins isolated from *L. cupanioides*.

from *Smelophyllum capense* [67] and *Lepisanthes rubiginosa* [68] in the Sapindaceae family. Phytochemical screenings of the extracts of *L. cupanioides* have indicated the presence of several secondary metabolites, such as alkaloids, phenolics, saponins, tannins and anthraquinones [22], cardiac glycoside, steroids, and flavonoids [36]. These metabolites, however, need to be isolated, characterized, as well as screened for biological activities.

## 1.6 Conclusion

Medicinal plants have been utilized and employed in the clinical traditional medicine since time immemorial. They are sources of biologically active principles, and are utilized as crude drugs (extracts) or as pure compounds (isolates) in treating various forms of human ailments and health challenges. Plant natural products are enormous in chemical diversity, and have shown to have fewer or no side effects as well as lesser/no toxicity over synthetic counterparts. Hence, they are “warehouse” for chemical entities in discovery, development and design of novel therapeutic agents.

*L. cupanioides* has been employed in folklore medicine for treating many diseases. Its uses have made researchers to investigate medicinal potential of this plant as claimed by traditional healers in sub-Saharan African countries. Antibacterial, anti-fungal, anticancer, antiprotozoal, antioxidant, anti-inflammatory, antidiabetic, anti-diarrhoeal, cytotoxicity activities as well as sexual prowess of *L. cupanioides* as reported in literature have been fully reviewed in this paper. However, this plant needs to be further investigated, especially as regards the recommended dose that should be administered to various illness. Except for the investigation reported by Okore and his colleagues [38] on antibacterial activity, every other antibacterial activity reported in this review showed that many strains of bacteria are susceptible to the plant extracts, thereby indicating broad-spectrum activity of the phytochemicals present in *L. cupanioides*. Selective susceptibility of some Gram-negative bacteria to the extracts of *L. cupanioides* speaks volume of the need to explore it for novel drugs against them, as these pathogens are known for highly restrictive permeable barrier, which limits the penetration of most compounds [69]. Also, mechanisms of interaction of the extracts with the pathogens should be studied and elucidated to aid in the development and design of new therapeutics. Few phytochemicals have been isolated from *L. cupanioides*, and they are all triterpenoid saponins. This calls for further research on the phytochemistry and pharmacology of *L. cupanioides*. We look for more bioactive constituents with an unusual carbon skeleton and biological activities in the future. This will not only broaden our knowledge, but also create awareness on the potential of this medicinal plant both for the local people, and the scientists who work on drug discovery.

**Author contribution:** All the authors have accepted responsibility for the entire content of this submitted manuscript and approved submission.

**Research funding:** This work was supported by the National Research Foundation (NRF), South Africa (Ref: Grant Number 116110).

**Conflict of interest statement:** The authors declare no conflict of interest.

## References

- Oliveira I, Sousa A, Ferreira IC, Bento A, Estevinho L, Pereira JA. Total phenols, antioxidant potential and antimicrobial activity of walnut (*Juglans regia* L.) green husks. *Food Chem Toxicol* 2008;46: 2326–31.
- Gurib-Fakim A. Medicinal plants: traditions of yesterday and drugs of tomorrow. *Mol Aspect Med* 2006;27:1–93.
- Verma S, Singh SP. Current and future status of herbal medicines. *Vet World* 2008;1:347.
- World Health Organization. The world traditional medicines situation. *Issues Chall* 2011;3:1–14.
- Bello MO, Abdul-Hammed M, Ogunbeku P. Nutrient and anti-nutrient phytochemicals in *Ficus exasperata* Vahl leaves. *Int J Sci Eng Res* 2014;5:2177–81.
- Abu-Lafi S, Rayan B, Kadan S, Abu-Lafi M, Rayan A. Anticancer activity and phytochemical composition of wild *Gundelia tournefortii*. *Oncol Lett* 2019;17:713–7.
- Dutta T, Paul A, Majumder M, Sultan RA, Emran TB. Pharmacological evidence for the use of *Cissus assamica* as a medicinal plant in the management of pain and pyrexia. *Biochem Biophys Rep* 2020; 21:100715.
- Ibrahim N, Kebede A. *In vitro* antibacterial activities of methanol and aqueous leave extracts of selected medicinal plants against human pathogenic bacteria. *Saudi J Biol Sci* 2020;27:2261–8.
- Maryam M, Te KK, Wong FC, Chai TT, Gary K, Gan SC. Antiviral activity of traditional Chinese medicinal plants *Dryopteris crassirhizoma* and *Morus alba* against dengue virus. *J Integr Agriv* 2020;19:1085–96.
- Moreno MA, Zampini IC, Isla MI. Antifungal, anti-inflammatory and antioxidant activity of bi-herbal mixtures with medicinal plants from Argentinean highlands. *J Ethnopharmacol* 2020;253:112642.
- Altemimi A, Lakhssassi N, Baharlouei A, Watson DG, Lightfoot DA. Phytochemicals: extraction, isolation, and identification of bioactive compounds from plant extracts. *Plants* 2017;6:42.
- Newman DJ, Cragg GM. Natural products as sources of new drugs over the 30 years from 1981 to 2010. *J Nat Prod* 2012;75:311–35.
- Newman DJ, Cragg GM. Natural products as sources of new drugs from 1981 to 2014. *J Nat Prod* 2016;79:629–61.
- Angerhofer CK, Guinaudeau H, Wongpanich V, Pezzuto JM, Cordell GA. Antiplasmodial and cytotoxic activity of natural bisbenzylisoquinoline alkaloids. *J Nat Prod* 1999;62:59–66.
- Klayman DL. Qinghaosu (artemisinin): an antimalarial drug from China. *Science* 1985;228: 1049–55.
- Kingston DG. Taxol, an exciting anticancer drug from *Taxus brevifolia*: an overview. In: *Human medicinal agents from plants*. ACS symposium series, ACS Publication, Washington; 1993, vol 534: 138–48 pp.
- Rashid S, Ahmad M, Zafar M, Anwar A, Sultana S, Tabassum S, et al. Ethnopharmacological evaluation and antioxidant activity of some important herbs used in traditional medicines. *J Tradit Chin Med* 2016;36:689–94.

18. Burkill HM. The useful plants of West Tropical Africa, vol 5, Families S–Z, Addenda. Kew, Richmond, United Kingdom: Royal Botanic Gardens; 1985.
19. Keay RWJ. Trees of Nigeria. New York, USA: Oxford University Press; 1989:191 p.
20. Chauhan NS, Sharma V, Dixit VK, Thakur M. A review on plants used for improvement of sexual performance and virility. *BioMed Res Int* 2014;2014:1–19.
21. Hermans M, Akoègninou A, van der Maesen J. Medicinal plants used to treat malaria in Southern Benin. *Econ Bot* 2004;58:S239–52.
22. Ajiboye TO, Nurudeen QQ, Yakubu MT. Aphrodisiac effect of aqueous root extract of *Lecaniodiscus cupanioides* in sexually impaired rats. *J Basic Clin Physiol Pharmacol* 2014;25:241–8.
23. Soladoye MO, Ikotun T, Chukwuma EC, Ariwaado JO, Ibhanesebor GA, Agbo-Adediran OA, et al. Our plants, our heritage: preliminary survey of some medicinal plant species of Southwestern University Nigeria Campus, Ogun State, Nigeria. *Ann Biol Res* 2013;4:27–34.
24. Olusola JA, Oyeleke OO. Survey and documentation of medicinal plants in Wildlife Park of Federal University of Technology, Akure, Nigeria. *Int J Life Sci Res* 2015;3:238–46.
25. Borokini TI, Clement M, Dickson NJ, Edagbo DE. Ethnobiological survey of traditional medicine practice for skin related infection in Oyo State, Nigeria. *Topclass J Herb Med* 2013;2:103–10.
26. Segun PA, Ogbole OO, Ajaiyeoba EO. Medicinal plants used in the management of cancer among the Ijebus of Southwestern Nigeria. *J Herb Med* 2018;14:68–75.
27. Lawal IO, Uzokwe NE, Igboanugo ABI, Adio AF, Awosan EA, Nwogwugwu JO, et al. Ethno medicinal information on collation and identification of some medicinal plants in Research Institutes of South-West Nigeria. *Afr J Pharm Pharmacol* 2010;4:001–7.
28. Aworinde DO, Erinoso SM. Ethnobotanical investigation of indigenous plants used in the management of some infant illnesses in Ibadan, South-Western Nigeria. *Afr J Tradit, Complementary Altern Med* 2015;12:9–16.
29. Diallo A, Traore MS, Keita SM, Balde MA, Keita A, Camara M, et al. Management of diabetes in Guinean traditional medicine: an ethnobotanical investigation in the coastal lowlands. *J Ethnopharmacol* 2012;144:353–61.
30. Yemitan OK, Adeyemi OO. CNS depressant activity of *Lecaniodiscus cupanioides*. *Fitoterapia* 2005;76:412–8.
31. Gbadamosi IT, Okolosi O. Botanical galactogogues: nutritional values and therapeutic potentials. *J Appl Biosci* 2013;61:4460–9.
32. Adeniyi A, Asase A, Ekpe PK, Asitoakor BK, Adu-Gyamfi A, Avekor PY. Ethnobotanical study of medicinal plants from Ghana; confirmation of ethnobotanical uses, and review of biological and toxicological studies on medicinal plants used in Apra Hills Sacred Grove. *J Herb Med* 2018;14:76–87.
33. Sofidiya MO, Jimoh FO, Aliero AA, Afolayan AJ, Odukoya OA, Familoni OB. Antioxidant and antibacterial properties of *Lecaniodiscus cupanioides*. *Res J Microbiol* 2008;3:91–8.
34. Ogbole OO, Segun PA, Fasinu PS. Antimicrobial and antiprotozoal activities of twenty-four Nigerian medicinal plant extracts. *South Afr J Bot* 2018;117:240–6.
35. Kafu ES, Adebisi O. Phytochemical and antibacterial activity of three medicinal plants found in Nasarawa State. *Int J Sci Res Publ* 2015;5:164–8.
36. Kazeem AA, Ashafa AOT. Evaluation of cytotoxic effects and antimicrobial activities of *Lecaniodiscus cupanioides* (Planch.) leaf extract. *Trans Roy Soc S Afr* 2017;72:33–8.
37. Oboh IE, Obasuyi O, Akerele JO. Phytochemical and comparative antibacterial studies on the crude ethanol and aqueous extracts of the leaves of *Lecaniodiscus cupanioides* Planch (Sapindaceae). *Acta Pol Pharm* 2008;65:565–9.
38. Okore VC, Ugwu CM, Oleghe PO, Akpa PA. Selective anti-candidal action of crude aqueous pod extract of *Lecaniodiscus cupanioides*: a preliminary study on *Candida albicans* obtained from an AIDS patient. *Sci Res Essays* 2007;2:043–6.

39. Ncube NS, Afolayan AJ, Okoh AI. Assessment techniques of antimicrobial properties of natural compounds of plant origin: current methods and future trends. *Afr J Biotechnol* 2008;7:1797–806.
40. Gibbons S. Anti-staphylococcal plant natural products. *Nat Prod Rep* 2004;21:263–77.
41. Nazemiyeh H, Rahman MM, Gibbons S, Nahar L, Delazar A, Ghahramani MA, et al. Assessment of the antibacterial activity of phenylethanoid glycosides from *Phlomis lanceolata* against multiple-drug-resistant strains of *Staphylococcus aureus*. *J Nat Med* 2008;62:91–5.
42. Alaoui HL, Oufdoui K, Mezrioui NE. Determination of several potential virulence factors in non-01 *Vibrio cholerae*, *Pseudomonas aeruginosa*, faecal coliforms and streptococci isolated from Marrakesh groundwater. *Water Sci Technol* 2010;61:1895–905.
43. Adeyemi OO, Yemitan OK, Adeogun OO. Analgesic activity of the aqueous root extract *Lecaniodiscus cup anioides*. *W Afr J Pharmacol Drug Res* 2004;20:10–4.
44. Nafiu MO, Abdulsalam TA, Jimoh RO, Kazeem MI. Ameliorative effect of *Lecaniodiscus cupanioides* (Sapindaceae) aqueous root extract in loperamide-induced constipated rats. *Trop J Pharmaceut Res* 2015;14:1057–62.
45. Ogbunugafor HA, Okpuzor J, Igwo-Ezike MN, Ezekwesili CN, Nebedum JO, Ekechi AC, et al. Anti-inflammatory medicinal plants: the effect of three species on serum antioxidant system and lipids levels in rats. *NISEB J* 2011;11:105–13.
46. Oladimeji-Salami JA, Akindede AJ, Adeyemi OO. Effects of ethanolic dried leaf extract of *Lecaniodiscus cupanioides* on antioxidant enzymes and biochemical parameters in rats. *J Ethnopharmacol* 2014;155:1603–8.
47. Nafiu MO, Abdulsalam TA, Akanji MA. Phytochemical analysis and antimalarial activity aqueous extract of *Lecaniodiscus cupanioides* root. *J Trop Med* 2013;2013:1–4.
48. World Health Organization. Trypanosomiasis, human African (sleeping sickness). Geneva, Switzerland: World Health Organization; 2013. factsheet 259.
49. Adesegun SA, Coker HA, Hamann MT. Antifungal triterpenoid saponins from *Lecaniodiscus cupanioides*. *Res J Phytochem* 2008;2:93–9.
50. Straadt IK, Kongstad KT, Stærk D. Identification of fungal plasma membrane H<sup>+</sup>-ATPase inhibitors in *Lecaniodiscus cupanioides* by HPLC-HRMS-SPE-NMR. In: Poster session presented at the 36th Danish NMR meeting, Lund, Sweden; 2015.
51. Ugorji OL, Okore VC. Biophysical characteristics of Clotrimazole creams formulated with saponin from seeds of *Lecaniodiscus cupanoides*. *Afr J Pharmaceut Res Dev* 2014;6:24–9.
52. Adesegun SA, Coker HAB, Hamann MT. Anti-cancerous triterpenoid saponins from *Lecaniodiscus cupanioides*. *J Nat Prod* 2014;7:155–61.
53. Ogbole OO, Segun PA, Adeniji AJ. *In vitro* cytotoxic activity of medicinal plants from Nigeria ethnomedicine on Rhabdomyosarcoma cancer cell line and HPLC analysis of active extracts. *BMC Compl Alternative Med* 2017;17:494–504.
54. Suffness M, Pezzuto JM. Assays related to cancer drug discovery. In: Hostettmann K, editor. *Methods in plant biochemistry*. London: Assays for Bioactivity, Academic Press; 1991, vol 6:71–133 pp.
55. Joshua ZP, Timothy AG. Toxicity studies of the aqueous root extract of *Lecaniodiscus cupanioides* on albino rats. *Sci World J* 2011;6:27–9.
56. Ayokun-nun AA, Adewale AR, Adekilekun A, Agbomekhe Y, Adedayo SM. Kinetics of inhibitory effect of ethyl acetate leaf fraction of *Lecaniodiscus cupanoides* on enzymes linked to carbohydrate metabolism: an *in vitro* assessment. *Adv Herb Med* 2017;3:37–51.
57. Saliu JA. Redox potential and antidiabetic properties of *Lecaniodiscus cupanioides in vitro*. *SF J Anal Biochem* 2018:1–9.
58. Nurudeen QO, Ajiboye TO. Aqueous root extract of *Lecaniodiscus cupanioides* restores the alterations in testicular parameters of sexually impaired male rats. *Asian Pac J Reprod* 2012;1:120–4.

59. Nurudeen QO, Ajiboye TO, Yakubu MT, Oweh OT, Nosarieme O. Aqueous root extract of *Lecaniodiscus cupanioides* restores nitric oxide/cyclic guanosine monophosphate pathway in sexually impaired male rats. *J Ethnopharmacol* 2015;175:181–4.
60. Muanya CA, Odukoya OA. Lipid peroxidation as index of activity in aphrodisiac herbs. *Plant Sci* 2008;3:92–8.
61. Olujobi OJ. Evaluation of the nutritive composition of five indigenous tree leaves used as vegetable in Ekiti State. *J Agric Environ Sci* 2015;4:185–97.
62. Dike MC. Proximate, phytochemical and nutrient compositions of some fruits, seeds and leaves of some plant species at Umudike, Nigeria. *ARPN J Agric Biol Sci* 2010;5:7–16.
63. Abe AI, Wakeel OK, Olapade MK. Bioassay-guided fractionation of antinociceptive effect of *Lecaniodiscus cupanioides* using mice. *Eur J Pharmaceut Med Res* 2019;6:88–95.
64. Oritsegbemi TN, Uwumarongie OH. Phytochemical and antidiarrhoeal evaluation of the hexane and methanol extracts of the leaf of *Lecaniodiscus cupanioides* Planch (Sapindaceae). *J Pharmaceut Allied Sci* 2015;12:2210–8.
65. Joseph OO, Fayomi OSI, Adenigba OA. Effect of *Lecaniodiscus cupanioides* extract in corrosion inhibition of normalized and annealed mild steels in 0.5 M HCl. *Energy Procedia* 2017;119:845–51.
66. Encarnación R, Kenne L, Samuelsson G, Sandberg F. Structural studies on some saponins from *Lecaniodiscus cupanioides*. *Phytochemistry* 1981;20:1939–42.
67. Lavaud C, Voutquenne L, Massiot G, Le Men Olivier L, Delaude C. Triterpenoid saponins from *Smelophyllum capense* (Sapindaceae). Belgium: Bulletin de la Societe Royale des Sciences de Liege; 1994, vol 63:455–63 pp.
68. Adesanya SA, Martin MT, Hill B, Dumontet V, Van Tri M, Sévenet T, et al. Rubiginoside, a farnesyl glycoside from *Lepisanthes rubiginosa*. *Phytochemistry* 1999;51:1039–41.
69. Helen IZ, Cesar AL, Gnanakaran S. Permeability barrier of gram-negative cell envelopes and approaches to bypass it. *ACS Infect Dis* 2015;11:512–22.





Emmanuel M. Halilu\*, Abdullahi M. Abdurrahman,  
Sylvester N. Mathias, Chinenye J. Ugwah-Oguejiofor,  
Muntaka Abdulrahman and Saadu Abubakar

## 2 Phytochemical and antioxidant activity of *Cadaba farinosa* Forssk stem bark extracts

**Abstract:** *Cadaba farinosa* is used in traditional medicine for treatment of cancer, diabetes, and rheumatism. The research was aimed at evaluating the phytochemical and antioxidant activity of the extracts. The powdered stem bark was extracted successively with the aid of Soxhlet extractor using n-hexane, ethyl acetate, and methanol. The resulting extracts were concentrated on rotary evaporator and the percentage yields were calculated. The phytochemical and TLC profiles of the extracts were studied. The antioxidant activity of the extracts and ascorbic acid (standard) were determined using 2, 2-diphenyl-1-picrylhydrazyl (DPPH) free radical assay. The total phenolic content of the extracts and tannic acid (standard) were evaluated using Folin–Ciocalteu reagent. The percentage yields of n-hexane, ethyl acetate, and methanol extracts were found to be 1.19, 1.37, and 13.93%, respectively. The phytochemical screening revealed the presence of tannins, flavonoids, saponins, cardiac glycosides, alkaloids, and triterpenoids. The TLC profiles of the extracts revealed the presence of compounds as evidenced from their  $R_f$  values. The total phenolic content of ethyl acetate and methanol extracts were found to be 135 and 112 mg, respectively. The free radical scavenging activity demonstrated by the extracts was comparable to ascorbic acid. The ethyl acetate extract had higher phenolic content and demonstrated the highest free radical scavenging with  $IC_{50}$  31.07 mg/mL. The results of research have provided strong preliminary evidence of antioxidant activity which may be because of phenolic compounds in the extracts.

**Keywords:** acute-toxicity; antioxidant; *Cadaba farinosa*; free-radical.

---

\*Corresponding author: Emmanuel M. Halilu, Department of Pharmacognosy and Ethnomedicine, Faculty of Pharmaceutical Sciences, Usmanu Danfodiyo University, Sokoto, Nigeria, E-mail: emshelia2002@gmail.com

Abdullahi M. Abdurrahman and Sylvester N. Mathias, Department of Pharmacognosy and Ethnomedicine, Faculty of Pharmaceutical Sciences, Usmanu Danfodiyo University, Sokoto, Nigeria

Chinenye J. Ugwah-Oguejiofor, Department of Pharmacology and Toxicology, Faculty of Pharmaceutical Sciences, Usmanu Danfodiyo University, Sokoto, Nigeria

Muntaka Abdulrahman, Department of Pharmaceutical and Medicinal Chemistry, Faculty of Pharmaceutical Sciences, Usmanu Danfodiyo University, Sokoto, Nigeria

Saadu Abubakar, Department of General Studies, College of Agriculture and Animal Science, Wurno, Sokoto, Nigeria

This article has previously been published in the journal *Physical Sciences Reviews*. Please cite as: E. M. Halilu, A. M. Abdurrahman, S. N. Mathias, C. J. Ugwah-Oguejiofor, M. Abdulrahman and S. Abubakar "Phytochemical and antioxidant activity of *Cadaba farinosa* stem bark extracts" *Physical Sciences Reviews* [Online] 2021, 7. DOI: 10.1515/psr-2020-0088 | <https://doi.org/10.1515/9783110710823-002>

## 2.1 Introduction

An antioxidant is a molecule which acts as a defense mechanism that protects against oxidative damage caused by free radicals. It prevents/retards the oxidation caused by free radicals and it is thought that, sufficient assimilation of antioxidant is supposed to protect human against diseases whose causes are linked to free radicals [1]. A free radical is any atom or molecule possessing unpaired electrons. They include: The reactive oxygen species (ROS) and reactive nitrogen species (RNS). These free radicals are produced by our body and to stabilize the body's natural function, but the excess amount could cause cell and tissue damage [2]. It can also cause oxidative damage to proteins, lipids and DNA and chronic diseases such as cancer, diabetes, aging, and other degenerative diseases in humans [3]. Antioxidant can be broadly defined as any substance that delays or inhibits oxidative damage to a target molecule [4]. The characteristic features of antioxidants are their ability to scavenge the free radicals because of their redox hydrogen donors and singlet oxygen quencher [5, 6]. Antioxidants can be natural (from plants) or synthetic. Natural antioxidants from plants include: flavonoids, tannins, carotenoids and others. Synthetic antioxidants include: Butylated hydroxyl toluene, butylated hydroxyl anisol, and tetra butyl hydroquinone. In recent past, the usage of synthetic antioxidants in foods, cosmetics, and pharmaceuticals are gradually being replaced with natural antioxidants that are considered to be safer without any side effects [7]. Today, there is renewed interest by researchers to evaluate medicinal plants for the presence of antioxidant possessing phytochemicals such as phenols, flavonoids, and tannins which have received more attention for their potential role in prevention of human diseases [8].

Medicinal plants have been used for thousands of years by the ancient civilizations for treatment of various diseases and illnesses [9, 10]. Medicinal plants contain one or more compounds in their organs that can be used for therapeutic purposes. *Cadaba farinosa* Forssk (Plate 2.1) belongs to the family Capparaceae. The plant is widely used in treatment of diabetes, cancer, inflammation and anthelmintic, and as purgative [11]. The leaves of the plant are used in traditional medicine for treatment of sores, wounds, haemorrhage, colic, conjunctivitis, stomach ache, and snake bite [12, 13]. The leaves and flower buds are considered to be purgative, antisyphilitic, anthelmintic, antiphlogistic, stimulant, antiscorbutic, purgative, urinary tract infection, hemorrhoids, and cure liver damage. The roots are burned and the ash is used to neutralize venom from snakebites. The ash is also rubbed on the skin to relieve general body pains. An infusion prepared from the roots, mixed with those of *Moringa oleifera*, is used for treatment of trypanosomiasis in animals. The leaves and roots are used in traditional veterinary medicine to treat anthrax. In Burkina Faso it is used as a cure for hemorrhagic septicemia and as appetite suppressant [14]. Previous studies on the phytochemical constituents of the aqueous leaves extract of *C. farinosa* revealed the presence of alkaloids, flavonoids, and terpenoids [15]. The toxicity profile of the aqueous stem bark extract in wistar rats revealed that acute oral administration of aqueous stem bark extract of *C. farinosa* was

safe up to 5000 mg/kg [16]. Also, the aqueous leaf extract of *C. farinosa* significantly increases the white blood cell counts (WBC) and MCHC [15]. There is a growing concern all over the world about cancer and diabetes whose causes have been linked to free radicals. Therefore, the research was aimed at evaluating the phytochemical and anti-oxidant activity of the stem bark extracts.

## 2.2 Methodology

### 2.2.1 Location, identification, collection, and preparation of plant sample

The plant is located beside the medicinal plant Garden of the Faculty of Pharmaceutical Sciences, Usmanu Danfodiyo University, Sokoto–Nigeria. The plant was identified by a Pharmacognosist at the Department of Pharmacognosy and Ethnomedicine. The voucher specimen with number PCG/UDUS/CAPP/0002 was prepared and deposited at the herbarium of the department for reference.

The stem bark of the plant was collected in January, 2018 where it was carefully removed with aid of a cutlass and dried under shade for 14 days. After which it was size reduced to moderately fine powder using wooden pestle and mortar. The powder was weighed and then stored in a plastic container for further use.

### 2.2.2 Extraction of plant material

The powdered plant sample (65 g) was extracted successively with the aid of Soxhlet extractor where it was first extracted using 1600 mL of n-hexane for 16 h with the



**Plate 2.1:** *Cadaba farinosa* in its natural habitat.

heating mantle set at 68 °C (at the boiling point of n-hexane). The extract obtained was concentrated at reduced pressure using rotary evaporator. The marc (residue) was removed, air dried and weighed, and then extracted using ethyl acetate and subjected to similar treatment as described above. The final marc obtained was extracted with methanol. The percentage yields of the successive extracts were calculated as follows:

$$\% \text{ yield} = \frac{\text{weight of Extracted sample}}{\text{weight of raw material}} \times 100$$

### 2.2.3 Preliminary phytochemical screening of the extracts of *C. farinosa*

The successive extracts were screened for the presence of alkaloids, tannins, anthraquinones, saponins, flavonoids, steroids, triterpenoids, and cardiac glycosides using the methods described by Halilu et al. [17].

### 2.2.4 Thin layer chromatographic studies

The TLC separation was carried out on a precoated silica gel 60 backed aluminum plate (F<sub>254</sub>). The separation profiles of the extracts were determined in suitable solvents systems. The n-hexane extract was resolved using solvent systems made of n-hexane/ethyl acetate (8:2, 7:3, 6:4, and 5:5) respectively. The ethyl acetate extract was resolved using solvent systems composed of n-hexane/ethyl acetate (8:2, 7:3, 6:4, and 5:5), respectively. The methanol extract was partially resolved using solvent system composed of n-hexane/methanol/ethyl acetate/water (8:1:1).

### 2.2.5 Determination of total phenolic content

The total phenolic contents of the extracts were determined by slightly modifying the method described by Wolfe et al. [18]. An aliquot of the extract (0.5 mL of 1:10 g/L) was mixed with 5 mL Folin–Ciocalteu reagent (previously diluted in water 1:10 v/v) and 4 mL (75 g/L) of sodium carbonate. The tubes were vortexed for 15 s and allowed to stand for 30 min at 40 °C for color development. The gallic acid (standard) was also prepared in similar manner as the extracts. The absorbance was measured using spectrophotometer at 765 nm.

### 2.2.6 Qualitative TLC screening of antioxidant compounds

The screening was carried out by modifying slightly the method described by Halilu et al. [17]. In this method, the spot of each extract was made with capillary tube where

three drops of the dilute solution of the extracts were spotted at the same point to form a circular spot and then allowed to dry. The freshly prepared DPPH solution was made by dissolution in methanol and was sprayed evenly on the TLC plate of each extract. The formation of yellow or white spot(s) against purple background indicates the presence of antioxidant compound(s).

### 2.2.7 Quantitative antioxidant studies

The free radical scavenging activity of the extract was assayed using DPPH free radical. The method described by Halilu et al. [17] was adopted. A solution of 0.135 mM DPPH in methanol containing 0.02–0.1 mg of the extracts was used. The reaction mixture was vortexed and kept in the dark at room temperature for 30 min. The absorbance of the reaction mixture was measured using spectrophotometer at 517 nm. Ascorbic acid was used as standard. The ability to scavenge DPPH radical was calculated as follows:

$$\text{DPPH radical scavenging activity \%} = \frac{\text{Abs control} - \text{Abs sample}}{\text{Absorbance of control}} \times 100$$

where; Abs<sub>control</sub> = Absorbance of DPPH + methanol; Abs<sub>sample</sub> = Absorbance of DPPH + sample extract.

### 2.2.8 Data analysis

The data obtained were analyzed using SPSS version 20 statistical software and Microsoft Excel 2016.

## 2.3 Results and discussion

### 2.3.1 Extraction of plant material

The mass of the successive extracts obtained and the percentage yields are presented in Table 2.1. The results indicate how much each solvent can extract soluble constituents from the powdered plant sample depending on the nature of the solvent and the nature of the phytochemicals. The result indicated that the methanol has the highest extraction capacity which is seen from Table 2.1. This observation may be attributed to the polar nature of methanol [17]. This trend continued from the moderately polar solvent (ethyl acetate) to the non polar solvent (n-hexane) as shown in Table 2.1. This observed trend is attributed to the nature of the extracting solvents. This shows that most of the components of the plant are soluble in methanol. This finding is in agreement with the results of Halilu et al. [17] which reported that different

phytochemicals have different degrees of solubility in different solvents depending on their polarity.

### 2.3.2 Preliminary phytochemical screening

The phytochemical screening revealed the presence of some plant secondary metabolites (Table 2.2). The presence of these metabolites in the plant guarantees its survival in the ecosystem. These metabolites are found to exhibit some pharmacological and toxicological effects in humans and other animals [19]. Also, according to Gnanavel et al. [19]; the most important secondary metabolites include terpenoids, phenolics, flavonoids, alkaloids, and glycosides which act as an important source for single bioactive ingredients in modern medicines and nutraceuticals. Secondary metabolites have a very good antioxidant property which can be used as an effective natural antioxidants source in nutraceuticals and modern drugs [17, 19]. The results of the phytochemical screening revealed *C. farinosa* as an excellent reservoir of phytochemicals with antioxidants; and this result agrees with the findings of Umesh et al. [20, 21].

### 2.3.3 Thin layer chromatography

TLC is rapid, efficient, reliable, and economical screening technique for the identification of unknown chemical constituents in natural drugs [22]. The results of the TLC analysis of the successive extracts (Table 2.3) revealed the presence of some chemical compounds as seen from the number of spots and the corresponding  $R_f$  values. It is clear from the result that the solvent systems used for the resolution of the ethyl acetate and methanol extracts were not suitable as the number of spots are fewer than expected. This may be due to the composition of solvent systems which could not provide the desired solubility for the relative movement of the constituents by capillary action. But in all, the result showed that *C. farinosa* contains phytochemicals which may be responsible for its antioxidant and other pharmacological properties.

**Table 2.1:** Mass and percentage yields of extracts.

Extract	Mass (g) of extract	Yield (%)
n-hexane	0.8	1.2
Ethyl acetate	0.9	1.4
Methanol	9.0	13.9

**Table 2.2:** Summary of Phytochemicals in *Cadaba farinosa* stem bark extracts.

Metabolites	Result
Saponins	+
Flavonoids	+
Tannins	+
Cardiac glycosides	+
Alkaloids	+
Triterpenoids	+
Anthraquinones	-

Key: + = Present, - = Not detected.

**Table 2.3:** TLC separation profiles of the extracts.

Extracts	Solvent system	Spot	$R_f$
n-hexane	n-hexane: EtOAc (8:2)	1	0.88
		2	0.85
		3	0.80
		4	0.76
		5	0.69
		6	0.42
		7	0.20
		8	0.14
EtOAc	n-hexane: EtOAc (2:8)	1	0.40
		2	0.10
Methanol	methanol:EtOAc:water (8:1:1)	1	0.75
		2	0.69
		3	0.64
		4	0.08

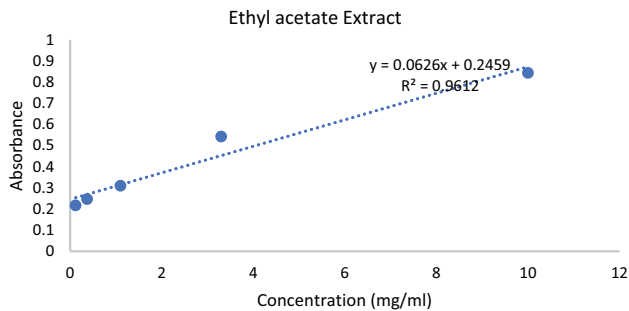
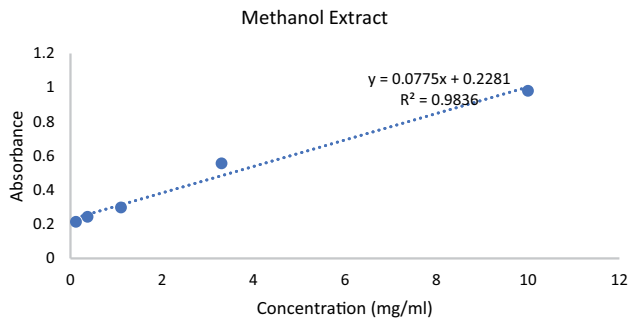
### 2.3.4 Total phenolic content

The total phenolic contents of the extracts have been expressed as gallic acid equivalent. The results are presented in Table 2.4 and Figures 2.1–2.3. The gallic acid equivalent of the ethyl acetate and methanol extracts were obtained from the calibration curve of the gallic acid (Figure 2.3). The gallic acid equivalence of ethyl acetate extract was found to be 135 mg/g while that of methanol was found to be 112 mg/g equivalence of gallic acid. This result indicates that the ethyl acetate extract had higher content phenolic compounds than methanol. This is possible because ethyl acetate is known as the best solvent for extraction of flavonoids and other related compounds [23]. Sushant et al. [24] claimed that extracts with higher phenolic and flavonoid contents could be a good source of natural antioxidants.



**Table 2.4:** Absorbance of extracts and gallic acid.

Conc. (mg/ mL)	Ethyl acetate absorbance	Methanol absorbance	Conc. gallic acid (mg/mL)	Gallic acid absorbance
0.1	0.22	0.21	0.08	0.36
0.4	0.25	0.24	0.16	0.84
1.1	0.31	0.30	0.31	2.03
3.3	0.54	0.56	0.63	3.00
10.0	0.84	0.98	1.25	3.00

**Figure 2.1:** Plot of absorbance of ethyl acetate extract against concentration.**Figure 2.2:** Plot of absorbance of methanol extract against concentration.

### 2.3.5 Qualitative and quantitative antioxidant studies

TLC silica gel layers in the form of a dot-blot test is an easy and fast test that has been developed to compare the total free radical scavenging activity of various food samples including plants [25]. Dots of extracts stained with a methanolic solution of the DPPH radical turned yellow, with a color intensity depending on the radical scavenging

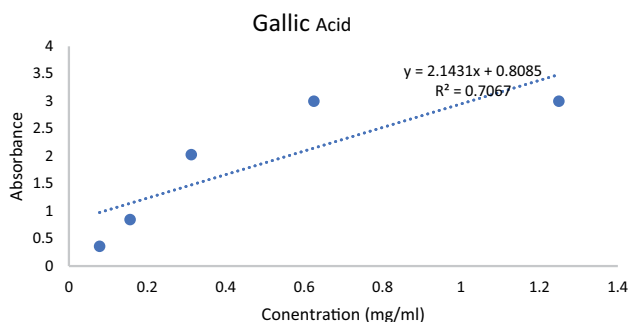


**Figure 2.3:** Calibration curve of gallic acid (standard).

capacity of compounds present in the extracts [25]. The qualitative screening of the n-hexane, ethyl acetate and methanol extracts revealed some antioxidant activity as the extracts produced yellow spots against purple background on TLC plates. The results are presented on Plates 2.2–2.4. The result showed that ethyl acetate extract had the highest antioxidant activity when compared that of n-hexane and methanol extract [17, 26, 27]. This shows that there is a direct relationship between phenolic content and antioxidant activity [24, 28]. It can be deduced that the higher the phenolic content, the higher the antioxidant activity.

To ascertain the observation from the qualitative screening, the DPPH photometric assay was conducted (Table 2.5 and Figure 2.4). The quantitative antioxidant assay of the extracts revealed different degrees of activity. The DPPH scavenging capacity of medicinal plants has been attributed to phenolics (e.g., flavonoids), terpenoids, and other phytochemicals [1, 17, 29]. The quantitative antioxidant assay of the extracts revealed different degrees of activity. The ethyl acetate showed the highest free radical scavenging activity with  $IC_{50}$  of 31.07 mg/mL. The  $IC_{50}$  of n-hexane and methanol extract could not be determined possibly because of low inhibitory activity they exhibited. This is in concordance with result obtained by Umesh et al. [20].

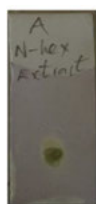


Plate 2

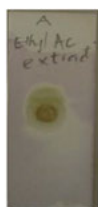


Plate 3

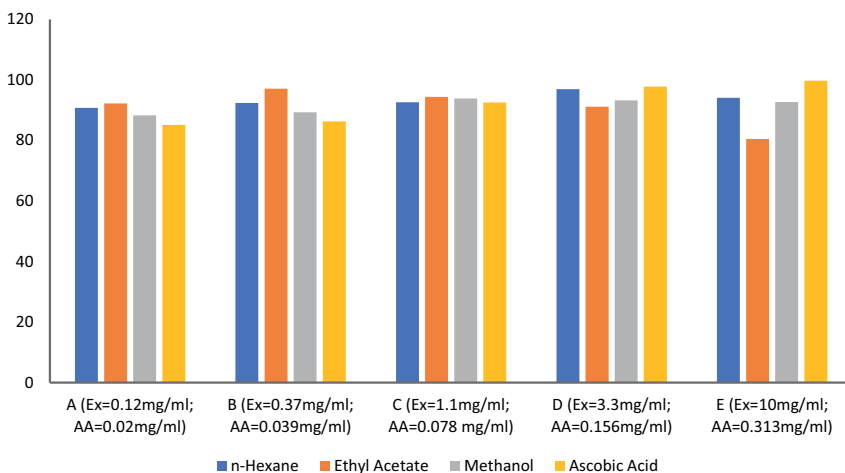


Plate 4

**Plates 2.2–2.4:** Showed the antioxidant potentials of n-hexane, ethyl acetate, and methanol extracts, respectively.

**Table 2.5:** Percentage inhibitions of the extracts and ascorbic acid.

Conc. (mg/mL)	n-hexane % inhibition	Ethyl acetate % inhibition	Methanol % inhibition	Ascorbic acid conc. (mg/mL)	% Inhibition of ascorbic acid
0.12	90.80	92.27	88.30	0.02	85.13
0.37	92.43	97.07	89.30	0.04	86.30
1.10	92.63	94.40	93.83	0.08	92.57
3.30	96.97	91.17	93.27	0.16	97.83
10.0	94.07	80.53	92.67	0.31	99.73

**Figure 2.4:** Antioxidant activity of the extracts at different concentrations compared with ascorbic acid.

## 2.4 Conclusion

The phytochemical studies on *C. farinosa* extracts revealed the presence of flavonoids and tannins. These classes of compounds are reputed for their free radical scavenging activity. The antioxidant activity demonstrated by the various extracts may be because of these phytochemicals. It can be deduced from this research that the antioxidant activity demonstrated by the extracts are directly related to their phenolic contents. The higher the phenolic content an extract contains, the higher the antioxidant activity it demonstrates. Therefore, the ethyl acetate extract exhibited higher antioxidant activity than the n-hexane and methanol extracts.

**Acknowledgements:** The authors express their sincere appreciation to Mr. Aliyu A. Garba of the laboratory of the Department of Pharmacognosy and Ethnomedicine for the assistance in running the phytochemical screening and the determination of the antioxidant activity.

**Author contributions:** All the authors have accepted responsibility for the entire content of this submitted manuscript and approved submission.

**Research funding:** None declared.

**Conflict of interest statement:** The authors declare no conflicts of interest regarding this article.

## References

1. Jayachitra A, Krithiga N. Study on the antioxidant property in selected plant extracts. *Int J Aromatic Med Plants* 2012;2:495–500.
2. Sen S, Chakaraborty R, Sridhar C, Reddy T, Biplab D. Free radicals, antioxidants, diseases and phytomedicines: current status and future prospects. *Int J Pharmaceut Sci Rev Res* 2010;3:91–100.
3. Aiyegoro OA, Okoh AI. Preliminary phytochemical screening and *in vitro* antioxidant activities of the aqueous extract of *Helichrysum longifolium* DC. *BMC Compl Alternative Med* 2010;10:10–21.
4. Yamagishi S, Matsui T. Nitric oxide, a janus faced therapeutic target for diabetic microangiopathy-friend or foe? *Pharmacol Res* 2011;64:187–94.
5. Wu YY, Li W, Xu Y, Jin EH, Tu YY. Evaluation of the antioxidant effect of four main theaflavin derivatives through chemiluminescence and DNA damage analysis. *J Zhejiang Univ Sci B* 2011;12:744–51.
6. Anokwuru CP, Esiaba I, Ajibaye O, Adesuyi AO. Polyphenolic content and antioxidant activities of *Hibiscus sabdariffa* Calyx. *Res J Med Plant* 2011;5:557–66.
7. Meenakshi S, Umayaparrathi S, Arumugan M, Balasubramanian T. *In vitro* antioxidant properties of FTIR analysis of two sea weeds of gulf of manner. *Asian Pac J Trop Biomed* 2011;1(1 Suppl): s66–70.
8. Upadhyah NK, Kumar MS, Gupta A. Antioxidant, cytoprotective and antibacterial effect of sea buckthorn (*Hippophae ramnoides* L.) leaves. *Food Chem Toxicol* 2010;48:3443–8.
9. Samuelson G, Bohlin L. *Drugs of natural origin: a treatise of pharmacognosy*, 6th ed. Stockholm, Sweden: Swedish Pharmaceutical Society, Swedish Pharmaceutical Press; 2009:17–22 pp.
10. Halilu EM, Ugwah-Oguejiofor CJ, October N, Abubakar K. Isolation of oleanolic acid from *Parinari curatellifolia* (Planch Ex. Benth) stem bark and evaluation of its anticonvulsant and sedative activities in rodents. *Trop J Nat Prod Res* 2019;3:17–21.
11. Umesh BT, Anuj M, Vaibhav U, Avinash G, Hemalatha S, Goswani DV. Hepatoprotective and Antioxidant activity of root of *Cadaba farinosa*, forsk against CCl<sub>4</sub> induced hepatotoxicity in rats. *J Pharmaceut Res* 2010;3:1–5.
12. Betti JL, Mebere YSR. An ethnobotanical study of medicinal plants used in the Kalamaloué National Park, Cameroon. *J Med Plants Res* 2011;5:1447–58.
13. Alshaimaa HA, Ali M, Souad H, Djaltou A, Mahdi J, Zemed A, et al. Medicinal plants and their uses by people in the region of Randa Djibouti. *J Ethnopharmacol* 2013;148:701–13.
14. Dramane P, Adama H, Noufou O, Samson G. Ethnobotanical study of medicinal plants used as anti-obesity remedies in the Nomad and Hunter communities of Burkina Faso. *Medicines* 2016;3:1–24.
15. Abdulrrahman AM, Aisha A, Hauwa K, Aliyu Khadijah A, Solomon MG, Anthony P, et al. Determination of haematological effects of aqueous leaf extract of *Cadaba farinosa* in adult wistar rats. *Int J Innovat Res Dev* 2019;8:245–9.
16. Solomon MG, Muhammad AA, Umar M, Musa A, Emmanuel Meshelia H, Saleh Illela A. Histological effects of aqueous stem bark extract of *Cadaba farinosa* on gastrointestinal tract of wistar rats. *Global J Med Res* 2019;19:1–8.

17. Halilu EM, Sani J, Abdullahi S, Umaru ML, Abiodun DJ. Phytochemical screening, free radical scavenging and antibacterial activity of *Cassia sieberiana* root bark extracts. *J Pharm Bioresour* 2017;14:75–82.
18. Wolfe K, Wu X, Liu RH. Antioxidant activity of apple peels. *J Agric Food Chem* 2003;51:609–14.
19. Gnanavel V, Veluchamy P, Anand PR. Phytochemical and pharmacological importance of plant secondary metabolites in modern medicine. *Bioorg Phase Nat Food Overv* 2018;13:135–56.
20. Umesh BT, Hemalatha S, Anuj M. Pharmacognostic and phytochemical investigation root of *Cadaba farinosa* forsk. *Int J Pharma Bio Sci* 2010;1:1–13.
21. Umesh BT, Vaibhav U. Phyto-pharmacological perspective of *Cadaba farinosa* forsk. *Am J Phytomed Clin Ther* 2013;1:11–22.
22. Pascual ME, Carretero ME, Slowing KV, Villar A. Simplified screening by TLC of plant drugs. *Pharmaceut Biol* 2002;40:139–43.
23. Nisha T, Leykkha S, Lee HT, Hock EK, Krishnamurthy NP, Kin WK. Extraction and recovery of phytochemical components and antioxidative properties in fruit parts of *Dacryodes rostrata* influenced by different solvents. *J Food Sci Technol* 2018;55:2523–32.
24. Sushant A, Manoj KB, Krishna D, Puspa K, Roshani G, Niranjana K. Total phenolic content, flavonoid content and antioxidant potential of wild vegetables from Western Nepal. *Plants* 2019;8:96.
25. Soler-Rivas C, Juan CE, Harry JW. An easy and fast test to compare total free radical scavenger capacity of foodstuffs. *Phytochem Anal* 2000;11:330–8.
26. Halilu ME, October N, Balogun M, Lall N, Abubakar MS. Studies of *in vitro* antioxidant and cytotoxic activities of extracts and isolated compounds from *Parinari curatellifolia* (chrysobalanaceae). *J Nat Sci Res* 2013;3:149–54.
27. Kumar S, Rajat S, Sudarshan O. Evaluation of antioxidant activity and total phenol in different varieties of *Lantana camara* leaves. *BMC Res Notes* 2014;7:560.
28. Mas AJ, Heng YK. Total phenolic content and antioxidant and antibacterial activities of *Pereskia bleo*, Hindawi. *Adv Pharmacol Sci* 2019;2019:4:7428593.
29. Giovanna P, Simonetta B. Correlations between phenolic content and antioxidant properties in twenty-four plant species of traditional ethnoveterinary use in the Mediterranean area. *Pharmaceut Biol* 2011;49:240–7.

Katso Binang and David T. Takuwa\*

### 3 Development of reverse phase-high performance liquid chromatography (RP-HPLC) method for determination of selected antihypertensive active flavonoids (rutin, myricetin, quercetin, and kaempferol) in medicinal plants found in Botswana

**Abstract:** The aim of the study was to develop a rapid, efficient, and cheap chromatographic method for determining four selected antihypertensive active flavonoid compounds in medicinal plants in Botswana. The determination of rutin, quercetin, and kaempferol in selected medicinal plants was conducted in less than 6 min using the developed reverse phase-high performance liquid chromatography (RP-HPLC) method with a 2.7  $\mu\text{m}$  Ascentis C18 express column (150  $\times$  4.60 mm i.d) at 340, 360, and 368 nm detection wavelengths and mobile phase of methanol and 0.068% of formic acid solution in isocratic elution. Validation results showed good selectivity, linearity ( $r^2 > 0.99$ ), high percentage recoveries (90.2–104.7%), and precision (% RSD < 2) for  $n = 3$ , confirming suitability of the method for determination of the investigated flavonoids in *Zingiber officinale* (ginger). Application of the developed RP-HPLC method was performed in selected medicinal plants (*Lippia javanica*) (*mosukujane*), *Myrothamnus flabellifolius* (*galalatshwene*), and *Elephantorrhiza elephantina* (*mositsana*) used to manage hypertension by herbalists in Botswana. *M. flabellifolius* a very commonly used plant for managing hypertension was found to contain highest amounts of rutin and myricetin, whereas nothing was detected for *E. elephantina*.

**Keywords:** flavonoids; hypertension; kaempferol; myricetin; quercetin; rutin.

### 3.1 Introduction

The use of traditional medicinal plants is most common in developing countries, especially in Africa where they are readily available as compared to synthesized drugs. Herbal medicine is effective, with limited side effects, and affordable than modern medicine. *Myrothamnus flabellifolius* and *Lippia javanica* are widely spread medicinal

---

\*Corresponding author: David T. Takuwa, Department of Chemistry, University of Botswana, Private Bag UB 00704, Gaborone, Botswana, E-mail: takuwadt@ub.ac.bw

Katso Binang, Department of Chemistry, University of Botswana, Private Bag UB 00704, Gaborone, Botswana

This article has previously been published in the journal Physical Sciences Reviews. Please cite as: K. Binang and D. T. Takuwa "Development of reverse phase-high performance liquid chromatography (RP-HPLC) method for determination of selected antihypertensive active flavonoids in medicinal plants found in Botswana" *Physical Sciences Reviews* [Online] 2021, 7. DOI: 10.1515/psr-2020-0209 | <https://doi.org/10.1515/9783110710823-003>

plants known to exist in southern part of Africa, including Botswana [1]. These medicinal plants are aromatic bush plants commonly used as herbal tea to treat coughs, asthma attack, scratches, muscle pains, insect bites, and skin disorders such as skin rash [2–4] stroke, shingles, diabetes mellitus, and hypertension [5]. Phytochemical studies have shown that *M. flabellifolius* contains flavonoids, anthocyanins, alkaloids, steroids, terpenoids, triterpenes, cardiac glycosides, saponins, phlobatanins, and tannins [6]. Different scientific studies have revealed that *L. javanica* constitute phytochemicals in substantial levels such as flavonoids, alkaloids, amino acids, phenolic acids, and saponins [7].

*Elephantorrhiza elephantina* commonly known as the “elephant root” [8], is a multipurpose medicinal plant that is also found in Botswana. The plant is well known for treatment of various cardiovascular ailments such as hypertension, diabetes mellitus, and stomach disorder [9, 10]. In addition, *E. elephantina* displayed very promising ethnomedicinal and biological activities such as antioxidant, antidiabetic, and other important immunological activities, which include antibacterial, antifungal, anti-inflammatory, antimutagenic, antiplasmodial, and antibabesial [11]. The phytochemical study of this plant produced more than 20 compounds from its dried rhizome and root extracts that included flavonoids such as epigallocatechin gallate (EGCg), epicatechin (EC), quercetin, epicatechin gallate (ECg), kaempferol, and their polymeric derivatives [11]. *Zingiber officinale* (ginger) is also widely known for reducing effects of hypertension [12]. *Z. officinale* is an underground rhizome commonly known as ginger, belonging to the family, *Zingiberaceae* [13]. Studies on phytochemical analysis of this plant have shown that it contains over 400 different compounds with gingerols identified as major active group [14]. The compounds isolated from this plant include terpenoids, triterpenoids, glycosides, phenolic compounds, and flavonoids [15]. The identified compounds are associated with pharmacological activities that include antibacterial, antidiabetic, antimalarial, antimicrobial, and antioxidant [16]. In this study, the above four plants were selected for screening of selected compounds that are known to display antidiabetic properties using the reverse phase-high performance liquid chromatography (RP-HPLC) method developed.

To determine the above plants for antidiabetic activities, their extracts were subjected to Angiotensin converting enzyme (ACE) inhibition activity. According to Shafaei et al. [17], ACE inhibitors suppress production of angiotensin II enzyme of which when allowed to enter the body stream, it will cause blood vessels to become narrower raising blood pressure, hence ACE inhibition has become a significant control measure for hypertension. In earlier investigations, flavonoid compounds have been identified as potential *in-vitro* ACE inhibitors [17, 18] through generation of chelate complexes with the active center of ACE [19]. Flavonoids are a group of polyphenol compounds widely distributed throughout the plant kingdom. These are categorized, according to their chemical structure; into flavonols, flavones, flavonones, isoflavones, catechins, anthocyanins, and chalcones [20]. They have a wide spectrum of pharmacological properties with confirmed health beneficial effects in hypertension and other cardiovascular

diseases such as stroke, heart attack, and diabetes. Scientific studies has revealed that the most active flavonoids (having ACE inhibitory activity of above 30%) are luteolin > rutin > rhoifolin > quercetin > kaempferol > apigenin > diosmetin > narigenin K > epicatechin > genistein > hesperetin and diosmin in their decreasing order [19]. Based on availability of compounds in our laboratory and limited funds to purchase more flavonoids; myricetin, rutin, quercetin, kaempferol were selected for development of RP-HPLC method and subsequent application to above medicinal plants found in Botswana (*L. javanica*) (*mosukujane*), *M. flabellious* (*galalatshwene*), and *E. elephantina* (*mositsana*) and *Z. officinale*. Apigenin was used as an internal standard (IS). Different scientific studies have demonstrated that quercetin, rutin, myricetin, and kaempferol are part of flavonoid compounds obtainable from plant extracts that can be used as potential natural ACE inhibitors for managing hypertension, which could make it possible for medicinal plants containing these flavonoids to be used as alternative medicine for managing hypertension [21–28]. As such, our selection of flavonoids to be used in our study was largely guided by the antihypertensive activities of rutin, myricetin, quercetin, and kaempferol.

## 3.2 Experimental

### 3.2.1 Instruments and apparatus

Agilent 1260 infinity series Agilent technologies (Waldbronn, Germany) assembled with ultraviolet diode array detector (UV DAD) 1260 series was used for HPLC analysis.

### 3.2.2 Chemicals and reagents

The HPLC grade methanol, formic acid and flavonoid standards (>98% HPLC grade): rutin, myricetin, quercetin, kaempferol, and apigenin were purchased from Sigma Aldrich (Steinheim, Germany). Deionized water used was purified with a Milli-Q system purchased from Millipore (Bedford, USA).

### 3.2.3 Preparation of flavonoid standards

The flavonoids standards (rutin, myricetin, quercetin, and kaempferol) were each weighed accurately to 0.005 g and dissolved in 2 ml of methanol. The solution was transferred into 10.0 ml volumetric flask and filled to the mark with (60:40 v/v) of methanol to water to make a stock solution of 50 ppm. The stock solution was filtered using 0.45 µm membrane filter to remove any solid particles and stored at 4 °C in the dark for further analysis. The



solvents used for standard solutions were HPLC grade (>99%) methanol and deionized water that was degassed and filtered using vacuum in a Millipore filter.

### 3.2.4 Preparation of medicinal plant samples

Fresh plant materials were harvested from parent trees in Moshupa Village, west of the capital city Gaborone in Botswana. Ginger was bought from local supermarkets in Gaborone. The part of the medicinal plant collected was rinsed with deionized water to remove soil and dust, air dried, ground, and sieved through 500  $\mu\text{m}$  sieves and approximately weighed to 100.0 g and stored as a representative sample. For each plant sample, 0.0250 g of the plant powder was accurately weighed and prewashed with hexane, filtered and dried, then added to 5 ml methanol in ultrasonicator bath for 15 min. The extract of each part of the plant was kept and used for determination with the developed RP-HPLC method.

### 3.2.5 HPLC-DAD-UV-Vis separation of flavonoid standards

The chromatographic separation of the flavonoid standards was performed using Agilent 1260 infinity series coupled with DAD-UV-Vis. The column used for separation of the standards was a 2.7  $\mu\text{m}$  C18 Ascentis express column (150  $\times$  4.60 mm i.d) maintained at 35  $^{\circ}\text{C}$  column temperature. Chromatographic conditions were optimized to obtain baseline resolution of the flavonoid standards. The mobile phase composition of formic acid and methanol was varied with the aim of getting optimum baseline resolution of the standards. At a volume of 20  $\mu\text{L}$  the standards were injected manually using a syringe and this procedure was repeated in triplicates. The retention times and peak areas of the injected standards were computed using Agilent 3D ChemStation.

### 3.2.6 Statistical analysis

All standard peak areas and retention times were calculated in triplicate and presented as means  $\pm$  Standard deviation (SD). Analysis of variation (ANOVA) was used to determine the differences between standard means and considered significant if  $P < 0.05$ .

## 3.3 Results and discussion

### 3.3.1 Development of RP-HPLC method

The methanolic flavonoid standards were scanned through 300–500 nm wavelength range. The maximum absorbance for the flavonoid were observed at 371.21, 374.21,

357.05, 368.90, and 336.08 nm wavelengths for quercetin, myricetin, rutin, kaempferol, and apigenin, respectively. The values obtained were used as a guide in setting the parameters of UV–Vis detector in HPLC instrument ranging from 350–380 nm. In a study by Arora and Itanker [29], it was established that in UV spectral analysis of flavonoids, there were two bands identified; band A, which lies in the 350–385 nm range for flavanols (kaempferol, quercetin, myricetin, and rutin) and for apigenin which is a flavone, whose absorption band was between 310 and 350 nm. In band B, it was found that in the 250–290 nm range, the behavior for all the above flavonoid subgroups was similar. In analyzing the UV spectra for band B for the four standards, it was observed that they were all within the ranges 310–385 nm, which was in agreement with results obtained by Arora and Itanker [29]. HPLC determination of the compounds was carried out using UV–VIS-DAD detector, and maximum wavelength absorption peak for each compound was also set and used for the respective determination of the analyte, which further increased the sensitivity and limit of detection (LOD) of analytes under consideration.

In developing a chromatographic system for eluting and resolving rutin, myricetin, quercetin, kaempferol, and apigenin, various chromatographic parameters such as organic content of mobile phase, flow rate, ratio of aqueous, and organic phase were evaluated to obtain the shortest overall run time, symmetrical peak shapes, baseline resolution, selectivity, and high number of chromatographic plates (good efficiency). The optimal baseline resolution was obtained with an isocratic elution at a flow rate of 0.85 ml/min and total analysis time of 6 min, using a composition of 40% of 0.068% formic acid solution and 60% methanol (v/v), Figure 3.1. The specific retention times for both the calibration and IS were; rutin (RT 2.09 min), myricetin (RT 2.48 min), quercetin (RT 3.41 min), kaempferol (RT 4.96 min), and IS – Apigenin (RT 5.38 min), all eluting under 6 min, Figure 3.1. It was further observed that the chromatographic method

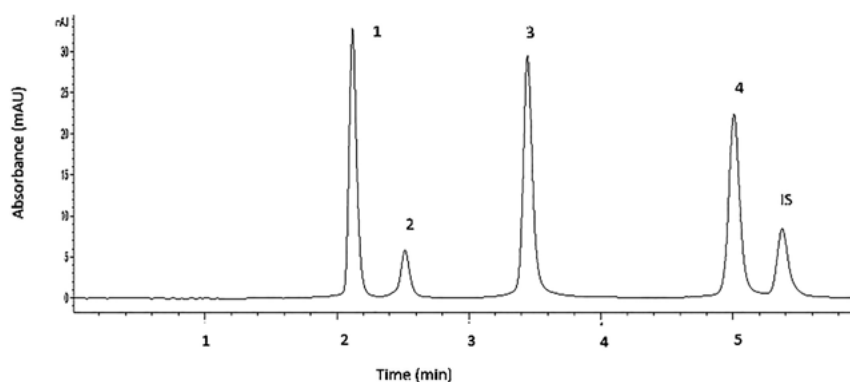


**Figure 3.1:** RP-HPLC chromatogram for determination of flavonoid standards: (1-rutin, 2-myricetin, 3-quercetin, 4-kaempferol, and IS-apigenin) using Ascentis Express C18 column, flow rate 0.85 ml/min and 0.068% formic acid solution and 60% methanol (v/v) as mobile phase.

developed was more rapid than those conducted in earlier studies. According to Kumar et al. [30], optimal resolution was obtained using a mobile phase consisting of water (solvent A)/acetonitrile with 0.02% trifluoroacetic acid (solvent B) in gradient elution, where 10 phenolic compounds were resolved, inclusive of the five flavonoids in this study; rutin (RT: 6.94 min), quercitrin (RT: 9.68 min), myricetin (RT: 11.40 min), quercetin (RT: 13.85 min), apigenin (RT: 15.53 min), and kaempferol (RT: 15.97 min). Ghasemzadeh et al. [6] and Olszewska [31] also obtained resolution of the same compounds with a total run time much higher than those obtained in this study.

### 3.3.2 Fitness for purpose

The figures of merit were determined for the RP-HPLC method developed and performance parameters validated according to International Conference on Harmonization (ICH) and Food and Drug Administration (FDA) guidelines shown in Table 3.1. In general, all parameters were satisfactory as per guidelines from ICH and FDA, show in Table 3.1. The linearity between peak ratio and concentration were validated with calibration curves obtained with standard solutions at six concentrations of each standard (Table 3.2). Satisfactory linearity ( $r^2 > 0.99$ ) was obtained for all compounds leading to acceptance of method as per guideline of FDA, Table 3.1. In previous studies, it has been shown that it is possible to obtain linearity of  $r^2 > 0.99$  for methods used to determine the above flavonoids in flowers [30], different plant extracts [31], different plant parts of *Sonchus arvensis* [32] and *Moringa oleifera* leaves [33]. The sensitivity of the method developed, with the experimental conditions described was demonstrated with LOD

**Table 3.1:** Validation parameters and the acceptance criteria according to the International Conference on Harmonization and Food and Drug Administration.

Validation parameter	Acceptance criteria	Validation guideline
Precision	<2% RSD	International Conference on Harmonization (ICH)
Repeatability		
Linearity	<0.999 (80–120% range of target concentration)	Food and Drug Administration (FDA)
Accuracy	80–120%	Food and Drug Administration (FDA)
<b>System suitability</b>		
Retention time	<1% RSD	International Conference on Harmonization (ICH)
Tailing time	Tf < 2.0	
Resolution	Rs > 2	
Theoretical plates	N > 2000	

**Table 3.2:** Data for calibration graphs, limit of detection, and limit of quantification for the four flavonoid standards in *Zingiber officinale*.

Standard	LOD	LOQ	Concentration range ( $\mu\text{g/ml}$ )	Coefficient	Equation
Rutin	0.51	1.55	2.00–12.00	0.9995	$y = 0.1376x + 0.906$
Myricetin	0.76	2.29	2.00–12.00	0.9998	$y = 0.0409x + 0.06$
Quercetin	0.57	1.72	2.00–12.00	0.999	$y = 0.1165x + 0.816$
Kaempferol	0.75	2.27	2.00–12.00	0.9991	$y = 0.1074 + 1.966$

and Limit of quantification (LOQ) determination (Table 3.2). To calculate LOD and LOQ of the four standards, the slope of the calibration curve as obtained from linear regression was used together with SD of the  $y$ -intercept ( $\delta$ ) using expression  $3\delta/S$  and  $10\delta/S$  to calculate LOD and LOQ, respectively. LOD was in the range 0.51–0.76 and LOQ ranging from 1.55 to 2.29 for the four flavonoids; rutin, myricetin, quercetin, and kaempferol, Table 3.2. The LOD and LOQ obtained in this study were much higher than those obtained for the same flavonoids when determined in leaves, stem and roots of *S. arvensis* [32]. However, the LOD and LOQ were comparable for methods developed for the determination of the flavonoids in several plants [30, 31]. The results for LOD and LOQ of compounds in this study were satisfactory as demonstrated by identification of full baseline resolved peak, making it possible for integration to be conducted on the peaks of the selected flavonoids.

Accuracy of the method was tested by recovery studies using the standard addition method. The overall recovery percentages for all the compounds were in the range 89–104% with relative standard deviation (RSD) less than 2% as shown in Table 3.3. The RSD values obtained for these compounds were within the guidelines outlined in

**Table 3.3:** Recovery studies for rutin, myricetin, quercetin, and kaempferol from *Zingiber officinale*.

	Standard added ( $\mu\text{g/ml}$ )	Recovery- (%)	RSD (%)
Rutin	12	$84.2 \pm 0.3$	0.3
	10	$100.9 \pm 1.3$	1.3
	8	$104.5 \pm 0.3$	0.3
Myricetin	12	$83.1 \pm 0.6$	0.1
	10	$102.7 \pm 1.5$	1.4
	8	$99.9 \pm 0.9$	0.9
Quercetin	12	$89.8 \pm 0.3$	0.4
	10	$83.1 \pm 0.1$	0.1
	8	$97.6 \pm 0.4$	0.4
Kaempferol	12	$107.3 \pm 1.6$	1.5
	10	$105.7 \pm 0.1$	0.1
	8	$101.0 \pm 0.3$	0.3

Table 3.1, qualifying the developed method fit for the intended purpose. The precision was expressed as RSD and according to the results displayed % RSD was less than 2% for both repeatability and intermediate precision, being in the range of 0.08–1.53% which demonstrated acceptable precision for the proposed method as according to ICH validation guidelines by comparing Tables 3.1 and 3.4. The results obtained in this study are in agreement with previous studies indicating possibilities of developing a precise and accurate method for determination of these flavonoids in plants using RP-HPLC [30, 32, 33].

In summary, all the figures of merit for fitness of intended purpose of the developed RP-HPLC method were satisfactory, which qualified this method to be reliably used in the determination of the selected flavonoids in medicinal plants.

### 3.3.3 Application of the optimized method on the selected medicinal plants

Identification of the flavonoid compounds in the selected medicinal plants was achieved by spiking and matching the retention times of the compounds with those of the working standards. Figure 3.2 a–d below show chromatogram peaks of flavonoids in the plant samples using the RP-HPLC method developed. In general, it was observed that quercetin and kaempferol were not detected in all the medicinal plants selected for this study. In previous studies, quercetin has been found to be highest flavonoid compared

**Table 3.4:** Retention times and %RSD values indicating repeatability and intermediate precision of the flavonoid compounds in *Zingiber officinale*.

Compound	Repeatability	
	Retention time (min) ± STDEV (n = 6)	RSD (%)
Rutin	2.09 ± 0.01	0.51
Myricetin	2.48 ± 0.03	1.03
Quercetin	3.40 ± 0.04	1.09
Kaempferol	4.94 ± 0.03	0.66
Apigenin (IS)	5.27 ± 0.06	1.09
Compound	Intermediate precision	
	Retention time (min) ± STDEV (n = 6)	RSD (%)
Rutin	2.08 ± 0.02	1.14
Myricetin	2.48 ± 0.04	1.59
Quercetin	3.37 ± 0.05	1.35
Kaempferol	4.93 ± 0.05	0.91
Apigenin(IS)	5.30 ± 0.08	1.48

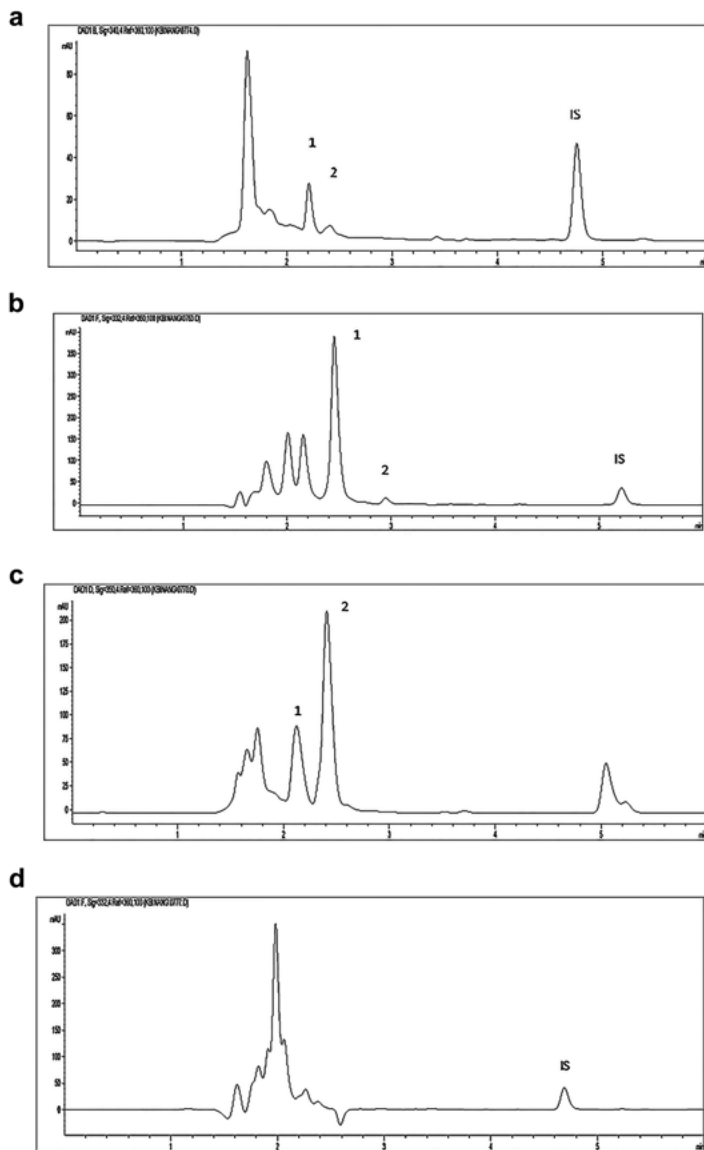


**Figure 3.2:** (a) Chromatogram peaks of *Zingiber officinale* extract indicating presence of (1) rutin and (2) myricetin as determined using the developed RP-HPLC method. (b) Chromatogram peaks of *Myrothamnus flabellios* extract indicating presence of (1) rutin and (2) myricetin as determined using the developed RP-HPLC method. (c) Chromatogram peaks of *Lippia javanica* indicating presence of (1) rutin and (2) myricetin as determined using the developed RP-HPLC method. (d) Chromatogram peaks of *Elephantorrhiza elephantina* extract indicating no detection of the flavonoids determined using the developed RP-HPLC method.

to myricetin and kaempferol; onions (quercetin 1.497 mg/g and kaempferol 0.832 mg/g) in onion leaves [34] and in berries (quercetin 1.58 mg/g) [35]. However, in the same study of berries [35], kaempferol was obtained from only two out of 25 berries studied. In another study, Yang et al. [36] concluded that kaempferol and quercetin were predominately found in cruciferous plants, when determining flavonoids in 91 edible plant species. For *E. elephantina* both quercetin and kaempferol were obtained in earlier study and their absence in this study could be attributed to use of different method of extraction of the flavonoids in plants [11]. Surprisingly, none of the flavonoids in this study was obtained in *E. elephantina*. In previous studies, several flavonoids such as kaempferol, quercetin, dihydroxy kaempferol, ethyl  $\beta$ -D galactopyranoside, quercetin - 3 - O -  $\beta$  - D - glucoside, trans - 3 - O - galloyl - 3,3',5,5',7 - pentahydroxyflavan and taxifolin - 3' - O - glucoside and (+) - catechin, ethyl gallate, and methyl gallate were obtained in *E. elephantina* [11, 37]. The strongest peak at retention time of 2 min in *E. elephantina* could not be elucidated since the study involved the use of only four flavonoids, and that peak could possibly be one of any of the flavonoids mentioned above.

Rutin and myricetin were obtained in varying quantities in the other three plants studied, with exception of *E. elephantina*. The actual amounts of each identified flavonoids are shown in Table 3.5. *M. flabellios* had the most content of rutin (24.43 mg/g) and myricetin (574.19 mg/g) as compared to the other plants, followed by *L.javanica* and *Z. officinale* (Table 3.5). In previous studies involving 91 edible plant species, myricetin was not obtained in all the plant species [36], as well as in not being found in *M. oleifera* leaves [33]. When determining myricetin in 10 herbal plants, it was found in only one plant out of the 10 studied [38]. In studies where myricetin was obtained, it was found in trace quantities [30, 32, 34, 35], making *M. flabellios* to be a very rich source of this flavonoid. According to information obtained from local herbalists, *M. flabellios* is the most common and preferred plant used in the management of hypertension and as such, high rutin and myricetin values in this plant tend to support that practice. There are other various numerous flavonoid compounds that have been identified in *M. flabellios* from other studies which included naringenin, quercetin (Quercetin-3-O-glucuronide, quercetin-7-O-glucuronide, galloyl quercetin-3-O-rhamnoside), epicatechin, epigallocatechin, including their 3-O-galloylated analogs

**Table 3.5:** Quantitative determination of detected flavonoid compounds in study plants.

	Rutin (mg/g)	Myricetin (mg/g)	Quercetin (mg/g)	Kaempferol (mg/g)
<i>Myrothamnus flabellios</i>	24.43	574.18	nd	nd
<i>Lippia javanica</i>	6.52	246.76	nd	nd
<i>Zingiber officinale</i>	1.77	10.52	nd	nd
<i>Elephantorrhiza elephantina</i>	nd	nd	nd	nd

All analyzes are the mean of triplicate measurements  $\pm$  standard deviation; Results expressed in mg/g dry weight; nd: not detected.

[1, 6, 25]. Those findings further indicate that *M. flabellious* has the potential to manage hypertension based on the antihypertensive phytochemical compounds that it possesses. In Botswana, *M. flabellious* and *L. javanica* are also used as preferred herbal teas for medicinal benefits, which are also supported by the respective high values of rutin and myricetin obtained in this study. The myricetin obtain in *M. flabellious* and *L. javanica* was not surprising since previous study has noted that this compound is a naturally occurring flavonoid with antidiabetic and hypoglycemic pharmacological properties in teas, berries, fruits, vegetables, and medicinal herbs [39]. In regards *Z. officinale* rhizomes, only rutin and myricetin were detected in much lower quantities than those obtained from *M. flabellious* and *L. javanica* (Figure 3.2 a and Table 3.5). In an earlier study where carbon dioxide was used to extract flavonoids that included rutin, quercetin, and kaempferol from *Z. officinale* leaves and rhizomes, all the three (rutin, quercetin, and kaempferol) were obtained [6]. However, the amount of the flavonoids extracted depended on the age of *Z. officinale* plant and extraction method [6], which could partly explain why the same compounds may not have been obtained in our study. It should be noted that currently there is no standardized method of extraction for flavonoids in medicinal plants for HPLC determination, hence different observations shall be obtained by different researchers for both qualitative and quantitative analyses of the same compounds in the same species of the medicinal plants. In most cases, extraction of flavonoids from medicinal plants and any analysis being performed is through modification of the general procedure that is commonly used. In the absence of standardized methods of extractions of flavonoid in medicinal plants, the different chemicals used would most likely extract different compounds at different percentage yield of flavonoids in the same plants using the same analytical methods. Even though analyte recovery could be used to develop reliable extraction methods of flavonoids, limitations in availability of certified reference materials for flavonoids in plant sample still remains a challenge to successfully develop extraction method that could possible lead to standardized extraction methods of flavonoids in medicinal plants.

### 3.4 Conclusion

The developed RP-HPLC in this study has secured a validated a method fit for the purpose for determination of rutin, myricetin, quercetin, and kaempferol in medicinal plants within a relatively short analysis time, than most of the previous studies. The shorter analysis time has advantage of using fewer chemicals in the mobile phase; hence reduction in hazardous waste to the environment and reducing costs since fewer chemicals will be used per analysis. In addition, time shall be saved with sample high throughput within a given time, making this method more efficient. The analytical method established from the study can be used as a quick screen to pave way for further research on plants identified as potential health alternatives for treating hypertension



and other chronic diseases. According to the phytochemical results of antihypertensive compounds in the selected plants; *Z. officinale*, *M. flabelliosus* (*galalatschwene*), *L. Javanica* (*mosukujane*), and *E. elephantina* (*mositsana*), it is promising that the plant kingdom has potential to provision of flavonoids for hypertension alleviation. With increased interests from pharmaceutical industries the scale up to industrial applications still needs to be explored and optimized for sustainable utilization and exploitation of medicinal plants and cytotoxicity studies conducted on a variety of medicinal plants for possible human consumption. In this study, using the results obtained, *M. flabelliosus* can be selected as medicinal plant of interest for further analysis to confirm its antihypertensive property to be used as an alternative medicine to manage hypertension. The results obtained are also in support of observation from traditional herbalists that, *M. flabelliosus* has a potential to use in the management of hypertension, which shall have a large bearing in rural areas where conventional medication for hypertension is limited in Botswana.

**Author contributions:** All the authors have accepted responsibility for the entire content of this submitted manuscript and approved submission.

**Conflict of interest statement:** The authors declare no conflicts of interest regarding this article.

## References

1. Quiñones M, Sánchez D, Mugerza B, Miguel M, Aleixandre A. Mechanisms for antihypertensive effect of CoccoanOX, a polyphenol-rich cocoa powder, in spontaneously hypertensive rats. *Food Res Int* 2011;5:1203–8.
2. Motlhanka DM, Mathapa G. Antioxidant activities of crude extracts from medicinal plants used by diabetic patients in Eastern Botswana. *J Med Plants Res* 2012;6:5460–3.
3. Kumar Gupta S, Sharma A. Medicinal properties of *Zingiber officinale* Roscoe—a review. *J Pharm Biol Sci* 2014;9:124–9.
4. Cheikhoussef A, Summers RW, Kahaka G. Qualitative and quantitative analysis of phytochemical compounds in Namibian *Myrothamnus flabellifolius*. *Int Sci Technol J Namibia* 2015;5:71–83.
5. Ho SC, Su MS. Optimized heat treatment enhances the anti-inflammatory capacity of ginger. *Int J Food Prop* 2015;19:1884–98.
6. Ghasemzadeh A, Jaafar HZ, Rahmat A. Elevated carbon dioxide increases contents of flavonoids and phenolic compounds, and antioxidant activities in Malaysian young ginger (*Zingiber officinale* Roscoe.) varieties. *Molecules* 2010;15:7907–22.
7. Anjarwalla P, Ofori DA, Stevenson PC. Pesticidal plant leaflet. Kenya: World Forestry Centre; 2011: 2–4 pp.
8. Anwar MA, Al Disi SS, Eid AH. Anti-hypertensive herbs and their mechanisms of action: part II. *Front Pharmacol* 2016;6:1–24.
9. Kwape TE, Majinda RRT, Chaturvedi P, Kwape TE, Majinda RRT, Chaturvedi P. Antioxidant and antidiabetic potential of *Myrothamnus flabellifolius* found in Botswana. *Cogent Biol* 2016;2:1–10.
10. Arika WM, Ogola PE, Abdirahman YA, Mawia AM, Wambua FK, Nyamai DW, et al. In vivo safety of aqueous leaf extract of *Lippia javanica* in mice models. *Biochem Physiol Open Access* 2016;1:1–9.

11. Maaliki D, Shaito AA, Pintus G, El-Yazbi A, Eid AH. Flavonoids in hypertension: a brief review of the underlying mechanisms. *Curr Opin Pharmacol* 2019;45:57–65.
12. Setshogo MB, Mberekhi C. Loristic diversity and uses of medicinal plants sold by street vendors in Gaborone, Botswana. *Afr J Plant Sci Biotechnol* 2011;5:69–74.
13. Adhami S, Siraj S, Farooqi H. Unexplored medicinal plants of potential therapeutic importance : a review. *Trop J Nat Prod Res* 2018;2:3–11.
14. Ojulari LS, Olatubosun OT, Okesina KB, Owoyele BV. The effect of *Zingiber officinale* (ginger) extract on blood pressure and heart rate in healthy humans. *J Dent Med Sci* 2014;13:73–6.
15. Maroyi A. Elephantorrhiza elephantina: traditional uses, phytochemistry, and pharmacology of an important medicinal plant species in Southern Africa. *Evid base Compl Alternative Med* 2017;11–12:1–18.
16. Alaba AE, Olaokun OO. Preliminary screening of leaf extracts of *Elephantorrhiza elephantina* for phytochemicals and antioxidant activity. *South Afr J Bot* 2018;115:315–25.
17. Hettihewa SK, Hemar Y, Vasantha Rupasinghe HP. Flavonoid-rich extract of *actinidia macrosperma* (a wild kiwifruit) inhibits angiotensin-converting enzyme in vitro. *Foods* 2018;7:1–9.
18. Guerrero L, Castillo J, Quiñones M, García-Vallvé S, Arola L, Pujadas G, et al. Inhibition of angiotensin-converting enzyme activity by flavonoids: structure-activity relationship studies. *PLoS One* 2012;7: e49493.
19. Mazid M, Khan TA, Mohammad F. Role of secondary metabolites in defense mechanisms of plants. *Biol Med* 2011;3:232–49.
20. de Wet H, Ramulondi M, Ngcobo ZN. The use of indigenous medicine for the treatment of hypertension by a rural community in northern Maputaland, South Africa. *South Afr J Bot* 2016;103: 78–88.
21. Loizzo MR, Said A, Tundis R, Rashed K, Statti GA, Hufner A, et al. Inhibition of angiotensin converting enzyme (ACE) by flavonoids isolated from *Ailanthus excels* (Roxb) (Simaroubaceae). *Phytother Res* 2007;21:32–6.
22. Patil S, Rao N, Somaskhekarappa H, Rajashekhar K. Antigenotoxic potential of Rutin and Quercetin in swiss mice exposed to gamma radiation. *Biomed J* 2014;37:305–13.
23. Niture N, Ansari A, Naik S. Anti-hyperglycemic activity of rutin in streptozotocin-induced diabetic rats: an effect mediated through cytokines, antioxidants and lipid biomarkers. *Indian J Exp Biol* 2014;52:720–7.
24. Bennett CJ, Jung SK, Lee KW, Lee HJ. Potential therapeutic antioxidants that combine the radical scavenging ability of myricetin and the lipophilic chain of vitamin E to effectively inhibit microsomal lipid peroxidation. *Bioorg Med Chem* 2004;8:2079–98.
25. Mendes-Junior L, Montero M, Carvalho Ados S, Quiroz T, Braga VA. Oral supplementation with the rutin improves cardiovascular baroreflex sensitivity and vascular reactivity in hypertensive rats. *Appl Physiol Nutr Metabol* 2013;38:305–13.
26. Grochowski DM, Locatelli M, Granica S, Cacciagrano F, Tomczyk M. A review on the dietary flavonoid tilirosin. *Compr Rev Food Sci Food Saf* 2018;17:1395–421.
27. Gasparotto A, Gasparotto FM, Lourenço ELB, Crestani S, Stefanello MEA, Salvador MJ, et al. Antihypertensive effects of isoquercitrin and extracts from *Tropaeolum majus* L.: evidence for the inhibition of angiotensin converting enzyme. *J Ethnopharmacol* 2011;134:363–72.
28. Arora S, Itankar P. Extraction, isolation and identification of flavonoid from *Chenopodium album* aerial parts. *J Tradit Complementary Med* 2018;8:476–82.
29. Kumar N, Bhandari P, Singh B, Gupta AP, Kaul VK. Reversed phase-HPLC for rapid determination of polyphenols in flowers of rose species. *J Separ Sci* 2008;31:262–7.
30. Olszewska MA. New validated high-performance liquid chromatographic method for simultaneous analysis of ten flavonoid aglycones in plant extracts using a C18 fused-core column and acetonitrile-tetrahydrofuran gradient. *J Separ Sci* 2012;35:2174–83.

31. Khuluk RH, Yunita A, Rohaeti E, Syafitri UD, Linda R, Lim LW, et al. An HPLC – DAD method to quantify flavonoids in *Sonchus arvensis* and able to classify the plant parts and their geographical area through principal component analysis. *Separations* 2021;8:1–10.
32. Shervington LA, Li BS, Shervington AA, Alpan N, Patel R, Muttakin U, et al. A comparative HPLC analysis of myricetin, quercetin and kaempferol flavonoids isolated from Gambian and Indian *Moringa oleifera* leaves. *Int J Chem* 2018;10:28–37.
33. Miean KH, Mohamed S. Flavonoid (myricetin, quercetin, kaempferol, Luteolin and apigenin) content of edible tropical plants. *J Agric Food Chem* 2018;49:3106–12.
34. Hakkinen SH, Karenlampi SO, Heinonen IM, Mykkanen HM, Torrenen AR. Content of the flavonols quercetin, myricetin, and kaempferol in 25 edible berries. *J Agric Food Chem* 1999;47:2274–9.
35. Yang RY, Lin S, Kuo G. Content and distribution of flavonoids among 91 edible plants species. *Asia Pac J Clin Nutr* 2008;17:275–9.
36. Veloso CC, Soares GL, Perez AC, Rodrigues VG, Silva FC. Pharmacological potential of maytenus species and isolated constituents, especially tingenone, for treatment of painful inflammatory diseases. *Sociedade Brasileira de Farmacognosia* 2017;27:533–40.
37. Kulevanova S, Stefova M, Panovska TK, Stafilo T. HPLC identification and determination of myricetin, quercetin, kaempferol and total flavonoids in herbal drugs. *Macedonian Pharm Bull* 2002;1:25–30.
38. Chang CJ, Tzeng TF, Liou SS, Chang YS, Liu IM. Myricetin increases hepatic peroxosome proliferator activated receptor protein expression and decreases plasma lipids and adiposity in rats. *Evid base Compl Alternative Med* 2012;2012:615–23.
39. Ghasemzadeh A, Jaafar HZ, Rahmat A. Identification and concentration of some flavonoid components in Malaysian young ginger (*Zingiber officinale Roscoe*) varieties by a high performance liquid chromatography method. *Molecules* 2010;15:6231–43.

Marthe Carine Djuidje Fotsing, Dieudonné Njamen,  
Zacharias Tanee Fomum and Derek Tantoh Ndinteh\*

## 4 Synthesis of biologically active heterocyclic compounds from allenic and acetylenic nitriles and related compounds

**Abstract:** Cyclic and polycyclic compounds containing moieties such as imidazole, pyrazole, isoxazole, thiazoline, oxazine, indole, benzothiazole and benzoxazole benzimidazole are prized molecules because of the various pharmaceutical properties that they display. This led Prof. Landor and co-workers to engage in the synthesis of several of them such as alkylimidazolenes, oxazolines, thiazolines, pyrimidopyrimidines, pyridylpyrazoles, benzoxazines, quinolines, pyrimidobenzimidazoles and pyrimidobenzothiazolones. This review covers the synthesis of biologically active heterocyclic compounds by the Michael addition and the double Michael addition of various amines and diamines on allenic nitriles, acetylenic nitriles, hydroxyacetylenic nitriles, acetylenic acids and acetylenic aldehydes. The heterocycles were obtained in one step reaction and in most cases, did not give side products. A brief discussion on the biological activities of some heterocycles is also provided.

**Keywords:** acetylenic nitriles; allenic nitriles; biological activity; heterocycles; Michael addition.

### 4.1 Introduction

Professor Landor and co-workers embarked in 1973 on the synthesis of enamino nitriles via the nucleophilic addition of amines to allenic nitriles. The work was later expanded to the synthesis of heterocyclic compounds by the double Michael addition of various amines to different nitrile substituents. This resulted in the synthesis of cyclic and

---

In memory of Prof. Zacharias Tanee Fomum (June 20, 1945–March 14, 2009)

---

\*Corresponding author: Derek Tantoh Ndinteh, Department of Chemical Sciences, University of Johannesburg, Doornfontein Campus, P.O. BOX 17011, Johannesburg, 2028, South Africa, E-mail: dndinteh@uj.ac.za

Marthe Carine Djuidje Fotsing, Department of Chemical Sciences, University of Johannesburg, Doornfontein Campus, P.O. BOX 17011, Johannesburg, 2028, South Africa

Dieudonné Njamen, Department of Animal Biology and Physiology, Laboratory of Animal Physiology, University of Yaoundé I, Faculty of Sciences, P.O. Box, 812 Yaoundé, Yaoundé, Cameroon

Zacharias Tanee Fomum, Department of Organic Chemistry, University of Yaoundé I, Faculty of Sciences, P.O. Box, 812 Yaoundé, Yaoundé, Cameroon

This article has previously been published in the journal *Physical Sciences Reviews*. Please cite as: M. C. D. Fotsing, D. Njamen, Z. T. Fomum and D. T. Ndinteh "Synthesis of biologically active heterocyclic compounds from allenic and acetylenic nitriles and related compounds" *Physical Sciences Reviews* [Online] 2021, 7. DOI: 10.1515/psr-2020-0210 | <https://doi.org/10.1515/9783110710823-004>

heterocyclic compounds such as imidazolines, imidazoles, oxazolines, thiazolines, oxazoles, thiazoles, pyrazoles, benzimidazoles, hexahydrobenzimidazoles, tetrahydropyrimidines, dihydrooxazines and benzothiazoles; just to name a few; which are biological potent compounds. The chemistry revolves around the Michael addition. In this review, particular emphasis will be placed on the different class of compounds generated and their biological usefulness.

## 4.2 Usefulness of heterocycles

Heterocycles are present in natural and in synthetic organic compounds of medicinal interest [1]. Raloxifene, an *S* heterocycle, is an FDA drug used for the treatment of breast cancer. Ritonavir, which is also an *S* heterocycle, is a potent antiviral agent [2]. The benzimidazole moiety can be found in drugs such as omeprazole, albendazole and astemizole [3]. The imidazole ring is a constituent of several important natural products including purine, histamine and histidine [4] (Figure 4.1). Purine, a nitrogen-containing heterocycle, is found abundantly in nature. It is the core structure of adenine and guanine in ribonucleic acid (RNA) and deoxyribonucleic acid (DNA) [5, 6]. They are present in other vital molecules such as chlorophyll, heme, vitamins B1 and B12, penicillin, benzodiazepines and most of the alkaloids [3, 7].

Benzothiazole based compounds (Figure 4.2) display interesting pharmacological properties such as anticancer [8, 9], antimicrobial [10], anticonvulsant [11], antiviral [12], antitubercular [13], antimalarial [14], antihelmintic [15], analgesic [16], anti-inflammatory [17], antidiabetic [18] and fungicidal activities [19, 20]. Bipyridines derivatives and quinolinyl heterocycles display very interesting antimycobacterial activity [21–23]. Quinolines [24] and structurally related heterocycles are currently used in

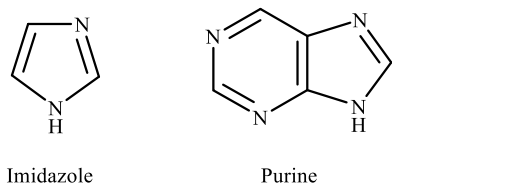


Figure 4.1: Some naturally occurring heterocycles.

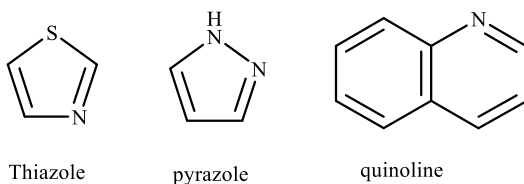


Figure 4.2: Some other heterocycles.

the clinic as antimalarials [25]. They also possess antibacterial and antifungal activities [23]. Pyridopyrimidines [26] have applications in various areas of medicine such as anti-cancer [27], antiviral [28], anti-inflammatory [29], [30]. Thiazoles [31] and their derivatives exhibit antibacterial [32], antifungal [33] and anti-inflammatory [34, 35]. Pyrazoles [36] exhibit significant biological properties such as antihyperglycemic [37], analgesic [38], anti-inflammatory [39], antipyretic [40], antibacterial [41], hypoglycemic [42] and sedative-hypnotic [34] activities.

## 4.3 Heterocycles synthesis

### 4.3.1 Double Michael addition

The Michael addition or 1, 4-addition is the nucleophilic addition of active methyles or any other nucleophile to activated olefins such as  $\alpha$ ,  $\beta$ -unsaturated carbonyl compound as shown in Scheme 4.1.

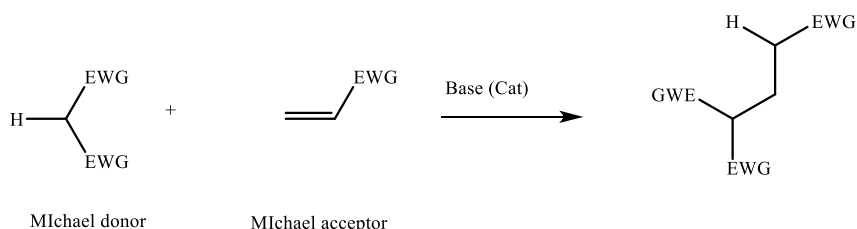
The synthesized heterocycles were all prepared via the double Michael addition. The different Michael acceptors were allenic nitriles, acetylenic nitriles, hydroxyacetylenic nitriles, acetylenic acids and acetylenic aldehydes.

This vast research area was pioneered by Landor and Fomum in 1974 when they embarked on the synthesis of imidazolines by Michael in addition to allenic and acetylenic nitriles.

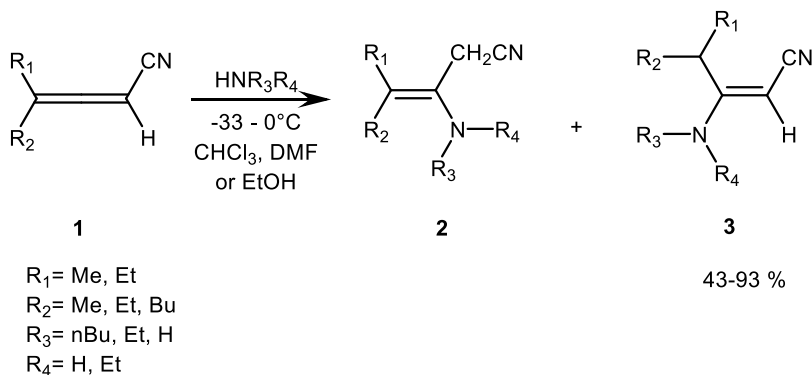
### 4.3.2 Heterocyclic compounds by Michael addition to allenic nitriles

#### 4.3.2.1 Synthesis of $\beta$ -ketonitriles

Fomum et al. reported on the Michael addition of amines to the 2,3 double bond of allenic nitriles, **1** to obtain unconjugated compound **2** and then conjugated enaminic nitriles, **3** in relatively good yields [43] (Scheme 4.2).



**Scheme 4.1:** The Michael addition general reaction.



**Scheme 4.2:** Synthesis of conjugated and unconjugated enaminic nitriles.

At first, separate and distinct mechanisms were postulated for the formation of the two adducts. But after careful consideration, it was concluded that the unconjugated enaminic nitriles **2** rearranges when heated at high temperatures to compound **3** which is conjugated. The reaction was later applied to the synthesis of most heterocycles. Total conversion of the unconjugated adduct to the conjugated one is best achieved by heating the reaction mixture between 150 and 200 °C for 2 h to obtain a yield of up to 90%. The successful conversion of the unconjugated enaminic nitriles to the conjugated one can be confirmed using infra-red spectroscopy. Compound **2** shows low-intensity stretching bands at 2250 and 1660  $\text{cm}^{-1}$  for the CN and the C=C bonds, respectively. The conjugated adduct **3** displays intense stretching bands at 2190 and 1590  $\text{cm}^{-1}$  for the previously mentioned functional groups. However, the enaminic nitriles were not isolated and only  $\beta$ -ketonitriles were, after acid-catalysed hydrolysis [43].

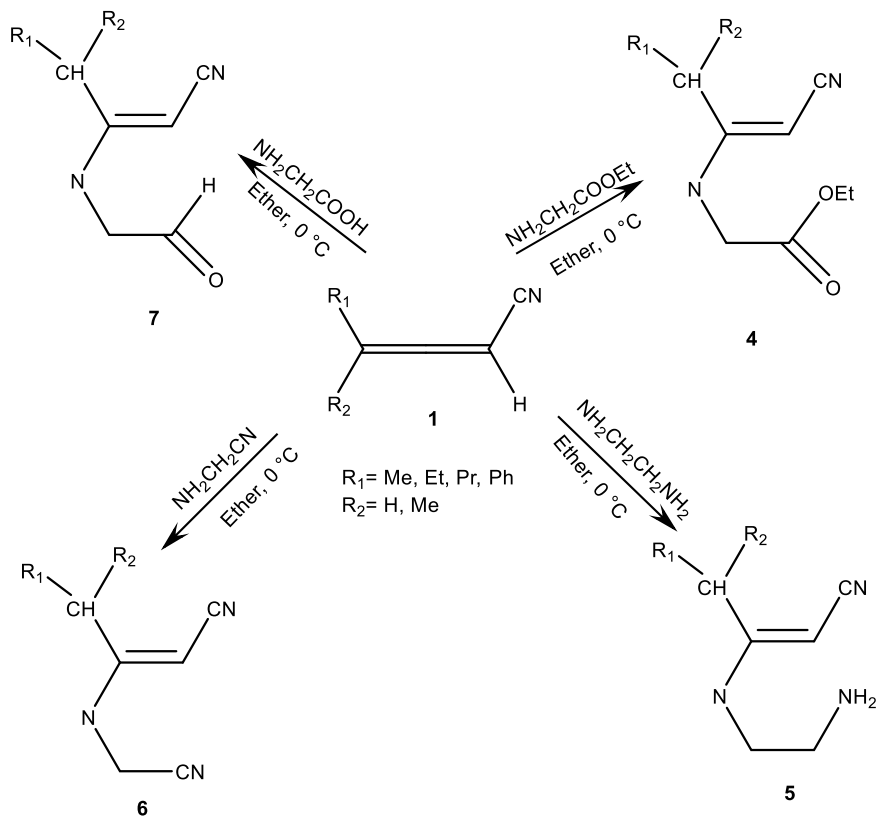
#### 4.3.2.2 Synthesis of imidazoline

Different Michael adducts were obtained from the reaction of acetylenic nitriles on ethylene or phenylethylene diamine,  $\alpha$ -amino-acids,  $\alpha$ -amino-esters and  $\alpha$ -amino-nitriles (Scheme 4.3).

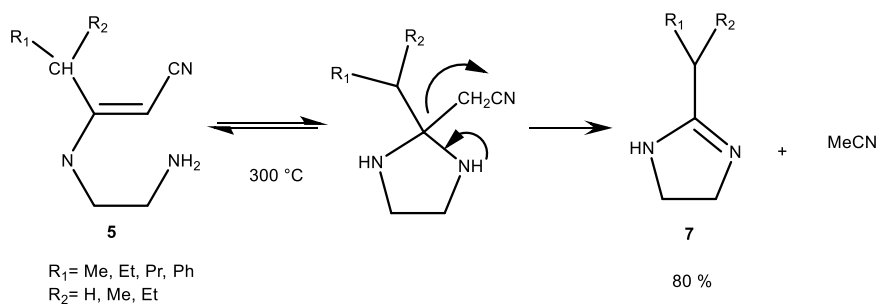
However, only the conjugated adduct from ethylenediamine and allenic nitriles **5** cyclised readily to give 2-alkylimidazolines **7** in good yields [44] (Scheme 4.4).

2-alkylimidazolines resulted from a second intramolecular Michael addition between the primary amine group and the first carbon of the double bond, which resulted in the formation of an unstable imidazoline that eliminates acetonitrile on distillation to yield the stable adduct **7**.

Similarly, when *o*-phenylenediamine **8** and 1,2-diaminocyclohexane **10** were used, 2-alkylbenzimidazoles **9** and 2-alkylheptahydrobenzimidazoles **11** were obtained respectively (Scheme 4.5) [45].



**Scheme 4.3:** Synthesis of the conjugated enaminic nitriles.

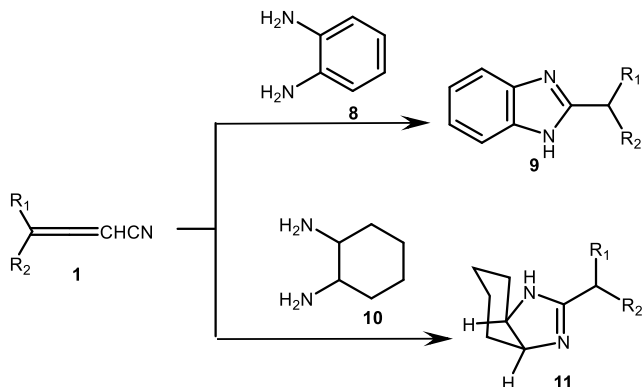


**Scheme 4.4:** Synthesis of 2-alkylimidazolines.

#### 4.3.2.3 Synthesis of oxazolines and thiazolines

The addition of equimolar amounts of ethanolamines, *o*-aminophenols,  $\beta$ -aminoethanethiols or *o*-aminobenzenethiols to allenic nitriles **1** followed by the cyclisation





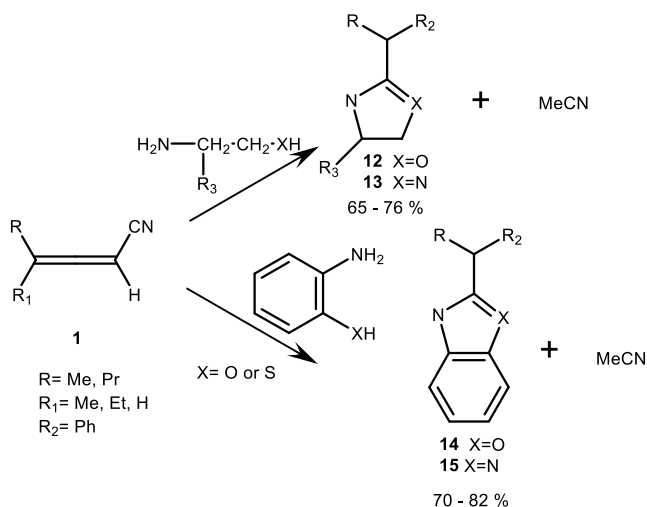
**Scheme 4.5:** Synthesis of 2-alkylbenzimidazoles and 2-alkylheptahydroimidazoles.

of the resulting compounds gave oxazolines and thiazolines in excellent yields (Scheme 4.6) [46].

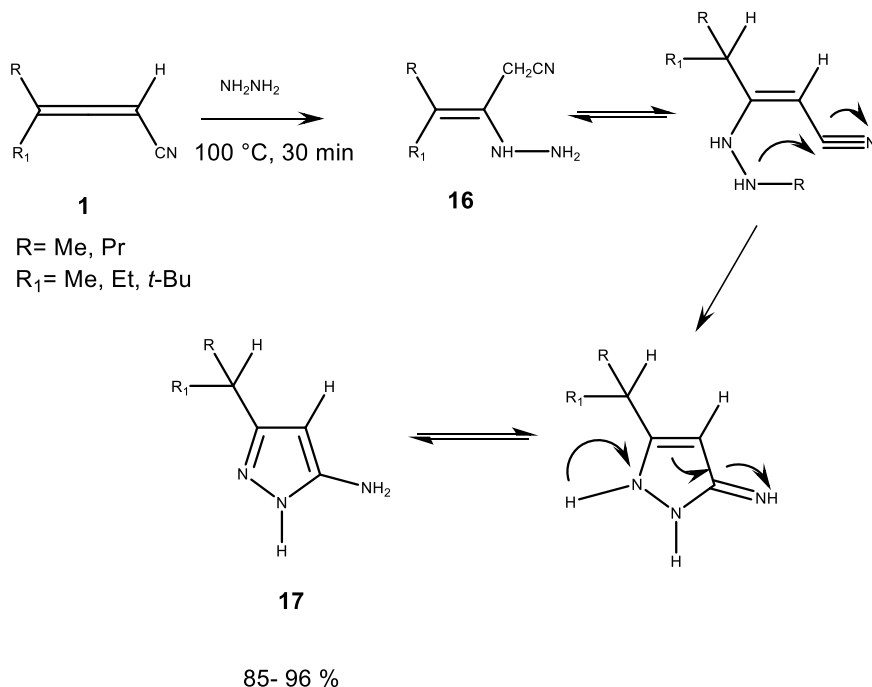
The oxazolines (X=O) **12** were easily distilled at atmospheric pressure whereas the thiazolines (X=N) **13** cyclised only after being heated and treated with a catalytic amount of base.

#### 4.3.2.4 Synthesis of pyrazoles

Pyrazoles **17** were also reported and resulted from the nucleophilic addition of hydrazine on allenic nitriles (Scheme 4.7).



**Scheme 4.6:** Synthesis of oxazolines and benzoxazolines (X=O) and thiazolines and benzoxazolines (X=S).



**Scheme 4.7:** Synthesis of 5-alkyl-3-aminopyrazoles.

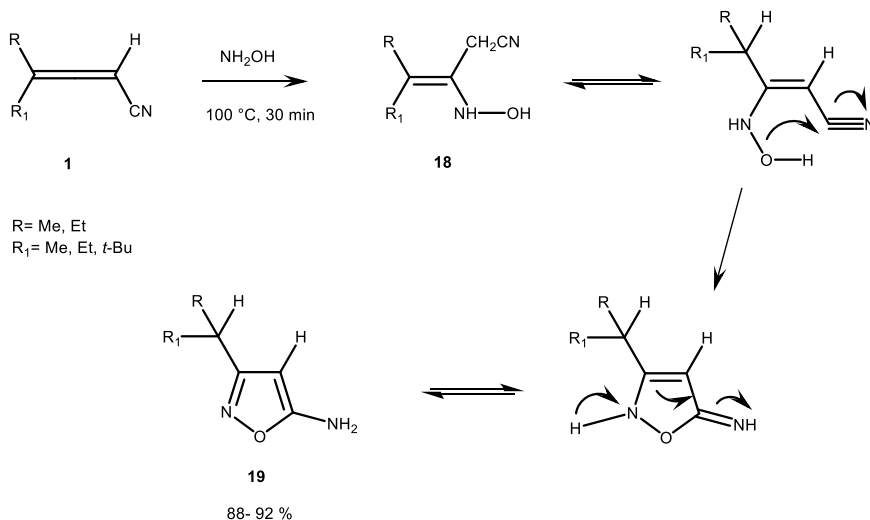
In another instance, hydrazine was substituted with hydroxylamine to yield 3-alkyl-5-amino, 5-amino-3-phenyl **19** and 3-amino-5-phenyl-isoxazoles in excellent yields (Scheme 4.8) [47].

The mechanism of the reaction can be summarised in an intramolecular 5-*Exo-Dig* [48] ring closure of the conjugated Michael adduct. The UV spectra of the synthesized isoxazoles were in agreement with the data reported in the literature.

#### 4.3.2.5 Synthesis of 3-H indoles

During the synthesis of pyrazoles **17** using hydrazine, cyclisation occurs immediately. Hence, neither the conjugated nor the unconjugated one could be isolated. However, when substituted hydrazine such as phenylhydrazine, was used, the unconjugated Michael adduct was first formed and transformed into the conjugated adduct. The latter one was isolated in quantitative yield. In another attempt to synthesize phenyl-substituted pyrazoles, 3-H indole **20** were isolated, even though it was first identified as impurity [49].

When phenylhydrazine and 4-methylhexa-2,4-diene-nitrile were mixed at room temperature then heated to 80 °C, an exothermic reaction took place and yielded a

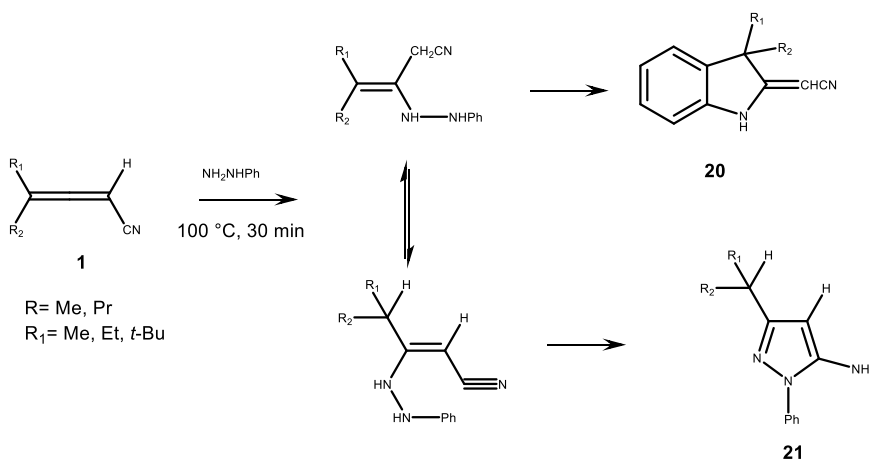


**Scheme 4.8:** Synthesis of isoxazoles from hydroxylamine.

mixture of pyrazoles **21** and 3-H indoles **20** in approximately equal proportions (Scheme 4.9) [50].

The characteristically shielded enaminic proton and the exchangeable hydrogen could be well-identified in the <sup>1</sup>H NMR spectra. As pyrazoles only resulted from the conjugated adduct, it was assumed that indoles could only derive from the unconjugated adduct.

The unconjugated adduct undergoes a [3, 3] sigmatropic rearrangement, followed by a phototropic rearrangement to the substituted aniline. The latter one then cyclises



**Scheme 4.9:** Synthesis of phenyl-substituted pyrazoles and 3-H indoles.

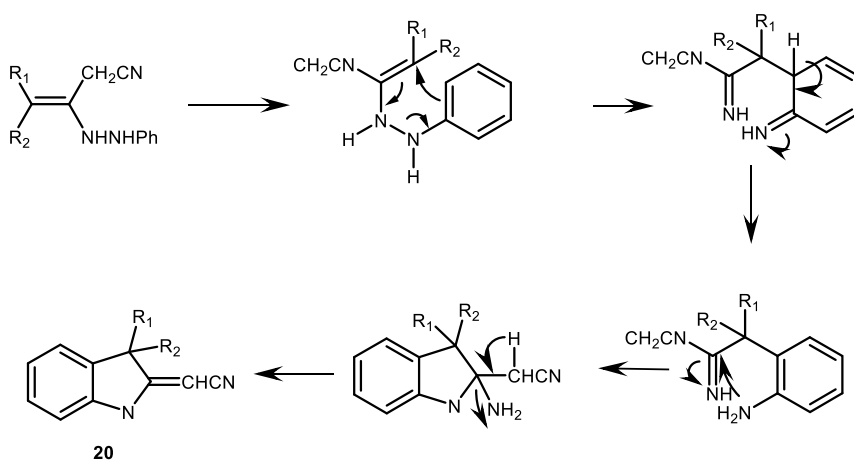
by nucleophilic addition of the imine, followed by elimination of ammonia to give **20** (Scheme 4.10) [50]. Table 4.1 presents the relative yields of indoles and pyrazoles depending on the substituents on the allenic nitriles.

No by-product resulting from another possible sigmatropic rearrangement of the conjugated adduct was detected.

#### 4.3.2.6 Synthesis of 2- and 4-imino (1, 2-a)pyridopyrimidines from allenic nitriles and 2-aminopyridine

The synthesis of pyrido (1, 2-a) pyrimid-4-ones **23** was also reported. This time, 2-amino and 2,3-diaminopyridine **22**, were used as nucleophiles. After 48 h under reflux, the pyridopyrimidines were collected in excellent yields [51].

Spectroscopic features such as a strongly hydrogen-bonded hydroxyl in the infra-red and a deshielded OH in the NMR spectra confirm the proposed structures.



**Scheme 4.10:** Reaction mechanism of 3-H indoles synthesis.

**Table 4.1:** Relative yields of indoles and pyrazoles synthesis.

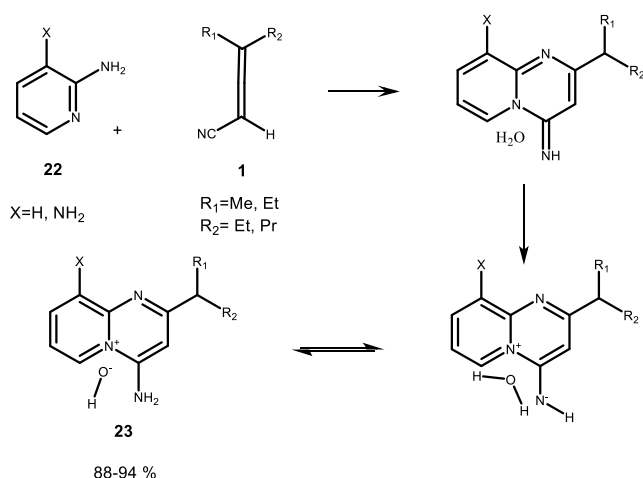
Entry	Indoles (%)	Pyrazole (%)
$R_1 = \text{Me}$	50	50
$R_2 = \text{Et}$		
$R_1 = \text{Et}$	41	59
$R_2 = \text{Et}$		
$R_1 = \text{Ne}$	39	61
$R_2 = \text{Pr}$		

When 4, 4-dialkylallenyl nitriles are used, 4-iminopyridopyrimidines **23** are synthesized (Scheme 4.11), but when 4-monoalkylallenyl nitriles are used, 2-iminopyridopyrimidines **24** are produced as shown in Scheme 4.12.

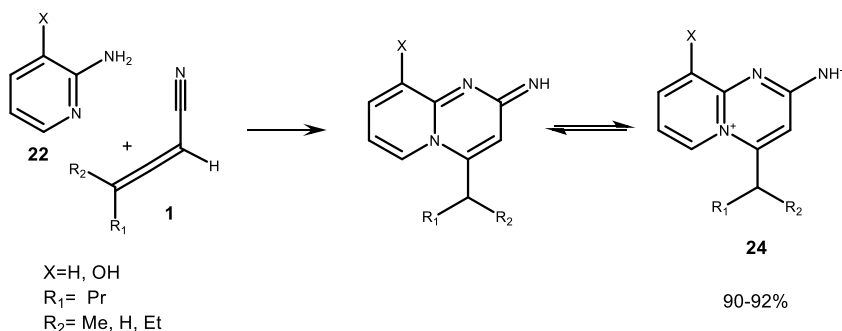
Steric hindrance from the 4-alkyl groups on the allenyl nitrile favours a nucleophilic attack by the side chain amino group at the Michael position for 4,4-disubstituted allenyl nitriles to yield 4-iminopyridopyrimidines.

When 3-hydroxy-2-aminopyridine is used as a nucleophile, only 2-imino derivatives are obtained, with both the mono and dialkyl allenic nitriles.

The assignment of structure 4-iminopyridopyrimidines was based mainly on a comparison of UV spectra [51]. However, a detailed study of  $^1\text{H}$  and  $^{13}\text{C}$  NMR spectra later revealed that 2-iminopyridopyrimidines **24** were always initially formed by prior attack of the ring nitrogen on the central carbon of the allene [52].



**Scheme 4.11:** Synthesis of 2-alkyl-4-iminopyrido (1, 2a)pyrimidines.



**Scheme 4.12:** Synthesis of 4-alkyl-2-iminopyrido (1, 2a)pyrimidines.

When the pyridopyridines were refluxed in 95% ethanol for the required time, pyridyl ketones **25** were obtained in good yields (Scheme 4.13) [52].

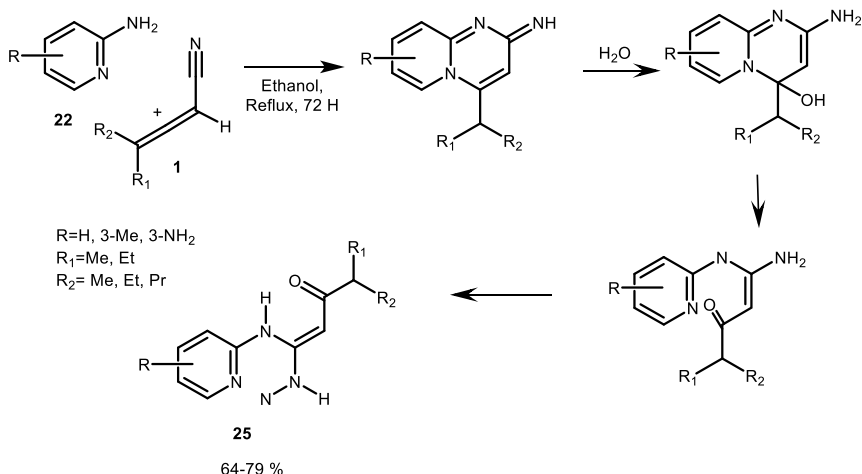
The NH proton engaged in the hydrogen bond with the carbonyl is observed downfield around 14 ppm. The ketonic carbonyl around 198 ppm is seen in  $^{13}\text{C}$  NMR spectrum.

#### 4.3.2.7 Synthesis of pyrimido(1, 2-a)pyrimidines from allenic nitriles and 2-aminopyridine

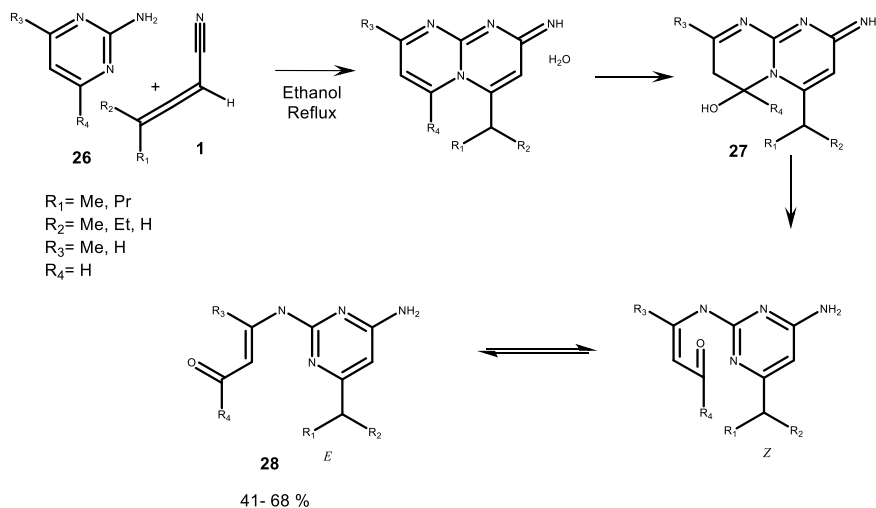
In another instance, pyrimidopyrimidines and their hydrolysis products were reported [53].

In this case, the pyrimido[1,2a] pyrimidines were obtained from the double Michael addition of 2-aminopyrimidine or 2-amino-4-methylpyrimidine on allenic nitriles (Scheme 4.14).

When  $R_4 = \text{H}$ , the product which is an aldehyde, results from the attack of  $\text{H}_2\text{O}$  on carbon 6. In that case, the *E* form from the ring chain tautomerism dominates. The *J* coupling constant between the  $\text{H}^1$  and  $\text{H}^2$  is between 8 and 10 Hz. Where  $R_3 = \text{Me}$  and  $R_4 = \text{H}$ , the product is in the *Z* form and in this case the coupling constant between the protons is 4 Hz. In addition, a strong hydrogen bonding between NH and the carbonyl can be confirmed with a signal around 13 ppm in the  $^1\text{H}$  NMR spectrum. All other spectroscopic data are in accord with the proposed structures.



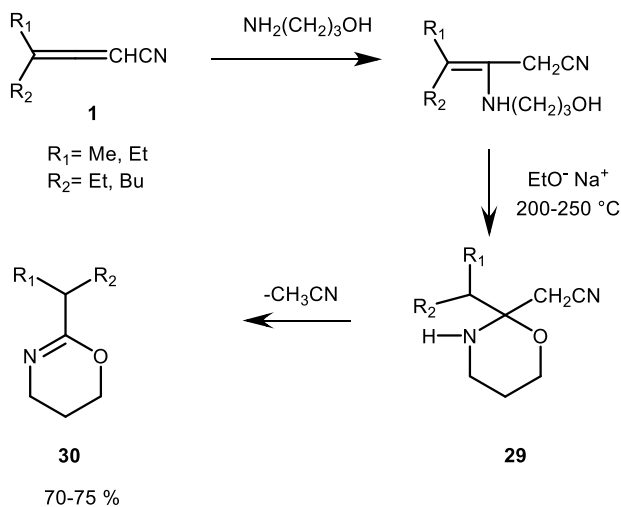
**Scheme 4.13:** Synthesis of pyridyl ketones.



**Scheme 4.14:** Synthesis of other pyridyl ketones and aldehydes.

#### 4.3.2.8 Synthesis of dihydrooxazines, tetrahydropyridines and tetrahydropyrimidines

Treatment of enaminic nitriles from 3-hydroxypropylamine and  $\alpha$ -allylic nitriles with a catalytic amount of sodium ethoxide yielded dihydrooxazines **30** in 70–75% yield with no other by-product formed (Scheme 4.15) [54].



**Scheme 4.15:** Synthesis of dihydrooxazines.

However, when the enamino nitriles were heated at 300 °C in the absence of the catalyst [54], a mixture of dihydrooxazines **30** and tetrahydropyridines **31** in the respective ratio of 30 and 70% were obtained as shown in Scheme 4.16.

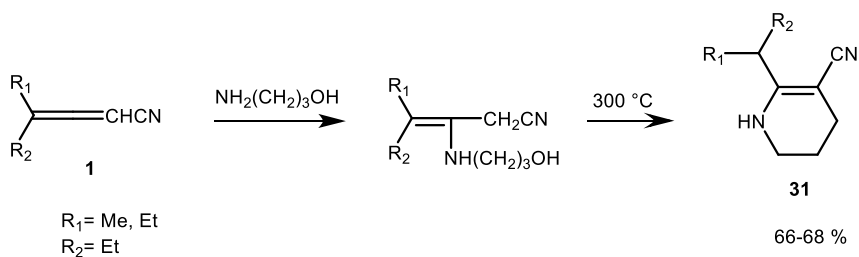
This was rationalised by postulating either the dehydration of the amine nitrile followed by ring expansion or a sigmatropic rearrangement of N-allylenamine followed by a concerted sigmatropic ring closure to give **31**.

The Michael adduct and the bis adduct were formed in the respective yields of 80 and 20% when 1,2 diaminopropane was used. The thermal cyclisation of the Michael adduct gave the tetrahydropyrimidines **32** (Scheme 4.17).

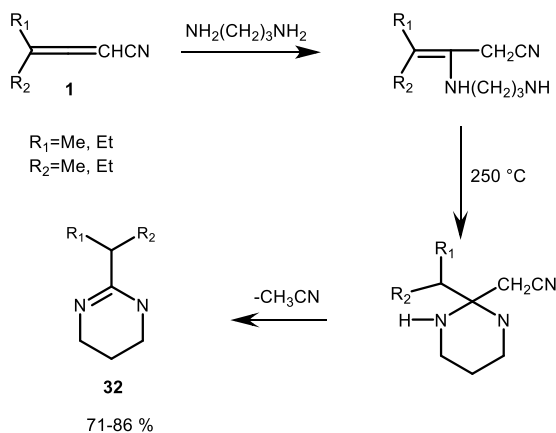
#### 4.3.2.9 Synthesis of six-membered thiazines

In the presence of sodium ethoxide, 5-alkyl-6-cyano-2,3-dihydro-4H-1,4-thiazines **34** were formed in excellent yields from allenyl nitriles **1** and 2-aminoethanethiol (Scheme 4.18) [55].

The mechanism behind the synthesis of **34** was presented as a ring expansion of the thiazolidine intermediate **33** as its anion, followed by oxidation of the sulphide into

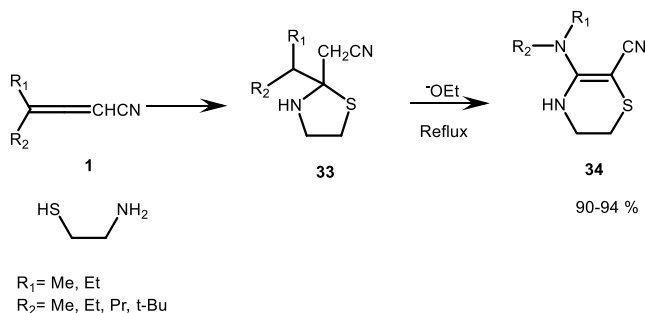


**Scheme 4.16:** Synthesis of tetrahydropyridines.



**Scheme 4.17:** Synthesis of tetrahydropyrimidines.





**Scheme 4.18:** Synthesis of 5-alkyl-6-cyano-2,3-dihydro-4H-1,4-thiazines.

disulphide and a ring closure followed by proton shift [56, 57]. But one of the drawbacks of this reaction is the non-cyclisation of neither the N- nor the S-adducts when bulky substrates such as o-aminothiophenol are used.

When the reaction was carried out with 0.5 mol equiv of NaOEt, maximum yields were obtained [58]. The scope of the dihydrothiazine synthesis was extended by treating allenic nitriles with cysteine and cystine and their ester to obtain 3-carboxy and 3-methoxycarbonyl-5,6-dihydrothiazines which are optically active chiral compounds [58].

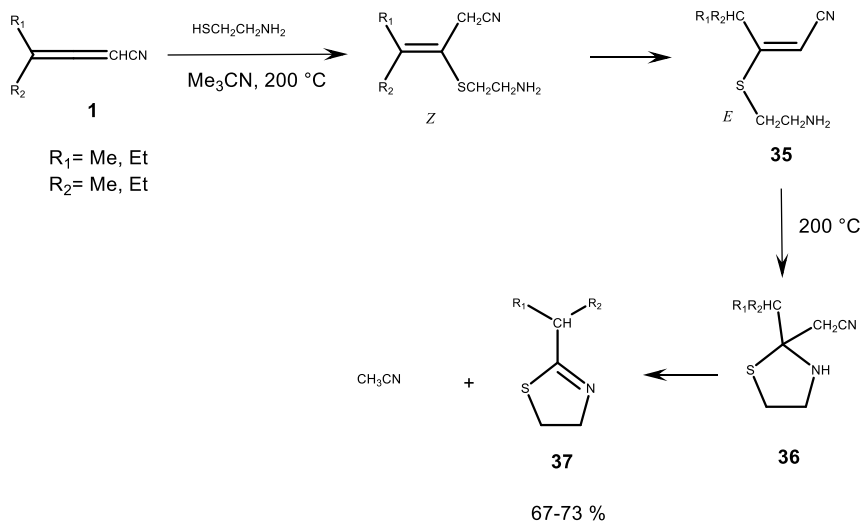
#### 4.3.2.10 Synthesis of thiazolines and benzothiazoles

Thiols when added to allenyl nitriles in the presence of a catalytic amount of base in refluxing acetonitrile produced unconjugated adducts which were converted to conjugated ones after being heated in ethanol under basic conditions. Upon heating the conjugated adducts, thiazolines were formed in about 70% yields. In the same manner, benzothiazoles were also obtained from 2-aminothiophenol in 80% yield (Scheme 4.19) [59].

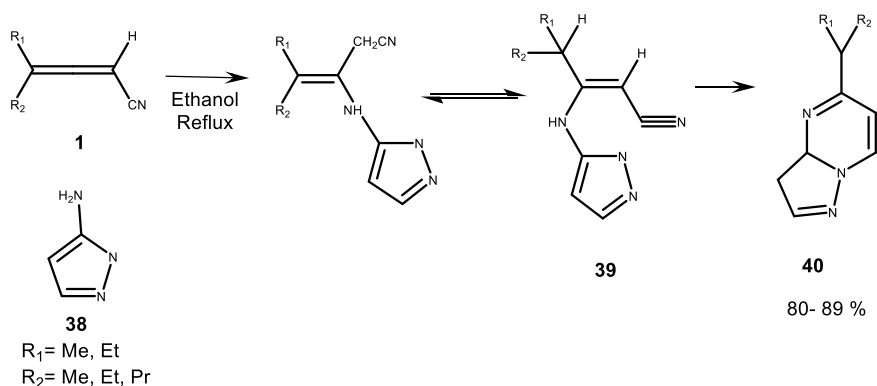
The suggested mechanism for the formation of thiazolines and benzothiazoles is a Michael attack from the amine and a 5-exotrig ring closure. Even though both the *E* and *Z* can undergo the ring closure, the *E* form which offers less hindrance to the attack of the nucleophile in the Michael position would be expected to react faster. At high temperatures, the two isomers are in equilibrium and the 5-exotrig ring closure displaces the equilibrium and therefore favours the *E* form and the thiazoline formation.

#### 4.3.2.11 Synthesis of pyrazolopyrimidines

5-alkyl-7-aminopyrazolo[1,5- $\alpha$ ]-pyrimidines **40** were obtained in good yield from allenic nitriles and 3-aminopyrazoles (Scheme 4.20) [60].



**Scheme 4.19:** Synthesis of thiazolines from allenic nitriles.



**Scheme 4.20:** Synthesis of pyrazolopyrimidines.

The products are obtained after 21 days in refluxed ethanol. However, the reaction time can be shortened to four days when Dimethylformamide is used as a solvent. However, lower yields are obtained in the latter case, because of dimerization of the allenic nitrile to the cyclobutene dimer competes with the intended reaction. To avoid a mixture of adducts **39** (*E* and *Z*) and the product **40**, prolonging the reflux time was needed. The reported spectroscopic data were in accord with the proposed structures.

#### 4.3.2.12 Synthesis of aminopyridylpyrazoles

Aminopyridylpyrazoles were reported and resulted from the double Michael addition of 2-hydrazinopyridine on allenic nitriles (Scheme 4.21) [61]. The reaction proceeds without solvent and also when using chloroform as a solvent to yield 5-amino-3-alkyl-1-(2-pyridyl)imidazoles in excellent yields.

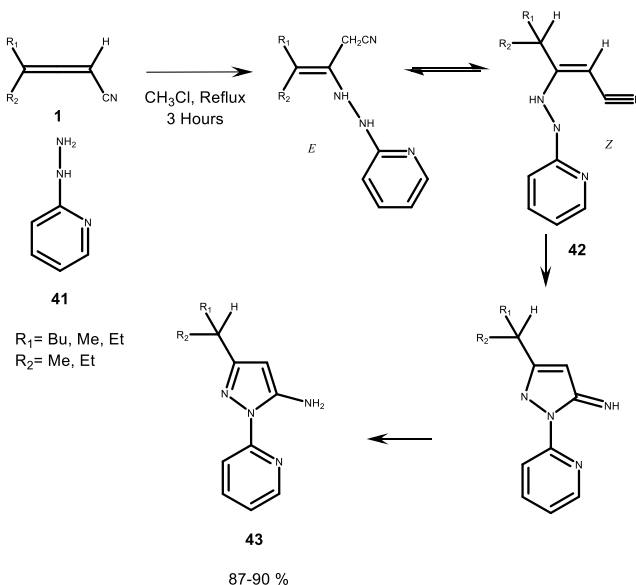
The reaction was spontaneous and occurred within 2 min in the absence of solvent. However, polymerisation of the pyrazoles is caused by the high temperatures induced by the exothermic reactions, hence the product was a mixture made of 20% of the polymerised pyrazoles and **43**. When the reaction was carried out in refluxed chloroform, cyclisation was completed within 3 h and no by-products were identified.

The *Z* form of the enaminic nitriles dominates and cyclises through the imino intermediate to yield the expected aminopyridylpyrazoles **43**.

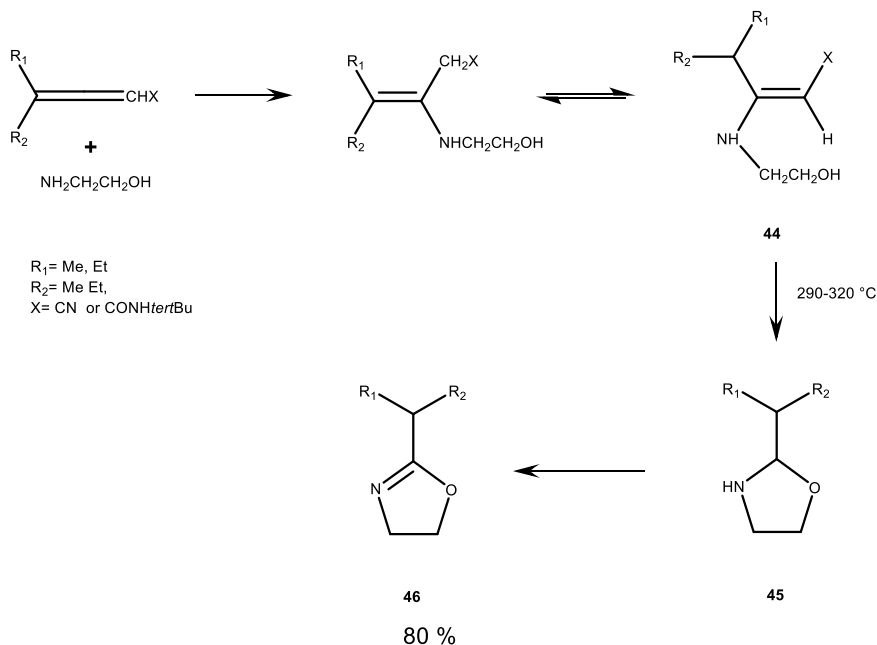
In the  $^1\text{H}$  NMR of aminopyridylpyrazoles, the chemical shift of  $\text{H}_4$  can be found around 4.70 ppm and appears as a singlet. The aromatic protons appear in the expected regions.

#### 4.3.2.13 Synthesis of oxazolines and benzoxazoles

Oxazolines were obtained from ethanolamines and allenic nitriles and amides in a two-stage reaction (Scheme 4.22) [62].



**Scheme 4.21:** Synthesis of pyridylpyrazoles.



**Scheme 4.22:** Synthesis of oxazolines.

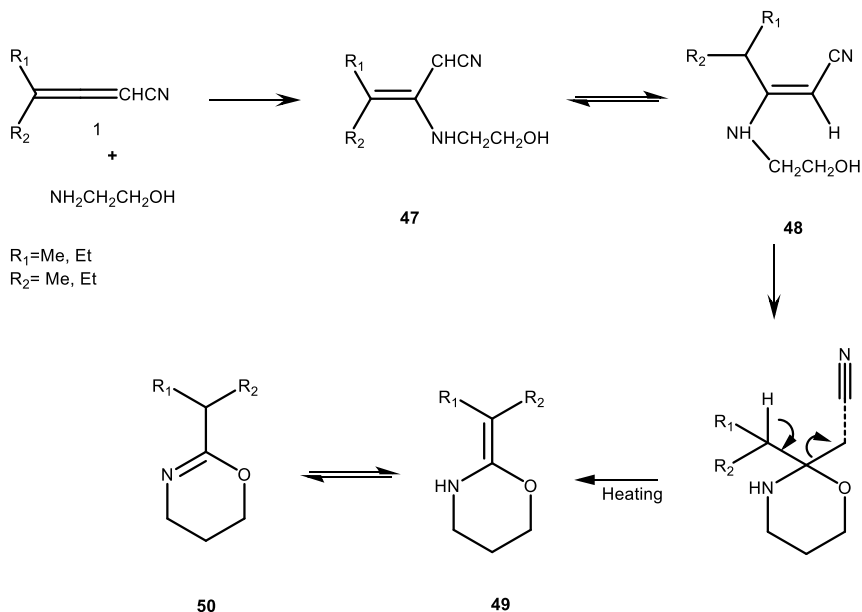
The first step was the nucleophilic addition of the amino group to the Michael carbon, to give conjugated enamine adducts, followed by the pyrolysis of these adducts at 290–320 °C which led to ring closure to yield an oxazolidine. The latter one undergoes elimination of either acetonitrile or a substituted acetamide to finally give oxazoline **46**.

When *o*-aminophenol was used, the reaction was slower. But oxazoines or benzoxazoles were isolated in good yields.

#### 4.3.2.14 Synthesis of 1, 3-oxazines

1, 3-Oxazines were derived from the nucleophilic attack of 3-aminopropan-1-ol on allenic nitriles to give Michael adducts which cyclise when heated. Ring closure of the adduct by a second Michael addition yields the expected product (Scheme 4.23) [63].

In this case, only the conjugated enamino nitrile was isolated as a mixture of *E* and *Z* forms. Upon heating the enamino nitriles in the presence of sodium ethoxide, a mixture of 2-alkylidene-3,4,5,6-tetrahydro-2H-1,3-oxazine and 2-alkyl-5,6-dihydro-4H-1,3-oxazine was obtained in 60–80% yield. When an acid is used instead of sodium ethoxide, the main product obtained is 2-alkyl-3-cyanotetrahydropyridine, that could



**Scheme 4.23:** Synthesis of 1, 3-oxazines.

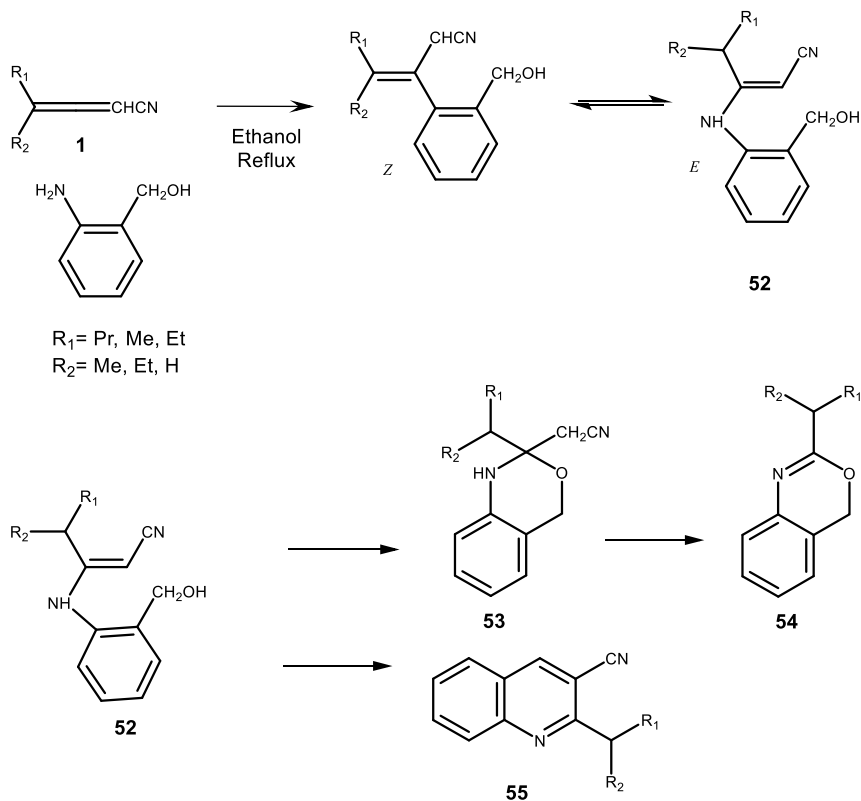
result from the dehydration of **48** followed by a sigmatropic rearrangement which is succeeded by an intramolecular 'ene' reaction.

When diaminopropane was used as a nucleophile, 2-alkyltetrahydropyrimidines were obtained in good yields.

#### 4.3.2.15 Synthesis of benzoxazines and cyanoquinolines

4H-3,1-benzoxazines **53** and 3-cyanoquinolines **54** were obtained from the reaction of allenic nitriles and o-aminobenzylalcohol in refluxing ethanol (Scheme 4.24) [64]. The reaction proceeds through the formation of the enaminic nitrile that slowly cyclise to dihydro-4H-3,1-benzoxazines. The latter eliminates acetonitrile when heated to yield the expected product. The 2-alkyl-3-cyanoquinolines **55** are obtained in 60–70% yield.

When the starting materials are heated in refluxed ethanol, the relative amounts of **52** and **53** depends on the reaction time and the substituents on the allene. After 70 h of reflux, **52** was the main product. To obtain **55**, the enaminic nitrile **52** containing trace amounts of **53** was heated at 300 °C and distilled. The only product is **55** which shows a nitrile band in the infra-red near 2220 cm<sup>-1</sup> and an NMR signal at  $\delta = 8.42$  for the characteristic proton at position 4. The mechanism of the reaction involves dehydration, ring closure and finally dehydrogenation.

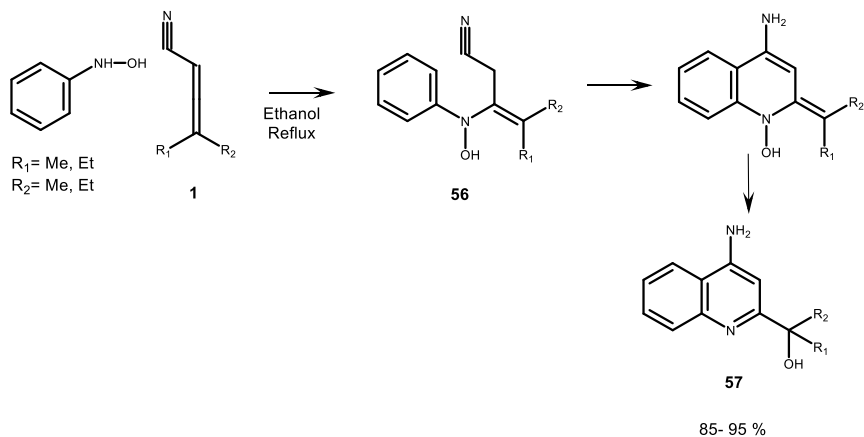


**Scheme 4.24:** Synthesis of benzoxazines and cyanoquinolines.

#### 4.3.2.16 Synthesis of 4-amino-2-alkylquinolines

Isoxazoles were previously obtained from hydroxylamine and allenic nitriles [47]. However, when hydroxylamine was substituted with phenylhydroxylamine, 2-alkylidene-4-amino-1,2-dihydroquinoline were obtained instead (Scheme 4.25) [65].

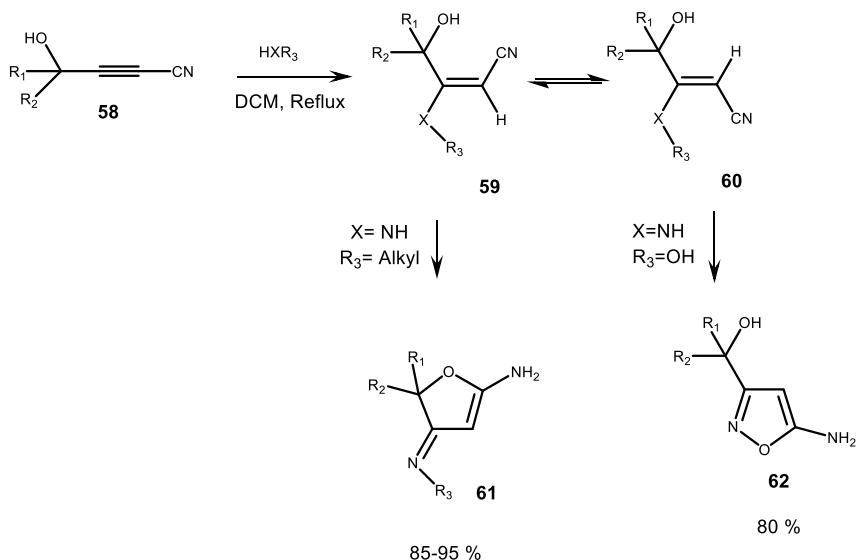
The reaction proceeds through the unconjugated adduct ring that closes ortho to the nitrogen on the benzene ring to form 2-alkylidene-4-amino-1,2-dihydro-1-hydroxyquinoline. The electrophilic ring closure of the unconjugated adduct **56** was considerably faster than a proton shift to the conjugated adduct. The instability of the intermediate was followed by a 1,3-hydroxy shift to give 4-amino-2-(1-hydroxyl)quinolines **57**. The proposed product could be further confirmed by a peak around  $\delta = 51$  ppm in the  $^{13}\text{C}$  NMR spectra assigned to the 2-(1-hydroxylalkyl) side chain with a quaternary carbon.



**Scheme 4.25:** Synthesis of quinolines.

#### 4.3.2.17 Synthesis of dihydrofurans

Dihydrofurans **61** were obtained from the Michael addition of HXR on 4-hydroxybut-2-ynenitriles **58**. When X was nitrogen and R a non-bulky alkyl group, and under basic conditions, the adducts forms cyclised spontaneously to give 5-amino-3-imino-2,3-dihydrofurans in good yields (Scheme 4.26) [66].



**Scheme 4.26:** Synthesis of dihydrofurans.

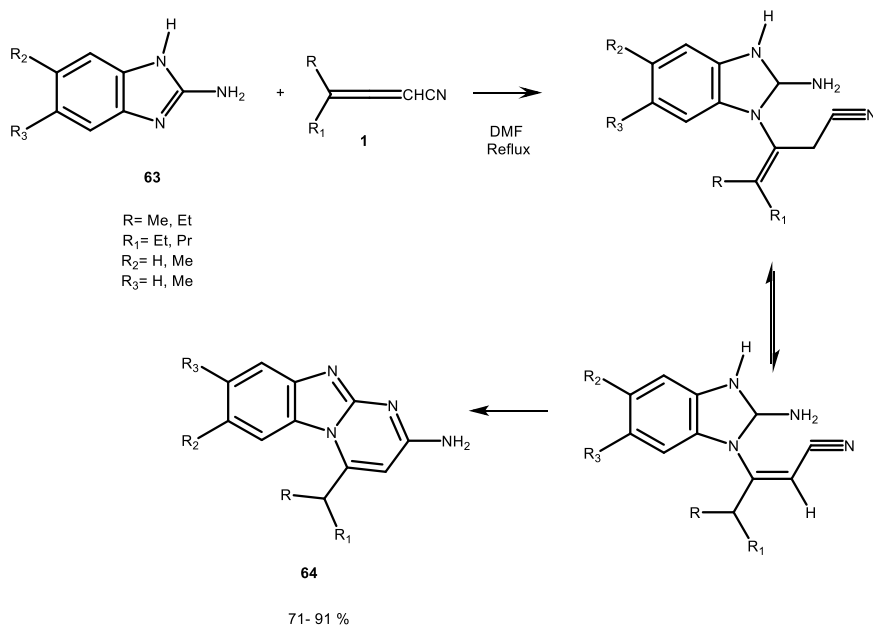
When hydroxylamine is used as a nucleophile, **62** is obtained as a pure product. However, phenylhydroxylamine only yields furans. Interference between the phenyl group and the bulky side chain destabilises the transition state and favour the furan formation.

Oxygen or sulphur adducts are formed under basic conditions but do not cyclise to furans.

#### 4.3.2.18 Synthesis of pyrimido(1,2a)benzimidazoles

Aminobenzimidazoles **63** and allenic nitriles **1** reacted via a double Michael addition in refluxed DMF to yield pyrimidobenzimidazoles in excellent yields (Scheme 4.27) [67].

Compound **64** was the product of an initial attack from the ring nitrogen of 2-aminobenzimidazole on the Michael carbon of the allenic nitrile. The resulting unconjugated adduct converts to the conjugated one that undergoes a second intramolecular Michael addition. Some of the spectroscopic highlights of pyrimidobenzimidazoles are the vinylic proton around  $\delta = 6$  ppm in the  $^1\text{H}$  NMR spectrum and the broad twin stretching bands in the infra-red spectrum between 3150 and 3450  $\text{cm}^{-1}$  because of  $\text{NH}_2$ .



**Scheme 4.27:** Synthesis of pyrimidobenzimidazoles.



### 4.3.3 Synthesis of heterocycles from acetylenic nitriles

#### 4.3.3.1 Synthesis of imidazolines

The double Michael attack of  $\text{NH}_2\text{CH}_2\text{C}(\text{Et}_2)\text{NH}_2$  on phenylacetylene nitriles **65** resulted in the formation of 2-phenyl imidazolines **66** in good yields (Scheme 4.28) [45].

Phenylpropyne nitrile reacts at the Michael carbon to yield the unconjugated adduct that rearranges to the conjugated one. 2-Phenyl-imidazolines are obtained by elimination of acetonitrile.

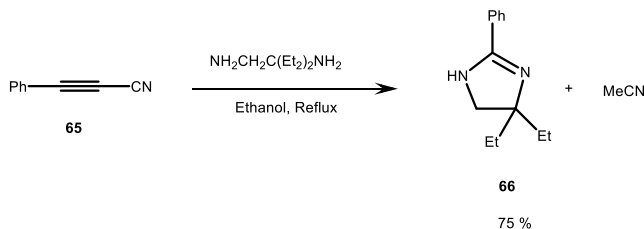
#### 4.3.3.2 Synthesis of benzothiazoles

The addition of equimolar amounts of aminobenzenethiols **67** to acetylenic nitriles **65** followed by the cyclisation of the resulting compounds gave benzothiazoles **68** in good yields (Scheme 4.29) [46].

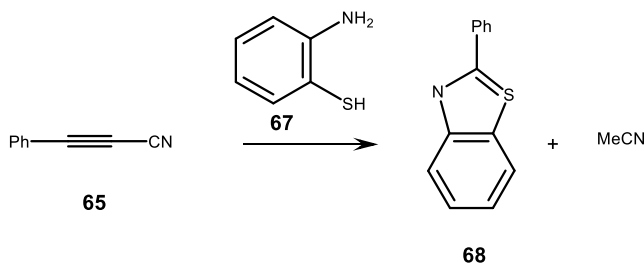
The reaction proceeds smoothly without the formation of any by-product. The corresponding Michael adduct cyclises when treated with a catalytic amount of sodium ethoxide. Distillation at atmospheric pressure gives acetonitrile followed by the benzothiazoles **68**.

#### 4.3.3.3 Synthesis of pyrazoles

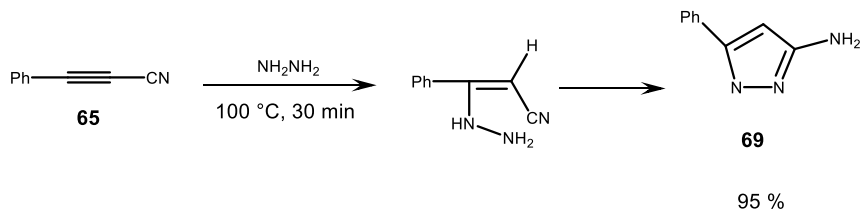
On mixing equivalent amounts of hydrazine hydrate and acetylenic nitriles, 5-phenyl-3-aminopyrazoles **69** were obtained in excellent yields (Scheme 4.30) [46].



**Scheme 4.28:** Synthesis of imidazolines.



**Scheme 4.29:** Synthesis of benzothiazoles.



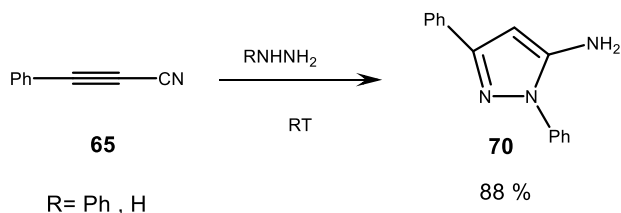
**Scheme 4.30:** Synthesis of 5-phenyl-3-aminopyrazoles.

When hydrazine [50] and the phenyl-substituted hydrazine [49] were used, 5-amino-3-phenylpyrazole **69** and 1,3-diphenyl-5-aminopyrazole **70** were formed respectively. In this case, no other product such as indole was detected, as the acetylene **65** can only form the conjugated adduct (Scheme 4.31).

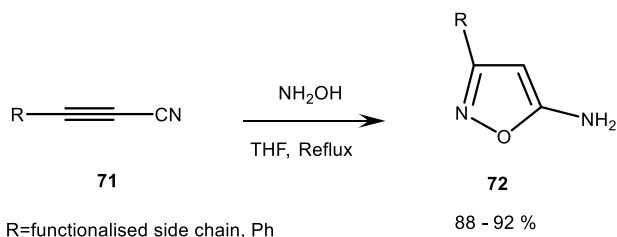
Compounds **70** are characterised by a maximum absorption in the UV spectra at  $\lambda = 204\text{--}207\text{ nm}$ . The infra-red spectra show a broadband for the NH stretching centred on  $\nu = 3200\text{ cm}^{-1}$ . Characteristic protons signal such as the =CH is found in expected regions.

Upon substitution of hydrazine with hydroxylamine, isoxazoles **72** were formed in excellent yields (Scheme 4.32) [47].

When the acetylenic nitrile was substituted by a functionalised side chain, 3-alkyl-5-aminoisoxazoles were formed in good yields (85%). However, when phenylpropynitrile **65** was used, a mixture of 5-amino-3-phenylisoxazole and 3-amino-5-phenylisoxazole was obtained in a 3:1 ratio.



**Scheme 4.31:** Synthesis of 1,3-diphenyl-5-aminopyrazole.



**Scheme 4.32:** Synthesis of isoxazoles.

The 5-amino compound ratio was increased to up to 95% when the cyclisation took place at 0 °C in ethanol.

#### 4.3.3.4 Synthesis of pyridyl ketones

Phenylpropenenitrile **65** reacted with 2-aminopyridine **21** to give 2-imino-4-phenyl-pyrido [1, 2a]pyrimidines which after hydrolysis yield pyridyl ketones **75** (Scheme 4.33) [52].

The obtained 2-imino-4-phenyl-pyrido [1,2a]pyrimidines are hydrolysed to ketones with ease.

When 2-aminopyrimidine **25** is used, the hydrolysis products are aldehydes (Scheme 4.34) [53].

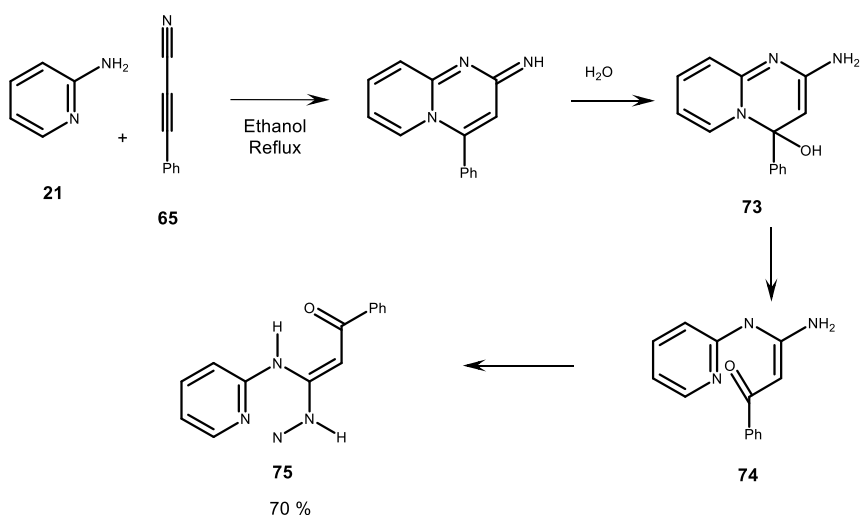
#### 4.3.3.5 Synthesis of dihydrofurans

Conjugated adducts were formed from a nucleophilic attack of HXR<sub>3</sub> on 4-hydroxybut-2-ynenitriles. When X was O or S, the adducts were isolated, but when X=N, they spontaneously cyclised to give imino and amino furans (Scheme 4.35) [68].

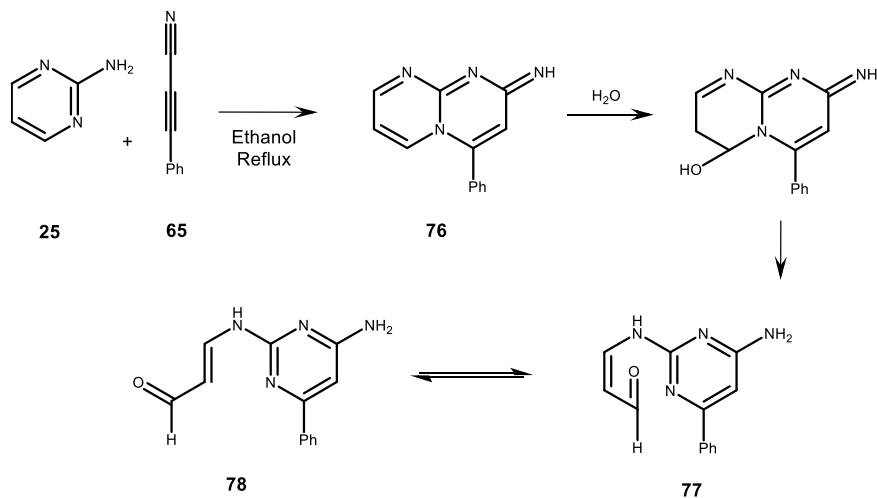
The reaction proceeds in reflux conditions and when the amine attacks the acetylenic nitrile, the *E* isomer is predominantly formed. The latter closes to yield dihydrofurans.

#### 4.3.3.6 Synthesis of 5-aryl-7-aminopyrazolo [1, 5a]pyrimidine

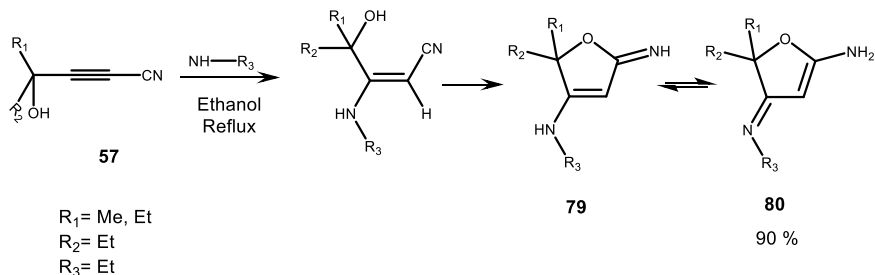
5-phenyl-7-aminopyrazolo[1,5a]pyrimidine **81** were obtained from the double Michael addition of 3-aminopyrazole **38** on phenylpropenenitrile in good yields (Scheme 4.36) [60].



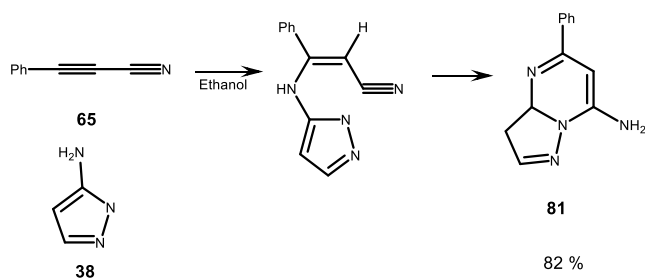
**Scheme 4.33:** Synthesis of 2-iminopyridopyrimidines and pyridyl ketones.



**Scheme 4.34:** Synthesis of 2-iminopyrimidopyrimidines and pyridyl aldehydes.



**Scheme 4.35:** Synthesis of 5-amino-2,2-dialkyl-3-(alkylimino)-2,3-dihydrofurans.



**Scheme 4.36:** Synthesis of 5-phenyl-7-aminopyrazolo [1,5- $\alpha$ ]pyrimidine.

The reaction is complete after 14 days in ethanol and the product is isolated in good yields without any by-product. After the nucleophilic attack of 3-aminopyrazole on the electrophile, the resulting adduct cyclises to afford pyrazolopyrimidines.

### 4.3.3.7 Synthesis of pyridylpyrazoles

5-amino-3-phenyl-1-(2-pyridyl)pyrazoles **83** resulted from the double Michael addition of 2-hydrazinopyridine **41** on phenylpropynenitrile in excellent yields (Scheme 4.37) [61].

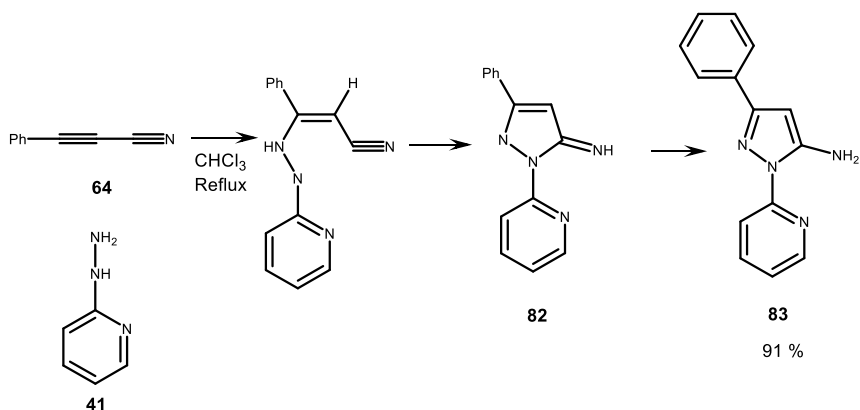
2-Hydrazinopyridine react neatly with phenylpropyne nitrile to afford 5-amino-3-phenyl-1-(2-pyridyl)pyrazole in chloroform for 12 h under reflux conditions.

From hydroxyacetylenic nitriles and of 2-hydrazinopyridine, pyrazoles were also obtained. In this case, after the formation of the intermediary adduct, the hydroxyl group could have reacted with the cyano group to yield aminofurans. But this does not occur, as any aminofuran formed is readily converted into pyrazole.

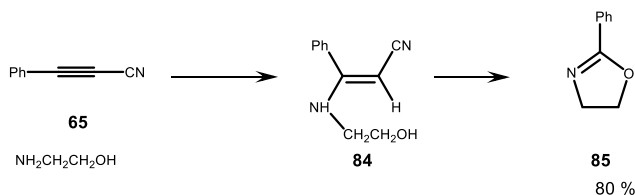
### 4.3.3.8 Synthesis of oxazolines

Benzoxazolines **78** were obtained in good yield from ethanolamines and phenylpropynenitrile (Scheme 4.38) [62].

A concerted *cis*-elimination mechanism can account for the formation of oxazolines. After the nucleophilic addition of the ethanolamine, the conjugated enaminic



**Scheme 4.37:** Synthesis of 5-amino-3-phenyl-1-(2-pyridyl)pyrazole.



**Scheme 4.38:** Synthesis of oxazolines.

adduct is obtained. During pyrolysis of the adduct, ring closure and elimination of acetonitrile yield the final product **85**.

#### 4.3.3.9 Synthesis of cyanoquinoline

Phenylpropynenitrile was heated under reflux with *o*-amino-benzyl alcohol to afford a crystalline adduct in 96% yield. After heating the adduct **87**, 2-phenyl-4H-3,1-benzoxazine, **88** and 2-phenyl-3-cyanoquinoline, **89** were obtained with 15 and 70% yield respectively as shown in Scheme 4.39 [64].

Compound **88** results from the intramolecular attack of the hydroxyl group followed by elimination of acetonitrile. The mechanistic steps involved in the formation of **89** include dehydration, ring closure and dehydrogenation.

#### 4.3.3.10 Synthesis of quinolines

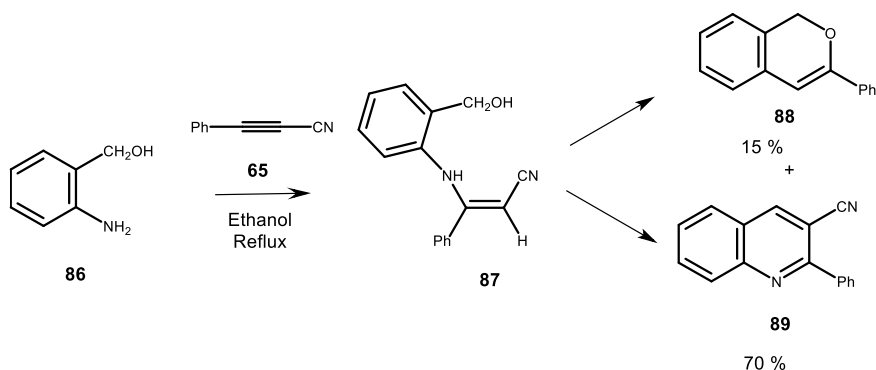
Phenylpropynenitrile and phenylhydroxylamine **95** gave 4-amino-2-(2-hydroxyphenyl)quinoline, but in 8% yield (Scheme 4.40) [65].

The reaction proceeds for 20 h under reflux in ethanol. The initial attack of phenylhydroxylamine yields 1-hydroxyl-4-imino-2-(phenyl)quinoline **91** that undergoes a 1,3-hydroxy shift to afford 4-amino-2-(2-hydroxyphenyl)quinoline **95**.

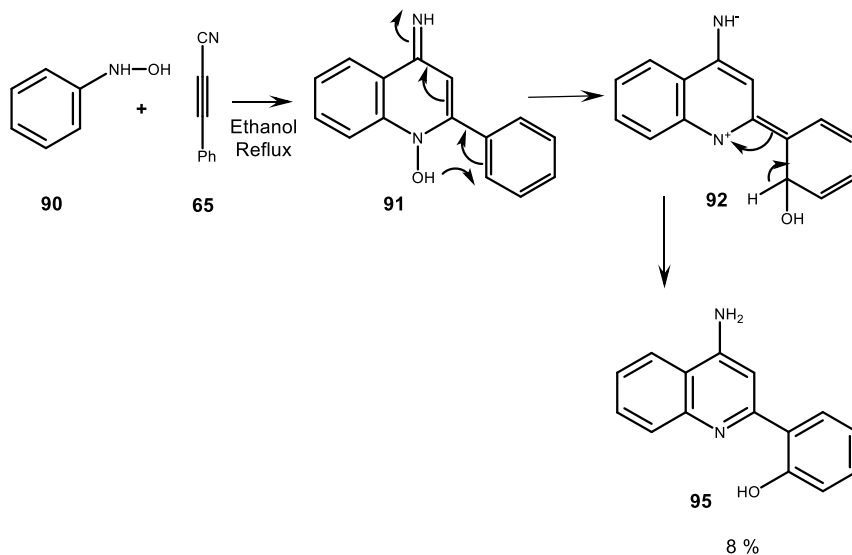
#### 4.3.3.11 Synthesis of pyrimidobenzimidazoles

When 3-phenylpropynenitrile was allowed to react with 2-aminobenzimidazole **62** and its 5,6-dimethyl derivative, 2-amino-4-phenylpyrimido[1,2-*a*]benzimidazoles, **87** were obtained in high yields (Scheme 4.41) [69].

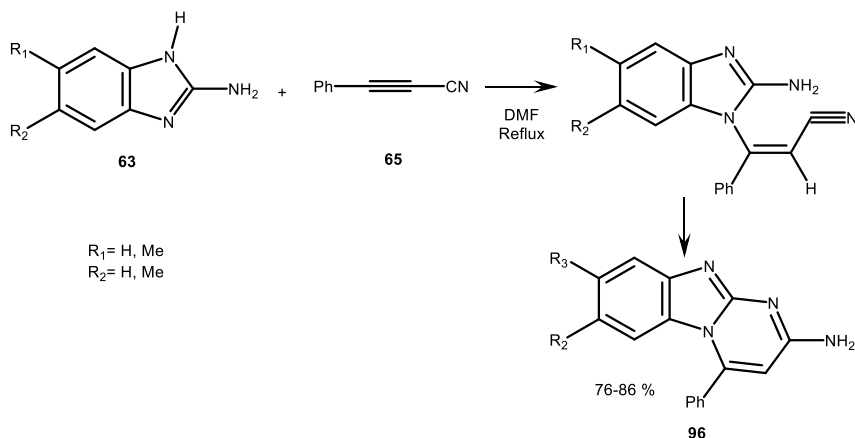
The reaction of phenylacetylene nitriles and the benzimidazoles very likely proceeded by the initial attack of the ring nitrogen of the benzimidazole to the acetylenic



**Scheme 4.39:** Synthesis of cyanoquinolines.



**Scheme 4.40:** Synthesis of cyanoquinolines.

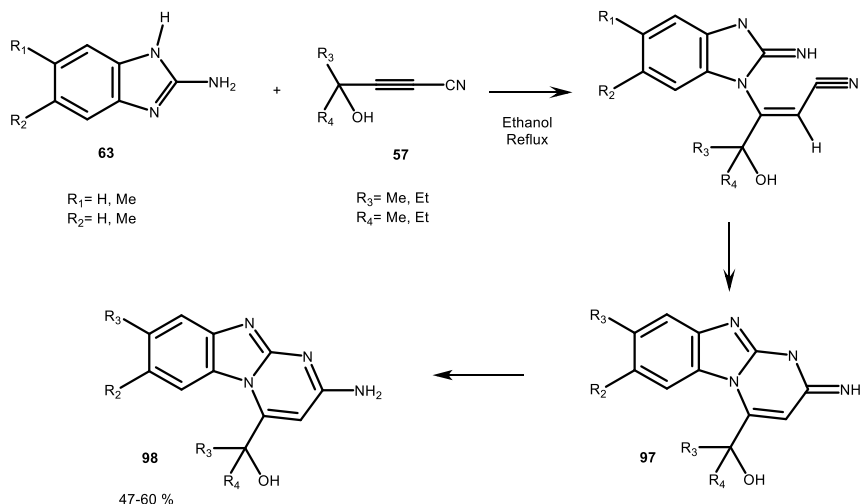


**Scheme 4.41:** Synthesis of 2-amino-4-phenylpyrimidobenzimidazoles.

$\beta$ -carbon, followed by cyclisation to give compound **96** (Scheme 4.42). The rate-determining step is the conjugate addition. All the spectroscopic and mass spectral data are in accord with the proposed structures.

When hydroxyacetylenic nitriles were used, 2-amino-4-(hydroxyalkyl)pyrimido [1,2-a]benzimidazoles, **98** were synthesized in good yields [70].

A protic solvent is required for the synthesis of pyrimidobenzimidazoles from hydroxyacetylenic nitriles and 2-aminobenzimidazoles.



**Scheme 4.42:** Synthesis of pyridobenzimidazoles.

However, when the reaction took place in DMF, it was found that (2, 2-dialkyl-2, 3-dihydrooxazo[3,2-a]benzimidazolylidene)ethane nitriles, **100** were formed (Scheme 4.43).

The formation of **100** proceeds only in the presence of an aprotic solvent and requires an activation energy higher than that needed for the formation of pyrimidobenzimidazoles **98**.

#### 4.3.4 Synthesis of heterocycles from acetylenic acids

The conjugate addition of 2-aminobenzothiazole **92** to the acetylenic acids in butanol, followed by cyclocondensation, gave the corresponding 2H-pyrimido[2,1-b]benzothiazol-2-ones **95** in 68–86% yield (Scheme 4.44) [71].

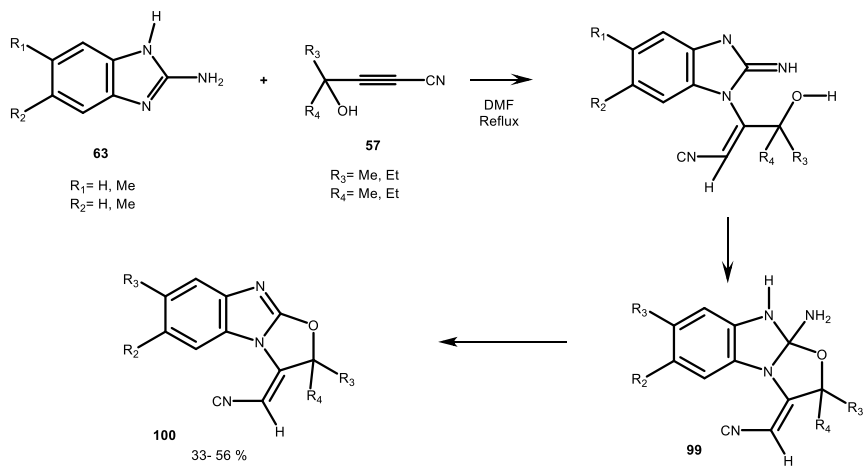
Pyrimidobenzothiazolones are formed when alkynoic acids are attacked at the  $\beta$ -carbon atom by the ring nitrogen atom of 2-aminobenzothiazole.

#### 4.3.5 Synthesis of heterocycles from acetylenic aldehydes

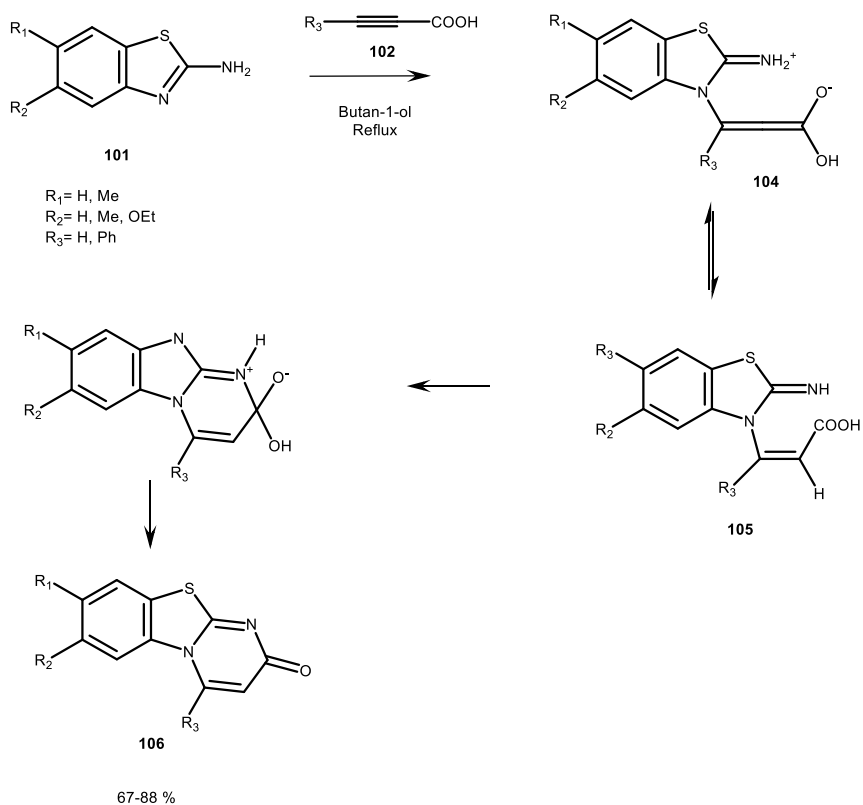
Acetylenic aldehydes **107** reacted with aminobenzimidazoles by conjugate addition to yield 4-pentyl and 4-phenylpyrimido[1,2-a]benzimidazoles **110** (Scheme 4.45) [69].

The reaction proceeds by the initial attack of the imino ring nitrogen of the benzimidazole to the acetylenic aldehyde, followed by cyclisation and dehydration to give compounds **110**. The  $^1\text{H}$  NMR signals of  $\text{H}_2$  and  $\text{H}_3$  are found in low fields around  $\delta = 8$  and 6 ppm, respectively.

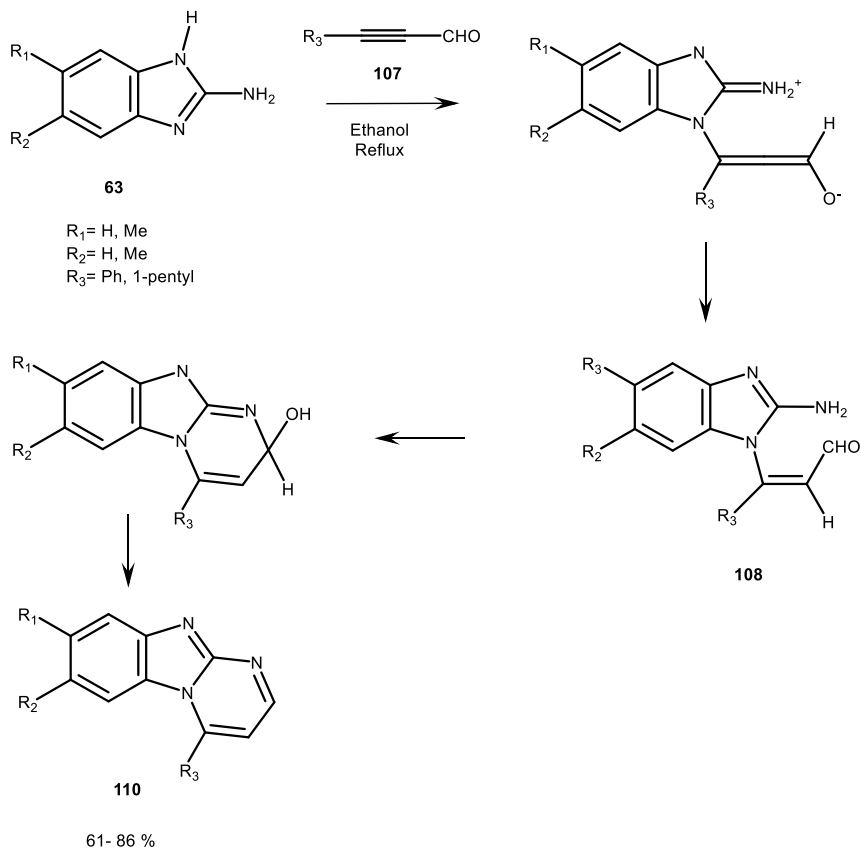




**Scheme 4.43:** Synthesis of oxazolo benzimidazolide ethane nitriles.



**Scheme 4.44:** Synthesis of pyrimidobenzothiazolones.



**Scheme 4.45:** Synthesis of pyrimidobenzimidazoles.

## 4.4 Biological applications of heterocycles

Some of the synthesized products were screened for potential biological activity.

### 4.4.1 Pyrimidopyrimidines

2-(1-Ethylpropyl)-4-iminopyrido (1, 2-a) pyrimidine monohydrate was subjected to pharmacological screening and was found to possess antiarrhythmic, antielectroshock and neuroleptic properties. 2-(1-Ethylpropyl)-4-iminopyrimido (1, 2-a) pyrimidine monohydrate was also screened and displayed diuretic, anti-oedema, anti-allergy and anti-ulcer effects (Schemes 4.11 and 4.12) [72].

#### 4.4.2 Pyrazolopyrimidines

5-isopropyl-7-aminopyrazolo[1,5- $\alpha$ ]-pyrimidine **40** displayed interesting pharmacological properties and can be used as an antihistamine, anticholinergic and a bronchodilator (Scheme 4.20).

#### 4.4.3 Aminopyridylpyrazoles

5-amino-3-pent-3yl-1-(2-pyridylpyrazole) **43** were screened for biological activity and were found to possess antielectroshock properties and were GABA antagonist (Scheme 4.21).

#### 4.4.4 Pyrimido(1,2a)benzimidazoles

The pyrimidobenzimidazoles **64** were found to possess the slight microbial activity and some antiarrhythmic effect. After the structure-activity relationship study, the pyrimidobenzimidazole moiety was found to be responsible for the activity and not the alkyl side chain. After screening, 2-Amino-7, 8-dimethyl-4-phenylpyrimido [1, 2-a]benzimidazole **96** found to be non-toxic and as a metabolic agent displayed diuretic properties.

#### 4.4.5 Oxazoles

5-amino-3-phenylisoxazole **78** exhibits significant activity as a behavioural depressor and muscle relaxing agent. It also showed significant anti-hypertensive and anti-oedema properties. It also possesses slight cataleptic, anti-electric shock, analgesic, GABA antagonism, anti-arrhythmic, platelet, aggregation inhibition, ADP, *in vitro*, platelet aggregation inhibition, collagen, *in vitro* diuretic and gastric irritation properties [73].

#### 4.4.6 Pyrimidobenzothiazolones

Substituted and unsubstituted 2H-pyrimido[2, 1-b] benzothiazol-2-ones **106** were identified as a new group of GABA<sub>A</sub>/benzodiazepine receptor ligands [74]. They can also be used as antibacterial and antifungal agents [75].

### 4.5 Current biological relevance of heterocycles

The presence of the thiazole core structure in drug design and the development of novel therapeutic agents have been reported [76, 77]. Researchers are focused on the

development of new antimicrobial agents with novel targets because the incidence of fungal infections is rapidly growing because of unselective antifungal activities and easily gained resistance [78, 79].

Sarojini et al. reported the synthesis 2-substituted 4-(2,5-dichloro thienyl)-1,3-thiazoles as a novel inhibitor of the L-glutamine: D-fructose-6-phosphate amidotransferase (GlcN-6-P synthase) [80]. A series of 2,4-disubstituted thiazole Schiff bases were synthesized by Bizzarri and co-workers and screened for their antifungal activity against 20 pathogenic *Candida* spp. and were found to be more active than clotrimazole and fluconazole [81]. Thiazole-bearing compounds also display antitubercular activities. In a study by Makam and co-workers, a series of 2-(2-hydrazinyl) thiazole derivatives were synthesized and evaluated against *M.tuberculosis*. Among the synthesized compounds, ethyl-4-methyl-2-[(E)-2-[1-(pyridin-2-yl)ethylidene]hydrazin-1-yl]-1,3-thiazole-5-carboxylate showed noticeable inhibitory activity against *Mycobacterium tuberculosis* with MIC value of 12.5 mM [82]. One of the most important biological properties of thiazole derivatives is its anticancer properties. Some were tested against malignant cancer cells and interesting results were reported [82–84]. Thiazoles derivatives were also reported to be valuable antiviral [85, 86], anticancer [83, 87] and anti-convulsant [88, 89] agents.

The biological activities of benzimidazole involve several biological mechanisms. Recent literature reports have shown the various substituted derivatives of benzimidazoles nucleus derivatives exhibiting remarkable biological activities. They have been reported to possess antitumor/antiproliferative/anticancer activity [90–92], antimicrobial including anti-HIV [93], cysticidal activities [94], antioxidant [95] and anti-inflammatory activities [96]. They also have a very good activity against *M. tuberculosis* [97].

The benzoxazole ring is a core structure found in a wide class of natural and synthetic compounds possessing anti-measles [98], antimicrobial [99], antifungal [100] and antibacterial [101] activities. Benzothiazoles and their derivatives exhibit antimicrobial [102], antitumor [103] and antiviral [104] activities.

The world is currently facing an unprecedented public health emergency of international concern because of the outbreak that originated in China in December 2019. The coronavirus responsible for the outbreak was named SARS CoV-2 by the World Health Organization. Heterocycles including indoles, pyrazoles, benzothiazoles, quinolines, pyridines, pyrimidines, thiazoles and their derivatives have been explored for activity against coronaviruses and may act as lead structures for the design and development of potent SARS CoV-2 inhibitors [105].

## 4.6 Conclusion

Double Michael addition of nucleophiles such as ethylenediamine, ethanoamine, o-aminophenols,  $\beta$ -aminoethanethiols, aminobenzothiols, 2-aminopyridines, 2-aminopyrimidines, phenylhydroxylamine, 2-aminobenzimidazoles, 2-aminobenzothiazoles to

allenic and acetylenic nitriles, hydroxyacetylenic nitriles, acetylenic acids, acetylenic aldehydes at various reaction conditions resulted in the synthesis of interesting heterocyclic systems such as imidazolines, imidazoles, oxazolines, benzoxazoles, quinolines, pyridopyrimidines, pyrimidopyrimidines, pyridobenzimidazoles, pyridobenzothiazoles in moderate to excellent yields. Only pyrimidobenzothiazolones, oxazoles, pyrimido[1,2a]benzimidazoles, aminopyridylpyrazoles, pyrazolopyrimidines and pyrimidopyrimidines biological activities have been reported by Fomum et al. The synthesized heterocycles must be tested on various fungi, bacteria and viruses and on challenging aspects of human health such as diabetes, Alzheimer's disease, tuberculosis, multiple drugs resistant cancers and coronaviruses.

**Acknowledgments:** The authors are grateful to the Department of Chemical Sciences of the University of Johannesburg. They are further grateful to the National Research Foundation of South Africa (NRF) for financial support to Marthe C. D. Fotsing (through grant No. 116740).

**Author contributions:** All the authors have accepted responsibility for the entire content of this submitted manuscript and approved submission.

**Research funding:** This work was supported by the National Research Foundation of South Africa (NRF) (through grant No. 116740).

**Conflict of interest statement:** The authors declare no conflicts of interest regarding this article.

## References

1. Shafiee A. Introduction for the special issue on bioactive heterocycles. *Eur J Med Chem* 2015;97: 14176.
2. Pathania S, Narang RK, Rawal RK. Role of sulphur-heterocycles in medicinal chemistry: an update. *Eur J Med Chem* 2019;180:486–508.
3. Bansal Y, Silakari O. The therapeutic journey of benzimidazoles: a review. *Bioorg Med Chem* 2012; 20:6208–36.
4. Shalini K, Sharma P, Kumar N. Imidazole and its biological activities: a review. *Chem Sin* 2010;1:36–47.
5. Legraverend M, Grierson DS. The purines: potent and versatile small molecule inhibitors and modulators of key biological targets. *Bioorg Med Chem* 2006;14:3987–4006.
6. Lim FPL, Dolzhenko AV. 1,3,5-triazine-based analogues of purine: from isosteres to privileged scaffolds in medicinal chemistry. *Eur J Med Chem* 2014;85:371–90.
7. Rescifina A. Book-reviews. *Eur J Med Chem* 2005;40:1071–2.
8. Huang S-T, Hsei I-J, Chen C. Synthesis and anticancer evaluation of bis(benzimidazoles), bis(benzoxazoles), and benzothiazoles. *Bioorg Med Chem* 2006;14:6106–19.
9. Sharma PC, Sharma D, Sharma A, Bansal KK, Rajak H, Sharma S, et al. New horizons in benzothiazole scaffold for cancer therapy: advances in bioactivity, functionality, and chemistry. *Appl Mater Today* 2020;20:100783.
10. Singh M, Singh SK, Gangwar M, Nath G, Sing SK. Design, synthesis and mode of action of some benzothiazole derivatives bearing an amide moiety as antibacterial agents. *RSC Adv* 2014;4: 19013–23.

11. Siddiqui N, Pandeya SN, Khan SA, Stables J, Rana A, Alam M, et al. Synthesis and anticonvulsant activity of sulfonamide derivatives-hydrophobic domain. *Bioorg Med Chem Lett* 2007;17:255–9.
12. Akhtar T, Hameed S, Al-Masoudi NA, Loddo R, Colla PL. *In vitro* antitumor and antiviral activities of new benzothiazole and 1,3,4-oxadiazole-2-thione derivatives. *Acta Pharm* 2008;58:135–49.
13. Palmer FJ, Trigg RB, Warrington JV. Benzothiazolines as antituberculous agent. *J Med Chem* 1971;14:248–51.
14. Burger A, Sawhney SN. Antimalarials. III. Benzothiazole amino alcohols. *J Med Chem* 1968;11:270–3.
15. Suresh CH, Rao JV, Jayaveera KN, Subudhi SK. Synthesis and anthelmintic activity of 3-(2-hydrozino benzothiazole)-substituted indole-2-one. *Int J Pharm* 2013;2:257–61.
16. Siddiqui N, Alam M, Siddiqui AA. Synthesis and analgesic activity of some 2-[[4-(alkyl thioureido) phenyl] sulphonamido]-6-substituted benzothiazoles. *Asian J Chem* 2004;16:1005–8.
17. Gurupadayya BM, Gopal M, Padmashali B, Vaidya VP. Synthesis and biological activities of fluoro benzothiazoles. *Indian J Heterocycl Chem* 2005;15:169–72.
18. Pattan SR, Suresh C, Pujar VD, Reddy VVK, Rasal VP, Koti BC. Synthesis and antidiabetic activity of 2-amino [5'-(4- sulphonylbenzylidene)-2,4-thiazolidinedione]-7-chloro-6-fluorobenzothiazole. *Indian J Chem B Org* 2005;44:2404–8.
19. Singh SP, Segal S. Study of fungicidal activities of some benzothiazoles. *Indian J Chem* 1988;27B:941–3.
20. Keri RS, Patil MR, Patil SA, Budagumpi S. A comprehensive review in current developments of benzothiazole-based molecules in medicinal chemistry. *Eur J Med Chem* 2015;89:207–51.
21. Danac R, Mangalagu II. Antimycobacterial activity of nitrogen heterocycles derivatives: bipyridine derivatives. Part III [13,14]. *Eur J Med Chem* 2014;74:664–70.
22. Rachakonda V, Alla M, Kotipalli SS, Ummani R. Design, diversity-oriented synthesis and structure activity relationship studies of quinolinyl heterocycles as antimycobacterial agents. *Eur J Med Chem* 2013;70:536–47.
23. Shchegolkov EV, Shchur IV, Burgart YV, Slepukhin PA, Evstigneeva NP, Gerasimova NA, et al. Copper(II) and cobalt(II) complexes based on methyl trifluorosallylate and bipyridine-type ligands: synthesis and their antimicrobial activity. *Polyhedron* 2020;194:114900.
24. Shiro T, Fukaya T, Tobe M. The chemistry and biological activity of heterocycle-fused quinolinone derivatives: a review. *Eur J Med Chem* 2014;97:397–408.
25. Kaur K, Jain M, Reddy RP, Jain R. Quinolines and structurally related heterocycles as antimalarials. *Eur J Med Chem* 2010;45:3245–64.
26. Gale JB. Recent advances in the chemistry and biology of retinoids. *Prog Med Chem* 1993;30:1–55.
27. Wei L, Malhotra SV. Synthesis and cytotoxicity evaluation of novel pyrido[3,4-d]pyrimidine derivatives as potential anticancer agents. *Med Chem Commun* 2012;3:1250–7.
28. Cody V, Pace J. Structural analysis of *Pneumocystis carinii* and human DHFR complexes with NADPH and a series of five potent 6-[5'-([omega]-carboxyalkoxy)benzyl]pyrido[2,3-d]pyrimidine derivatives. *Acta Crystallogr D* 2011;67:1–7.
29. Dehbi O, Tikad A, Bourg S, Bonnet P, Lozach O, Meijer L, et al. Synthesis and optimization of an original V-shaped collection of 4-7-disubstituted pyrido[3,2-d]pyrimidines as CDK5 and DYRK1A inhibitors. *Eur J Med Chem* 2014;80:352–63.
30. Buron F, Mérou JY, Akssira M, Guillaumet G, Routier S. Recent advances in the chemistry and biology of pyridopyrimidines. *Eur J Med Chem* 2015;95:76–95.
31. Prakash TB, Dinneswara Reddy G, Padmaja A, Padmavathi V. Synthesis and antimicrobial activity of (1, 4-phenylene) bis (arylsulfonylpyrazoles and isoxazoles). *Eur J Med Chem* 2014;82:347–54.
32. Vicini P, Geronikaki A, Anastasia K, Incerti M, Zani F. Synthesis and antimicrobial activity of novel 2-thiazolylimino-5-arylidene-4-thiazolidinones. *Bioorg Med Chem* 2006;14:3859–64.
33. Bae S, Hahn H-G, Nam KD, Mah H. Solid-phase synthesis of fungitoxic 2-imino-1,3-thiazolines. *J Comb Chem* 2005;7:7–9.

34. Flynn DL, Belliotti TR, Boctor AM, Connor DT, Kostlan CR, Nies DE, et al. Styrylpyrazoles, styrylisoaxazoles, and styrylisothiazoles. Novel 5-lipoxygenase and cyclooxygenase inhibitors. *J Med Chem* 1991;34:518–25.
35. Sondhi SM, Singh J, Kumar A, Jamal H, Gupta PP. Synthesis of amidine and amide derivatives and their evaluation for anti-inflammatory and analgesic activities. *Eur J Med Chem* 2009;44:1010–5.
36. Dadiboyena S, Nefzi A. Synthesis of functionalized tetrasubstituted pyrazolyl heterocycles – a review. *Eur J Med Chem* 2011;46:5258–75.
37. Stauffer SR, Coletta CJ, Tedesco R, Nishiguchi G, Carlson K, Sun J, et al. Pyrazole ligands: structure-affinity/activity relationships and estrogen receptor-alpha-selective agonists. *J Med Chem* 2000; 43:4934–47.
38. Fink BE, Mortensen DS, Stauffer SR, Aron ZD, Katzenellenbogen JA. Novel structural templates for estrogen-receptor ligands and prospects for combinatorial synthesis of estrogens. *Chem Biol* 1999;6:205–19.
39. Harrington WR, Sheng S, Barnett DH, Petz LN, Katzenellenbogen JA, Katzenellenbogen BS. Activities of estrogen receptor alpha- and beta-selective ligands at diverse estrogen responsive gene sites mediating transactivation or transrepression. *Mol Cell Endocrinol* 2003;206:13–22.
40. Baraldi PG, Tabrizi MA, Romagnoli S, Fruttarolo R, Merighi F, Varani K, et al. Pyrazolo[4,3-e] 1,2,4-triazolo[1,5-c]pyrimidine ligands, new tools to characterize A3 adenosine receptors in human tumor cell lines. *Curr Med Chem* 2005;12:1319–29.
41. Stauffer SR, Huang YR, Aron ZD, Coletta CJ, Sun J, Katzenellenbogen BS, et al. Triarylpyrazoles with basic side chains. *Bioorg Med Chem* 2001;9:151–61.
42. Ashton WT, Hutchins SM, Greenlee WJ, Doss GA, Chang RSL, Lotti VJ, et al. Nonpeptide angiotensin II antagonists derived from 1H-pyrazole-5-carboxylates and 4-aryl-1H-imidazole-5-carboxylates. *J Med Chem* 1993;36:3595–605.
43. Fomum ZT, Greaves PM, Landor PD, Landor SR. Allenes. Part XXVI. The synthesis of enaminic nitriles by the nucleophilic addition of amines to allenic nitriles. *J Chem Soc, Perkin Trans 1* 1973;1:1108–11.
44. Fomum ZT, Landor PD, Landor SR. Novel synthesis of imidazolines and imidazoles by Michael addition to allenic or acetylenic nitriles. *J Chem Soc Chem Commun* 1974:706a. <https://doi.org/10.1039/c3974000706a>.
45. Landor SR, Landor PD, Fomum ZT, Mpango GWB. Allenes. Part 38. Imidazolines, benzimidazoles, and hexahydrobenzimidazoles from 1,2-diamines and allenic or acetylenic nitriles. *J Chem Soc, Perkin Trans 1* 1979;1:2289–93.
46. Fomum ZT, Landor PD, Landor SR, Mpango GB. Oxazolines, thiazolines, oxazoles, thiazoles and pyrazoles from allenic and acetylenic nitriles. *Tetrahedron Lett* 1975;16:1101–4.
47. Fomum ZT, Asobo PF, Landor SR, Landor PD. Allenes. Part 42. nucleophilic addition of hydroxylamine to allenic and acetylenic nitriles; synthesis of 3-alkyl-5-amino,5-amino-3-phenyl-, and 3-amino-5-phenyl-isoxazoles. *J Chem Soc, Perkin Trans 1* 1984;1:1079–83.
48. Baldwin JE. Rules for ring closure. *J Chem Soc Chem Commun* 1976:734–6. <https://doi.org/10.1039/c39760000734>.
49. Landor SR, Landor PD, Fomum ZT, Mpango GM. N-phenylpyrazoles and 3H-indoles from allenic nitriles. A novel fischer-indole reaction. *Tetrahedron Lett* 1977;18:3743–6.
50. Fomum ZT, Landor SR, Landor PD, Mpango GWP. Allenes. Part 39. The synthesis of 3-alkyl-5-aminopyrazoles and 3H-Indoles from allenic or acetylenic nitriles. *J Chem Soc Perkin Trans 1* 1981:2997–3001. <https://doi.org/10.1039/p19810002997>.
51. Fomum ZT, Mbafor JT, Landor PD, Landor SR. Synthesis of 2- and 4-imino(1,2-a)pyridopyrimidines from allenic nitriles and 2-aminopyridines. *Tetrahedron Lett* 1981;22:4127–8.
52. Landor SR, Landor PD, Johnson A, Fomum ZT, Mbafor JT, Nkengfack AE, et al. Part 47. Pyrido[1,2-a] pyrimidines and their hydrolysis products from allenic and acetylenic nitriles. *J Chem Soc, Perkin Trans 1* 1988;1:975–9.

53. Landor SR, Johnson A, Fomum ZT, Nkengfack AE. Allenes. Part 50. Pyrimido[1,2-a]pyrimidines and pyrimido[1,6-a]pyrimidines and their hydrolysis products from allenic nitriles and phenylpropenenitrile. *J Chem Soc Perkin Trans I* 1989;609–13. <https://doi.org/10.1039/p19890000609>.
54. Landor SR, Landor PD, Fomum ZT, Mbafor JT. Novel syntheses of dihydrooxazines, tetrahydropyrimidines and tetrahydropyridines from allenyl nitriles. *Heterocycles* 1981;16:1889–92.
55. Fomum ZT, Mbafor JT, Landor SR, Landor PD. A novel synthesis of 5-alkyl-6-cyano-2,3-dihydro-4H-1,4-thiazines. *Heterocycles* 1982;19:465–8.
56. McMillan I, Stoodley RJ. A novel rearrangement of methyl 6-chloropenicillanate. *Tetrahedron Lett* 1966;7:1205–10.
57. Kitchin J, Stoodley RJ. Studies related to dihydro-1,4-thiazines. Part consequences of I83-sulphur migrations stereochemica. *J Chem Soc, Perkin Trans 1* 1985;1:2460–4.
58. Landor SR, Landor PD, Seliki-Muruumu J, Fomum ZT, Mbafor JT. Allenes. Part 48. A new general method for the synthesis of dihydro-4H-1, 4- thiazines. *J Chem Soc, Perkin Trans 1* 1988;1:1759–63.
59. Landor SR, Landor PD, Fomum ZT, Mbafor JT. Allenes-41: the addition of thiols to allenyl- and phenylpropynyl- nitrile and the formation of thiazolines and benzothiazoles. *Tetrahedron* 1984; 40:2141–9.
60. Fomum ZT, Asobo PF, Ifeadike PN. Heterocycles of biological importance. Part 1. Novel synthesis and biological activity study of 5-alkyl and 5-aryl-7-aminopyrazolo[1,5-a]-pyrimidines from allenic or acetylenic nitriles and 3-aminopyrazole. *J Heterocycl Chem* 1984;21:1125–8.
61. Fomum ZT, Ifeadike PN. Heterocycles of biological importance. Part 2. Novel synthesis and pharmacological evaluation of 5-amino-3-alkyl-1-(2-pyridyl)pyrazoles and 5-amino-3-phenyl-1-(2-pyridyl)pyrazole from allenic or acetylenic nitriles and 2-hydrazinopyridine. *J Heterocycl Chem* 1985;22:1611–4.
62. Fomum ZT, Nkengfack AE, Mpango GWP, Landor SR, Landor PD. Allenes. Part 44. Formation of oxazolines and benzoxazoles from allenic nitriles and amides and from phenylpropenenitriles. *J Chem Res* 1985;69:69.
63. Fomum ZT, Johnson A, Landor SR, Landor PD, Mbafor JT, Nkengfack AE, et al. Part 45. 2-alkyltetrahydropyrimidines, 2-alkylidetetrahydro-1,3-oxazines, 2-alkyl-5,6-dihydro-4H-1,3-oxazines and 2-alkyl-3-cyano-1,3,5,6-tetrahydropyridines from allenic nitriles. *J Chem Res* 1987:188–9.
64. Fomum ZT, Nkengfack AE, Landor SR, Landor PD. Allenes. Part 46. Synthesis of 1,2-dihydro-4H-3,1-benzoxazines, 4H-3,1-benzoxazines, and 3-cyanoquinolines from allenic and acetylenic nitriles. *J Chem Soc, Perkin Trans 1* 1988;1:277–81.
65. Landor SR, Fomum ZT, Asobo PF, Landor PD, Johnson A. Allenes. Part 49. 4-amino-2-(1-hydroxyalkyl)quinolines from phenylhydroxyl- amine and allenic nitriles. *J Chem Soc Perkin Trans I* 1989: 251–4. <https://doi.org/10.1039/p19890000251>.
66. Landor SR, Asobo PF, Fomum ZT, Roberts R. 5-amino-3-imino-2,3-dihydrofurans and 3-Amino-5-imino-2,5-dihydrofurans from 4,4- dialkyl-4- hydroxybut-2-yenenitriles. *J Chem Soc Perkin Trans I* 1991:1201–4. <https://doi.org/10.1039/p19910001201>.
67. Asobo PF, Wahe H, Mbafor JT, Nkengfack AE, Fomum ZT, Sopbue EF, et al. Heterocycles of biological importance. Part 5. The formation of novel biologically active pyrimido[1,2-a]benzimidazoles from allenic nitriles and aminobenzimidazoles. *J Chem Soc, Perkin Trans 1* 2001;1:457–61.
68. Fomum ZT, Asobo FA, Landor SR, Landor PD. A novel synthesis of 5-amino-2,3- or 5-lmino-2,5-dihydrofurans. *J Chem Soc Chem Commun* 1983:1455–6. <https://doi.org/10.1039/c39830001455>.
69. Wahe H, Asobob PF, Cherkasova RA, Nkengfackb AE, Folefocb GN, Fomum ZT, et al. Heterocycles of biological importance. Part 6. The formation of novel biologically active pyrimido [1, 2- a] benzimidazoles from electron deficient alkynes and 2-aminobenzimidazoles. *Arkivoc* 2003;2003:170–7.



70. Wahe H, Asobo PF, Cherkasov RA, Fomum ZT, Döpp D. Heterocycles of biological importance: Part 8. Formation of pyrimido[1,2-a]benzimidazoles and oxazolo[3,2-a] benzimidazoles by conjugate addition of 2-aminobenzimidazoles to 4-hydroxy-2-alkynenitriles. *Arhivoc* 2004;2004:130–7.
71. Wahe H, Mbafor JT, Nkengfack AE, Fomum ZT. Heterocycles of biological importance : Part 7. Synthesis of biologically active pyrimido [2, 1-b] benzothiazoles from acetylenic acids and 2-aminobenzothiazoles. *Arhivoc* 2003;2003:107–14.
72. Fomum ZT, Mbafor JT, Nkengfack AE. Heterocycles of biological importance. Part 4. a comparative study of the pharmaceutical potential of 2-(1-ethylpropyl)-4-iminopyrimido (1, 2-a)pyrimidine monohydrate and 2-(1-ethylpropyl)-4-iminopyrimido (1, 2-a)pyrimidine monohydrate. *Rev Sci Tech* 1985;2:73–88.
73. Fomum ZT, Asobo PF. Heterocycles of biological importance. Part 3. 5-amino-3-phenylisoxazole: a behaviour depressing, muscle relaxing anti-hypertensive and anti-edema compound. *Rev Sci Tech* 1984;1:105–12.
74. Ai J, Wang X, Wahe H, Fomum ZT, Sterner O, Nielsen M, et al. 2-oxo-2H-pyrimido[2,1-b]benzothiazoles inhibit brain benzodiazepine receptor binding *in vitro*. *Pharmacology* 2000;60:175–8.
75. Gupta S, Ajmera N, Gautam N, Sharma R, Gautam DC. Novel synthesis and biological activity study of pyrimido [2, 1- b] benzothiazoles. *Indian J Chem* 2009;48:853–7.
76. Sharma PC, Bansal KK, Sharma A, Sharma D, Deep A. Thiazole-containing compounds as therapeutic targets for cancer therapy. *Eur J Med Chem* 2020;188:112016.
77. Kashyap SJ, Garg VK, Sharma PK, Kumar N, Dudhe R, Gupta JK, Thiazoles: having diverse biological activities. *Med Chem Res* 2012;21:2123–32.
78. Strasfeld L, Chou SWC. Antiviral drug resistance: mechanisms and clinical implications. *Infect Dis Clin* 2011;24:413–37.
79. Molnar A. Antimicrobial resistance awareness and games. *Trends Microbiol* 2019;27:1–3.
80. Milewski S, Gabriel I, Olchowy J. Enzymes of UDP-GlcNAc biosynthesis in yeast. *Yeast* 2006;23:1–14.
81. Chimenti F, Bizzarri B, Bolasco A, Secci D, Chimenti P, Granese A, et al. Synthesis and biological evaluation of novel 2,4-disubstituted-1,3-thiazoles as anti-Candida spp. agents. *Eur J Med Chem* 2011;46:378–82.
82. Makam P, Kankanala R, Prakash A, Kannan T. 2-(2-hydrazinyl)thiazole derivatives: design, synthesis and *in vitro* antimycobacterial studies. *Eur J Med Chem* 2013;69:564–76.
83. Mohammadi-Farani AR, Foroumadi A, Kashani MR, Aliabadi AR. N-phenyl-2-P-tolylthiazole-4-carboxamide derivatives: synthesis and cytotoxicity evaluation as anticancer agents. *Iran J Basic Sci Med* 2014;17:502–8.
84. Mahmoodi M, Aliabadi A, Emami S, Safavi M, Rajabalian S, Mohagheghi MA, et al. Synthesis and *in-vitro* cytotoxicity of poly-functionalized 4-(2-arylthiazol-4-yl)-4H-chromenes. *Arch Pharm (Weinheim)* 2010;343:411–6.
85. Liu Y, Jing F, Xu Y, Xie Y, Shi F, Fang H, et al. Design, synthesis and biological activity of thiazolidine-4-carboxylic acid derivatives as novel influenza neuraminidase inhibitors. *Bioorg Med Chem* 2011; 19:2342–8.
86. Wang W-L, Yao DY, Gu M, Fan MZ, Li JY, Xing YC, et al. Synthesis and biological evaluation of novel bisheterocycle-containing compounds as potential anti-influenza virus agents. *Bioorg Med Chem Lett* 2005;15:5284–7.
87. Aliabadi A, Shamsa F, Ostad SN, Emami S, Shafiee A, Davoodi J, et al. Synthesis and biological evaluation of 2-phenylthiazole-4-carboxamide derivatives as anticancer agents. *Eur J Med Chem* 2010;45:5384–9.
88. Ahangar N, Ayati A, Alipour E, Pashapour A, Foroumadi A., Emami S. 1-[(2-arylthiazol-4-yl)methyl] azoles as a new class of anticonvulsants: design, synthesis, *in vivo* screening, and *in silico* drug-like properties. *Chem Biol Drug Des* 2011;78:844–52.

89. Amin KM, Rahman DEA, Al-Eryani YA. Synthesis and preliminary evaluation of some substituted coumarins as anticonvulsant agents. *Bioorg Med Chem* 2008;16:5377–88.
90. Demirayak S, Kayagil I, Yurttas L. Microwave supported synthesis of some novel 1,3-diarylpyrazino[1,2-a]benzimidazole derivatives and investigation of their anticancer activities. *Eur J Med Chem* 2011;46:411–6.
91. Abonia R, Cortés E, Insuasty B, Quiroga J, Noguera M, Cobo J. Synthesis of novel 1,2,5-trisubstituted benzimidazoles as potential antitumor agents. *Eur J Med Chem* 2011;46:4062–70.
92. Refaat HM. Synthesis and anticancer activity of some novel 2-substituted benzimidazole derivatives. *Eur J Med Chem* 2010;45:2949–56.
93. Sharma D, Narasimhan B, Kumar P, Judge V, Narang R, De Clercq E, et al. Synthesis, antimicrobial and antiviral activity of substituted benzimidazoles. *J Enzym Inhib Med Chem* 2009;24:1161–8.
94. Francisca P, Jung-Cook H, Pérez-Villanueva J, Piliado JC, Rodríguez-Morales S, Palencia-Hernández G, et al. Synthesis and *in vitro* cysticidal activity of new benzimidazole derivatives. *Eur J Med Chem* 2009;44:1794–800.
95. Kuş C, Ayhan-Kılıçgil G, Özbey S, Kaynak FB, Kaya M, Çoban T, et al. Synthesis and antioxidant properties of novel N-methyl-1,3,4-thiadiazol-2-amine and 4-methyl-2H-1,2,4-triazole-3(4H)-thione derivatives of benzimidazole class. *Bioorg Med Chem* 2008;16:4294–303.
96. Achar KCS, Hosamani KM, Seetharamareddy HR. In-vivo analgesic and anti-inflammatory activities of newly synthesized benzimidazole derivatives. *Eur J Med Chem* 2010;45:2048–54.
97. Gong Y, Karakaya SS, Guo X, Zheng P, Gold B, Ma Y, et al. Benzimidazole-based compounds kill *Mycobacterium tuberculosis*. *Eur J Med Chem* 2014;75:336–53.
98. Sun A, Prussia A, Zhan W, Murray EE, Doyle J, Cheng LT, et al. Nonpeptide inhibitors of measles virus entry. *J Med Chem* 2006;49:5080–92.
99. Alper-Hayta S, Arisoy M, Temiz-Arpaci Ö, Yıldız I, Aki E, Özkan S, et al. Synthesis, antimicrobial activity, pharmacophore analysis of some new 2-(substitutedphenyl/benzyl)-5-[(2-benzofuryl)carboxamido]benzoxazoles. *Eur J Med Chem* 2008;43:2568–78.
100. Ertan T, Yıldız I, Tekiner-Gulbas B, Bolelli K, Temiz-Arpaci O, Ozkan S, et al. Synthesis, biological evaluation and 2D-QSAR analysis of benzoxazoles as antimicrobial agents. *Eur J Med Chem* 2009;44:501–10.
101. Sun L-Q, Chen J, Bruce M, Deskus JA, Epperson JR, Takaki K, et al. Synthesis and structure-activity relationship of novel benzoxazole derivatives as melatonin receptor agonists. *Bioorg Med Chem Lett* 2004;14:3799–802.
102. Shi D-Q, Rong S-F, Dou G-L. Efficient synthesis of 2-arylbenzothiazole derivatives with the aid of a low-valent titanium reagent. *Synth Commun* 2010;40:2302–10.
103. Gilchrist TL. *Heterocyclic chemistry*, 3rd ed. England: AddisonWesley Longman, Ltd.; 1998.
104. Lednicher D. *Strategies for organic drugs synthesis and design*. New York: Wiley & Sons; 2008.
105. Negi M, Chawla PA, Faruk A, Chawla V. Role of heterocyclic compounds in SARS and SARS CoV-2 pandemic. *Bioorg Chem* 2020;104:104315.



Djellouli Fayrouz\*, Dahmani Abdallah and Hassani Aicha

## 5 Experimental investigation of ternary mixture of diclofenac sodium with pharmaceutical excipients

**Abstract:** The goal of this work was the study of drug-excipient interactions of ternary mixtures between diclofenac sodium when introduced with excipients commonly explored in solid dosage formulas such as microcrystalline cellulose and stearic acid obtained by three methods. Differential scanning calorimetry (DSC) (DSC), Fourier transform infrared spectroscopy (FTIR), scanning electron microscopy (SEM), and the structural characterization technique of diffraction (XRPD) were used to investigate the characterization and potential physical and chemical interactions of solid products of diclofenac sodium with excipients prepared by different methods. This work revealed a possible interaction between diclofenac sodium, microcrystalline cellulose, and stearic acid in mixture prepared by microwave irradiation also; it was found compatibility for ternary mixtures prepared by physical mixture and co evaporation methods. Results of this study can be useful in the development of the method of preparation and select adequate excipients with suitable compatibility.

**Keywords:** compatibility; diclofenac sodium; DSC; interaction; ternary.

### 5.1 Introduction

Frequently, the formulation of drug involves the research of multicomponent systems established on drug–drug and drug-excipient mixtures. It is clearly known that the interactions of drug-excipient can profoundly affect the technical and biopharmaceutical qualities of solid dosage forms [1–5]. In the course of the formulation of new drug, it is important to evaluate physical and chemical interactions between drug-excipient which can strongly affect the physical–chemical properties and biological activities of the final dosage form such as chemical–physical stability, propriety

---

**\*Corresponding author: Djellouli Fayrouz**, Laboratoire de Thermodynamique et Modélisation Moléculaire, Faculté de Chimie, USTHB, Alger, Algeria; and Laboratoire de Recherche sur les Produits Bioactifs et la Valorisation de la Biomasse BP 92, 16050 Vieux Kouba, Alger, Algeria, E-mail: alafa2006@yahoo.fr

**Dahmani Abdallah**, Laboratoire de Thermodynamique et Modélisation Moléculaire, Faculté de Chimie, USTHB, Alger, Algeria

**Hassani Aicha**, Laboratoire de Recherche sur les Produits Bioactifs et la Valorisation de la Biomasse BP 92, 16050 Vieux Kouba, Alger, Algeria

This article has previously been published in the journal *Physical Sciences Reviews*. Please cite as: D. Fayrouz, D. Abdallah and H. Aicha "Experimental investigation of ternary mixture of Diclofenac sodium with pharmaceutical excipients" *Physical Sciences Reviews* [Online] 2021, 7. DOI: 10.1515/psr-2020-0111 | <https://doi.org/10.1515/9783110710823-005>

of solubility, rate of dissolution, and criteria of biodisponibility [5–11]. Thermal analysis methods find wide application in drug chemistry, starting with the testing of raw materials, demonstration of stability, compatibility of compositions, and preparation of new formulations [10–14] (Table 5.1).

The technique of scanning calorimetry (DSC) (DSC) has shown to be a rapid and specific process for evaluating and predicting chemical–physical interactions between an active ingredient and pharmaceutical excipients [12, 14]. Interactions analysis is performed by analyzing the differences in thermograms DSC of the drug mixed with the excipient through the comparison to the individual drug DSC [11]. During the preparation of the mixtures, the excipients (in 1:1:1 portions) are introduced in a way that ensures good adhesion [14].

Physical or chemical interactions in the solid state between the constituents do not certainly show an structural (physic–chemical) incompatibility, but it is well known that the presence (appearance) of new DSC responses (new peaks), change or disappearance of current peak and/or change in the value of heat of fusion are signs of non compatibility [14].

It is crucial to note that the techniques and the method of preparation of the mixtures play a determining role in the final behavior of the materials and therefore their properties. Therefore, for each physical or chemical property there is a corresponding characterization technique [8].

The excipients used as additives drug are recognized to help administration and moderate the release of the active constituent. Physical and chemical interactions between drugs and excipients can modify the physico–chemical nature, the degree of

**Table 5.1:** Temperature of pure diclofenac sodium (DHNa), microcrystalline cellulose (MCC), and acid stearic (AS) and ternary mixtures prepared by physical mixture (PM), co evaporation (CE), and microwave irradiation (MW). 1: PM; 2: CE; 3: MW.

	<i>Tonset</i> (°C)
DHNa	50.69
	71.74
	113.62
	158.36
MCC	259
	37
AS	66.47
PM	65.49
	78.22
	86.72
CE	61.65
	74.19
	240
MW	62.06

stability and biological response of drug products, and subsequently, their therapeutic efficiency and safety [2]. Microcrystalline cellulose (MCC) is extensively used in a variety of oral and topical medication. It is also widely required in cosmetics and nutrition products. Then, MCC is used as inactive filler in tablets and as a thickener and stabilizers in industrial foods.

Diclofenac sodium is a NSAIDs (non steroidal anti inflammatory) drug presented in numerous pharmaceutical dosage forms [15]. It reveals a complex in solid state and can be present in different hydrate phases. Wide literature is accessible on physico-chemical and spectral characteristics for diclofenac sodium non hydrated form, and, its crystalline edifice and thermal behavior have been detailed in literature [15–24]. A tetrahydrate form of diclofenac has been previously described [18–21]. It was showed that diclofenac sodium hydrate (DSH) has physicochemical characteristics dissimilar from Diclofenac sodium anhydrous that can affect the physico-chemical and pharmaceutical properties of the finished product [23].

Compatibility of diclofenac sodium with excipients was investigated by DSC [25–29] and was found to exhibit interactions with povidone. Stearic acid, PEG 6000, although it is compatible with starch, microcrystalline cellulose, and titanium dioxide [26].

Tita [7] used a thermal analysis TG/DTG and DSC as selection techniques for determination the physico-chemical concordance between diclofenac sodium and its physical binary mixtures with several different excipients: starch, microcrystalline cellulose, colloidal silicon, di-oxide, lactose (monohydrate and anhydre), polyvinylpyrrolidone, magnesium stearate, and talc.

The spectral response of TG/DTG and DSC of diclofenac sodium and each excipient were discussed and related with those of binary mixtures. The investigated spectroscopy like: Fourier transformed infrared spectroscopy (FTIR) and the structural identification technique such as X-ray powder diffractometry (XRPD) was explored as complementary methods to support the understanding of the experimental results. Based on screening calorimetry results, supported by IR and diffraction characterisations, diclofenac sodium was discovered to be non-compatible with lactose monohydrate, anhydre, povidone, and magnesium stearate, respectively.

Recently, Nugrahani et al. [30] synthesized a novel salt co crystal in the form of an unstable diclofenac – sodium – proline monohydrate with the aim of increasing the solubility and dissolution of diclofenac sodium (compared to isolated diclofenac sodium).

In our work, DSC, FTIR, SEM, and XRPD experimental analyses were investigated in order to evaluating the interaction between diclofenac sodium with excipients usually required in solid dosage systems: microcrystalline cellulose as diluent, and stearic acid as lubricant on 1:1:1 mass/mass drug-exciipient ternary mixtures prepared by three different methods: physical mixture (PM), co evaporation (CE), and microwave irradiation (MW).

## 5.2 Materials and methods

### 5.2.1 Materials

Diclofenac sodium and microcrystalline cellulose were procured from Saidal Laboratories, Algeria. Stearic acid was obtained from Merck Company with purity greater than 0.98 (in mass fraction). All these products were used without further purification.

### 5.2.2 Sample preparation

The diclofenac sodium and microcrystalline cellulose, also stearic acid mixtures at 1:1:1 w/w/w ratio was mixed by three diverse methods: physical mixture (PM), co evaporation (CE) and microwave irradiation (MW).

Physical mixture of DHNa/cellulose/A.S (PM) was individually weighed and was obtained by mixing them in a ceramic mortar for 5 min. The mortar and pestle implements are required to grind lightly the sample.

Co evaporated mixture of diclofenac sodium and microcrystalline cellulose and stearic acid mixtures (CE) was dissolved in 20 mL of DMSO, and was subjected to magnetic stirring at 60 °C for 2 h and the obtained clear solution was evaporated at room temperature, MW-irradiated sample of DHNa/cellulose/A.S (MW) was individually weighed and was dissolved in 20 mL of DMSO, and was subjected to stirring at ambient temperature for 30 min and the obtained solution was subjected to microwave irradiation at 300 W for 10 min.

### 5.2.3 Infrared spectroscopy

The FTIR data was recorded using an spectrophotometer NICOLET model 6700 equipped with a DTGS detector coupled to a microscope NICOLET CONTINUμM, the latter is equipped with an MCT detector/A (Mercury Cadmium Telluride) in the frequency interval of 400–4000  $\text{cm}^{-1}$  with a resolution of 10  $\text{cm}^{-1}$  using potassium bromide discs method. The drug and each mixture were prepared with dried KBr powder and compacted to a 12 mm disc by a particular press (hydraulic) at 10 tonnes strength compression for 30 s.

### 5.2.4 Differential scanning calorimetry

While the DSC analysis, the samples are introduced in the sealed aluminum sample holders.

The fluid nitrogen atmosphere was used to record the DSC curve at 5 °C/min of the constant heating rate (the interval of the used temperature is maintained between: 25–300 °C). In this experimental stage, the heat flux DSC (DSC131, Setaram) was employed.

The phase transformation temperatures were directly obtained from the recorded curves using the user-friendly interface software previously delivered with the DSC apparatus accessories.

Approximately 5 mg of samples were used in this characterization. The masses of the samples were thought by  $\pm 0.0002$  g accuracy via a balance of the Mettler H31 type. The melting point of indium was required as a standard to adjust the operation of DSC apparatus. The error intervals of the measurements are maintained to be  $\pm 0.20$  K for the  $T^\circ$  temperatures and  $\pm 0.40$  kJ/mol for the enthalpy of fusion.

### 5.2.5 X-ray powder diffraction

The X-ray diffraction spectra for free samples as well as those of ternary mixture were recorded using the X-ray diffractometer (ITAL STRUCTURES-Diffractomètre APD2000) at 30 kV, 30 mA over a range of 10–100°, at the rate of scanning fixed to  $2^\circ 2\theta \text{ min}^{-1}$ ,  $2\theta$ , using CuK radiation wavelength 1.5405 Å.

### 5.2.6 Scanning electron microscopy

The scanning electron microscope of the type of FEI Quanta 600, functioning between 3 and 30 kV was exploited to obtain the electron micrograph of crystals.

The studied samples were fixed to a metal stub (double sided adhesive tape). After this step, the samples are heated in under vacuum with gold in an inert argon atmosphere (prior to observation).

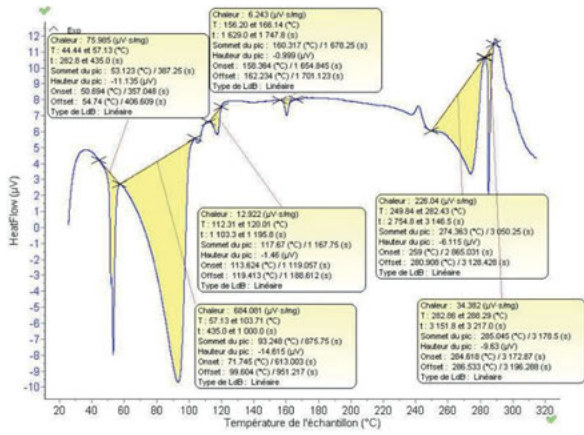
## 5.3 Discussion of experimental results

### 5.3.1 DSC

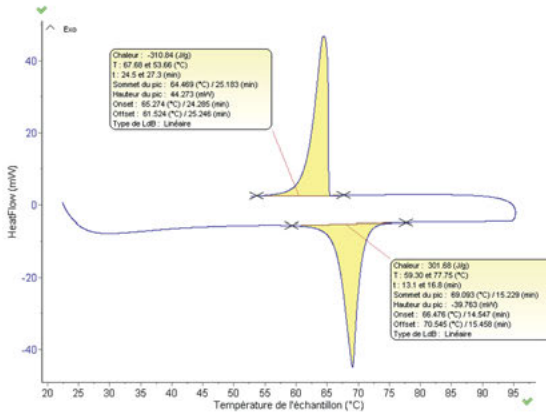
The DSC graphical response of diclofenac sodium DHNa displays two sharp endothermic peaks Tonset at 50.69 °C, and Tonset 71.74 °C indicated two transition phases as indicated in the literature [8]. Two small endothermic peaks were observed at 113.62 and 158.36 °C. This was probably because of some structural rearrangements and an endothermic effect at 259 °C, equivalent to the melting point. Then, the final decomposition of drug is purely exothermic phenomena. The thermogram DSC for diclofenac sodium was similar to the published DSC thermogram [29]. The DSC thermogram for the acid has shown single endothermic peak corresponding to the melting at, 55.25 °C.

The DSC curves of individual sample and the respective tri components systems obtained by physical mixture preparation; PM, co evaporation, CE and MW irradiation techniques are shown in Figure 5.1 and Figure 5.2, respectively. Modifications were recorded in the DSC response of DHNa in comparison with ternary mixture.

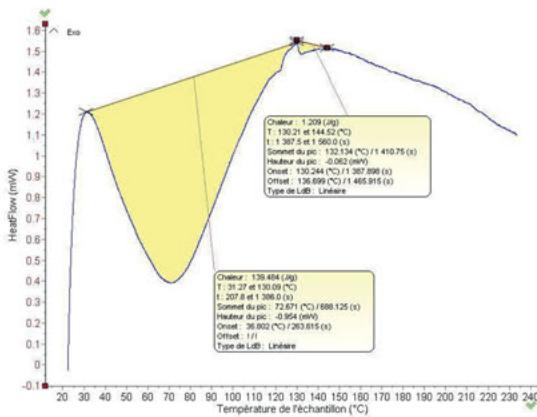




DHNa



AS



MCC

Figure 5.1: DSC thermogram of pure diclofenac sodium (DHNa), microcrystalline cellulose (MC), and acid stearic (AS).

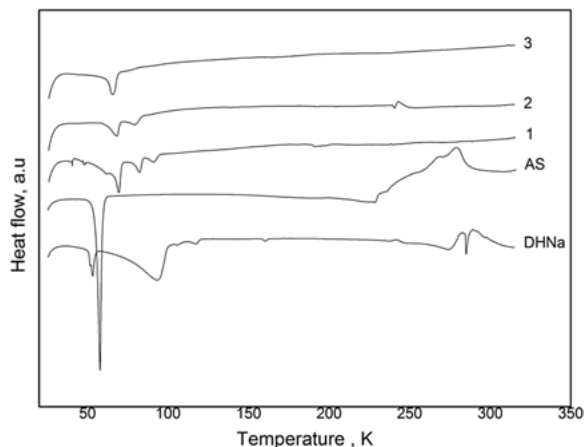


**Figure 5.2:** DSC thermogram of pure diclofenac sodium (DHNa), and acid stearic (AS) and ternary mixtures prepared by physical mixture (PM), co evaporation (CE), and microwave irradiation (MW). 1: PM; 2: CE; 3: MW.

The curve of the ternary systems prepared by PM has shown three endothermic events shifted to 65.49; 78.22; and 86.72 °C, these slight modifications in the responses of the endothermic phenomena of drug might be due to the efficient of excipients involvement in the drug [9].

The DSC curve for ternary systems prepared by CE, where the melting point of the drug moves to greater temperatures of Tonset = 61.65, 74.19, 240 °C, respectively, which can be attributed to the melting point followed by decomposition.

Consequently, the endothermic interval of DHNa was commonly conserved, with simply small modifications in rappings of enlargement or displacement to inferior temperatures. These slight fluctuations can be because of the involvement of the mixture constituents, which let down their purity and cannot be considered indications of efficient incompatibility [5].

Transformations were detected in the DSC responses of ternary systems prepared by MW, (sample 3) has shown one endothermic event at Tonset = 62.06 °C. At the melting point of DHNa, the endothermic peak disappeared. These results indicated the occurrence of a strong interaction in the solid state.

### 5.3.1.1 FTIR

FTIR has been used as a complementary analysis to inspect the physical reactivity appeared between drug and multi components mixtures (excipients) and to clarify the DSC results. The FTIR response of pure diclofenac sodium displayed a characteristic bands at 3386  $\text{cm}^{-1}$  due to NH stretching of the secondary amine, 1558  $\text{cm}^{-1}$  owing to  $\text{C}=\text{O}$  stretching of the carboxyl ion, 1393  $\text{cm}^{-1}$  resulted from C–N stretching and at

$767\text{ cm}^{-1}$  because of C–Cl stretching band of the O–H at  $3257\text{ cm}^{-1}$ , stretching vibrations of C=C at  $1453/1469\text{ cm}^{-1}$ , followed by C–O–CH<sub>3</sub> stretching at  $1305\text{ cm}^{-1}$ . The FTIR spectra (Figure 5.3) did not illustrate confirmation on chemical interaction in samples at the solid state. Furthermore, the FT-IR bands of ternaries combinations can be taken as the superposition of the separate ones with inexistence of deficiency, change, or enlargement in the vibration bands of DHNa. It was found the nonappearance of chemical interactions between DHNa and microcrystalline cellulose, and stearic acid, indicating that the change displayed in DSC responses can be assigned to a possible interaction of the physical type.

### 5.3.1.2 XRPD

X-ray powder diffraction has been investigated for quantitative–qualitative analysis and confirmation of structural crystallinity. Samples (PM; CE; and MW) were crystalline character (Figure 5.4) and showed several diffraction peaks with differences, both in positions and intensity ratios distinguishing itself from the pure DHNa that could be recognized to an interaction in drug-excipients mixtures. Some of the characteristics peaks of the drug are found in mixtures, and DHNa demonstrating the same crystalline structure.

Noticeably, the intensity of some peaks is lower for MW as compared to their corresponding mixtures PM and CE, which can be attributed to a possible interaction.

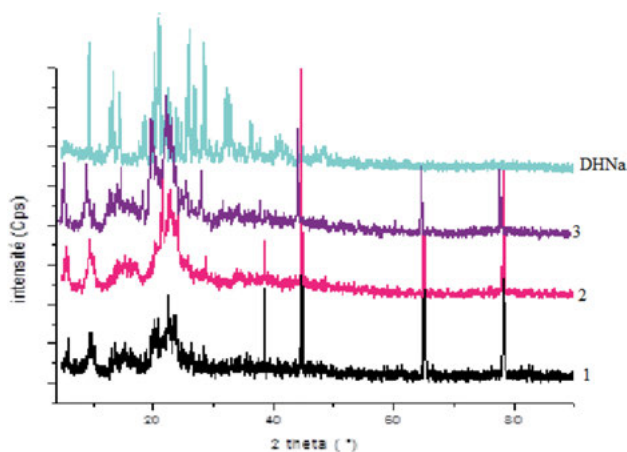


**Figure 5.3:** X-ray powder diffraction of pure diclofenac sodium (DHNa) and ternary mixtures prepared by physical mixture (PM), co evaporation (CE), and microwave irradiation (MW). 1: PM; 2: CE; 3: MW.

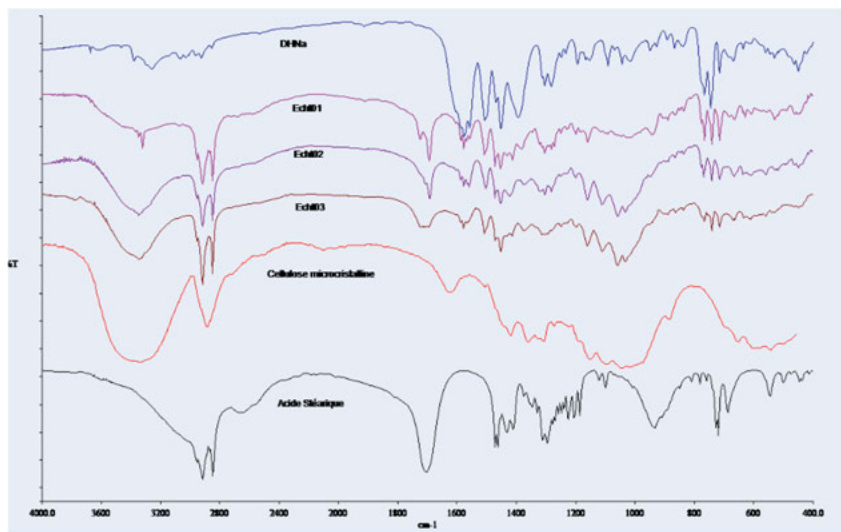


**Figure 5.4:** FTIR spectrum of pure diclofenac sodium (DHNa), microcrystalline cellulose (MCC) and acid stearic (AS), and ternary mixtures prepared by physical mixture (PM), co evaporation (CE), and microwave irradiation (MW). 1: PM; 2: CE; 3: MW.

### 5.3.2 SEM

Scanning electron microscopy (SEM) is a method permits viewing of the morphology of surface compounds (constituents and mixtures), it is recommended when there are typical differences in their crystal behaviors. The SEM technique cannot provide any data about the chemical structure/thermal compartment of drug constituents. The SEM photomicrographs taken at different magnifications are given in Figure 5.5. It was detected that DHNa/MC/As mixture is characterized by different morphology and shaped crystals.

## 5.4 Conclusions

In the present work, experimental data of DSC with combination of SEM analysis with spectroscopic techniques, such as XPRD and FTIR were effectively engaged to evaluate the physical–chemical interaction of diclofenac sodium with the different excipients. The changes found in the DSC response recommended a possible interaction of diclofenac sodium with microcrystalline cellulose and stearic acid in the mixture prepared by MW irradiation. A small change was observed in the ternary systems

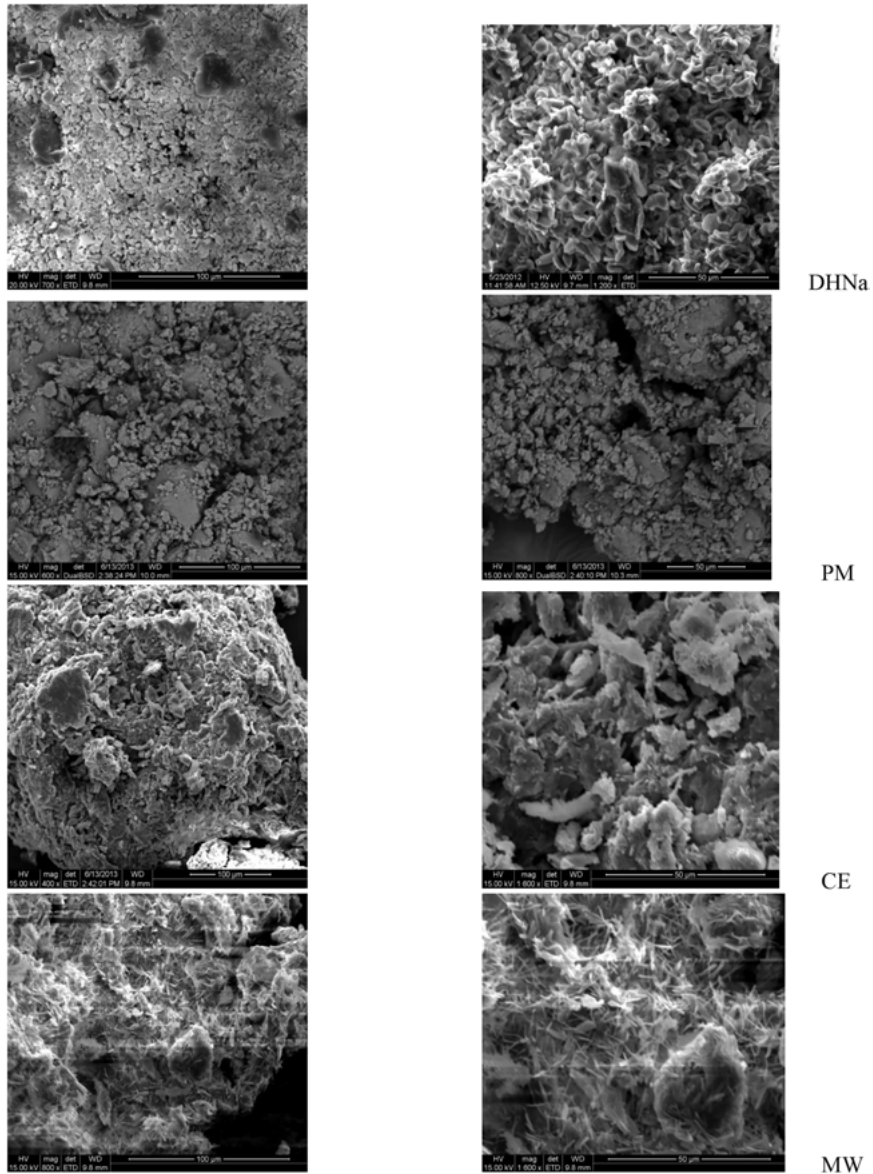


**Figure 5.5:** Scanning electron micrographs at different magnifications of pure diclofenac sodium (DHNa), and ternary mixtures prepared by physical mixture (PM), co evaporation (CE), and microwave irradiation (MW).

prepared by physical mixture; PM, and co evaporation (CE), which suggested compatibility, and could be because of the mixing of the components.

Results of this study can be useful in the development of the method of preparation and select adequate excipients with suitable compatibility.

**Author contributions:** All the authors have accepted responsibility for the entire content of this submitted manuscript and approved submission.

**Research funding:** This scientific work was financial sustained by CNEPRU Project (MESRS) N° E00220130108.

**Conflict of interest statement:** The authors declare no conflicts of interest regarding this article.

## References

1. Jackson K. Drug excipient interactions and their effect on absorption. *Pharm Sci Technol* 2000;3: 336–45.
2. Rowe RC, Sheskey PJ, Quinn ME. Handbook of pharmaceutical excipients, 6th ed. London: Pharmaceutical Press; 2009.
3. Giron D. Applications of thermal analysis in the pharmaceutical industry. *J Pharmaceut Biomed Anal* 1986;4:755–70.
4. Barboza F, Vecchia DD, Tagliari MP, Silva MAS, Stulzer HK. Differential scanning calorimetry as a screening technique in compatibility studies of acyclovir extended release formulations. *Pharm Chem J* 2009;43:363–8.
5. Vueba ML, Veiga F, Sousa JJ, Pina ME. Compatibility studies between ibuprofen or ketoprofen with cellulose ether polymer mixtures using thermal analysis. *Drug Dev Ind Pharm* 2005;31:943–9.
6. Bharate SS, Bharate SB, Bajaj AN. Interactions and incompatibilities of pharmaceutical excipients with active pharmaceutical ingredients: a comprehensive review. *J Excipients Food Chem* 2010;1: 3–26.
7. Tita B, Fulias A, Bandur G, Ledeti I, Tita D. Application of thermal analysis to study the compatibility of sodium diclofenac with different pharmaceutical excipients. *Rev Chim* 2009;62:443–54.
8. Crowley P, Martini L. Drug-excipient interactions. *Pharm Technol Eur* 2001;13:26–34.
9. Ozawa T. Thermal analysis-review and prospect. *Thermochim Acta* 2000;355:35–42.
10. Verma RK, Garg S. Compatibility studies between isosorbide mononitrate and selected excipients used in the development of extended release formulations. *J Pharmaceut Biomed Anal* 2004;35: 449–58.
11. Tomassetti M, Catalani A, Rossi V, Vecchio S. Thermal analysis study of the interactions between acetaminophen and excipients in solid dosage forms and in some binary mixtures. *J Pharmaceut Biomed Anal* 2005;37:949–55.
12. Marini A, Berbenni V, Moioli S, Bruni G, Vecchio S, Cofrancesco P, et al. Drug-excipient compatibility studies by physico-chemical techniques. The case of indomethacin. *J Therm Anal Calorim* 2003;73:529–45.
13. Mura P, Faucci MT, Manderioli A, Bramanti G, Ceccarelli L. Compatibility study between ibuprofen and pharmaceutical excipients using differential scanning calorimetry, hot-stage microscopy and scanning electron microscopy. *J Pharmaceut Biomed Anal* 1998;18:151–63.
14. Chuasuwan B, Binjesoh V, Polli JE, Zhang H, Amidon G, Junginger HE, et al. Biowaiver monographs for immediate release solid oral dosage form: diclofenac sodium and diclofenac potassium. *J Pharmacol Sci* 2009;98:1206–19.
15. Bartolomei M, Rodomonte A, Antonietta E, Minelli G, Bertocchi P. Hydrate modifications of the non-steroidal anti-inflammatory drug diclofenac sodium: solid-state characterization of a trihydrate form. *J Pharmaceut Biomed Anal* 2007;45:443–9.
16. Bucci R, Magri AD, Magri AL. Determination of diclofenac salts in pharmaceutical formulations. *Fresenius' J Anal Chem* 1998;362:577–82.

17. Tudja P, Khan MZ, Mestrovic E, Horvat M, Golja P. Thermal behaviour of diclofenac sodium: decomposition and melting characteristics. *Chem Pharm Bull* 2001;49:1245–50.
18. Palomo ME, Ballesteros MP, Frutos P. Analysis of diclofenac sodium and derivatives. *J Pharmaceut Biomed Anal* 1999;21:83–94.
19. Bettini R, Giordano F, Donini C, Massimo G, Catellani PL, Colombo P. Swelling force development as a result of hydrate formation in diclofenac sodium or nitrofurantoin tablets. *Pharmaceut Sci* 2000;10:335–9.
20. Fini A, Garuti M, Fazio G, Alvarez-Fuentes J, Holgado MA. Diclofenac salts. I. fractal and thermal analysis of sodium and potassium diclofenac salts. *J Pharmacol Sci* 2001;90:2049–57.
21. Fini A, Fazio G, Rosetti F, et al. Diclofenac salts. III. Alkaline and earth alkaline salts. *J Pharmacol Sci* 2005;94:2416–31.
22. Reck G, Faust G, Dietz G. X-ray crystallographic studies of diclofenac-sodium-structural analysis of diclofenac-sodium tetrahydrate. *Pharmazie* 1988;43:771–4.
23. Muangsin N, Prajaubsook M, Chaichit N, Siritaedmukul K, Hannongbua S. Crystal structure of a unique sodium distorted linkage in diclofenac sodium pentahydrate. *Anal Sci* 2002;18:967–8.
24. Bartolomei M, Bertocchi P, Antoniella E, Rodomonte A. Physico-chemical characterisation and intrinsic dissolution studies of a new hydrate form of diclofenac sodium: comparison with anhydrous form. *J Pharmaceut Biomed Anal* 2006;40:1105–13.
25. Pygall SR, Griffiths PC, Wolf B, Timmins P, Melia CD, et al. Solution interactions of diclofenac sodium and meclofenamic acid sodium with hydroxypropyl methylcellulose (HPMC). *Int J Pharm* 2011;312:55–62.
26. Al Gohary OMN. Preformulation stability screening of diclofenac sodium and mebeverine hydrochloride with tablet excipients and polymers using differential scanning calorimetry. *Pharm Ind* 1998;60:168–73.
27. Velasco MV, Ford JL, Rowe P, Rajabi-Siahboomi AR. Influence of drug: hydroxypropylmethylcellulose ratio, drug and polymer particle size and compression force on the release of diclofenac sodium from HPMC tablets. *J Contr Release* 1999;57:75–85.
28. Llinàs A, Burley JC, Box KJ, Glen RC, Goodman JM. Diclofenac solubility: independent determination of the intrinsic solubility of three crystal forms. *J Med Chem* 2007;50:979–83.
29. Christian MA, LP K. Analytical profiles of drug substances, Florey K, editor. New York: Academic Press; 1990:123–41 pp.
30. Nugrahani I, Kumalasari RA, Auli WN, Horikawa A, Uekusa H. Salt cocrystal of diclofenac sodium-L-proline: structural, pseudopolymorphism, and pharmaceuticals performance study. *Pharmaceutics* 2020;12:690.

Thabile Lukhele, Denise Olivier, Marthe C. D. Fotsing,  
Charlotte M. Tata, Monisola I. Ikhile, Rui W. M. Krause,  
Sandy Van Vuuren and Derek Tantoh Ndinteh\*

## 6 Ethnobotanical survey, phytoconstituents and antibacterial investigation of *Rapanea melanophloeos* (L.) Mez. bark, fruit and leaf extracts

**Abstract:** *Rapanea melanophloeos* is traditionally used in South Africa in the treatment of ailments of the skin, pulmonary and gastro intestinal tract. This study was aimed at giving an overview of these traditional uses and comparing the phytochemicals and antibacterial activities of various crude extracts of the leaves, fruits and bark in order to validate these uses. The three plant parts were extracted using petroleum ether (PE), ethyl acetate (EtOAc), methanol (MeOH) and water. Various phytochemicals were compared using TLC, while alcohol precipitable solids (APS), non-polar terpenes and amino acids were analysed by GC-MS. Antibacterial activity was determined against three Gram-positive and three Gram-negative strains by microdilution assays. Caryophyllene oxides,  $\alpha$ -cadinol and (–)-spathulenol were identified in the PE extracts. All nine essential amino acids were present in fruit extracts in significantly higher levels than in the leaves and bark; 255.1, 23.4 and 21.3 mg/g respectively. Most of the extracts showed good antibacterial activity, especially against the Gram-positive pathogens (MIC of  $\leq 1$  mg/mL), the EtOAc extracts exhibited the best activity with the fruit having an MIC values of  $0.1 \pm 0.2$  mg/mL against *Staphylococcus epidermidis* and *Enterococcus faecalis*, 0.05 mg/mL against *Bacillus cereus*. Results from this study validate the ethnomedicinal uses of *R. melanophloeos* extracts for ailments of bacterial etiology. The plant had a rich supply of secondary metabolites, APS and amino acids and TLC and antibacterial activities of the extracts showed slight variations in chemical composition due to geographic distribution.

---

\*Corresponding author: **Derek Tantoh Ndinteh**, Department of Applied Chemistry, Faculty of Science, University of Johannesburg, PO Box 17011, Doornfontein 2028, Johannesburg, South Africa, E-mail: dndinteh@uj.ac.za

**Thabile Lukhele, Marthe C. D. Fotsing, Charlotte M. Tata and Monisola I. Ikhile**, Department of Applied Chemistry, Faculty of Science, University of Johannesburg, PO Box 17011, Doornfontein 2028, Johannesburg, South Africa

**Denise Olivier**, SEOBI, 19 Mountain Street, Derdepoort 0186, South Africa

**Rui W. M. Krause**, Department of Chemistry, Rhodes University, Grahamstown 6140, South Africa

**Sandy Van Vuuren**, Department of Pharmacy and Pharmacology, Faculty of Health Sciences, University of the Witwatersrand, 7 York Road, Parktown 2193, South Africa

This article has previously been published in the journal Physical Sciences Reviews. Please cite as: T. Lukhele, D. Olivier, M. C. D. Fotsing, C. M. Tata, M. I. Ikhile, R. W. M. Krause, S. V. Vuuren and D. T. Ndinteh "Ethnobotanical survey, phytoconstituents and antibacterial investigation of *Rapanea melanophloeos* (L.) Mez. bark, fruit and leaf extracts" *Physical Sciences Reviews* [Online] 2021, 6. DOI: 10.1515/psr-2020-0143 | <https://doi.org/10.1515/9783110710823-006>



**Keywords:** alcohol precipitable solids, amino acids, antibacterial activity, phytochemicals, *Rapanea melanophloeos*

## 6.1 Introduction

There are approximately 100 species from the *Rapanea* genus (one of 37 genera in the Myrsinaceae family) spread throughout tropical areas worldwide [1–3]. Only two of these species are indigenous to South Africa; *Rapanea melanophloeos* (L.) Mez. [4], and *Rapanea gilliana* (Sond.) Mez. [5–7]. *R. melanophloeos* generally occurs in coastal regions and also flourishes in tropical Afromontane as well as riverine areas. These areas include the Cape Peninsula, Free State, Limpopo and Mpumalanga provinces in South Africa [8], and ranges through Malawi [4], as far north as Tanzania [9] and Kenya [10]. It stretches from Zimbabwe [11] to Burundi, Rwanda, Uganda [12], Ethiopia [13], Democratic Republic of Congo [14] and as far west as Cameroon [15], Nigeria [16] and Benin [17]. The morphological characteristics of *R. melanophloeos* include medium-sized to large evergreen trees of variable heights (5–20 m) with straight trunks which may be fluted at the base in large specimens. The bark is thick and grey, often with small diamond shaped spots (raised areas). The leaves are thick and leathery, 50–130 mm in length, hairless, simple, entire-margined, oblong or oblong-lanceolate shaped and occur clustered mainly at the ends of the branches. When the leaves are young, they appear pale green with maroon petioles but become darker above and paler below with distinct purplish petioles (up to 15 mm long) when mature. The blades often have numerous small dark green streaks (secretory cavities) visible when held up to the light. The flowers are very small, whitish or creamy yellow with a faint scent and occur clustered mainly below the leaves on the older wood. Male and female flowers are borne on separate trees and are visible from winter months. The edible fruits appear in spring as heavy clusters of small (up to 5 mm in diameter) thinly-fleshed, one-seeded berries, green when young and purple when mature, all along the stem. It is also common to find flowers and fruits growing at the same time all through summer [4, 7, 8, 18–20].

In southern Africa, approximately seven species of Myrsinaceae have been recorded from four genera (*Embelia*, *Myrsine*, *Maesa* and *Rapanea*) [5] whose plants are known to be useful as traditional medicines especially for the treatment of gastro-intestinal ailments and as anthelmintics (for both livestock and humans) [21, 22]. *R. melanophloeos* bark is a popular ingredient in various medicinal preparations, its decoctions are used as expectorants and emetics [23] against pain and to strengthen the heart [22–24]. The seeds are used traditionally as anthelmintics against roundworms by grinding them and making hot decoctions thereof [25].

This study was aimed at giving detailed account of the ethnobotanical uses of *R. melanophloeos* by summarizing what is available in literature from as early as 1775. Traditional practitioners in Swaziland were interviewed to supplement the available literature. Since various major compounds are already known from the species, a

further aim of this study was to elaborate on the phytochemical variation where the profiles of *R. melanophloeos* samples from different localities in Swaziland and South Africa were compared as a means to establish whether external factors such as climate, geographical location and growth conditions give rise to phytochemical variation in wild harvested specimens. Furthermore, plants which are rich in mucilage are often prescribed to treat coughs, improve digestion and may be used for topical application to treat inflamed skin [26], where such plants usually also contain high levels of alcohol precipitable solids (APS) (polysaccharides and glycoproteins) [27]. From the slimy appearance of *R. melanophloeos* plant material upon extraction with water, and from its medicinal uses as expectorants, the presence of APS was anticipated and consequently quantified in the various plant samples taken. GC-MS was used to identify three of the major non-polar components in the petroleum ether extracts as the bark may be burnt as incense [28]. Since *R. melanophloeos* fruits are also edible and its bark is used as a tonic (to strengthen the heart) [22], the amino acid content of the various plant parts were determined to evaluate the respective nutritional values. Lastly, the phytochemical composition and antibacterial activities (microdilution assays) of various bark, fruit and leaf extracts were investigated and compared to determine the possibility of plant part substitution as a means of conservation of the species [29].

## 6.2 Materials and methods

### 6.2.1 Ethnobotanical survey

A literature search was conducted in Web of science and Google Scholar databases (1775 to December 2017). The scope of the work was Swaziland and surrounding areas of South Africa. Interviews were conducted with a taxonomist based at the Malkerns Research Station, Mr. Zachariah Dlamini (who also helped with the identification of the species), and Mr. Msibi, a herbalist based at the Manzini Muti Market in Swaziland.

### 6.2.2 Plant material

Leaves, fruits and bark were collected from a total of 22 mature plants across six Afromontane sites; five in the Highveld of Swaziland (Sicunusa, Nhlngano, Bhunya, Fonteyn, and Lundzi) and one in the KwaZulu-Natal province of South Africa (Karkloof). Voucher specimens were deposited at the University of Johannesburg Herbarium (JRAU) (the voucher numbers are listed with the provenances in Table 6.1). The plant materials were dried under shade at ambient temperature and ground to fine powder using a Waring commercial blender (Model 32BL79, Dynamics Corporation, USA).

### 6.2.3 Preparation of plant extracts and alcohol precipitable solids (APS)

The ground plant parts were successively extracted with 10 mL/g of petroleum ether (PE), ethyl acetate (EtOAc), methanol (MeOH) (technical grade, Saarchem Chemicals) and water (distilled and deionized).

Table 6.1: *Rapanea melanophloeos* collection sites, voucher specimen numbers and mean yields.

Locality or provenance (altitude)	Voucher number	Sample reference numbers	Plant parts gathered <sup>a</sup>	Mean yields per plant part extraeach locality				
				% yield (g/g dry weight) with STD <sup>b</sup>				
				PE	EtOAc	MeOH	H <sub>2</sub> O	APS <sup>c</sup>
Swaziland								
Sicunusa (A)	T.Lukhele 01	A1	L, B, F	L: 1.7 ± 0.4	L: 1.1 ± 0.2	L: 11.7 ± 4.1	L: 5.7 ± 2.4	L: 6.0 ± 1.1
Manzini (1259 m)	T.Lukhele 16	A2	L, B	B: 0.5 ± 0.1	B: 0.9 ± 0.4	B: 12.4 ± 1.8	B: 3.2 ± 1.7	B: 3.0 ± 2.0
Nhlangano (B)	T.Lukhele 17	A3	L, B	F: 2.9	F: 2.3	F: 10.6	F: 5.9	F: 4.4
	T.Lukhele 02	B1	L, B	L: 1.5 ± 0.2	L: 1.3 ± 0.2	L: 16.1 ± 3.0	L: 4.5 ± 1.2	L: 2.2 ± 2.4
	T.Lukhele 03	B2	L, B, F					
Shiselweni (1053 m)	T.Lukhele 14	B3	L, B, F	B: 0.5 ± 0.2	B: 0.7 ± 0.1	B: 16.5 ± 1.4	B: 3.5 ± 2.6	B: 2.0 ± 1.7
	T.Lukhele 15	B4	L, B					
	T.Lukhele 18	B5	L, B, F	F: 3.8 ± 0.6	F: 2.4 ± 0.5	F: 12.7 ± 2.3	F: 3.1 ± 0.2	F: 4.6 ± 1.9
	T.Lukhele 19	B6	L, B, F					
Bhunya (C)	T.Lukhele 04	C1	L, B	L: 1.8 ± 0.2	L: 1.1 ± 0.0	L: 16.7 ± 3.8	L: 4.8 ± 0.6	L: 3.3 ± 2.4
Manzini (1069 m)	T.Lukhele 05	C2	L, B					
	T.Lukhele 06	C3	L, B	B: 0.5 ± 0.1	B: 0.7 ± 0.4	B: 18.0 ± 4.0	B: 3.8 ± 2.1	B: 1.3 ± 1.1
	T.Lukhele 07	C4	L, B					
Fonteyn (D)	T.Lukhele 09	D1	L, B, F	L: 1.8 ± 0.3	L: 1.4 ± 0.2	L: 16.6 ± 3.2	L: 4.8 ± 1.4	L: 3.1 ± 2.2
Hhohho (1333 m)	T.Lukhele 10	D2	L, B	B: 0.6 ± 0.1	B: 0.9 ± 0.4	B: 17.4 ± 4.1	B: 2.9 ± 1.3	B: 3.4 ± 1.2
	T.Lukhele 11	D3	L, B	F: 3.3	F: 4.7	F: 12.9	F: 6.4	F: 6.1
	T.Lukhele 12	D4	L, B					
	T.Lukhele 13	D5	L, B					
Lundzi (E)	T.Lukhele 08	E1	L, B	L: 1.7	L: 1.3	L: 12.8	L: 4.4	L: 0.8
Manzini (1505 m)				B: 0.5	B: 0.8	B: 15.4	B: 1.7	B: 0.8
South Africa								
Karkloof (F)	I.Johnson 1214	F1	L, B	L: 2.4 ± 0.2	L: 0.9 ± 0.1	L: 16.1 ± 1.9	L: 8.7 ± 0.7	L: 0.7 ± 0.1
KwaZulu-Natal (1362 m)	I.Johnson 1215	F2	L, B	B: 2.2 ± 0.8	B: 0.6 ± 0.2	B: 10.5 ± 2.4	B: 2.9 ± 1.1	B: 0.7 ± 0.1
	I.Johnson 1216	F3	L, B					

<sup>a</sup>L = leaves; B = bark; F = fruit; <sup>b</sup>mean and STD calculated where there were more than one sample; mean obtained when extracting the various plant parts sequentially with solvents of different polarities; <sup>c</sup>APS = alcohol precipitable solids.

The mixtures were agitated in a mechanical shaker for 1 h and allowed to stand at room temperature for 24 h. Filtrates were collected through Whatman No. 1 filter paper and concentrated under a fume hood. Water extracts were freeze-dried with a WirTis freeze dryer. Extraction thus afforded four different types of crude extracts for each plant part which were weighed and kept at  $-4\text{ }^{\circ}\text{C}$  in tightly closed vials until use (Table 6.1).

APS are soluble in boiling water, but precipitate when the solution contains more than 75% EtOH [30]. The APS were extracted from the leaf, fruit and bark samples by soaking 1 g powdered dry plant material in 10 mL boiling water and allowing the mixture to stand for 24 h at room temperature. The mixtures were filtered through cotton wool and EtOH (96%) was added to the filtrate to make up a 75% (v/v) ethanolic solution. Each solution was shaken vigorously and left to stand at room temperature for 1 h to allow for APS to completely precipitate before each mixture was centrifuged at 4100 rpm for 20 min. The supernatant was decanted, freeze dried and its amino acid content determined by GC-MS. The precipitate (white gelatinous solid) was left to dry in the fume-hood under a stream of air, weighed and the percentage APS calculated (Table 6.1).

#### 6.2.4 TLC variation study

The plant extracts were reconstituted in the relevant extraction solvent to a final concentration of 10 mg/mL. Fifteen microliter of each extract solution was spotted on aluminium-backed TLC plates (Macherey Nagel Silica gel 60 F<sub>254</sub>). Plates were developed separately in the following solvent systems: hexane:diethyl ether (3:2), hexane:EtOAc (2:3), butanol:CH<sub>3</sub>COOH:water (4:1:1) and EtOAc:HCOOH:CH<sub>3</sub>COOH:water (100:11:11:26) for the PE, EtOAc, MeOH and water extracts respectively. Chromatograms were visualized under UV light (Camac Universal UV lamp) at 254 and 366 nm before being sprayed with vanillin-sulphuric acid spray reagent (1 g vanillin in 194 mL ethanol and 5 mL sulphuric acid) [31] and heated at 110 °C for a few minutes until optimal colour development.

#### 6.2.5 GC-MS analyses of PE extract

After extraction, the dried PE extracts of the leaf, fruit and bark samples were reconstituted in 5 mL spectroscopic grade n-hexane (Sigma-Aldrich), mixed gently with a vortex and filtered through a 0.45 µm nylon filter. An aliquot of 1.5 mL of each sample solution was transferred into a GC sample vial and capped for analysis by means of a Varian 3800 Capillary GC coupled to a Saturn 2000 MS. The GC was fitted with a TRX-5MS (5% diphenyl-95% dimethylpolysiloxane) column (30 m × 0.25 mm). The samples were injected (1.0 µL; analyses in duplicate), inlet temperature of 250 °C and a flow rate of 1 mL/min. The initial oven temperature was held at 50 °C for 1 min, which then increased to 210 °C at 4 °C/min, with a second ramp to 300 °C at 45 °C/min. Mass spectrometry was accomplished in EI mode at 35–600 *m/z*. The mass spectra of the compounds in the extracts were compared with those of known compounds in the GC-MS library database (NIST 08). Table 6.2 contains a summary of the results.

#### 6.2.6 Amino acid extraction and analyses

Identification and quantification of free amino acids in the aqueous filtrate remaining after the APS were removed, was accomplished by means of an Agilent GC with a LECO Pegasus high-throughput time-of-flight mass spectrometer (HR-GC-MS-TOF) instrument. Amino acids are normally not volatile enough to inject in GC due to their high polarity. Consequent derivatisation provided increased volatility, thermal stability and an adequate detector response for such analysis. An EZ fast-Free amino acid Phenomenex analysis kit (obtained from Separations) was used for the derivatisation: A 100 µL of

**Table 6.2:** Retention times and mass fragments of five major compounds from GC-MS analysis of the PE extracts of *R. melanophloeos*.

Compound no. in Figure 6.2	Retention time (minutes)	Mass fragments ( <i>m/z</i> )*	Tentative identity from NIST 08 library
a	14.34	<u>43</u> , 119, 205	(-)-spathulenol ( <b>6</b> )
b	20.10	<u>43</u> , 109, 188, 220	Caryophyllene oxide ( <b>7</b> )
c	25.38	<u>43</u> , 121, 204	$\alpha$ -cadinol ( <b>8</b> )
d	30.12	73, 268, <u>355</u>	Unidentified
e	34.02	73, <u>356</u> , 401	Unidentified

\*Major mass fragments, underlined = base peak.

aqueous extract (dried extract re-suspended in 1 mL MeOH: H<sub>2</sub>O–1:1) and 100  $\mu$ L of an internal standard (0.2 mM norvaline) was pipetted onto a solid phase extraction (SPE) sorbent tip with a strong affinity for amino acids. The adsorbed extract was consequently washed with 200  $\mu$ L of n-propanol to ensure that compounds such as proteins, lipids and inorganic salts that could interfere with the chromatographic analyses were removed. The extracted amino acids were deprotonated and washed from the stationary phase in the sorbent tip by using a sodium hydroxide and n-propanol (3:2) solution (200  $\mu$ L). A chloroform mixture containing the derivatising agent (50  $\mu$ L alkyl chloroformate) was added to the extracted amino acids, vortexed and left for a minute or more to react. Thereafter, 100  $\mu$ L of iso-octane was added to the mixture in order to extract the derivatised amino acids. In this instance, the formation of two layers was observed with the organic top layer containing the derivatised amino acids. This layer (50  $\mu$ L) was removed with a pipette into a GC vial and dried under a stream of nitrogen. The dry amino acid extracts were reconstituted in 100  $\mu$ L of 80% iso-octane in chloroform for injection into the HR-GC-MS-TOF.

Calibration standards containing mixtures of amino acids used for quantification purposes were also provided in the kit. Four calibration levels (ranging from 50–200 nmol/mL) were used where different volumes of standard solution were pipetted together with 100  $\mu$ L of an internal standard (0.2 mM Norvaline) onto a solid phase extraction (SPE) sorbent tip as was the case with the extracts. The same method of derivatisation was followed as with the sample mixtures. The GC was fitted with a Zebtron ZB-AAA GC column (10 m  $\times$  0.25 mm). Samples were injected (1.5  $\mu$ L, split ratio 1:15) at 250  $^{\circ}$ C and a constant flow of 1.1 mL/min. The temperature program included an increase in temperature at 30  $^{\circ}$ C/min from 110–320  $^{\circ}$ C (hold 2 min). The MS source temperature was set at 240  $^{\circ}$ C with a scan range of 45–450 *m/z* and a sampling rate of 3.5 scans/sec. Analyses were done in duplicate and the mean values were reported. The results are summarized in Table 6.3.

### 6.2.7 Antibacterial activity by microdilution assay

Three Gram-positive [*Bacillus cereus* (ATCC 11778), *Enterococcus faecalis* (ATCC 29212) and *Staphylococcus epidermidis* (ATCC 2223)] and three Gram-negative strains [*Escherichia coli* (ATCC 8739), *Klebsiella pneumoniae* (ATCC 13883) and *Pseudomonas aeruginosa* (ATCC 9027)] were chosen with specific reference to skin, intestinal and respiratory ailments for which *R. melanophloeos* is mostly used. All cultures were obtained from either the National Health Laboratory Services or Davies Diagnostics. All test pathogens were grown overnight and diluted in Tryptone Soya Broth (TSB) to a ratio of 1:100, yielding an approximate inoculum size of  $1 \times 10^8$  colony forming units (CFU)/mL. The antibacterial activity of the extracts was evaluated by observing the minimum inhibitory

**Table 6.3:** Free amino acids detected in the aqueous extracts of the leaves, fruits and bark from *R. melanophloeos*.

Amino acid	Retention time (s)	Molar mass (g/mol)	Major ions ( $m/z^a$ )	Average concentration (mg/g dry weight) <sup>b</sup>		
				Leaves <sup>c</sup>	Fruits <sup>d</sup>	Bark <sup>e</sup>
Alanine	55.1	89.09	<u>130</u> , 158	0.8	<b>7.1</b>	0.5
Glycine	60.7	75.06	<u>116</u> , 162	tr	2.1	tr
$\alpha$ -amino butyric acid	66.6	103.12	144, 172	nd	0.2	nd
Valine	72.0	117.14	<u>116</u> , 143, 158	0.6	1.7	0.4
$\beta$ -amino iso-butyric acid	75.9	103.12	116, 130, 143, 172, 231	0.9	0.9	1.0
Isoleucine	84.3	131.17	<u>130</u> , 143, 157, 172	1.3	4.0	1.3
Leucine	87.5	131.17	<u>172</u>	0.7	1.9	0.5
Threonine	100.2	119.12	<u>101</u> , 119, 143, 160, 203	0.1	<b>7.2</b>	tr
Serine	102.5	105.09	<u>60</u> , 74, 101, 116, 146, 174, 203	0.7	<b>10.6</b>	0.7
Proline	105.9	114.12	<u>70</u> , 114, 156	0.8	<b>33.9</b>	0.4
Asparagine	112.2	132.11	<u>69</u> , 113, 129, 141, 155	tr	4.9	tr
Aspartic acid	145.8	132.09	<u>88</u> , <u>99</u> , 114, 130, 156, 174, 184, 216, 244	tr	<b>14.2</b>	tr
Methionine	147.0	146.18	<u>61</u> , 75, 88, 101, 114, 129, 143, 156, 175, 190, 203, 217, 277	nd	0.8	nd
Glutamic acid	167.8	146.12	<u>84</u> , 100, 128, 142, 155, 170, 188, 215, 230, 258	0.4	<b>30.7</b>	1.3
Phenylalanine	168.2	165.19	<u>74</u> , 91, 103, 120, 131, 148, 164, 190, 206, 234	2.2	4.5	2.5
$\alpha$ -amino adipic acid	186.6	161.16	<u>98</u> , 124, 142, 169, 184, 244, 272	1.0	0.7	0.1
Glutamine	205.5	146.13	<u>84</u> , 100, 114, 142, 155, 187, 215	1.0	4.5	0.5
Lysine	246.6	147.18	<u>170</u> , 185, 198, 213, 240, 300	3.1	<b>5.8</b>	3.1
Histidine	257.6	155.14	<u>81</u> , 94, 110, 121, 136, <u>153</u> , 180, 196, 224, 282, 310	3.1	3.1	3.3
Tyrosine	274.4	181.19	<u>107</u> , 164, 156, 169, 200, 257	1.9	<b>9.4</b>	1.4
Tryptophan	291.0	205.22	<u>130</u> , 143, 229, 332	4.0	<b>10.4</b>	3.9
Cystine	322.2	118.06	<u>74</u> , 104, 116, 132, 146, 174, 188, 206, 216, 248	0.8	1.5	0.4
Total				23.4	255.1	21.3

<sup>a</sup>major ions are underlined; <sup>b</sup>Concentrations > 5 mg/g in bold print; <sup>c</sup> $n = 11$ ; <sup>d</sup> $n = 6$ ; <sup>e</sup> $n = 6$  (not all samples were subjected to amino acid quantification due to limited amounts of extract); nd = non detected, tr = traces, <0.1 mg/g.

concentration (MIC) using the microdilution assay adapted from Eloff [32]. Only the PE, EtOAc and MeOH extracts were subjected to antibacterial assay since the MeOH and aqueous extracts showed similar TLC profiles and the MeOH extract yields were much larger than those obtained for the aqueous extracts. The PE and EtOAc extracts were reconstituted in acetone while the MeOH extracts were reconstituted in 50% (v/v) aqueous dimethyl sulfoxide (DMSO), to a starting concentration of 32 mg/mL in all instances. Where extracts were found to be highly active, starting concentrations were subsequently lowered to 5, 3.2 or 0.5 mg/mL. An eight-fold serial dilution of extracts was carried out aseptically in 96-well microtitre plates (100  $\mu$ L extract per well) under a laminar flow hood using sterile water. All wells were inoculated with 100  $\mu$ L of the relevant culture under ambient laboratory conditions. Microtitre plates were tightly sealed with sterile seal plate films to avoid evaporation of solvent and the plates were incubated at 37 °C for 24 h to stimulate bacterial growth. *p*-iodonitrotrazolum violet (INT) (Sigma-Aldrich) (0.2 mg/mL)(40  $\mu$ L) was added to all wells and the plates were left to stand at ambient laboratory conditions for 6 h. The formation of a red/pink complex signified microbial growth and minimum inhibitory concentration was defined as the lowest concentration that inhibited the colour change of INT. To validate microbial sensitivity, ciprofloxacin (0.01 mg/mL) was included as a positive control for all tested bacterial strains, while acetone and 50% aqueous DMSO were included as negative controls to evaluate antimicrobial susceptibility of the solvents. All assays were repeated twice to ensure that a standard error of not more than one dilution factor was obtained.

## 6.3 Results and discussion

### 6.3.1 Ethnobotanical knowledge

In southern Africa *R. melanophloeos* is known as the Cape beech (due to its resemblance to the European beech trees), *Kaapse boukenhoutorbeukeboom* (Afrikaans), *isiQwane-sehlatior isiQwandwemshube* (Xhosa), *Khubalwane, isiQalaba-sehlathi* [33] or *uMaphipha* (Xhosa, Zulu), *inhluthe, isicalabi, isihluthi-wentaba, umaphiphakhubaloor uvukakwabaflikhubalo* (Zulu), *Mogôñô* (northern Sotho), *Shitsuvane* (Tswana), *Tshikonwa* (Vhenda) [34], *Maphipha* or *Dzilidzili* (siSwati), *Tshididiri* (Vhenda) and *Mudonera* (Shona) [4, 8, 35, 36]. The bark and fruit are preferred as ethnomedicines, but the roots and leaves may also be used. Decoctions or infusions of the bark may be used (or rarely the roots are eaten) as emetics and expectorants [23], as well as for stomach [37] and muscular pain, ulcers, acidity, fever, haematemesis and to strengthen the heart [23, 24, 38]. For the treatment of diarrhoea, the bark or leaves are ground and boiled and the decoction is taken orally thrice daily [39]. Bark decoctions may further be used as mouthwash to treat toothache [7, 40] or to lower blood sugar [41]. For wounds, the bark is chewed or pulverized and applied locally [41]. The roots may be chewed as treatment for a sore throat or may be dried, powdered and applied to wounds [42]. The root and bark are used to treat palpitations and infusions of the ground bark may also be taken thrice daily by persons who “feels like crying” [22]. The fruits are mainly used for anthelmintic purposes where the dried fruit may be pulverized or ground and taken in milk, broth or beer [43–45]. The fruit is especially effective against roundworm or tapeworm where three to five fruits are eaten or the

seeds are ground with millet meal, cooked as a gruel and eaten [44]. In Kenya the fruit is also a popular treatment for gonorrhoea and heartburn [45]. Both the root (when eaten) [46] or the fruit (ground and taken in milk) [44, 47] are purgatives. The leaves are less popular and are reportedly used as astringents in the Cape in South Africa [48]. Apart from its medicinal uses, *R. melanophloeos* bark is also harvested from living trees to be used cosmetically against *umgqwaliso* (sorcery), where a paste of the bark is applied to the face and becomes light pink in colour once it has dried on the skin. The bark is also burnt as incense in preparation for rituals [28].

The *R. melanophloeos* plant parts may be used individually as described or in combination with other plants. In this instance, the barks of *R. melanophloeos* and *Pterocelastrus echinatus* N.E.Br. are used to treat general body aches (50 g of each is ground together and added to 1 L of warm water; one tablespoon of the mixture is taken thrice daily; interestingly, the use of sugar or maize porridge is prohibited while this treatment is used) [49]. *R. melanophloeosis* may also be taken together with either *P. entanisia* or *P. echinatus* as a tonic and for blood purification [pers. communication with Mr. Dlamini and Mr. Msibi]. These “cleansing” or “purifying” properties of *R. melanophloeos* bark renders it a very common ingredient in traditional herbal mixtures used in the Manzini province of Swaziland, whilst *P. prunelloides* or *P. echinatus* are said to function as “pain killers” in the combinations mentioned above [pers. communication with Mr. Mavuso]. While *R. melanophloeos* bark may be used on its own as a skin lightener, it may also be combined with the barks of *Cassipourea flanaganii* Alston, *C. gerrardii* Alston, *Sideroxylon inerme*, Krauss ex A.DC., *Olea capensis* Buchoz ex Roem. & Schult. and *Curtisia dentate* (Burm.f.) C.A.Sm. in a mixture known as *umMemezi* among Xhosa speakers [50], which is particularly used for skin lightening purposes [51], as a sunscreen [52] or for the treatment of pimples. The *umMemezi* is prepared by pouring a small amount of water onto a concave-shaped stone and rubbing the pre-soaked bark onto the stone until a thick mixture is formed. After cleansing the face, the mixture is gently and evenly applied to the face and neck as often as necessary even several times a day. Dold and Cocks [35] further emphasized the effectiveness of *R. melanophloeos* as an ethnoveterinary medicine in South Africa in the treatment of “heart water” disease where it is used in combination with *C. dentata* that is, the barks of the two species are boiled together for half an hour, cooled and given to cows (200 mL) followed by Coca-Cola™ (1 L).

### 6.3.2 Extract yields, APS content and TLC profiles

From the extraction yields obtained with solvents of various polarities (Table 6.1), it was observed that MeOH produced the highest yield of extracts. This trend is confirmed in another study [53] where the alcoholic leaf extract also returned the highest yield when compared to PE, DCM and water. Water extract yields were comparable with those obtained after APS extractions thus it may be deduced that APS contributes



significantly to the weight of water extractable compounds. Comparing the APS levels in *R. melanophloeos* with those obtained for Aloes, known for their high content of APS in the gel contained in their fleshy leaves (approximately 10–60%) [27, 30], it was evident that *R. melanophloeos* fruit in particular, produces great amounts of APS (4.4–6.1%) as well. Apart from the potential energy source (amylase and amylopectin) found in APS, cellulose is a structural component in plants that serve as fibre in the human diet. Polysaccharides are also suggested to exhibit wound-healing [54] and immune-stimulatory properties [55, 56] as are suggested ethnobotanical knowledge of *R. melanophloeos*. The glycoproteins in APS consist of carbohydrate chains attached to certain amino acids such as hydroxyproline, proline, lysine or tyrosine and are responsible for keeping cell walls intact [57].

Methanol and water seemed to extract the same classes of compounds as the TLC profiles for these extracts are almost identical (Figure 6.1c (leaves) and Figure 6.1d show the MeOH and water extracts respectively). The two plates were developed in different solvent systems but essentially the yellow zones in Figure 6.1c were representative of those in Figure 6.1d, where butanol:CH<sub>3</sub>COOH:water (4:1:1) (used for MeOH extracts) is the more polar solvent system of the two, able to migrate polar compounds such as tannins, saponins and phenolic glycosides further along the stationary phase. On the other hand, EtOAc:HCOOH:CH<sub>3</sub>COOH:water (100:11:11:26) (used for water extracts) had a greater component of acid (25%) which is able to establish better resolution between the polar compounds without excessive tailing. The yellow band in Figure 6.1c (leaves) is resolved to give four yellow zones (typical of phenolic glycosides such as flavonoids) at  $R_f = 0.19, 0.46, 0.63$  and  $0.67$  respectively (Figure 6.1d). While no flavonoids have been identified from *R. melanophloeos* to date, various flavonoid glycosides, e.g. kaempferol, quercetin, myricetin, quercitrin, myricitrin, mearnsitrin, mearnsetin, several of their derivatives and glycosides, as well as gallic acid, (–)-epicatechin, (–)-epigallocatechin, (–)-epigallocatechin-3-O-gallate and 3',5'-di-C-β-glucopyranosyl phloretin have been isolated from *Myrsine africana*, the southern African counter-part of *R. Melanophloeos* [55, 56, 58], The TLC analysis (Figure 6.1c) further confirms the presence of large amounts of glycosidic compounds especially in the fruits where the MeOH extracts exhibited dark grey to blue charred streaks (typical of glycosides such as triterpenoid, saponins) after treatment with vanillin/H<sub>2</sub>SO<sub>4</sub> spray reagent [31]. The presence of these saponins was confirmed by spraying duplicate plates with chromic acid as visualizing agent followed by heating at 100 °C (a method used for the detection of sugars) [30], where the saponin zones were visibly white on a yellow background. It is further evident that these or similar compounds are also present in the leaves and bark but in much smaller quantities. While literature supports the presence of at least four saponins in *R. melanophloeos* leaves [59], these compounds have not been identified in the bark or fruit. The TLC study certainly indicates the presence of the same or similar saponins in all the extracts. Large quantities of tannins were also visible in the MeOH extracts (red streaks from the origins on the TLC plates) particularly in the bark and leaves. Tannins and saponins are known to be highly bitter and may contribute to the

efficient anti-feedant activity exhibited by *R. melanophloeos* against *Schistocerca gregaria* [60]. The Myrsinaceae are known to accumulate mostly condensed tannins [38] also referred to as proanthocyanidins; consisting of flavonoid polymers or oligomers as opposed to the hydrolysable tannins consisting of sugar esters combined with a small ratio of trihydroxybenzene carboxylic acids. *R. melanophloeos* reportedly contains 11–15% tannins in the bark [61]. Tannins are reported to cause anthelmintic activity by binding to the gastrointestinal proteins of the host or to glycoprotein on the cuticle of the parasite and may cause death [62]. Previous reports indicating that the anthelmintic activity *R. melanophloeos* against the nematode parasite *Haemonchus contortus in vitro* was exhibited by the bark [63] but not the seeds [64] may possibly be explained through the TLC results revealing high levels of tannins in the bark and leaves but not in the fruit.

The chemical profiles (TLC, MeOH extracts – Figure 6.1c) for bark and leaves seemed similar and there was no great geographical variation for either the bark or leaves (water and MeOH extracts). A greater geographical variation was observed for the fruit (MeOH extracts), which could possibly be linked with the age of the fruit. The less polar extracts (EtOAc and PE) showed the lowest yields in all instances (Table 6.1) even though a greater amount of compounds mostly terpenes or benzoquinones (blue zones) [31, 65] were indicated using TLC (Figure 6.1a, b) in the case of bark and leaves. Reports of phytochemical studies of the medium polar DCM and non-polar PE extracts of the aerial parts from other *Rapanea* species (*Rapanea laetevirens*, *Rapanea umbellata*, *Rapanea lancifolia* and *Rapanea guyanensis*), revealed alkyl- and alkenyl resorcinols amongst the seed lipids [66], together with terpeno-*p*-hydroxy-benzoic acid derivatives [67] and dammarane-as well as cycloartane-type triterpenes [65] from the leaves, fruit and stems. These compounds all typically show blue-purple colouration when visualized on TLC, as was indicated in our findings. The fruit further seemed to produce the largest yields of PE and EtOAc extracts, possibly due to the fact that fruits often have a waxy layer on the surface to prevent dehydration. When comparing these non-polar and medium polar leaf and bark extracts, a great measure of geographical variation was evident as a function of geographical distribution, but also observed between samples from the same locality (for instance extracts from B1 and B2; Figure 6.1a). The same major terpene zones were however, present at  $R_f = 0.77$ , 0.85 and 0.92 in all the leaf and bark EtOAc extracts (Figure 6.1b). The terpenes at  $R_f = 0.77$  and 0.92 present in the leaves may be similar to those present in the fruit but the fruit contains an additional phenolic compound (red) which is not prominent in the leaves and bark. Flavonoids were also noted in the medium polar EtOAc extracts, presumably less glycosylated than those in the water and MeOH extracts.

### 6.3.3 Results of petroleum ether extract analysed by GC-MS

The PE extracts of the leaves, fruits and bark were subjected to GC-MS analysis in order to identify the major non-polar compounds and to ascertain whether there were

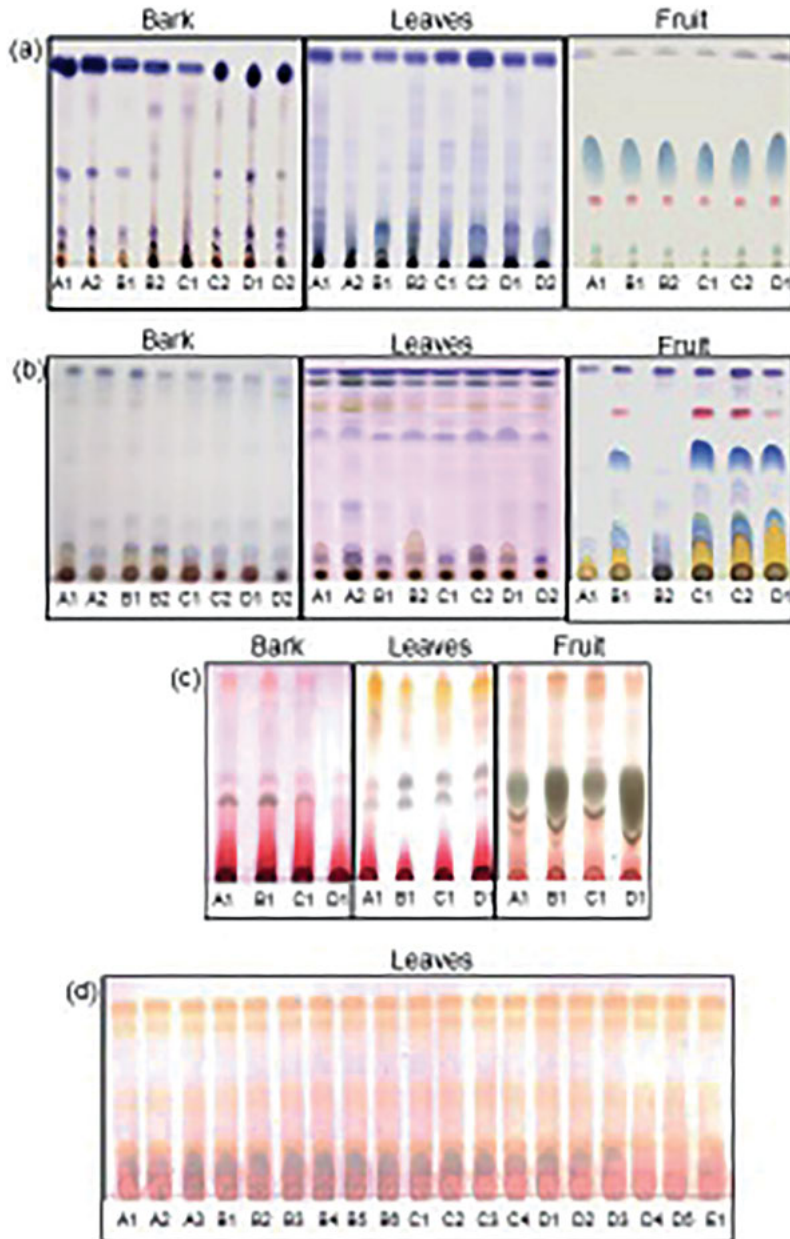


**Figure 6.1:** TLC comparison of the chemical components present in the stem bark, leaf and fruit extracts of *R. melanophloeos* extracted in (a) petroleum ether, developed in hexane-diethyl ether (3:2); (b) ethyl acetate-hexane (3:2); (c) methanol, developed in butanol-water-acetic acid (4:1:1). Vanillin-sulphuric acid was used as visualizing agent in all instances. Sample numbers: capital letter = locality, number = which plant sampled from the locality, e.g. A1 = Sicunusa, plant 1 (B = Nhlango, C = Bhunya, D = Fonteyn).

variations between samples from different localities. A variation pattern could be observed based on five main compounds that is, (-)-spathulenol (**6**), caryophyllene oxide (**7**) and  $\alpha$ -cadinol(**8**) (compound identities based on a >80% fit with compounds in the NIST library, not confirmed or quantified using isolated standards), together with two other unidentified compounds (Table 6.2; Table 6.2a – supplementary electronic material; Figure 6.2). These qualitative results confirmed the yields obtained (Table 6.1), where leaves and fruit contained similar yields of non-polar compounds and the bark either lacked most of the non-polar compounds or had them in very low concentrations. Plants from Swaziland (localities C, D, E) seemed to accumulate higher quantities of non-polar compounds with those from South Africa (locality F) also containing high levels of these compounds in the bark. Interestingly, the only reference of the bark being burnt as incense is in South Africa [28] corroborating the GC-MS results. In this instance, similar profiles were exhibited in most leaf and fruit extracts as well as bark extracts from locality F, where caryophyllene oxide (**7**) and  $\alpha$ -cadinol (**8**) were present in highest concentrations. Spathulenol (**6**) was also present in appreciable amounts in most leaves and fruits. Consequently, burning leaves instead of bark as incense may be promoted as conservation measure.

Where spathulenol (**6**) and caryophyllene oxide (**7**) are the major components of essential oils, the oils may further exhibit insect repellent [68] and antiparasitic properties, e.g. caryophyllene oxide (**7**) is insecticidal as well as an antifeedant [69]. In support of the traditional use where fruits are rather used for anthelmintic treatment than bark or leaves, it may very well be the non-polar essential oils in the fruit which are responsible for the anthelmintic effect. Essential oils rich in **6** [70], **7** [71] and **8** [72] have all been found to possess good anthelmintic activity, amongst various other antimicrobial activities. This notion is further supported by the modes of administration where the fruit are not necessarily extracted using any solvents, but are incorporated into the diet by eating the fruit raw or grinding it before taking it with milk, broth or beer [44].

Better representative results may also be obtained by rather extracting these volatile non-polar monoterpenes through steam distillation as is commonly used in the essential oil industry.

### 6.3.4 Amino acid analysis by means of GC-MS

The nutritional value of the fruit was shown clearly in its amino acid content (255.1 mg/g dry weight; (Table 6.3)) compared to that of the leaves (23.4 mg/g) and bark (21.3 mg/g). All nine essential amino acids (histidine, isoleucine, leucine, lysine, methionine, phenylalanine, threonine, tryptophan and valine) were present in the fruits. The amino acids present in the highest levels (>10 mg/g) were serine (10.6 mg/g), proline (33.9 mg/g), aspartic acid (14.2 mg/g), glutamic acid (30.7 mg/g) and tryptophan (10.4 mg/g). The presence of proline, lysine or tyrosine in appreciable levels is significant since they are the building blocks of the glycoproteins [57] suggested to be present in the APS.

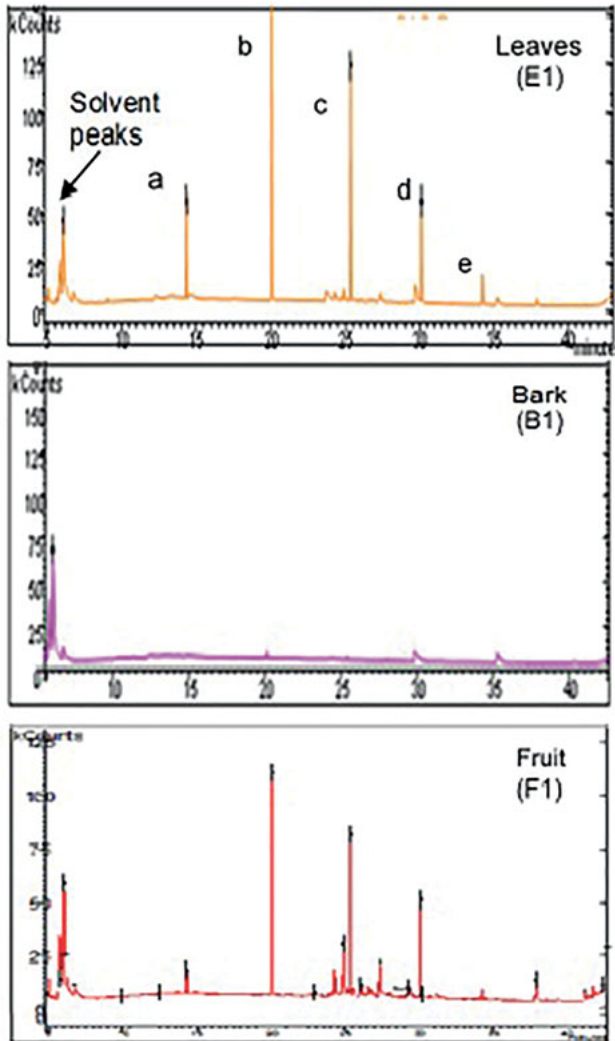


**Figure 6.2:** Examples of chromatograms obtained after GC-MS analysis of PE leaf, bark and fruit extracts from *Rapanea melanophloeos*.

Glutamate, the conjugate base of glutamic acid is an important neurotransmitter along with serotonin and dopamine amongst others [26]. Phenylalanine (4.5 mg/g; precursor to tyrosine) and tyrosine (9.4 mg/g) which are both precursors for dopamine and other catecholamine neurotransmitters (epinephrine and norepinephrine) as well as tryptophan (precursor for serotonin) [73] were present in high levels in the fruit. Aspartate (the conjugate base of aspartic acid) is the precursor to several amino acids, including four that are essential for humans that is, methionine, threonine, isoleucine, and lysine

(also present in the fruit at 0.8, 7.2, 4.0 and 5.8 mg/g respectively). Serine plays a key role in the phosphorylated (metabolic) pathway involved in various developmental events in plants [74, 75] and in humans it is particularly important in protein synthesis [76] and in neuromodulation [74]. D-Serine synthesized in the brain by serine racemase from its enantiomer L-serine serves as a neuromodulator by coactivating NMDA receptors and is a potent agonist at the glycine site of the NMDA-type glutamate receptor (NMDAR). For the receptor to open, glutamate and either glycine or D-serine must bind to it, where the latter is a more potent agonist at the glycine site [75]. Aspartate also stimulates NMDA receptors even though not as strongly as L-glutamate [77]. D-serine may be applied as potential treatment for schizophrenia [78] or as a potential biomarker in early Alzheimer's disease diagnosis [79]. Apart from the central nervous system, D-serine plays a further signalling role in peripheral tissues such as cartilage [80] and organs like the kidney [81] and corpus cavernosum [82].

Apart from the nourishing effect tonics provide through nutrients such as amino acids required for proper tissue health and organ function, the immuno-stimulatory effect suggested to be exhibited by *R. melanophloeos* saponins [83, 84] may be enhanced by the presence of appreciable levels of amino acids playing key roles in proper CNS functioning, so that the traditional claim of a tonic-effect (to strengthen the heart) for this species [85], [pers. communication with Mr. Dlamini and Mr. Msibi] is substantiated.

### 6.3.5 Antibacterial properties by means of MIC determination

The antibacterial activity of *R. melanophloeos* extracts was evaluated by determining their MIC values using the microdilution assay. In this study, MIC values below 8 mg/mL were considered weakly active [86], those exhibiting MIC values below 1 mg/mL were considered to have good activity [87] and values of less than 100 µg/mL were considered highly active [88]. These levels of activity were assigned based on the antibacterial activity of isolated compounds, where MIC values below 1 mg/mL are considered significant [87–89]. The pathogens were chosen on the basis of the infections they cause, so that the claims of traditionally using *R. melanophloeos* for the treatment of gastrointestinal (*E. faecalis*, *B. cereus*, *E.coli*), wound (*S. epidermidis*, *B. cereus*) and pulmonary infections (*P. aeruginosa*, *K. pneumoniae*) may be verified. In preliminary studies, the water extracts exhibited weak or no activity against the chosen pathogens and hence emphasis was placed on PE, EtOAc and MeOH extracts (Table 6.4).

The Gram-positive strains (*S. epidermidis* in particular) were more susceptible to all extracts probably due to the fact that Gram-negative bacteria have less penetrable cell walls. The EtOAc extracts (all plant parts) exhibited the best comparable activity against all the six pathogens (low MIC values of  $0.05 \pm 0.1$  mg/mL for *B. cereus* (Gram-positive) and  $0.5 \pm 0$  mg/mL for *Klebsiella pneumoniae* (Gram-negative)). MIC values exhibited for the EtOAc fruit extracts were reported as low as 0.0001 mg/mL against *S. epidermidis*

Table 6.4: Antibacterial effects of *R. melanophloeos* extracts against six bacterial strains.

Extracts with localities	Three gram-positive strains			Three gram-negative strains			
	<i>E. faecalis</i> ATCC 29212	<i>S. epidermidis</i> ATCC 2223	<i>B. cereus</i> ATCC 11778	<i>P. aeruginosa</i> ATCC 9027	<i>E. coli</i> ATCC 8739	<i>K. pneumoniae</i> ATCC 13883	
Petroleum ether	(mg/mL)	(mg/mL)	(mg/mL)	(mg/mL)	(mg/mL)	(mg/mL)	
Bark <sup>a</sup>	A	0.04	0.19	0.13	0.50	1.50	>8.00
	B	0.12	0.13	0.13	0.52	1.50	>8.00
	C	3.00	0.35	0.35	1.25	1.00	2.00
	D	0.12	0.19	0.13	0.50	2.00	2.00
	E	0.04	0.03	0.06	0.50	1.00	1.00
	F	0.12	0.13	0.13	0.50	1.50	1.00
Average	0.67 ± 1.3	0.18 ± 0.1	0.17 ± 0.1	0.80 ± 0.5	1.45 ± 0.5	1.44 ± 0.6	
Fruit <sup>b</sup>	A	0.13	0.13	0.25	0.50	2.00	>8.00
	B	0.38	0.15	0.14	1.13	1.13	0.88
	D	0.13	0.13	0.01	0.50	0.50	1.00
	Average	0.30 ± 0.4	0.15 ± 0.2	0.14 ± 0.2	0.92 ± 0.6	1.17 ± 0.5	0.90 ± 0.7
Leaves <sup>a</sup>	A	2.00	0.75	0.50	1.00	1.00	8.00
	B	1.50	0.63	1.75	1.50	2.00	>8.00
	C	0.25	0.75	0.35	1.00	1.50	8.00
	D	0.44	0.63	0.38	1.50	1.00	4.00
	E	1.00	0.38	1.00	0.50	0.50	>8.00
	F	0.75	0.50	0.75	1.00	1.00	4.00
Average	0.89 ± 0.7	0.61 ± 0.4	0.79 ± 1.6	1.15 ± 0.5	1.25 ± 0.5	5.50 ± 2.1	
Ethyl acetate	(mg/mL)	(mg/mL)	(mg/mL)	(mg/mL)	(mg/mL)	(mg/mL)	
Bark <sup>a</sup>	A	0.01	0.13	0.02	2.00	1.00	1.00
	B	0.04	0.13	0.27	1.50	1.00	1.75
	C	0.88	0.44	0.10	1.00	1.00	1.00

Table 6.4: (continued)

Extracts with localities	Three gram-positive strains			Three gram-negative strains		
	<i>E. faecalis</i> ATCC 29212	<i>S. epidermidis</i> ATCC 2223	<i>B. cereus</i> ATCC 11778	<i>P. aeruginosa</i> ATCC 9027	<i>E. coli</i> ATCC 8739	<i>K. pneumoniae</i> ATCC 13883
Petroleum ether	(mg/ml)	(mg/ml)	(mg/ml)	(mg/ml)	(mg/ml)	(mg/ml)
D	0.06	0.01	0.04	1.25	0.88	0.75
E	0.01	0.01	0.03	2.00	0.50	0.50
F	0.01	0.01	0.03	2.00	1.00	0.50
Average	0.20 ± 0.4	0.13 ± 0.2	0.09 ± 0.1	1.55 ± 0.5	0.92 ± 0.2	0.95 ± 0.8
Fruit <sup>b</sup>						
A	0.01	0.02	0.03	2.00	0.50	0.50
B	0.16	0.18	0.07	2.00	0.75	0.50
D	0.03	0.0001	0.003	2.00	0.50	0.50
Average	0.11 ± 0.2	0.12 ± 0.2	0.05 ± 0.1	2.00 ± 0.0	0.67 ± 0.3	0.50 ± 0.0
Leaves <sup>a</sup>						
A	0.50	0.25	0.25	0.50	1.00	4.00
B	0.38	0.25	0.32	0.50	0.50	5.00
C	0.13	0.19	0.11	0.50	1.11	2.00
D	0.32	0.19	0.50	0.50	0.50	3.00
E	0.50	0.13	0.25	1.00	0.50	2.00
F	0.13	0.19	0.25	0.50	0.50	2.00
Average	0.29 ± 0.2	0.20 ± 0.1	0.28 ± 0.2	0.55 ± 0.2	0.67 ± 0.5	3.00 ± 1.4
Methanol	(mg/ml)	(mg/ml)	(mg/ml)	(mg/ml)	(mg/ml)	(mg/ml)
Bark <sup>a</sup>						
A	1.00	0.50	1.00	2.00	1.00	1.00
B	0.88	0.50	1.00	3.00	1.00	1.00
C	0.50	0.50	1.00	4.00	1.00	1.50
D	0.50	0.50	1.00	4.00	1.00	1.00
E	0.50	0.50	1.00	4.00	1.00	1.00
F	0.75	0.50	1.00	3.00	1.00	1.00



Table 6.4: (continued)

Extracts with localities	Three gram-positive strains			Three gram-negative strains		
	<i>E. faecalis</i> ATCC 29212	<i>S. epidermidis</i> ATCC 2223	<i>B. cereus</i> ATCC 11778	<i>P. aeruginosa</i> ATCC 9027	<i>E. coli</i> ATCC 8739	<i>K. pneumoniae</i> ATCC 13883
Petroleum ether	(mg/mL)	(mg/mL)	(mg/mL)	(mg/mL)	(mg/mL)	(mg/mL)
Average	0.68 ± 0.2	0.50 ± 0.0	1.00 ± 0.0	3.40 ± 1	1.00 ± 0.0	1.10 ± 0.3
Fruit <sup>b</sup>						
A	4.00	1.00	2.00	2.00	4.00	1.50
B	2.00	1.06	2.00	3.00	2.00	3.5
D	2.00	0.50	2.00	2.00	2.00	2.00
Average	2.33 ± 0.8	0.96 ± 0.6	2.00 ± 0.0	2.67 ± 1.03	2.33 ± 0.8	1.45 ± 0.8
Leaves <sup>a</sup>						
A	0.50	1.00	0.31	2.00	1.00	1.50
B	1.00	1.00	1.00	1.00	1.00	1.00
C	0.75	0.88	0.75	1.50	1.00	1.00
D	0.88	1.00	0.75	3.00	1.00	1.00
E	0.75	0.13	1.00	2.00	1.00	1.00
F	0.75	1.00	1.00	1.50	1.00	1.00
Average	0.80 ± 0.3	0.89 ± 0.3	0.83 ± 0.3	1.80 ± 0.9	1.00 ± 0.0	1.05 ± 0.2
Controls	(mg/mL)	(mg/mL)	(mg/mL)	(mg/mL)	(mg/mL)	(mg/mL)
Negative: DMSO	>8.00	>8.00	>8.00	>8.00	>8.00	>8.00
Negative: acetone	>8.00	>8.00	>8.00	>8.00	>8.00	>8.00
Positive: ciprofloxacin (0.01 mg/mL)	$0.16 \times 10^{-3}$	$0.16 \times 10^{-3}$	$0.63 \times 10^{-3}$	$0.31 \times 10^{-3}$	$0.63 \times 10^{-3}$	$0.63 \times 10^{-3}$

Average MIC values (mg/mL, with STD) of all petroleum ether, ethyl acetate and methanol extracts of leaves, fruits and stem bark of *R. melanophloeos* against six bacterial strains associated with wounds as well as gastro-intestinal and respiratory ailments. <sup>a</sup>Samples/locality: A, B, C, D, E, F; <sup>b</sup>Samples/locality: A, B, D.

and 0.003 mg/mL against *B. cereus*, comparable to the positive control (ciprofloxacin; 0.00016 and 0.00063 mg/mL respectively). Both these values were reported for fruit from the same locality (D: Fonteyn, Hhohho district, Swaziland). Closer scrutiny with regards to the chemical composition of this particular extract (Figure 6.2b), showed a higher concentration of phenolic compounds (yellow and red zones) and terpenes (blue zones) when compared to other localities, for example Nhlangano, Shiselweni district (B), where the activities exhibited against the same pathogens were also significant (0.18 mg/mL against *S. epidermidis* and 0.07 mg/mL against *B. cereus*) but not as remarkable as those for D. Excellent activity was also observed for the EtOAc bark extracts against all three Gram-positive strains (0.01–0.88 mg/mL). Where activity against the Gram-negative pathogens was concerned, it was noted that all the EtOAc extracts showed good activity against *E. coli* (MIC of 0.5–1.11 mg/mL). The EtOAc leaf extracts were further observed to be most active against *P. aeruginosa* (MIC of 0.5–1.0 mg/mL) and weakly active against *K. pneumoniae* (MIC of 2.0–5.0 mg/mL), while the activities exhibited against the latter two pathogens by the fruit and bark was *vice versa*. The PE extracts also exhibited very good activity against all three Gram-positive strains (MIC of 0.01–3.0 mg/mL), though not as good as the EtOAc extracts. Comparable with the EtOAc extracts, the PE fruit extracts showed the best activity (MIC of 0.01–0.38 mg/mL), followed by the bark (MIC of 0.03–3.0 mg/mL). A few of the extracts showed good activity against some of the Gram-negative strains but 80% of the PE bark extracts were active (MIC of 0.5 mg/mL) against *P. aeruginosa*, contrary to the findings for the EtOAc bark extracts. The best activities for the MeOH extracts were observed for the bark against *E. faecalis* (MIC of 0.5–1.0 mg/mL) and *S. epidermidis* (MIC of 0.5 mg/mL), as well as those for the leaves against *E. faecalis* (MIC of 0.5–1.0 mg/mL). The leaf extracts from specific localities exhibited inconsistent activity against some of the pathogens for example; MeOH leaf extract E (Lundzi, Manzini district, Swaziland) had an MIC of 0.31 mg/mL against *S. epidermidis*, while 70% of the other MeOH leaf extracts had MIC values of 1.0 mg/mL. Phytochemical variation is thus clearly correlated with variation in antibacterial activity. The *E. coli* results obtained for the MeOH leaf extracts (average MIC  $0.67 \pm 0.16$  mg/mL) was comparable with those obtained for the EtOH leaf extracts reported by Madikizela et al. [53] (MIC ranging between 0.39 and 0.78 mg/mL), but the PE and EtOAc leaf extracts results presented here are much improved compared to the MIC reported (6.25 mg/mL) against *E. coli* for PE and DCM leaf extracts in the Madikizela et al. study [39]. The activities obtained for the MeOH bark extracts (MIC 0.5 mg/mL) also contradict the non-activity reported for *S. epidermidis* by Steenkamp et al. [90].

The significant activities exhibited by the EtOAc extracts may be ascribed to the affinity of embelin (**1**) and rapanone (**2**) to this solvent [48, 91] While the emphasis of this study was not on the identification or quantification of these two compounds in the extracts, they would probably be present since they have been noted to be the two major 2,5-dihydroxyalkylbenzoquinones identified in all plant parts of *R. melanophloeos*, where the fruit would yield the highest quantities [48, 60, 92]. While embelin (**1**) is

reportedly present in most cases, the presence of rapanone (**2**) was said to vary considerably [93]. Embelin (**1**) has been shown to exhibit significant activity against Gram-negative bacteria; *P. aeruginosa* (MIC 25 µg/mL), *E. coli* (MIC 45 µg/mL) and *K. pneumoniae* (MIC 50 µg/mL), as well as Gram-positive *B. cereus* (MIC 20 µg/mL) [94, 95]. Rapanone (**2**) on the other hand, is reportedly inactive against *E. Coli* and *P. aeruginosa* but highly active against *K. pneumoniae* (MIC 16–32 µg/mL) [96]. This selective activity has been ascribed to the specific chain length of its alkyl side-chain (C13). Chains of C7 and longer have been reported to produce similar but significant activity while longer chains have an influence on the selectivity against certain pathogens. It could thus be suggested that extracts (EtOAc bark and fruit extracts) that exhibited significant activity against *K. Pneumonia* contain appreciable amounts of **1** and **2**, while significant activity of extracts (EtOAc leaf extracts) against *P. aeruginosa*, *E. coli* and *B. cereus* may be ascribed to appreciable the amount of **1**. Caryophyllene oxide (**7**) and  $\alpha$ -cadinol (**8**) were detected in the PE extracts as major compounds together with spathulenol (**6**). These compounds may thus contribute to the antibacterial properties of the PE extracts since it was reported that the essential oil of *Cyperus kyllingia* Endl., which contains **7** and **8** as major compounds (12.17 and 19.32% respectively) exhibited moderate antibacterial activity against *E. coli* and *P. aeruginosa* (10 mg/mL resulted in 15 mm diameter inhibition zones for both pathogens) [72], as was the case in this study. In other essential oils, where **6** and **7** were the major compounds, an MIC of 2.0 mg/mL was reported against *E. Coli* [97], and an MIC of 5.0–9.0 µg/mL against *S. Epidermidis* [98]. The results presented in this study for the PE extracts against *S. epidermidis* also indicated good activity but not as remarkable as those presented by Cunico et al. [98] where this could indicate that higher quantities of **6** synergistically enhance activity against *S. epidermidis*. Myrsinoic acids B (**3**) and C (**4**) were isolated from the MeOH leaf extracts [99] and show potential as antibacterial agents where **3** exhibited MIC of 62.5, 31.25, 125 and 125 µg/mL against *Bacillus subtilis*, *Staphylococcus aureus*, *S. saprophyticus* and *Streptococcus pyogenes* respectively [100].

This study has successfully confirmed scientific justification of the ethnomedicinal uses of *R. melanophloeos* extracts especially for ailments of bacterial etiology. A comprehensive overview of traditional uses was done. Extract yields obtained for solvents from different polarities confirmed the presence of APS and amino acids as well as various classes of terpenoids and phenolic compounds. Close scrutiny of water and APS extract yields showed that APS contribute largely to most of the water extractable solids, thus explaining the mucilage observed in water extracts as well as the use of *R. melanophloeos* for treatment of respiratory ailments. Caryophyllene oxide,  $\alpha$ -cadinol and (–)-spathulenol have been identified in the fruit, leaves and bark extracts, where these terpenes may also contribute to the antibacterial properties of the PE extracts. The fruit yielded the highest levels and variety of amino acids compared to the leaves and bark, where all nine essential amino acids were present in the fruits. The amino acids present in the highest levels were proline, glutamic acid, aspartic acid, serine and tryptophan, not only confirming the presence of glycoproteins but also to

proper physiological functioning of living organisms. TLC and antibacterial activities of the leaf, bark and fruit extracts confirmed slight variations in chemical composition due to geographic distribution.

The noteworthy activities exhibited by the EtOAc and PE extracts warrant further research where the scope of the geographical variation could be widened and all the major active compounds identified, including the still unidentified medium polar saponins and flavonoids in all the plant parts. Soxhlet extraction with PE or hexane, steam distillation or CO<sub>2</sub> supercritical fluid extraction could be applied for improved extraction of the active non-polar compounds. Although the bark is the most popular in Southern African traditional medicine, similar significant antibacterial activity was observed for the fruits, especially where PE and EtOAc extracts were concerned. For the MeOH extracts, bark and leaves showed the best activities. Plant-part substitution should thus be promoted where possible as a means of conservation.

## 6.4 Conclusions

This study has successfully confirmed scientific justification of the ethnomedicinal uses of *R. melanophloeos* extracts especially for ailments of bacterial etiology. A comprehensive overview of traditional uses was done. Extract yields obtained for solvents from different polarities confirmed the presence of APS and amino acids as well as various classes of terpenoids and phenolic compounds. Close scrutiny of water and APS extract yields showed that APS contribute largely to most of the water extractable solids, thus explaining the mucilage observed in water extracts as well as the use of *R. melanophloeos* for treatment of respiratory ailments. Caryophyllene oxide,  $\alpha$ -cadinol and (-)-spathulenol have been identified in the fruit, leaves and bark extracts, where these terpenes may also contribute to the antibacterial properties of the PE extracts. The fruit yielded the highest levels and variety of amino acids compared to the leaves and bark, where all nine essential amino acids were present in the fruits. The amino acids present in the highest levels were proline, glutamic acid, aspartic acid, serine and tryptophan, not only confirming the presence of glycoproteins but also to proper physiological functioning of living organisms. TLC and antibacterial activities of the leaf, bark and fruit extracts confirmed slight variations in chemical composition due to geographic distribution.

The noteworthy activities exhibited by the EtOAc and PE extracts warrant further research where the scope of the geographical variation could be widened and all the major active compounds identified, including the still unidentified medium polar saponins and flavonoids in all the plant parts. Soxhlet extraction with PE or hexane, steam distillation or CO<sub>2</sub> supercritical fluid extraction could be applied for improved extraction of the active non-polar compounds. Although the bark is the most popular in Southern African traditional medicine, similar significant antibacterial activity was observed for the fruits, especially where PE and EtOAc extracts were concerned. For the

MeOH extracts, bark and leaves showed the best activities. Plant-part substitution should thus be promoted where possible as a means of conservation.

**Acknowledgments:** This work was funded by the University of Johannesburg through the Postgraduate Bursary Fund. The authors are grateful to the staff of the Swaziland Institute for Research in Traditional Medicine, Medicinal and Indigenous Food Plants (SIREMIP) for their assistance with plant collection.

**Author contributions:** All the authors have accepted responsibility for the entire content of this submitted manuscript and approved submission.

**Research funding:** This work was funded by the University of Johannesburg.

**Conflict of interest statement:** The authors declare no conflict of interest.

## References

1. Abraham I, Joshi R, Paedasani P, Pardasani RT. Recent advances in 1,4-benzoquinone chemistry. *J Braz Chem Soc* 2011;22:385–421.
2. Kupicha FK. Myrsinaceae, 1st ed. Zambia: Flora zambesiaca; 1983, 7.
3. Polhill R, Halliday P. Flora of tropical East Africa. Myrsinaceae. Netherlands: A.A. Balkema, Rotterdam; 1984.
4. Williams VL, Raimondo D, Crouch NR, Cunningham AB, Scott-Shaw CR, Lötter M, et al. *Rapanea melanophloeos* (L.) Mez. national assessment: red list of South African plants version 2017.1. 2016. [accessed 15 May 2017].
5. Dyer RA, Codd LEW, Rycroft HB. Flora of Southern Africa. Govt. Printer. Pretoria: Cape and Transvaal Printers Limited; 1963.
6. Palgrave KC. Trees of Southern Africa. South Africa: Struik Publishers; 2002.
7. De Sousa DP, Vieira YW, Dunlop RA, Cox PA, Banack SA, Rodgers KJ, et al. Histoire des plantes de la Guiane Française: rangées suivant la méthode sexuelle, avec plusieurs mémoires sur différents objets intéressans, relatifs à la culture & au commerce de la Guiane Française, & une notice des plantes de l'Isle-de-France. *J Ethnopharmacol* 1775;14:159–72.
8. van Wyk B-E, van Oudtshoorn B, Gericke N. *Erythrina lysistemon*. In: Medicinal plants of South Africa. South Africa: Briza Publications; 1997:124–5 pp.
9. Lovett JC, Bridson DM, Thomas DW. A preliminary list of the moist forest Angiosperm Flora of Mwanihana Forest Reserve, Tanzania. *Ann Mo Bot Gard* 1988;75:874–85.
10. Aerts R, Thijs KW, Lehouck V, Beentje H, Bytebier B, Matthyssen E, et al. Woody plant communities of isolated Afromontane cloud forests in Taita Hills, Kenya. *Plant Ecol* 2011;212:639–49.
11. Müller T. The distribution, classification and conservation of rainforests in Zimbabwe. In: African plants: biodiversity, taxonomy and uses. Kew: Royal Botanic Gardens; 1999.
12. Jolly D, Taylor D, Marchant R, Hamilton A, Bonnefille R, Buchet G, et al. Vegetation dynamics in central Africa since 18,000 yr BP: pollen records from the interlacustrine highlands of Burundi, Rwanda and Western Uganda. *J Biogeogr* 1997;24:495–512.
13. Hemp A. Continuum or zonation? Altitudinal gradients in the forest vegetation of Mt. Kilimanjaro. *Plant Ecol* 2006;184:27–42.
14. Hubau W, Van den Bulcke J, Bostoen K, Clist BO, Smith AL, Defoirdt N, et al. Archaeological charcoals as archives for firewood preferences and vegetation composition during the late Holocene in the Southern Mayumbe. *Veg Hist Archaeobotany* 2014;23:591–606.

15. Neba NE. Degradation of useful plants in Oku tropical montane cloud forest, Cameroon. *Int J Biodivers Sci Manag* 2006;2:73–86.
16. Ihuma JO, Chima UD, Chapman HM. Diversity of fruit trees and frugivores in a Nigerian montane forest and adjacent fragmented forests. *Int J Plant Anim Environ Sci* 2011;1:6–15.
17. Delvaux C, Sinsin B, Darchambeau F, Van Damme P. Recovery from bark harvesting of 12 medicinal tree species in Benin, West Africa. *J Appl Ecol* 2009;46:703–12.
18. Mez C. Myrsinaceae. *Das Pflanzenreich* 1902;4:1–437.
19. Palmer E, Pitman N. *Trees of South Africa*. Cape Town: A. A. Balkema Publishers; 1961.
20. Aublet F. *Histoire des plantes de la Guiane Française : rangées suivant la méthode sexuelle, avec plusieurs mémoires sur différens objets intéressans, relatifs à la culture & au commerce de la Guiane Française, & une notice des plantes de l'Isle-de-France*. London and Paris: P. F. Didot jeune; 1775.
21. Hutchings A. A survey and analysis of traditional medicinal plants as used by the Zulu, Xhosa and Sotho. *Bothalia* 1989;19:111–23.
22. Miller JS. Zulu medicinal plants: an inventory by A. Hutchings with A. H. Scott, G. Lewis, and A. B. Cunningham (University of Zululand). University of Natal Press, Pietermaritzburg. 1996. xiv + 450 pp. 21 × 29.5 cm. \$133.00. ISBN 0-86980-893-1. *J Nat Prod* 1997;60:955.
23. Watt J, Breyer-Brandwijk MJ. *The medicinal and poisonous plants of Southern and Eastern Africa*, 2nd ed. London: Livingstone; 1962.
24. Pujol J. *Naturafrika – the herbalist handbook*. Durban: Jean Pujol Natural Healers Foundation; 1990.
25. Nanyingi MO, Mbaria JM, Lanyasanya AL, Wagate CG, Koros KB, Kaburia HF, et al. Ethnopharmacological survey of Samburu district, Kenya. *J Ethnobiol Ethnomed* 2008;4:1–12.
26. Van Wyk B-E, Wink M. *Medicinal plants of the world*. Pretoria: Briza Publications; 2004.
27. Olivier DK. The ethnobotany and chemistry of South African traditional tonic plants. South Africa: PhD Thesis, Department of Chemistry, University of Johannesburg, <http://hdl.handle.net/10210/8094>; 2012. <http://hdl.handle.net/10210/8094>.
28. Dold AP, Cocks ML. Imbholha yesiXhosa: traditional Xhosa cosmetics. *Veld Flora* 2005;91:123–5.
29. Zschocke S, Rabe T, Taylor JLS, Jager AK, Van Staden J. Plant part substitution – a way to conserve endangered medicinal plants? *J Ethnopharmacol* 2000;71:281–92.
30. O'Brien C. Physical and chemical characteristics of Aloe gels, *S Afr J Bot*; 2005;77:988.
31. Wagner H, Blatt S. *Plant drug analysis. A thin layer chromatography atlas*, 2nd ed. New York: Springer-Verlag; 1996.
32. Eloff JN. A sensitive and quick microplate method to determine the minimal inhibitory concentration of plant extracts for bacteria. *Planta Med* 1998;64:711–3.
33. Gerstner J. A preliminary check list of Zulu names of plants. *Bantu Stud* 1941;15:277–301.
34. Williams VL, Raimondo D, Crouch NR, Cunningham AB, Scott-Shaw CR, Lötter M, et al. *Rapanea melanophloeos* (L.) Mez. national assessment: red list of South African plants version 2014. 2008. <https://treesa.org/rapanea-melanophloeos/>.
35. Dold AP, Cocks M l. Traditional veterinary medicine in the Alice district of the eastern Cape Province, South Africa. *South Afr J Sci* 2001;97:375.
36. Moll E. *Trees of Natal*. Cape Town: ABC Press; 1981.
37. Gerstner J. A preliminary check list of Zulu names of plants. *Bantu Stud* 1939;13:307–26.
38. Hutchings A, Scott AH, Lewis G, Cunningham A. *Zulu medicinal plants: an inventory*. Scottsville: University of Natal Press; 1996.
39. Madikizela B, Ndhala AR, Finnie JF, Van Staden J. Ethnopharmacological study of plants from Pondoland used against diarrhoea. *J Ethnopharmacol* 2012;141:61–71.
40. Chinemana F, Drummond RB, Mavi S, De Zoysa I. Indigenous plant remedies in Zimbabwe. *J Ethnopharmacol* 1985;14:159–72.

41. Neuwinger HD. African traditional medicine – a dictionary of plant use and applications. Stuttgart: Medpharm Scientific Publishers; 2000.
42. Van Wyk B, Van Wyk P, Van Wyk B-E. Photo guide to trees of Southern Africa, 2nd ed. South Africa: Briza Publishers; 2008.
43. Glover PE, Stewart J, Gwynne MD. Masai and Kipsigis notes on East African plants. Part II – domestic uses of plants. *East Afr Agric J* 1966;32:192–9.
44. Kokwaro JO. Medicinal plants of East Africa. Nairobi, Kenya: Literature Bureau; 1976.
45. Muthee JK, Gakuya DW, Mbaria JM, Kareru PG, Mulei CM, Njonge FK. Ethnobotanical study of anthelmintic and other medicinal plants traditionally used in Loitokitok district of Kenya. *J Ethnopharmacol* 2011;135:15–21.
46. Bally PRO. Native medicinal and poisonous plants of East Africa. *Bull Misc Inf* 1937;1937:10–26.
47. Lindsay RS. Medicinal plants of Marakwet, Kenya. Royal Botanic Gardens, Kew. In: African traditional medicine – a dictionary of plant use and applications. Stuttgart: Medpharm Scientific Publishers; 1978.
48. Midiwo JO, Yenesew A, Juma BF, Derese S, Ayoo JA, Aluoch AO, et al. Bioactive compounds from some Kenyan ethnomedicinal plants: Myrsinaceae, Polygonaceae and Psiadia punctulata. *Phytochemistry Rev* 2002;1:311–23.
49. Amusan OOG, Dlamini PS, Msonthi JD, Makhubu LP. Some herbal remedies from Manzini region of Swaziland. *J Ethnopharmacol* 2002;79:109–12.
50. Earle R. Can the Nubian change his skin, or the leopard his spots? *Afr Wildl* 1976;30:6–8.
51. La Cock GD, Briers JH. Bark collecting at Tootabie Nature Reserve, Eastern Cape, South Africa. *South Afr J Bot* 1992;58:505–9.
52. Bhat RB, Jacobs TV. Traditional herbal medicine in Transkei. *J Ethnopharmacol* 1995;48:7–12.
53. Madikizela B, Ndhlala AR, Finnie JF, Van Staden J. Ethnopharmacological study of plants from Pondoland used against diarrhoea. *J Ethnopharmacol* 2012;141:61–71.
54. Bruneton J. Pharmacognosy, phytochemistry, medicinal plants; 1995.
55. Manguro L, Midiwo JO, Kraus W. A new flavonol Tetraglycoside from *Myrsine Africana* leaves. *Nat Prod Res* 1996;9:121–6.
56. Kang L, Zhou JX, Shen ZW. Two novel antibacterial flavonoids from *Myrsine Africana* L. *Chin J Chem* 2007;25:1323–5.
57. Brielmann H, Kaufman P, Duke J, Cseke L, Warber S, Kirakosyan A. Natural products from plants, 2nd ed. CRC Press, Taylor and Francis; 2006.
58. Zou Y, Tan C, Zhu D. A new acetylated flavonoid glycoside from *Myrsine Africana* L. *Bull Kor Chem Soc* 2009;30:2111–3.
59. Othani K, Mavi S, Hostettmann K. Molluscicidal and antifungal triterpenoid saponins from *Rapanea melanophloeos* leaves. *Phytochemistry* 1993;33:83–6.
60. Midiwo J, Mwangi R, Ghebremeskel Y. Insect antifeedant, growth-inhibiting and larvicidal compounds from *Rapanea melanophloeos* (Myrsinaceae). *Int J Trop Insect Sci* 1995;16:163–6.
61. Venter F, Venter J-A. Making the most of indigenous trees. Pretoria: Briza Publications; 1996.
62. Max RA, Kimambo AE, Kassuku AA, Mtenga LA, Buttery PJ. Effect of tanniniferous browse meal on nematode faecal egg counts and internal parasite burdens in sheep and goats. *South Afr J Anim Sci* 2007;37:97–106.
63. Ombasa O, Kareru PG, Rukunga G, Mbaria J, Keriko JM, Njonge FK, et al. *In vitro* antihelmintic effects of two Kenyan plant extracts against *Haemonchus contortus* adult worms. *Int J Pharmacol Res* 2012;2:113–6.
64. Githiori JB, Höglund J, Waller PJ, Baker RL. Anthelmintic activity of preparations derived from *Myrsine Africana* and *Rapanea melanophloeos* against the nematode parasite, *Haemonchus contortus*, of sheep. *J Ethnopharmacol* 2002;80:187–91.

65. Januário AH, Da Silva MFDGF, Vieira PC. Dammarane and cycloartane triterpenoids from three *Rapanea* species. *Phytochemistry* 1992;31:1251–3.
66. Madrigal RV, Spencer GF, Plattner RD, Smith CR. Alkyl- and alkenylresorcinols in *Rapanea laetevirens* seed lipids. *Lipids* 1977;12:402–6.
67. Januário AH, Vieira PC, Da Silva MFDGF. Terpeno-p-hydroxybenzoic acid derivatives from *Rapanea umbellata*. *Phytochemistry* 1991;30:2019–23.
68. Cantrell CL, Klun JA, Bryson CT, Kobaisy M, Duke SO. Isolation and identification of mosquito bite deterrent terpenoids from leaves of American (*Callicarpa Americana*) and Japanese (*Callicarpa japonica*) beautyberry. *J Agric Food Chem* 2005;53:5948–53.
69. Bettarini F, Borgonovi GE, Fiorani T, Gagliardi I, Caprioli V, Massardo P, et al. Antiparasitic compounds from East African plants: isolation and biological activity of anonaine, matricarianol, canthin-6-one and caryophyllene oxide. *Int J Trop Insect Sci* 1993;14:93–9.
70. Kerala RTR, Francis MS, Soumya M. Essential oil composition of *Artemisia japonica* Thunb. *J Pharmacogn Phytochem* 2014;3:160–3.
71. Garg SC, Dengre SL. Composition of the essential oil from the leaves of *Buddleia asiatica* Lour. *Flavour Fragrance J* 1992;7:125–7.
72. Khamsan S, Liawruangrath B, Liawruangrath S, Teerawutkulrag A, Pyne S, Garson M. Antimalarial, anticancer, antimicrobial activities and chemical constituents of essential oil from the aerial parts of *Cyperus kyllingia* Endl. *Record Nat Prod* 2011;5:324–7.
73. Savelieva KV, Zhao S, Pogorelov VM, Rajan I, Yang Q, Cullinan E, et al. Genetic disruption of both tryptophan hydroxylase genes dramatically reduces serotonin and affects behavior in models sensitive to antidepressants. *PLoS One* 2008;3:e3301.
74. Tabatabaie L, Klomp LW, Berger R, De Koning TJ. L-serine synthesis in the central nervous system: a review on serine deficiency disorders. *Mol Genet Metabol* 2010;99:256–62.
75. Oliet SHR, Mothet JP. Regulation of N-methyl-D-aspartate receptors by astrocytic D-serine. *Neuroscience* 2009;158:275–83.
76. Dunlop RA, Cox PA, Banack SA, Rodgers KJ. The non-protein amino acid BMAA is misincorporated into human proteins in place of L-serine causing protein misfolding and aggregation. *PLoS One* 2013;8:e75376.
77. Chen PE, Geballe MT, Stansfeld PJ, Johnston AR, Yuan H, Jacob AL, et al. Structural features of the glutamate binding site in recombinant NR1/NR2A N-methyl-D-aspartate receptors determined by site-directed mutagenesis and molecular modeling. *Mol Pharmacol* 2005;67:1470–84.
78. Singh SP, Singh V. Meta-analysis of the efficacy of adjunctive NMDA receptor modulators in chronic schizophrenia. *CNS Drugs* 2011;25:859–85.
79. Madeira C, Lourenco MV, Vargas-Lopes C, Suemoto CK, Brandao CO, Reis T, et al. D-serine levels in Alzheimer's disease: implications for novel biomarker development. *Transl Psychiatry* 2015;5:e561.
80. Takarada T, Hinoi E, Takahata Y, Yoneda Y. Serine racemase suppresses chondrogenic differentiation in cartilage in a Sox9-dependent manner. *J Cell Physiol* 2008;215:320–8.
81. Ma M-C, Huang H-S, Chen Y-S, Lee S-H. Mechanosensitive N-methyl-D-aspartate receptors contribute to sensory activation in the rat renal pelvis. *Hypertension* 2008;52:938–44.
82. Ghasemi M, Rezaei F, Lewin J, Moore KP, Mani AR. D-serine modulates neurogenic relaxation in rat corpus cavernosum. *Biochem Pharmacol* 2010;79:1791–6.
83. Francis G, Kerem Z, Makkar HPS, Becker K. The biological action of saponins in animal systems: a review. *Br J Nutr* 2002;88:587.
84. Sun H-X, Xie Y, Ye Y-P. Advances in saponin-based adjuvants. *Vaccine* 2009;27:1787–96.
85. Hutchings A, Scott AH, Lewis G, Ab C. *Erythrina lysistemon* Hutch. In: *Zulu medicinal plants: an inventory*. South Africa: University of Natal Press; 1996:145 p.



86. Fabry W, Okemo PO, Ansong R. Antibacterial activity of East African medicinal plants. *J Ethnopharmacol* 1998;60:79–84.
87. Rios JL, Recio MC. Medicinal plants and antimicrobial activity. *J Ethnopharmacol* 2005;100:80–4.
88. Bueno J. *In vitro* antimicrobial activity of natural products using minimum inhibitory concentrations: looking for new chemical entities or predicting clinical response. *Med Aromatic Plants* 2012;01:1–2.
89. Gibbons S. Anti-staphylococcal plant natural products, 2nd ed. *Natural Product Reports*; 2004, 21:263–77 pp.
90. Steenkamp V, Fernandes AC, Van Rensburg CEJ. Antibacterial activity of Venda medicinal plants. *Fitoterapia* 2007;78:561–4.
91. Mosa R, Lazarus G, Oyediji A. *In vitro* anti-platelet aggregation, antioxidant and cytotoxic activity of extracts of some Zulu medicinal plants. *J Nat Prod* 2011;4:136–46.
92. Ghebremeskel Y. Chemical analysis of *Rapanea melanophloeos* (Myrsinaceae) alkybenzoquinones and some of their biological activities [M.Sc. thesis]. Department of Chemistry, University of Nairobi; 1991.
93. Mashimbye MJ. Chemical constituents of plants native to Venda [M.Sc. thesis]. Pietermaritzburg: Department of Chemistry, University of Natal; 1993.
94. Chitra M, Devi CSS, Sukumar E. Antibacterial activity of embelin. *Fitoterapia* 2003;74:401–3.
95. Radhakrishnan N, Gnanamani A, Mandal A. A potential antibacterial agent Embelin, a natural benzoquinone extracted from *Embelia ribes*. *Biol Med* 2011;3:1–7.
96. Omosa LK, Midiwo JO, Mbaveng AT, Tankeo SB, Seukey JA, Voukeng IK, et al. Antibacterial activities and structure–activity relationships of a panel of 48 compounds from Kenyan plants against multidrug resistant phenotypes. *SpringerPlus* 2016;5:1–15.
97. Hess SC, Peres MTL, Batista AL, Rodrigues JP, Tiviroli SC, Oliveira LGL, et al. Evaluation of seasonal changes in chemical composition and antibacterial activity. *Evaluation* 2007;30: 370–3.
98. Cunico MM, Lopes AR, Côcco LC, Yamamoto CI, Plochanski RCB, Miguel MD, et al. Phytochemical and antibacterial evaluation of essential oils from *Ottonia martiana* Miq. (Piperaceae). *J Braz Chem Soc* 2007;18:184–8.
99. Kimani N, Matasyoh J, Kibor AC. Antischistosomal benzoic acid derivatives from *Rapanea melanophloeos* against *Schistosoma mansoni* miracidia. *Research* 2014;1:1171.
100. Cruz AB, Kazmierczak K, Gazoni VF, Monteiro ER, Lais M, Martins P, et al. Bio-guided isolation of antimicrobial compounds from *Rapanea ferruginea* and its cytotoxic and genotoxic potential. *Res J Med Plant* 2013;71:1323–9.

---

**Supplementary Material:** The online version of this article offers supplementary material (<https://doi.org/10.1515/psr-2020-0143>).

Enitan Omobolanle Adesanya\*, Mubo Adeola Sonibare,  
Edith Oriabure Ajaiyeoba and Samuel Ayodele Egieyeh

## 7 Compounds isolated from hexane fraction of *Alternanthera brasiliensis* show synergistic activity against methicillin resistant *Staphylococcus aureus*

**Abstract:** Methicillin resistant *Staphylococcus aureus* (MRSA) has been classified as a “serious threat” by the centre for Disease Control, USA. *Alternanthera brasiliensis* plant, usually found on wasteland, belongs to the family Amaranthaceae. It is traditionally used for wound healing and has shown antimicrobial effect. Yet, this plant has not been fully explored for its antibacterial activity. Hence, this study evaluated isolated compounds from this plant for its activity against MRSA infections. The leaves extracts and fractions were prepared and concentrated *in vacuo* using a rotatory evaporator. Isolated compounds were obtained through vacuum liquid chromatographic (VLC) techniques and structurally elucidated with various spectroscopic techniques. Anti-MRSA assay of the fraction and compounds were evaluated by agar-well diffusion and broth-dilution methods while checkerboard assay was used to determine the fractional inhibitory concentration index (FIC<sub>i</sub>). The Gas Chromatography-Mass Spectrometry (GCMS) and High Performance Liquid Chromatography (HPLC) analysis revealed fatty acid and carboxylic acid components like hexadecanoic acid, bis (2-ethylhexyl) phthalate and Fettsäure. The compounds AbHD<sub>1</sub> and AbHD<sub>5</sub> were identified as hexadecanoic acid and di (ethylhexyl) phthalate. Anti-MRSA assay shows that *A. brasiliensis* hexane fraction (AbHF) and the compounds had zones of inhibitions (Z<sub>i</sub>) ranging from 7.3 ± 0.5 to 17.5 ± 0.5 mm with minimum inhibitory concentrations (MIC) between 1.22 × 10<sup>-5</sup> – 2.5 mg/mL. Synergistic effects were observed between AbHF and erythromycin, AbHF and ampicillin and AbHF and ciprofloxacin with FIC<sub>i</sub> 0.208–0.375 in K<sub>1</sub>St<sub>4</sub> strain while amoxicillin revealed antagonistic effects against M91 strain (4.67). Similarly, hexadecanoic acid and di (ethylhexyl) phthalate showed synergistic behaviour only with ampicillin against K<sub>1</sub>St<sub>4</sub> while the rest were antagonistic. The study revealed that hexadecanoic acid and di (ethylhexyl) phthalate isolated from *A. brasiliensis* showed synergistic activity in variations against MRSA isolate and strains.

---

\*Corresponding author: **Enitan Omobolanle Adesanya**, Department of Pharmacognosy, Faculty of Pharmacy, University of Ibadan, Ibadan, Nigeria, E-mail: enitadesanya@gmail.com. <https://orcid.org/0000-0002-1790-7579>

**Mubo Adeola Sonibare and Edith Oriabure Ajaiyeoba**, Department of Pharmacognosy, Faculty of Pharmacy, University of Ibadan, Ibadan, Nigeria

**Samuel Ayodele Egieyeh**, Pharmacology and Clinical Pharmacy, School of Pharmacy, University of the Western Cape, Cape Town, South Africa

This article has previously been published in the journal Physical Sciences Reviews. Please cite as: E. O. Adesanya, M. A. Sonibare, E. O. Ajaiyeoba and S. A. Egieyeh “Compounds isolated from hexane fraction of *Alternanthera brasiliensis* show synergistic activity against methicillin resistant *Staphylococcus aureus*” *Physical Sciences Reviews* [Online] 2021, 8. DOI: 10.1515/psr-2020-0113 | <https://doi.org/10.1515/9783110710823-007>

**Keywords:** *Alternanthera brasiliensis*; antibacterial; isolation; methicillin resistant *Staphylococcus aureus*; synergistic activity.

## 7.1 Introduction

*Methicillin-resistant Staphylococcus aureus* (MRSA) also known as multidrug-resistant *S. aureus* and oxacillin-resistant *S. aureus* (ORSA) is a bacterium responsible for several difficult to treat infections [1]. Due to resistance to beta-lactam antibiotics, which include the penicillin (methicillin, dicloxacillin, nafcillin, oxacillin, etc.) and the cephalosporin [2]. In the light of the foregoing, we need new antimicrobial treatments to keep up with the constantly emerging antibiotic resistance. Hence, the World Health Organization has included MRSA as an important antibiotic-resistant bacteria requiring the urgent need for new drugs [3]. Recent search for new antibiotic drug candidates have focused on compounds from nature because of their privileged structures and previous success as anti-infective [4].

*Alternanthera brasiliensis* Hort ex. Vilmorin is a species belonging to the flowering plants in the amaranth family, Amaranthaceae. The species of the genus *Alternanthera* are widespread flowering plants with most species occurring in the tropical Americas and others in Asia, Africa and Australia (Flora of North America) [5]. In general plants of this genus are known as joy weeds, or Joseph's coat (Integrated Taxonomic Information System [ITIS]) and a number of the species are known as notorious toxic weeds [6]. *Alternanthera brasiliensis* plant is the least explored for its medicinal activity and traditionally used for wound dressing and to prevent abortion [7]. Based on the ethnobotanical use of this plant for wound healing, this study evaluated extracts and isolated compounds from this plant for their activity against MRSA infections.

## 7.2 Materials and methods

### 7.2.1 Plant material

*Alternanthera brasiliensis* leaves were collected, identified and authenticated at the Forest Herbarium Ibadan (FHI) of Forestry Research Institute of Nigeria (FRIN), Ibadan, Oyo State where voucher specimens (FHI 110402) was deposited.

### 7.2.2 Plant extraction and fractionation

The leaves were air-dried for two weeks and milled with electric blender. The plant materials were macerated in absolute methanol for 120 h and filtered and the filtrate was subjected to low pressure distillation (Rotary Evaporator) at 40 °C to obtain waxy

mass called *concentrate* (crude extract). The crude extract was further partitioned using separating funnel with *n*-hexane according to Taib et al. [8] with slight modification. Briefly, a solution of 200 mL was constituted in ratio of 20:30:50% of methanol, water and *n*-hexane, respectively in a 250 mL separating funnel to obtain *n*-hexane fraction.

### 7.2.3 Isolation of compounds from the *A. brasiliensis*

The hexane fraction of *A. brasiliensis* (AbHF) leaves was subjected to purification with a vacuum liquid chromatography (VLC). The VLC was employed according to the method of Isah et al. [9] with some modifications for the isolation of compounds. Concisely, 25 g of the fraction was dissolved in methanol and filtered to eliminate undissolved lump. The filtrate was pre-adsorbed unto 10 g of silica gel and allowed to dry overnight. This was packed with 500 g silica gel (Hi Media Labs., India) and subjected to VLC. The column was eluted with different solvent system starting with 100% hexane and various ratios of hexane – EtOAc up to 100% EtOAc then DCM 100% followed by various ratios of DCM-MeOH by collecting 200 mL each. Based on their thin layer chromatographic (TLC) profiles on the TLC plates (Merck, Darmstadt, Germany), the sub-fractions were further pooled and tested for their anti-MRSA activities, the potent fractions were later subjected to column chromatography and eluted. Fraction AbHD was further purified via column chromatography to allow effective isolation of compounds AbHD<sub>1</sub> and AbHD<sub>5</sub> respectively.

### 7.2.4 High performance liquid chromatography (HPLC) analysis

The High performance liquid chromatography (HPLC) analysis was done using a Mobile phase –90% Acetonitrile/10% water with a phenomenex column of C18. Isocratic elution was run at 0.5 mL/min with a visible – UV diode array detector.

### 7.2.5 Gas Chromatography-Mass Spectrometry (GCMS) analysis

The Gas Chromatography-Mass spectrometry (GCMS) analysis of the AbHF was performed using the GC-MS machine (model Agilent technologies GC-7890 coupled with an MS-5975, USA.). The column (model Agilent technologies HP5MS) with length 30 m, internal diameter of 0.320 mm and thickness of 0.25  $\mu$ L. The oven temperature program, initial temperature is 80 °C held for 2 min at 12°/min to the temperature of 240° held for 6 min with the 1  $\mu$ L of sample injected. The interface temperature between GC and MS is 250 °C. The mode of analysis is split less injection and the scan ranges is from 50 to 500. The components data were analysed according to their library sources by comparing their retention indices and mass spectra fragmentation patterns with those stored on the computer library and published literature.

## 7.2.6 Nuclear Magnetic Resonance (NMR) analysis

The Nuclear Magnetic Resonance (NMR) spectra were recorded on a Bruker Ascend-500 spectrometer (Bruker Biospin Co., Karlsruhe, Germany) with  $^1\text{H}$  and  $^{13}\text{C}$  NMR at 400 MHz. The isolated compounds were prepared using deuterated methanol with tetramethylsilane (TMS) as an internal standard in 5 mm NMR tubes. Chemical shifts were expressed in parts per million ( $\delta$ ) according to the TMS signal. 2D NMR-Nuclear Overhauser Effect Spectroscopy (NOESY) and Heteronuclear single quantum coherence spectroscopy (HSQC) were applied for better structural assignments.

## 7.2.7 Antibacterial assay

### 7.2.7.1 Bacterial strains

The clinical MRSA strain MRSA-K<sub>1</sub>St<sub>4</sub> used was collected from the Department of Pharmaceutical Microbiology, Olabisi Onabanjo University Ago-Iwoye Ogun State, while the standard isolate MRSA-M91 was collected from the Department of Pharmaceutical Microbiology, University of Ibadan.

### 7.2.7.2 Agar well-diffusion assay and broth-dilution method

An agar-well diffusion and broth dilution method proposed by Clinical and Laboratory Standards Institute [10] and Mirtaghi et al. [11] were used for the assay to determine the zones of inhibitions (Zi) and Minimum Inhibitory Concentration (MIC), respectively.

### 7.2.7.3 Preparation of inoculum inoculation of plates

The MRSA strain and isolate were sub-cultured on nutrient broth and incubated at 37 °C for 24 h. Subsequently the nutrient agar was prepared according to standard procedure and autoclaved at 121 °C for 15 min, then allowed to cool to about 40 °C and dispensed into sterilized plates. These plates were allowed to gel (i.e. solidify), thereafter each inoculum was introduced unto the different gelatinized nutrient agar plates using a sterilized swab stick and standard cork-borer (6 mm in diameter) to bore four equidistant holes into each plates. Concentrations of 12.5, 25, 50 and 100 mg/mL of the hexane fractions, 1.25, 2.5, 5 and 10 mg/mL of sub-fraction AbHD and 25  $\mu\text{g}/\text{mL}$  of compounds AbHD<sub>1</sub> and AbHD<sub>5</sub> were prepared in that order and 0.2 mL of test solutions at the different concentrations were added into the wells. The plates were incubated at 37 °C for 24 h and the Zi measured using a metric ruler. Fifty micrograms per millilitre of ampicillin, amoxicillin, ciprofloxacin, erythromycin and gentamycin each were used as positive control while methanol and water as negative controls, respectively. Each antibacterial assay was carried out in triplicate.

#### 7.2.7.4 Broth dilution method (determination of MIC)

A twofold serial dilutions of the extract and fractions were prepared to obtain concentrations used to determine the MIC. In the 96 micro-wells plates, 0.1 mL of suspension of standard strain (M 91) and clinical isolate (K<sub>1</sub>St<sub>4</sub>) of MRSA was added individually and inoculated at 37 °C for 24 h, the lowest concentration that inhibited the growth of the organisms was regarded as the MIC.

#### 7.2.7.5 Checkerboard assay

To determine the synergistic interaction between antibiotics and the bioactive compounds, the checkerboard assay was employed according to Olajuyigbe [12] and Reuk-ngam et al. [13] with slight modifications to obtain the fractional inhibitory concentrations index (FIC<sub>i</sub>). This was done by determining the MIC of the drug and sample alone then in combination after incubation for 24 h at 37 °C, the FIC<sub>i</sub> was then calculated as;

$$\text{FIC}_i = (\text{MIC of sample A in combination} / \text{MIC of sample A alone}) \\ + (\text{MIC of antibiotic in combination} / \text{MIC of sample antibiotics alone})$$

Synergism by this method is then defined as FIC index  $\leq 1$ , additive effect as  $=1$ , indifference effect as  $>1$  and  $<4$  while antagonistic effect as  $>4$ .

### 7.2.8 Statistical analysis

The experimental results for the agar-well diffusion were expressed as mean  $\pm$  standard error of mean (SEM). Data were analysed using one way analysis of variance (ANOVA) and post-hoc test using Duncan analysis.

## 7.3 Results and discussion

### 7.3.1 Identification of potential compounds in *A. brasiliensis* hexane fraction

The GCMS analysis was done to assist in the potential identification of compounds from AbHF. Figure 7.1 shows the chromatogram of AbHF while the table (Appendix) shows a list of possible compounds with their retention time. Forty potential compounds that might be found in *A. brasiliensis* leaves hexane fraction were reported. The chromatogram of HPLC analysis shown in Figure 7.2 identified 13 likely components expected listed in a table (see Appendix).

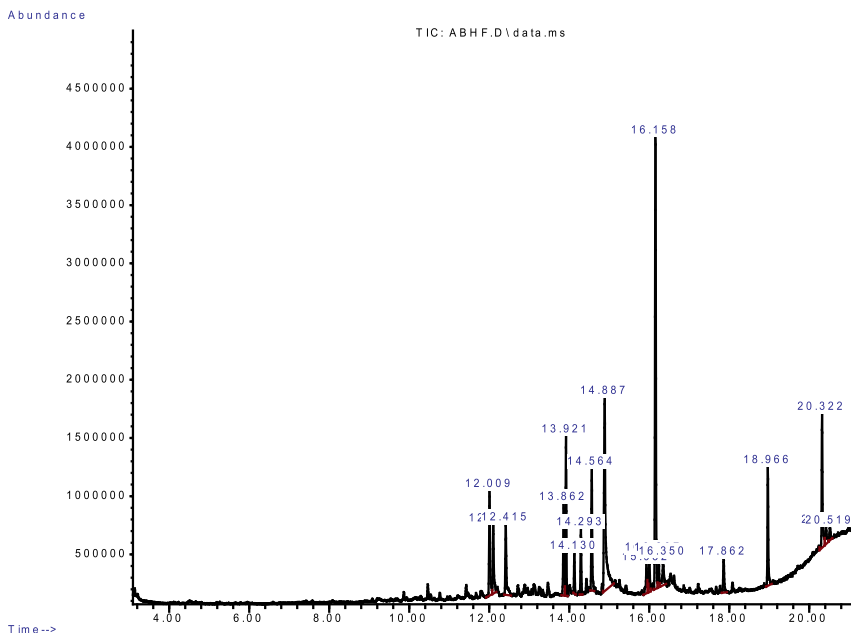


Figure 7.1: GCMS chromatogram of *A. brasiliensis* hexane fraction (This figure shows the retention time, absorbance and different peaks of compounds at which they were identified).

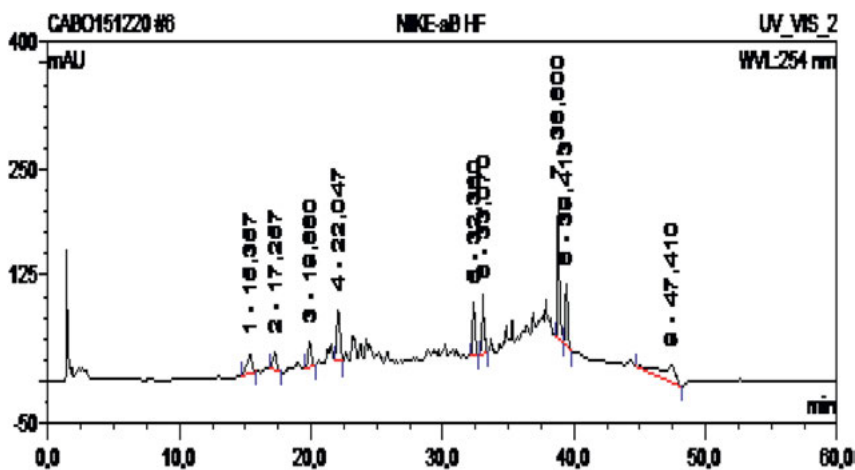


Figure 7.2: HPLC chromatogram of *A. brasiliensis* hexane fraction.

### 7.3.2 Isolation and structural elucidation of compounds from *A. brasiliensis* hexane fraction

Isolation and structural elucidation of compounds from AbHF identified compounds AbHD<sub>1</sub> and AbHD<sub>5</sub> using NMR (see Appendix). NOESY spectrum was used to determine

signals from protons that are close to each other and the spectrum are presented for compounds ABHD<sub>1</sub> and ABHD<sub>5</sub> (See appendix). HSQC spectrum showing hydrogen that were directly attached to carbons present in the compounds are presented (see Appendix). The spectroscopy identification assigned compound AbHD<sub>1</sub> as Hexadecanoic acid (palmitic acid) (Figure 7.3), formula C<sub>16</sub>H<sub>32</sub>O<sub>2</sub>. AbHD<sub>1</sub> (20 mg) was a yellow oil, with melting point of 66 °C and molecular mass of 256 g/mol.

The <sup>1</sup>H NMR spectrum of compound AbHD<sub>1</sub> displayed three major peaks; a triplet peak at  $\delta$  2.33 integrating for two protons ( $J = 6.8$  Hz), belonging to the methylene at position 2, that is the proton on the carbon directly connected to the carboxylic acid. An intense multiplet peak  $\delta$  1.23–1.40, integrating as 26H which represent protons of the methylenes between 3 and 15 positions, this indicates the presence of a long fatty chain on the molecule of compound AbHD<sub>1</sub>. Three typical protons appearing at  $\delta$  H 0.86 (3H, t,  $J = 6.8$  Hz, H-16); assigned to the terminal methyl group terminating the alkyl chain length at position 16. This further confirms the presence of the fatty alkyl chain in the fatty acid molecule of the compound.

The <sup>13</sup>C NMR spectrum indicated the presence of a carboxylic acid group appearing at  $\delta$  c 179.4 ppm, which is the most deshielded carbon in the <sup>13</sup>C NMR of compound AbHD<sub>1</sub>. Other upfield signals  $\delta$  34.1; assigned to carbon at position 2.  $\delta$  31.9 (C-14), 29.1–29.7; belonging to position 4–13 on the fatty acid, 24.9 (C-3) and 14.1 (C-16), which terminates the alkyl fatty acid. Comparing the <sup>1</sup>H and <sup>13</sup>C NMR spectra characteristics with literature according to Fadzil [14] heteronuclear single quantum coherence assignment shows a similar results (see Appendix).

Similarly, spectroscopy identification assigned Compound AbHD<sub>5</sub> as di ((2-ethylhexyl) phthalate) (Figure 7.4), a brownish-yellow powder, TLC R<sub>f</sub> = 0.87 Hex: ethyl acetate; (2:3). Composition: C<sub>24</sub>H<sub>38</sub>O<sub>4</sub>, Molecular mass: 390 g/mol.

The <sup>1</sup>H NMR spectrum of this phthalate dimer contains signals at  $\delta$ <sub>H</sub> 7.62 (2H, d,  $J = 5.6, 3.3$  Hz, H-1 and 4 of the *sp*-hybridized signal), 7.45 (2H, d,  $J = 5.6, 3.3$  Hz, H-2 and 3, of the aromatic region), 4.20 (4H, m, CH<sub>2</sub>-3' and 3''); assigned to the oxygenated methylene), 2.15 (2H, m, assigned to the methine peaks at 4' and 4'') on the side chain,  $\delta$ <sub>H</sub> 1.10–1.90 (16H, m; belonging to the methylene protons at 5', 6', 7', 9' and 5'', 6'', 7'' and 9'' respectively). Another peak at  $\delta$ <sub>H</sub> 0.80–0.90 (6H, t,  $J = 6.8$  Hz) belong to the methyl groups; *sp*<sup>3</sup> hybrid orbitals of the position 8'' and 10'' respectively.

The <sup>13</sup>C NMR of the phthalate contain 24 carbon resonances attributed to two quaternary most downfield carbons  $\delta$  167.8 (assigned to the carbonyl group of the

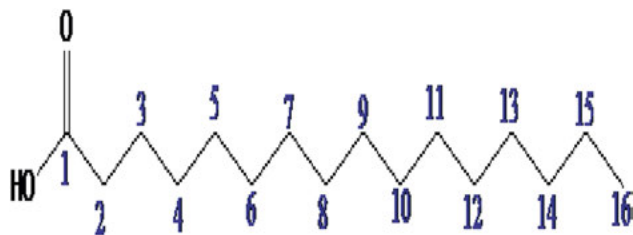


**Figure 7.3:** Structure of compound AbHD<sub>1</sub> – hexadecanoic acid (common name – palmitic acid).



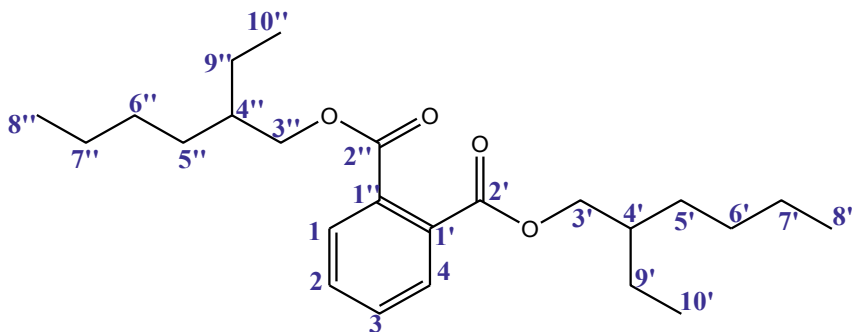


**Figure 7.4:** Structure of compound AbHD<sub>5</sub> (di (2-ethylhexyl) phthalate).

ester group at C-2' and 2'') of the dimer,  $\delta$  132.5 (assigned to the most deshielded aromatic carbon at C-1' and 1'' respectively), two aromatic methine carbon peaks at  $\delta$  130.9 (C-2 and 3), 128.8 (C-1 and 4) being *sp*-hybridized carbons and another *sp*-hybridized carbons signal at 24.8 (C-9' and 9''). Also, five *sp*<sup>2</sup>-hybridized carbon  $\delta$  68.2 (oxo-methylene carbon at C-3' and 3''), 30.4 (CH<sub>2</sub>-5' and 5''), 29.4 (C-6' and C-6''), 24.8 (C-9' and 9''), 23.8 (C-7' and 7'') and two methyl peaks of *sp*<sup>3</sup>-hybridized carbons  $\delta$  14.1 and 10.9 (C-8', 8'', C-10' and 10'' respectively).

The NOESY <sup>1</sup>H–<sup>1</sup>H correlation shows a spatial coupling of  $\delta_{\text{H}}$  4.20 (H-3'') with  $\delta_{\text{H}}$  2.15 (H-4'') and  $\delta_{\text{H}}$  0.80–0.90 (H-10'') since the compound is symmetrical, hence, 4.20 (H-3') will also correlates in space with  $\delta_{\text{H}}$  2.15 (H-4') and  $\delta_{\text{H}}$  0.80–0.90 (H-10'). Relating the <sup>13</sup>C NMR spectra characteristics with literature according to Nair et al. [15] heteronuclear single quantum coherence assignment shows a similar results (see Appendix).

### 7.3.3 Antibacterial assay

The bioassay fractionation potential of the hexane fraction and compounds isolated from *A. brasiliensis* leaves part are presented in Table 7.1. From the results, we see that hexane fraction of *A. brasiliensis* leaves part had activity at all the concentrations with a zone of inhibition (Zi) of range  $37 \pm 1.00$ – $47 \pm 2.67$  mm in diameter and MIC of 2.5 mg/mL against the standard strain of MRSA. The activity against the clinical strain was 50 mg/mL MIC concentration with Zi range  $09 \pm 0.58$ – $16 \pm 0.58$  mm in diameter. In addition, the tables shows that sub-fraction D of AbHF from VLC had activity at all the concentration tested against both clinical and standard strains. The Zi was between  $9 \pm 0.71$  mm and  $12 \pm 0.71$  mm, MIC 0.039 mg/mL against clinical strain while against standard strain, it had Zi between  $7.5 \pm 1.06$  mm and  $10 \pm 2.83$  mm, MIC 0.020 mg/mL. The isolated compounds AbHD<sub>1</sub> at 0.025 mg/mL showed Zi  $15 \pm 1.16$  mm and MIC  $1.22 \times 10^{-5}$  mg/mL against the clinical strain while against the standard strain it had Zi of  $14 \pm 2.08$  mm and MIC  $4.9 \times 10^{-5}$  mg/mL. Likewise, AbHD<sub>5</sub> had Zi of  $7.3 \pm 0.88$  mm and MIC  $1.22 \times 10^{-5}$  mg/

mL against the clinical strain while against the standard strain it had  $8.73 \pm 2.67$  mm and MIC  $4.9 \times 10^{-5}$  mg/mL.

Standard antibiotic drugs at 0.050 mg/mL concentrations were used as control drugs, ampicillin (beta-lactamase inhibitor antibiotics), amoxicillin (a beta-lactamase inhibitor antibiotics), ciprofloxacin (fluoroquinolones antibiotics) and erythromycin (a macrolide antibiotics) were selected and tested against both strains. The result from the table shows that ampicillin had no Zi at 0.05 mg/mL but had MIC of 0.05 mg/mL against the two strains while amoxicillin had Zi of 30 and 11 mm with MIC between  $1.56 \times 10^{-5}$  and  $3.9 \times 10^{-5}$  mg/mL, erythromycin had Zi of 30 and 26 mm with MIC between  $2.0 \times 10^{-5}$  and  $7.8 \times 10^{-5}$  mg/mL and ciprofloxacin 20 and 26 mm with MIC ranged  $1.56 \times 10^{-5}$ – $2.0 \times 10^{-5}$  mg/mL against both isolate but gentamycin had Zi 18 mm only against standard strain. The assay result revealed that both AbHF and isolated compounds (Hexadecanoic acid and di (ethylhexyl) phthalate) had good

**Table 7.1:** AntiMRSA assay of *A. brasiliensis* hexane fraction, AbHD<sub>1</sub> and AbHD<sub>5</sub>.

Plant Fraction	Bacteria	Concentrations (mg/mL)/Zones of inhibitions (mm)				MIC (mg/mL)
		25	50	75	100	
<i>A. brasiliensis</i> hexane fraction (AbHF)	M91	37 ± 1.00	42 ± 3.85	46 ± 4.81	47 ± 2.67	2.5
	K <sub>1</sub> St <sub>4</sub>	06 ± 0.00	09 ± 0.58	11 ± 0.58	16 ± 0.58	<2.5
Sub-fraction of AbHF		1.25	2.5	5	10	MIC (mg/mL)
AbHD	K1St4	9 ± 0.71	10 ± 0.71	10 ± 1.06	12 ± 0.71	0.039
	M <sub>91</sub>	7.5 ± 1.06	8.5 ± 0.71	8.5 ± 2.47	10 ± 2.83	0.020
Compound		0.025 (mg/mL)				
AbHD <sub>1</sub>	K1St4	15 ± 1.16	–	–	–	$1.22 \times 10^{-5}$
	M <sub>91</sub>	14 ± 2.08				$4.9 \times 10^{-5}$
AbHD <sub>5</sub>	K1St4	7.3 ± 0.88	–	–	–	$1.22 \times 10^{-5}$
	M <sub>91</sub>	8.73 ± 2.67				$4.9 \times 10^{-5}$
Control		0.05 (mg/mL)				
Ampicillin	M91	06				0.05
	K <sub>1</sub> St <sub>4</sub>	06				0.05
Amoxicillin	M91	30				$3.9 \times 10^{-5}$
	K <sub>1</sub> St <sub>4</sub>	11				$1.56 \times 10^{-5}$
Erythromycin	M91	30				$2.0 \times 10^{-5}$
	K <sub>1</sub> St <sub>4</sub>	26				$2.0 \times 10^{-5}$
Gentamycin	M91	18				$7.8 \times 10^{-5}$
	K <sub>1</sub> St <sub>4</sub>	00				Nd
Ciprofloxacin	M91	20				Nd
	K <sub>1</sub> St <sub>4</sub>	26				$1.5 \times 10^{-5}$
						$2.0 \times 10^{-5}$

Mean ± SEM, n – 3, Size of cork-borer 6 mm, ND, Not done.

anti-MRSA activity in comparison with the selected antibiotics. Also, from the assay isolated compounds had better inhibitory activities against the MRSA strain because they had lower MIC values than the antibiotic drugs used whereas for MRSA isolate they varied. Furthermore, this result has shown compounds isolated from *A. brasiliensis* can be used as antibiotic drug in the management of drug resistant.

This research also explored the level of synergism between common antibiotics and isolated compounds. FIC<sub>i</sub> was calculated and presented in Table 7.2. From the results, *A. brasiliensis* HF with ampicillin (beta-lactam drug) had FIC<sub>i</sub> 0.255 and 0.274; erythromycin 0.208 and 0.208 while ciprofloxacin 0.250 and 0.375 for both bacterial strain and isolate in that order. Synergistic effects were also, observed between AbHF, erythromycin and ciprofloxacin with FIC<sub>i</sub> range between 0.208 and 0.375 in K<sub>1</sub>St<sub>4</sub> while amoxicillin revealed antagonistic effects against M91 strain (4.67). The FIC<sub>i</sub> for AbHD<sub>1</sub> from the table reveals that with ampicillin 4.00098 and 1.000, erythromycin 4.49 and 4.13, ciprofloxacin 18.99 and 40.65 as well as amoxicillin gave 96.97 and 388.69 for both bacterial strain and isolate respectively. While compound AbHD<sub>5</sub> had 31.99 and 1.000 with ampicillin, 35.87 and 16.89 with erythromycin, 73.4 and 9.03 ciprofloxacin and 24.42 and 388.69 with amoxicillin for both bacterial strain and isolate correspondingly. The results from hexadecanoic acid and di (ethylhexyl) phthalate clearly reveals that it is with the clinical isolate that ampicillin had synergistic effect while other combination were antagonistic. This shows that synergism between ampicillin (a β-lactam drug) and hexadecanoic acid/di (hexylethyl) phthalate is a possible future solution to drug resistance especially in MRSA infections by altering resistance posed by the bacterial cell wall.

Generally, natural product have different antibacterial activity considering the existence of differences in polarity and secondary metabolites of plant material, solvent fractionation and mechanism of determining the presence of substances and affinities for

**Table 7.2:** Result of fractional inhibitory concentration (FIC) index.

Sample	Standard strain (M91)	Clinical isolate (K1St4)
AbHF + ampicillin	0.255 <sup>a</sup>	0.274 <sup>a</sup>
AbHF + erythromycin	0.208 <sup>a</sup>	0.208 <sup>a</sup>
AbHF + ciprofloxacin	0.250 <sup>a</sup>	0.375 <sup>a</sup>
AbHF + amoxicillin	4.67 <sup>c</sup>	3.30 <sup>b</sup>
AbHD <sub>1</sub> + ampicillin	4.00098 <sup>c</sup>	1.000 <sup>a</sup>
AbHD <sub>1</sub> + erythromycin	4.49 <sup>c</sup>	4.13 <sup>c</sup>
AbHD <sub>1</sub> + ciprofloxacin	18.99 <sup>c</sup>	40.65 <sup>c</sup>
AbHD <sub>1</sub> + amoxicillin	96.97 <sup>c</sup>	388.69 <sup>c</sup>
AbHD <sub>5</sub> + ampicillin	31.99 <sup>c</sup>	1.000 <sup>a</sup>
AbHD <sub>5</sub> + erythromycin	35.87 <sup>c</sup>	16.89 <sup>c</sup>
AbHD <sub>5</sub> + ciprofloxacin	73.4 <sup>c</sup>	9.03 <sup>c</sup>
AbHD <sub>5</sub> + amoxicillin	24.42 <sup>c</sup>	388.69 <sup>c</sup>

<sup>a</sup>Synergistic effect. <sup>b</sup>Indifferent effect. <sup>c</sup>Antagonistic effect *A. brasiliensis* hf – AbHF.

antimicrobial activity can contribute to the MIC result [16]. The mechanisms by which extracts can inhibit the growth of micro-organisms varied which can be due in part to the hydrophobic and lipophilicity nature of some compounds which can show greater interaction with lipid bi-layer of the cell membrane [17]. Such hydrophobic and lipophilicity interaction with the bacterial cell wall can even make the cell more permeable to antibiotics, leading to the interruption of vital cellular activity [18]. The penetration of antibiotics can be increased with various components of extract permeable to the cell membrane. Also, the interference with bacterial enzyme systems can be a potential mechanism of action. For instance, the mechanism of action can be obtained by the combination of antibiotic with extract at sub-inhibitory concentration applied directly to the culture medium, this method is called 'herbal shotgun or synergistic multi-effect targeting' [19]. It refers to the utilization of plants and drugs in an approach using mono- or multi-extract combinations, which can affect not only a single target but various targets, where the different therapeutic components collaborate in a synergistic manner [20]. This approach is not only for combinations of extracts but combination between natural products or extracts and synthetic products or antibiotics are also possible [21]. This combination therapy of fraction and compounds were the major focus of this research work and as noticed combinations with the fraction was a success but with isolated compounds it varied. Just like a comprehensive investigation conducted by Haq et al. [22] on synergistic relationship between crude extracts of *Jatropha curcas* pressed cake and seed oil with some commercial antibiotic confirms that synergism is possible and the activities of both extracts and antibiotics are improved. The results from this research support natural compound-conventional drug combination strategy to combat antibacterial resistance. Also, from this research work it was observed that the compounds reported belonged to fatty acid and carboxylic acid groups indicating that MRSA bacteria bilayer can only be penetrated by a hydrophobic compound as reported by Nagendra Prasad et al. [23]. The anti-MRSA assay results of the compounds comparing with result of the antibiotics used even at a lower concentration shows a better activity than the antibiotics. This is an indication that these two compounds can be a better options in the treatment of MRSA infections.

In a brief review by Okwu et al. [24] on anti-MRSA activities of extracts of some medicinal plants they mention 22 plants used in Nigeria that has potential anti-MRSA activities extracted from different plant parts and alcoholic solvents. They reported the MIC ranged between 0.05 and 4.0 mg/mL and concluded that these plant can be promising candidates for treatment of MRSA infections. Comparing the results of the MIC's of the plants reviewed by Okwu et al. [24] and the present research, is noteworthy that AbHF (MIC < 2.5 mg/mL) from methanolic extract is relatively also a future lead as an anti-MRSA agent.

Hexadecanoic acid (also known as palmitic acid) is used to produce soaps, cosmetics and industrial mold release agents. In cosmetics industry the concentration of palmitic acid is more than 10% of total composition this could be as a result of its usage to control

resistant bacteria causing skin diseases [25]. In a research of combination therapy using low-concentration oxacillin (a penicillinase-resistant  $\beta$ -lactam antibiotic, just like ampicillin) with palmitic acid to control clinical Methicillin-Resistant *S. aureus* by Yang et al. [25] they reported that palmitic acid at concentrations lower than 1 mg/mL exerted no significant effect on the growth of the MRSA mutant strain. Conversely, it started to inhibit the cell growth when the concentration was over 1 mg/mL. In relations to our study, it reveals a significant progress that at lower concentration of 0.025 mg/mL of palmitic acid with ampicillin had inhibition against the clinical isolate K<sub>1</sub>St<sub>4</sub>.

Likewise, in general phthalate have been used as softeners in poly-vinyl chloride (PVC) plastic and as vehicles for fragrance in cosmetics [26] and for packing of drug capsules but has been reported to possess anti-MRSA activity. For instance, *Streptomyces* a source of phthalates compounds as reported by Lee et al. [27] to possess anti-MRSA activity with MIC 12.5  $\mu$ g/mL. Also, Dirche et al. [28] reported di (2-ethylhexyl) phthalate having activity against methicillin-resistant *S. aureus* with inhibitory zones between 21 and 30 mm.

Due to the different multi-resistance mechanism strains posed by MRSA bacteria to various kinds of antibiotics because of their genetic and physical traits Gonzales et al. [29]; suggested that the use of a single antibiotic drug is not recommended. As a possible solution Tyer et al. [30] reported that drug combination is considered a simple method to avoid the complex resistance mechanism of *S. aureus* because multiple antibacterial agents, such as antibiotics, free fatty acids, flavonoids and surfactants, can exert synergistic effects arising from the complex activities of their combinations [18, 31]. They reported synergistic relationship between palmitic acid and oxacillin at low concentrations because there was an increase in inhibition against the MRSA strains.

## 7.4 Conclusion

In this study we evaluated the anti-MRSA potentials of AbHF leaves and compounds isolated from it. The two compounds that were identified from AbHF; hexadecanoic acid and di (ethylhexyl) phthalate belonging to fatty acid and carboxylic acid groups with potential anti-MRSA activities. The antibacterial assay result proved that both AbHF and isolated compounds (hexadecanoic acid and di-(ethylhexyl) phthalate) had better anti-MRSA activity than the selected antibiotics especially with ampicillin (a beta lactam drug that the bacterial cell wall is usually resistant to) result. Additionally, hexadecanoic acid and di (ethylhexyl) phthalate from *A. brasiliensis* can serve as antibiotic drugs in the management of drug resistant since they had lower MIC's than selected antibiotics because at reduced concentration of 0.25 mg/mL inhibitory activity was observed. Furthermore, synergistic relationship between selected antibiotic drugs with fractions and isolated compounds were studied and from the assay it reveals that synergistic

relationship varies between samples. This study has shown that AbHF and compounds possesses anti-MRSA activities. Conclusively, synergistic relationship between compounds isolated from *A. brasiliensis* and antibiotic drugs used in MRSA treatment is a possible solution to drug resistance by bacteria and this is the first time this plant is being reported for any activity.

**Author contributions:** All the authors have accepted responsibility for the entire content of this submitted manuscript and approved submission.

**Research funding:** None declared.

**Conflict of interest statement:** The authors declare no conflicts of interest regarding this article.

## 7 Appendix

**Table 7.A1:** Compounds identified from *Alternanthera brasiliensis* hexane fraction via GCMS analysis.

S/no	Retention Time (min)	Compound name
1	5.82	Ar-tumerone
2		Phenyl tiglate, 2-(1Z)-propenyl-
3		Tumerone
4		(Z)-.gamma.-Atlantone
5		(E)-.gamma.-Atlantone
6	4.40	Curlone
7		2-Methyl-6-(4-methylenecyclohex-2-en-1-yl)hept-2-en-4-one
8		Benzoic acid, 4-amino-, 4-acetoxy-, 2,2,6,6-tetramethyl-1-piperidinyl ester
9	4.71	2-Pentadecanone, 6,10,14-trimethyl
10		2-Undecanone, 6,10-dimethyl-
11	7.09	Neophytadiene
12		Bicyclo[3.1.1]heptane, 2,6,6-trimethyl-
13		Bicyclo [3.1.1] heptane, 2, 6, 6-trimethyl-, (1.alpha. 2. beta., 5.alpha.)
14	1.69	3,7,11,15-Tetramethyl-2-hexadecen-1-ol
15		1,4-Eicosadiene
16	2.89	9-Eicosyne
17		1-Hexadecyne
18	5.93	Hexadecanoic acid, methyl ester
19	17.06	<i>n</i> -Hexadecanoic acid
20	1.84	Methyl 10- <i>trans</i> ,12- <i>cis</i> -octadecadienoate
21		9,12-Octadecadienoic acid, methyl ester
22	1.90	11-Octadecenoic acid, methyl ester
23		9-Octadecenoic acid, methyl ester, (E)-
24		9-Octadecenoic acid (Z)-, methyl ester

Table 7.A1: (continued)

S/no	Retention Time (min)	Compound name
25	22.34	Phytol
26	1.59	Methyl stearate
27		Heptadecanoic acid, 16-methyl-, methyl ester
28	2.34	2-Methyl-Z,Z-3,13-octadecadienol
29		Cyanoacetylurea
30		1,19-Eicosadiene
31	2.05	4,8,12,16-Tetramethylheptadecan-4-olide
32		2(3H)-Furanone, 5-butyldihydro-4-methyl-
33	5.59	Bis(2-ethylhexyl) phthalate
34		Phthalic acid, di(2-propylpentyl)ester
35	6.69	Squalene
36		Supraene
37	1.40	Cyclotrisiloxane, hexamethyl-
38		Benzo[h]quinoline, 2,4-dimethyl-
39		1-methyl-4-phenyl-5-thioxo-1,2,4-triazolidin-3-one
40		Tetrasiloxane, decamethyl-

Table 7.A2: HPLC analysis of *A. brasiliensis* hexane fraction.

S/no	Likely component expected
1	Cyclo(polyvaly 1)
2	Cerebroside
3	9-OH-pinoresinol
4	Aureonitol
5	Fetts äure
6	Bastadin 2
7	Herbarin B
8	Indo-3-Carbaldehyde
9	Aloresin A
10	2,3-Dibromoaldsin
11	Septone
12	(E,Z) Paucin
13	(Z)-oct.2-ene 1,3,8-tricarboxylic acid

Table 7.A3: HSQC assignment of AbHD1.

Position	<sup>13</sup> C NMR Experimental	<sup>13</sup> C NMR Reported <sup>a</sup>	<sup>1</sup> H NMR Experimental	<sup>1</sup> H NMR Reported <sup>a</sup>	Type of Carbon
1	178.7	178.7	–	–	C
2	34.1	34.1	2.33 (2H, t, <i>J</i> = 8.0 Hz)	2.33 (2H, t, <i>J</i> = 8.0 Hz)	CH <sub>2</sub>
3	24.9	24.9	1.23–1.40 (2H, m)	1.61 (2H, m)	CH <sub>2</sub>

Table 7.A3: (continued)

Position	<sup>13</sup> C NMR		<sup>1</sup> H NMR		Type of Carbon
	Experimental	Reported <sup>a</sup>	Experimental	Reported <sup>a</sup>	
4	29.1	29.9–29.3	1.23–1.40 (2H, m)	1.28 (2H, m)	CH <sub>2</sub>
5	29.4	29.9–29.3	1.23–1.40 (2H, m)	1.28 (2H, m)	CH <sub>2</sub>
6	29.7	29.9–29.3	1.23–1.40 (2H, m)	1.28 (2H, m)	CH <sub>2</sub>
7	29.7	29.9–29.3	1.23–1.40 (2H, m)	1.28 (2H, m)	CH <sub>2</sub>
8	29.7	29.9–29.3	1.23–1.40 (2H, m)	1.28 (2H, m)	CH <sub>2</sub>
9	29.7	29.9–29.3	1.23–1.40 (2H, m)	1.28 (2H, m)	CH <sub>2</sub>
10	29.7	29.9–29.3	1.23–1.40 (2H, m)	1.28 (2H, m)	CH <sub>2</sub>
11	29.7	29.9–29.3	1.23–1.40 (2H, m)	1.28 (2H, m)	CH <sub>2</sub>
12	29.7	29.9–29.3	1.23–1.40 (2H, m)	1.28 (2H, m)	CH <sub>2</sub>
13	29.4	29.9–29.3	1.23–1.40 (2H, m)	1.28 (2H, m)	CH <sub>2</sub>
14	31.9	32.1	1.23–1.40 (2H, m)	1.28 (2H, m)	CH <sub>2</sub>
15	22.7	22.9	1.23–1.40 (2H, m)	1.28 (2H, m)	CH <sub>2</sub>
16	14.1	14.2	0.86 (3H, t, <i>J</i> = 8.0 Hz)	0.86 (3H, t, <i>J</i> = 8.0 Hz)	CH <sub>3</sub>

m, multiplet; t, triplet; *J* = coupling constant in Hertz. <sup>a</sup>Reported by Fadzil et al. [14].

Table 7.A4: HSQC assignment of compound ABHD5 [di(2-ethylhexyl) phthalate].

Position	<sup>1</sup> H NMR	<sup>13</sup> C NMR (Observed)	<sup>13</sup> C NMR ( <sup>a</sup> Reported)
1	7.62 (1H, dd, <i>J</i> = 5.6, 3.3 Hz)	128.8, CH	129.1, CH
2	7.45 (1H, dd, <i>J</i> = 5.6, 3.3 Hz)	130.9, CH	131.2, CH
3	7.45 (1H, dd, <i>J</i> = 5.7, 3.3 Hz)	130.9, CH	131.2, CH
4	7.62 (1H, dd, <i>J</i> = 5.7, 3.3 Hz)	128.8, CH	129.1, CH
1'	–	132.5, qC	132.8, qC
2'	–	167.8, qC	168.1, qC
3'	4.20 (2H, dd, <i>J</i> = 10.9, 5.8 Hz)	68.2, CH <sub>2</sub>	68.5, CH <sub>2</sub>
4'	2.15 (1H, m)	39.4, CH	39.1, CH
5'	1.10–1.90 (2H, m)	30.4, CH <sub>2</sub>	30.7, CH <sub>2</sub>
6'	1.10–1.90 (2H, m)	29.4, CH <sub>2</sub>	29.3, CH <sub>2</sub>
7'	1.10–1.90 (2H, m)	23.8, CH <sub>2</sub>	23.3, CH <sub>2</sub>
8'	0.80–0.90 (3H, t, <i>J</i> = 6.8 Hz)	14.1, CH <sub>3</sub>	14.4, CH <sub>3</sub>
9'	1.10–1.90 (2H, m)	24.8, CH <sub>2</sub>	24.1, CH <sub>2</sub>
10'	0.80–0.90 (3H, t, <i>J</i> = 6.8 Hz)	10.9, CH <sub>3</sub>	11.3, CH <sub>3</sub>
1''	–	132.5, qC	132.8, qC
2''	–	167.8, qC	168.1, qC
3''	4.20 (2H, dd, <i>J</i> = 10.9, 5.8 Hz)	68.2, CH <sub>2</sub>	68.5, CH <sub>2</sub>
4''	2.15 (1H, m)	39.4, CH	39.1, CH
5''	1.10–1.90 (2H, m)	30.4, CH <sub>2</sub>	30.7, CH <sub>2</sub>
6''	1.10–1.90 (2H, m)	29.4, CH <sub>2</sub>	29.3, CH <sub>2</sub>
7''	1.10–1.90 (2H, m)	23.8, CH <sub>2</sub>	23.3, CH <sub>2</sub>
8''	0.80–0.90 (3H, t, <i>J</i> = 6.8 Hz)	14.1, CH <sub>3</sub>	14.4, CH <sub>3</sub>
9''	1.10–1.90 (2H, m)	24.8, CH <sub>2</sub>	24.1, CH <sub>2</sub>
10''	0.80–0.90 (3H, t, <i>J</i> = 6.8 Hz)	10.9, CH <sub>3</sub>	11.3, CH <sub>3</sub>

<sup>a</sup>Reported by Nair et al. [15]. qC, quaternary carbon; dd, double doublet; m, multiplet; t, triplet.



138 — 7 Compounds isolated from hexane fraction of *Alternanthera brasiliensis*

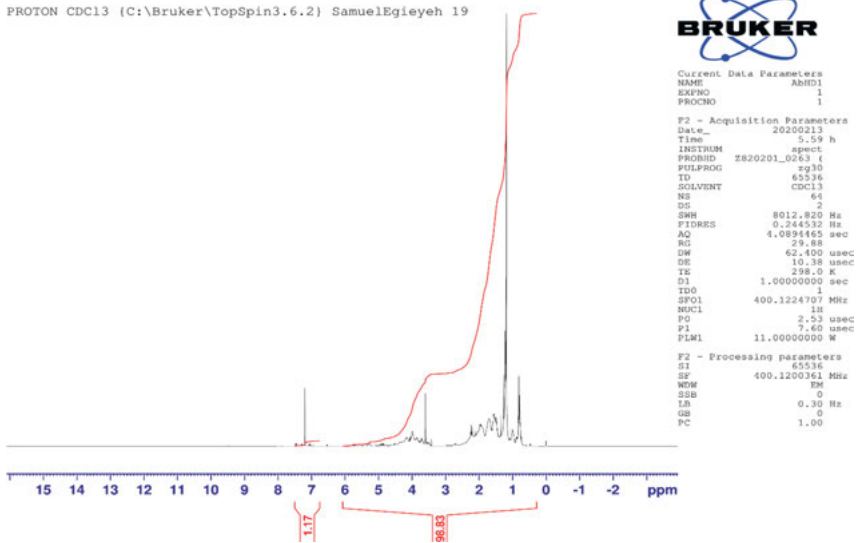


Figure 7.A1:  $^1\text{H}$  NMR spectrum of AbHD<sub>1</sub>.

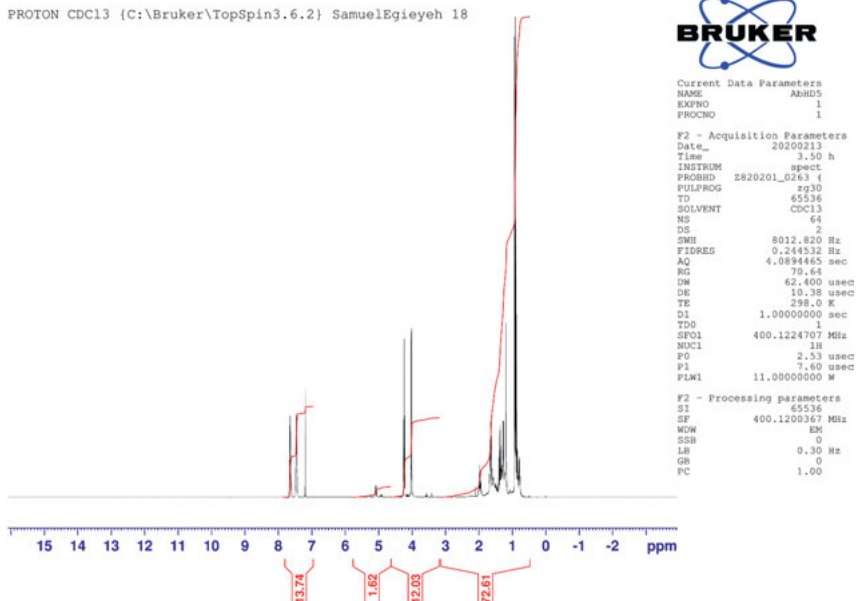
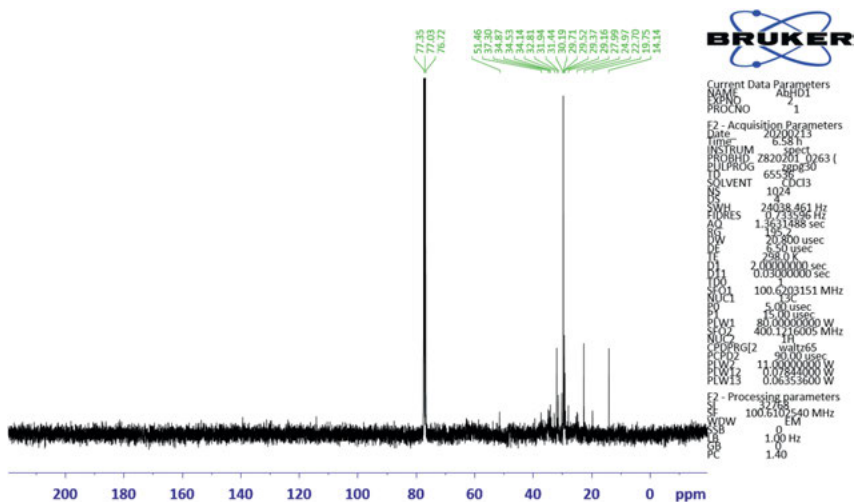
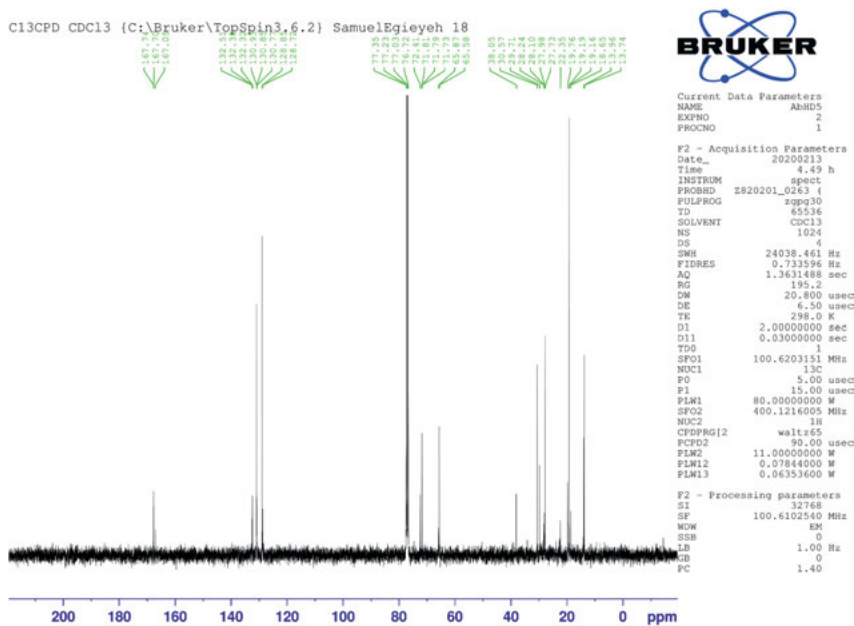


Figure 7.A2: Proton NMR of AbHD<sub>5</sub>.

Figure 7.A3: Carbon – 13 NMR of AbHD<sub>1</sub>.Figure 7.A4: Carbon 13 of AbHD<sub>5</sub>.

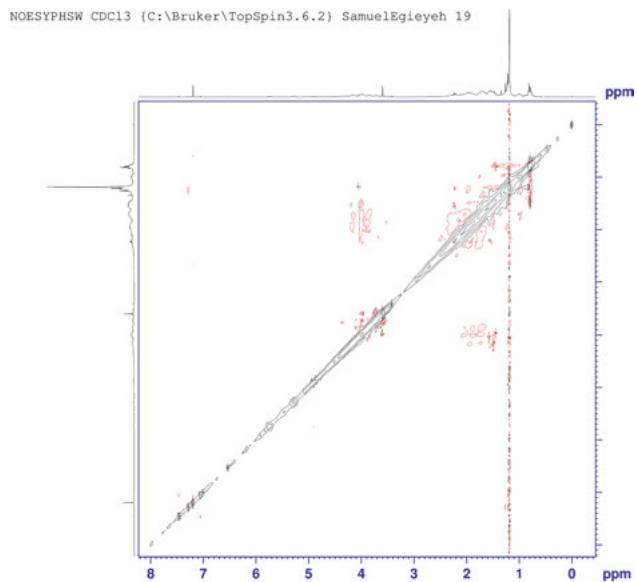


Figure 7.A5: NOESY of AbHD<sub>1</sub>.

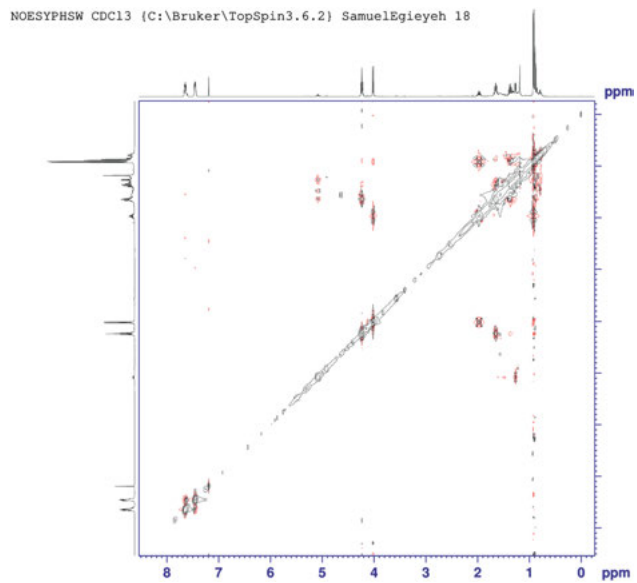


Figure 7.A6: NOESY of AbHD<sub>5</sub>.

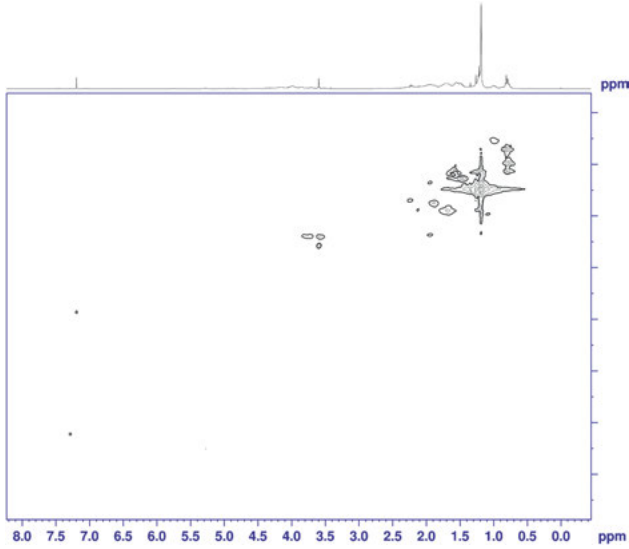


Figure 7.A7: HMQC of AbHD<sub>1</sub>.

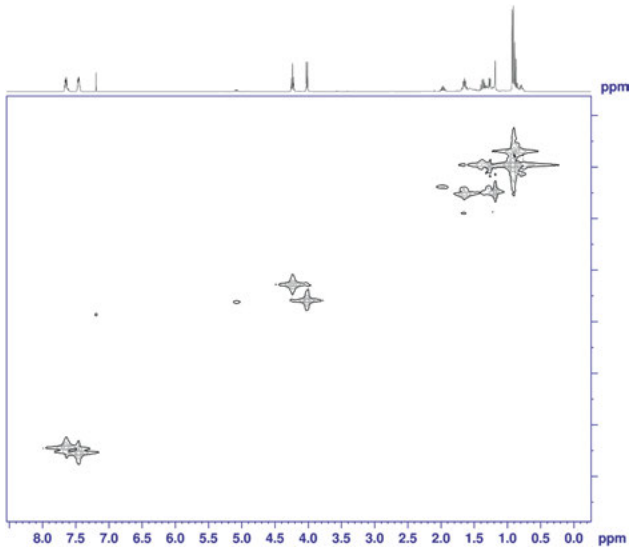


Figure 7.A8: HMQC of AbHD<sub>5</sub>.

142 — 7 Compounds isolated from hexane fraction of *Alternanthera brasiliensis*

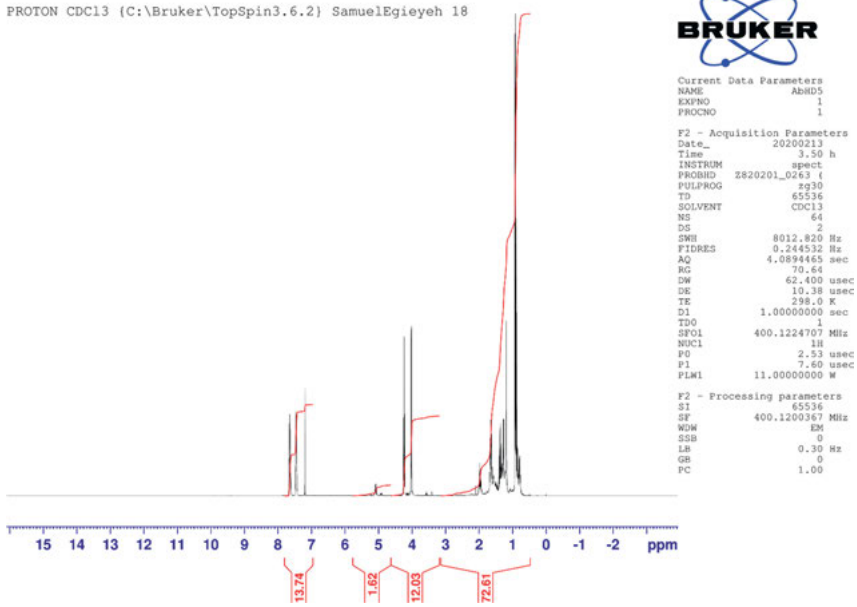


Figure 7.A9: Proton NMR of AbHD<sub>5</sub>.

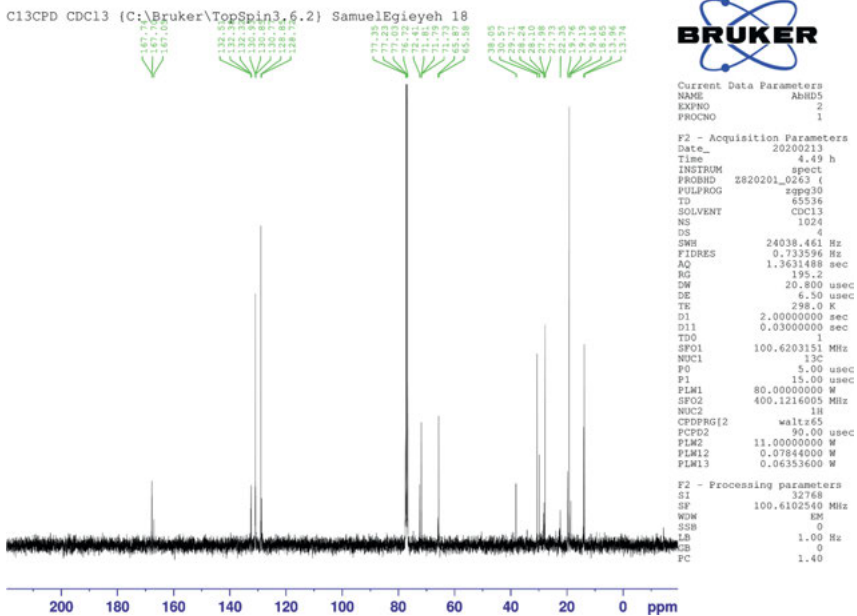


Figure 7.A10: Carbon 13 of AbHD<sub>5</sub>.

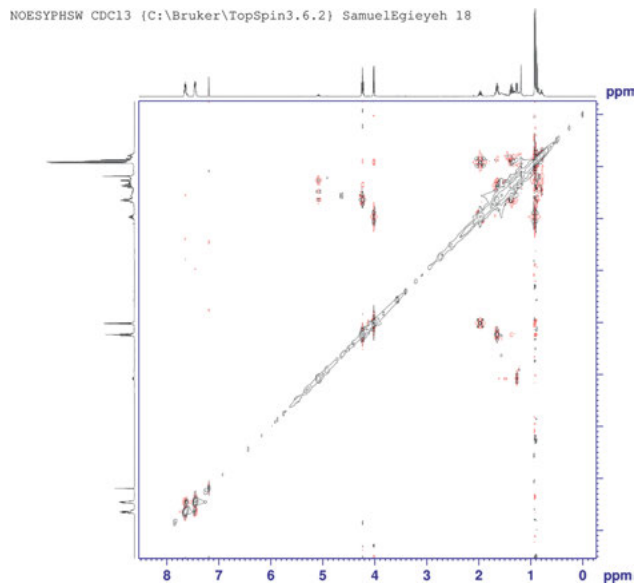


Figure 7.A11: NOESY of AbHD<sub>5</sub>.

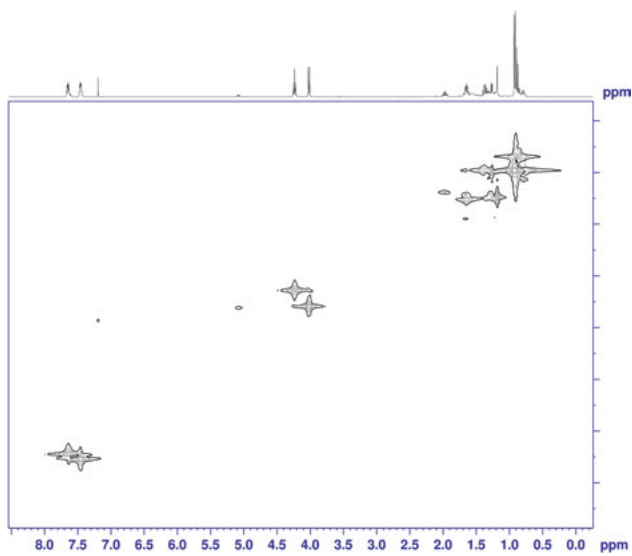


Figure 7.A12: HMQC of AbHD<sub>5</sub>.

## References

- Nichols H. All you need to know about MRSA. In: Newsletter January edition MedicalNewsToday. Brighton, UK: Healthline Media; 2020.
- Ramirez-Rueda R. Natural plant products used against methicillin-resistant *Staphylococcus aureus*. In: Fighting multidrug resistance with herbal extracts, essential oils and their components (p. 240) Chapter 2: Natural agents from plants used against methicillin-resistant *Staphylococcus aureus*. Netherlands: Elsevier; 2013.
- World Health Organisation. WHO publishes list of bacteria for which new antibiotics are urgently Needed. Geneva: World Health Organisation; 2017.
- Azman N, Hassan M, Nissapatorn V, Uthaipibull C. Anti-infective activities of 11 plants species used in traditional medicine in Malaysia. *Exp Parasitol* 2018;194:67–78.
- Sánchez-Del P, Motley T, Borsch T. Molecular phylogenetics of *Alternanthera* (Gomphrenoideae, Amaranthaceae): resolving a complex taxonomic history caused by different interpretations of morphological characters in a lineage with *C. Bot J Linn Soc* 2012;169:493–517.
- Tanveer A, Khaliq A. A review on genus *Alternanthera* weeds implications. Pakistan. *J Weed Sci Res* 2013;19:53–8.
- Burkill H. The useful plants of west tropical Africa. Kew: Royal Botanic Gardens; 2004.
- Taib C, Rai M, Kon K, Mat N, Farahziela A, Mohd M, et al. Antioxidant Properties of Crude Extract, Partition Extract, and Fermented Medium of *Dendrobium sabin* Flower. *Evid base Compl Alternative Med* 2017;2017:1–9. 2907219.
- Isah Y, Ndukwe I, Ayo R, Yakubu R. Vacuum liquid chromatographic isolation and characterization of beta-stosterol from the bark of *Sarcocephalus latifolius* (Smith Bruce). *J Chem Chem Sci* 2015;5: 480–8.
- Clinical Laboratory Standards Institute (formerly NCCLS) – Clinical and Laboratory Standards Institute. Performance standards for antimicrobial susceptibility testing, 18<sup>th</sup> informational supplement M100-S18. Wayne, PA: CLSI; 2016.
- Mirtaghi S, Torbati Nejad P, Mazandarani M, Livani F, Bagheri H. Evaluation of antibacterial activity of *Urtica dioica* L. leaf ethanolic extract using agar well diffusion and disc diffusion methods. *Med Lab J* 2016;10:15–21.
- Olajuyigbe O. Synergistic influence of tetracycline on the antibacteria activities of amoxicilin against resistant bacteria. *J Pharm Allied Health Sci* 2012;2:12–20.
- Renk-ngam N, Chimnoi N, Khunnawutmanotham N, Techasakul S. Antimicrobial activity of coronarin D and its synergistic potential with antibiotics. *BioMed Res Int* 2014;10:1155.
- Fadzil SR, Yap A, Choo Y. A new cyclopentylidene and other chemical constituents from Malaysian *Crotalaria pallida* (Siklopentilidena Baru dan Jujuk Kimia Lain daripada *Crotalaria pallida* Malaysia). *Sains Malays* 2017;46:1581–6.
- Nair JJ, Ndhala AR, Chukwujekwu JC, Van Staden J. Isolation of di (2-ethylhexyl) phthalate from a commercial South African cognate herbal mixture. *South Afr J Bot* 2012;80:21–4.
- Matias E, Santos K, Almeida T, Costa J, Coutinho H. Enhancement of antibiotic activity by *Cordia verbenacea* DC. *Acta Farm Bonaerense* 2010;29:1049–52.
- Al-Majmaie S, Nahar L, Rahman M, Nath S, Saha P, Talukdar A, et al. Anti-MRSA constituents from *Ruta chalepensis* (rutaceae) grown in Iraq, and in silico studies on two most active compounds, chalepentin and 6-hydroxy-rutin 3', 7-dimethyl ether. *Molecules* 2021;26:1114.
- Song R, Yu B, Friedrich D, Li J, Shen H, Krautscheid H, et al. Naphthoquinone-derivative as a synthetic compound to overcome the antibiotic resistance of methicillin-resistant *S. aureus*. *Commun Biol* 2020;3:529.

19. Carmona F, Pereira A. Herbal medicines: old and new concepts, truths and misunderstandings. *Rev Bras Farmacogn* 2013;23:379–85.
20. Matias E, Souza C, Tintino S, Guedes G, Medeiro C, Flaviana M, et al. Screening the *in vitro* modulation of antibiotic activity of the extracts and fractions of *Ocimum gratissimum* L. *Afr J Microbiol Res* 2012;6:1902–7.
21. Kali A. Antibiotics and bioactive natural products in treatment of methicillin resistant *Staphylococcus aureus*: a brief review. *Phcog Rev* 2015;9:29–34.
22. Haq A, Siddiqi M, Batool S, Islam A, Khan A, Khan S, et al. Comprehensive investigation on the synergistic antibacterial activities of *Jatropha curcas* pressed cake and seed oil in combination with antibiotics. *Amb Express* 2019;9:67–88.
23. Nagendra Prasad H, Karthik C, Manukumar H, Mailesha L, Mailu P. New approach to address antibiotic resistance: miss loading of functional membrane microdomains (FMM) of methicillin-resistant *Staphylococcus aureus* (MRSA). *Microb Pathog* 2019;127:106–15.
24. Okwu M, Olley M, Akpoka A, Izevbuwa O. Methicillin-resistant *Staphylococcus aureus* (MRSA) and anti-MRSA activities of extracts of some medicinal plants: a brief review. *AIMS Microbiol* 2019;5: 117–37.
25. Yang Y, Song H, Choi T, Bhatia S, Lee S, Park S, et al. Combination therapy using low-concentration oxacillin with palmitic acid and Span85 to control clinical methicillin-resistant *Staphylococcus aureus*. *Antibiotics* 2020;9:681–92.
26. Kim S, Park M. Phthalate exposure and childhood obesity. *Annu Pediatr Endocrinol Metabol* 2014; 19:69–75.
27. Lee L, Kemung H, Tan L, Khan T, Chan K, Pusparajah P, et al. Streptomyces as a prominent resource of future anti-MRSA drugs. *Front Microbiol* 2018;10:1–15.
28. Driche E, Belghit S, Zitouni A, Sabaou N, Badji B, Bijani C, et al. A new Streptomyces strain isolated from Saharan soil produces di-(2-ethylhexyl) phthalate, a metabolite active against methicillin-resistant *Staphylococcus aureus*. *Annu Microbiol* 2015;65:1341–50.
29. Gonzales P, Pesesky M, Bouley R, Ballard A, Biddy B, Suckow M, et al. Synergistic, collaterally sensitive  $\beta$ -lactam combinations suppress resistance in MRSA. *Nat Chem Biol* 2015;11:855–61.
30. Tyers M, Wright G. Drug combinations: a strategy to extend the life of antibiotics in the 21st century. *Nat Rev Microbiol* 2019;17:141–55.
31. Ng'uni T, Mothlalamme T, Daniels R, Klaasen J, Fielding B. Additive antibacterial activity of naringenin and antibiotic combinations against multidrug resistant *Staphylococcus aureus*. *Afr J Microbiol Res* 2015;9:1513–18.





Kafeelah Yusuf\*, Abdulrafiu Majolagbe and Sherifat Balogun

## 8 Evaluation of raw, treated and effluent water quality from selected water treatment plants: a case study of Lagos Water Corporation

**Abstract:** Water plays a significant role in maintaining human health and welfare. In this paper, eight selected water treatment plants (Ishasi, Iju, Adiyari, Mosan Okunola, Ikorodu, Otta-ikosi, Alausa and Akilo) controlled by Lagos Water Corporation were studied to evaluate raw, treated and effluent water quality. Sixteen parameters (pH, Turbidity, Electrical Conductivity (EC), Total Dissolved Solids (TDS), Total Alkalinity (TA), Total Hardness (TH), Calcium ( $\text{Ca}^{2+}$ ), Magnesium ( $\text{Mg}^{2+}$ ), Chloride ( $\text{Cl}^-$ ), Sulphate ( $\text{SO}_4^{2-}$ ), Nitrate ( $\text{NO}_3^-$ ), Phosphate ( $\text{PO}_4^{3-}$ ), Total Coliform (TC), Copper ( $\text{Cu}^{2+}$ ), Cadmium ( $\text{Cd}^{2+}$ ) and Lead ( $\text{Pb}^{2+}$ ) were determined for a period of three months (July–September 2018) using standard methods. The results showed that Cd was not detected; the TC exceeded the World Health Organization (WHO) limit while all other parameters were within the (WHO) guideline for drinking purposes with the exception of turbidity. The values of water quality index (WQI) designated 70.83% as excellent water, 20.83% as good water and 8.33% as poor water in respect to drinking uses. The Principal Component Analysis (PCA) extracts five components with eigenvalue  $>1.0$  and accounts for 78.22% of the total variance. The associated health risks were estimated for adults and children. The hazard quotients (HQ) were greater than one indicating an overall health risk for adults and children.

**Keywords:** health risks; PCA; raw; water samples; water treatment plants; WQI.

### 8.1 Introduction

Water resources and quality are imperative for urban development and ecological environment [1]. Surface water such as freshwater rivers, streams, dams, ponds, lakes, springs, etc. and ground waters such as borehole and well water are essential potable water supply globally. Anthropogenic activities such as industrial sewages, domestic wastewater, agricultural drainage water and/or natural processes such as bedrock weathering deteriorate surface and ground water quality thus compromising its suitability [1]. The quality of life is a reflection of water quality consumed as shown by

---

\*Corresponding author: Kafeelah Yusuf, Chemistry, Lagos State University, Lagos, Nigeria,  
E-mail: kafyusuf@yahoo.co.uk

Abdulrafiu Majolagbe, Chemistry, Lagos State University, Lagos, Nigeria

Sherifat Balogun, Lagos State Ministry of Commerce, Industry and Cooperatives, Lagos State Government, Lagos, Nigeria

This article has previously been published in the journal *Physical Sciences Reviews*. Please cite as: K. Yusuf, A. Majolagbe and S. Balogun "Evaluation of Raw, Treated and Effluent Water Quality from Selected Water Treatment Plants: a case study of Lagos Water Corporation" *Physical Sciences Reviews* [Online] 2021, 6. DOI: 10.1515/psr-2020-0114 | <https://doi.org/10.1515/9783110710823-008>

studies for 3.1% of deaths (1.7 million) and 3.7% of disability-adjusted-life-years (DALYs) (54.2 million) worldwide [2]. Water treatment is therefore geared toward removing the impurities associated with the water sources [3]. Water quality denotes suitability having removed the adverse variables in its composition [4].

The water quality index (WQI) was first developed by Horton in 1965 to express the quality of water. It simplifies complex datasets into easily and useable information. The index reflects the quality of water in a single value at a certain location and time based on some water parameters. This has been subjected to various studies [5].

Lagos, a tropical megacity in Nigeria, lacks proper disposal of wastewater which percolates into groundwater, polluting both the ground and surface waters.

This study aims to develop local water management strategies to prevent hazardous contamination by examining physical, chemical and microbiological parameters in raw, treated and effluent water samples from selected water treatment plants for a period of three months with the objectives to (i) compare the parameters analyzed in the raw, treated and effluent of the surface and groundwater supplying the treatment plants (ii) identify sources of pollution by multivariate statistical method, such as principal component analysis (PCA); (iii) assess the impacts on human health by calculating the WQI as well as the hazard index. The findings of this research will greatly assist policymakers in the provision of potable water to the citizenry.

## 8.2 Materials and methods

### 8.2.1 Sampling and sample preparation

Raw, treated and effluent water samples were collected in the months of July–September 2018. One hundred and forty-four surface and groundwater samples were collected for physicochemical analysis from four major waterworks (Iju, Adiyin, Ishasi and Otta-ikosi) and four mini-waterworks (Alausa, Akilo, Mosan and Ikorodu) undertaken by the Lagos Water Corporation. All physical parameters such as pH turbidity and electrical conductivity (EC) were evaluated at the site, 2.5 L of water (raw, treated and effluent) samples from each site were collected in sterile polypropylene bottles for chemical analysis, another 1 L each was collected (acidified) for metals (Cu, Cd and Pb), nutrients (SO<sub>4</sub>, NO<sub>3</sub> and PO<sub>4</sub>) and microbiological (Total coliform [TC]) analysis. All bottles were labelled, kept in the icebox for four Degree Celsius (4 °C) and transported to the laboratory.

### 8.2.2 Description of the study area

The study area is located in Lagos megacity as indicated in the global positioning system (GPS) data (Table 8.1). Water supply in the study area is undertaken by the Lagos

**Table 8.1:** Global positioning system where samples were obtained in selected water treatment plants.

Sampling point	Latitude	Longitude
Iju waterworks	6°40'30"N	3°19'58"E
Ishasi	6°30'0"N	3°10'0"E
Adiyan	6°41'27"N	3°20'23"E
Alausa	6°61'23"N	3°35'84"E
Akilo	6°34'59"N	3°19'59"E
Mosan Okunola	6°61'16"N	3°28'90"E
Ikorodu	6°35'59"N	3°29'59"E
Otta-ikosi	6°53'11"N	3°97'72"E

Water Corporation. The Lagos Water Supply System comprises four major waterworks (Adiyan, Iju, Isashi and Otta-ikosi), 27 mini-waterworks and 10 micro-waterworks. The four major waterworks derive their water from Rivers Ogun, Osun, Aye, Owo, Yewa and Iju. The groundwaters were sourced from two regional hydrogeological aquifers namely Abeokuta and Coastal Plain Sands Formations.

### 8.2.3 Analytical procedure

The pH was determined by Jenway 3505 pH meter; HACH – 2100N Turbidity meter for turbidity; Jenway 470 Conductivity meter for EC; alkalinity, Total Hardness (TH), chloride were determined by titrimetric methods. Trace Metals were digested and evaluated using AA Series Spectrometer, nitrate obtained by diphenoldisulphonic acid method, Microbial analysis (TC) were analyzed by membrane filtration technique. All analyses were carried out in accordance with standard methods for the examination of water and wastewater [6]. All chemicals used were of analytical grade, blanks were used for background correction and analyzed under the same conditions used for water samples. Accuracy was assessed by analyzing duplicate of water samples. All the sample containers were washed, soaked for 24 h and rinsed with distilled water. Water samples for metal analysis were acidified. All equipment was calibrated on daily basis using standard solutions.

## 8.3 Statistical analysis

### 8.3.1 Correlation analysis (CA)

“Pearson  $r$  correlation coefficients” was used to evaluate the linear relationship between various pairs of variables, with statistical significance set at  $p < 0.01$  and  $p < 0.05$ . The value of the correlation coefficient ranges between  $-1.0$  and  $+1.0$ .

### 8.3.2 Principal component analysis

PCA is a technique that transforms a set of interrelated variables into a set of uncorrelated variables. The newly formed variables (PCs) are linear combinations of the original set of variables. PCs with eigenvalues more than one were retained. The coefficients that are greater than 0.75 are considered as “strong”, 0.75–0.50 as “moderate”; and 0.50–0.30 as “weak” [7].

### 8.3.3 Water quality index

WQI is an effective tool for communicating information on the quality of water to the concerned citizenry and policymakers. It provides a detailed description of the quality of surface and groundwater for domestic uses [8]. In the present study, 15 parameters were considered for WQI calculation as shown in Table 8.2. The relative weight ( $w_i$ ) is the mean values for the weights of each parameter along with the references used as shown in Table 8.2. The calculated relative weight ( $W_i$ ) values of each parameter are given in Table 8.3. The WQI value can be obtained from the following equations

$$W_i = w_i \sum_{i=1}^n w_i \quad (8.1)$$

$$q_i = \frac{C_i}{S_i} \times 100 \quad (8.2)$$

$$S_{li} = W_i \times q_i \quad (8.3)$$

$$WQI = \sum_{i=1}^n S_{li} \quad (8.4)$$

where  $n$  is the number of parameters,  $w_i$  is the parameter weight and  $W_i$  is the relative weight,  $q_i$  is the rating factor,  $C_i$  is the concentrations of the parameters measured and  $S_{li}$  is the sub-indexes of parameters. The water quality rating includes five categories as defined in Table 8.4 [9]  $S_i$  is the standard of each parameter according to the international guidelines [10].

### 8.3.4 Health risk assessment

Health risk assessment such as average daily dose (ADD) and hazard quotient (HQ) were calculated using Equations (8.5) and (8.6), respectively

$$ADD_{\text{water oral ingestion}} = \frac{C_w \times IRW \times EF \times ED}{BW \times AT_n} \quad (8.5)$$

where ADD is the average daily dose from ingestion of metal in drinking water (mg/kg/

**Table 8.2:** Assigned weight values adopted from the literature.

Parameters	Reference numbers											Mean value
	[7]	[10]	[7]	[11]	[12]	[13]	[7]	[14]	[9]	[15]	[16]	
pH	4	4	4	4	4	3	1	3	4	4		3.44
EC	2		2	3		3	4		4			3.20
Turbidity	2		2	3						3		2.67
TDS				3		5		5	5	4	5	4.50
TH	1		1	2		3	2		3	3		2.33
Cl <sup>-</sup>		1		2	3	3		5	5	5	5	3.63
Mg <sup>2+</sup>		2		2	2	2		3	3		3	2.43
Ca <sup>2+</sup>		2		2	2	2		3	3		3	2.43
SO <sub>4</sub> <sup>2-</sup>				4	4	3		5	5	5	4	4.29
NO <sub>3</sub> <sup>-</sup>				5		5			5	5	5	5.00
PO <sub>4</sub> <sup>3-</sup>									1			1.00
TA	1		1	1		2	3					1.75
Cu		4									2	3.00
Pb					4						5	4.50

**Table 8.3:** WHO standards for water quality and calculated relative weight for each parameter.

Parameters	Unit	WHO (2011) standards (Si)	Weight (wi)	Relative weight (Wi)
pH		8.5	3.44	0.078
EC	µS/cm	1000	3.20	0.073
Turbidity	NTU	5	2.67	0.061
TDS	mg/L	500	4.50	0.102
TH	mg/L	100	2.33	0.053
Cl <sup>-</sup>	mg/L	250	3.63	0.082
Mg <sup>2+</sup>	mg/L	50	2.43	0.055
Ca <sup>2+</sup>	mg/L	75	2.43	0.055
SO <sub>4</sub> <sup>2-</sup>	mg/L	250	4.29	0.097
NO <sub>3</sub> <sup>-</sup>	mg/L	50	5.00	0.113
PO <sub>4</sub> <sup>3-</sup>	mg/L	0.5	1.00	0.023
TA	mg/L	200	1.75	0.04
Cu	µg/L	2000	3.00	0.068
Pb	µg/L	10	4.50	0.102
			Σwi = 44.61	ΣWi = 1.00

day); Cw was the contaminant mean concentration in water ( $\mu\text{gL}^{-1}$ ); IRW was the drinking water ingestion rate ( $\text{L day}^{-1}$ ) or incidental water ingestion rate ( $\text{L day}^{-1}$ ). This study used the standard amount of water intake of 2 L/day recommended by the WHO [13]; while EF of 365 days year<sup>-1</sup> recommended by the USEPA [16] was used. ED was the exposure duration (year), 26 for adults and six for children; The average body weight

**Table 8.4:** Water Quality Classifications for drinking based on WQI values [14].

WQI value	Class	Rank
<50	I	Excellent water
50.1–100	II	Good water
100.1–200	III	Poor water
200.1–300	IV	Very poor water
>300	V	Unsuitable for drinking

used is assumed to be 72 kg for adult and 32.7 kg for child, and  $AT_n$  was the averaging time for non-carcinogens (day), 25,550 for adults and 2190 for children [12].

### 8.3.5 Non-carcinogenic risk assessment

The non-carcinogenic toxicity (HQ) was estimated as shown in the equation below

$$HQ_{\text{water ingestion}} = \frac{ADD_{\text{water oral ingestion}}}{RfD_{\text{water oral ingestion}}} \quad (8.6)$$

Hazard index is the sum of the HQs for individual elements from both the applicable pathways mentioned previously, which is used to analyze the total potential non-carcinogenic risk. Risk levels can be divided into four different classifications according to the HQ or HI values. When HQ or HI < 0.1, the chronic risk is negligible and the cancer risk is very low; when  $0.1 \leq HQ$  or HI < 1, the chronic and cancer risks are low; when  $1 \leq HQ$  or HI < 4, the chronic and cancer risks are medium; if HQ or HI  $\geq 4$ , the chronic and cancer risks are very high.

## 8.4 Results and discussion

The mean and standard error mean of the parameters measured in raw, treated and effluent water samples from selected water treatment plants were presented in Table 8.5 and as box plot in Figure 8.1. The pH values of raw, treated and effluent water samples respectively ranged between 5.80–6.93, 5.89–7.23 and 5.85–6.90. The pH levels were moderately acidic and within the (WHO [10]) permissible limit (6.5–8.5) for drinking purposes. The lowest value of pH was recorded in Mosan (raw) and the highest value was recorded in Alausa (treated).

Turbidity is a measure of the water cloudiness; the present study had turbidity of water between 0.79 NTU and 125 NTU. The WHO limit recommends (five NTU). The turbidity obtained for this study is higher than 0.23–2.20 NTU reported by Adeniyi et al. [11]. The EC is related to the concentration of the ionized substances dissolved in water and an indication of the salinity of the water. The (EC) in water samples ranged between

**Table 8.5:** Descriptive statistics of water quality at selected water treatment plants.

(a) Parameter	Water sample	Alausa			Akilo			Mosan			Ishasi			WHO 2011 standard
		Mean	SEM	N	Mean	SEM	N	Mean	SEM	N	Mean	SEM	N	
pH	Raw	6.030	0.12	3	5.970	0.13	3	5.800	0.25	2	6.200	0.00	3	6.5–8.5
	Treated	7.233	0.19	3	7.033	0.03	3	6.445	0.56	2	6.667	0.03	3	
	Effluent	6.200	0.12	3	6.767	0.13	3	6.255	0.25	2	6.900	0.00	3	
Turbidity NTU	Raw	2.643	0.58	3	1.627	0.24	3	2.245	1.28	2	5.350	1.91	3	5
	Treated	4.063	2.67	3	2.153	0.46	3	1.520	1.04	2	6.217	5.06	3	
	Effluent	61.383	10.13	3	54.000	0.00	3	2.825	0.89	2	81.000	22.37	3	
TDS mg/L	Raw	20.000	1.15	3	0.260	0.00	3	24.500	1.50	2	180.667	1.20	3	500
	Treated	41.000	1.53	3	0.393	0.00	3	46.000	1.00	2	189.667	0.88	3	
	Effluent	23.000	3.61	3	0.000	0.00	3	57.500	1.50	2	224.667	1.45	3	
TH mg/L	Raw	2.200	0.12	3	6.200	2.19	3	0.240	0.04	2	0.800	0.06	3	
	Treated	5.733	0.35	3	4.000	0.23	3	0.500	0.02	2	1.133	0.25	3	
	Effluent	3.600	0.46	3	2.600	0.58	3	0.600	0.00	2	1.267	0.04	3	
EC µS/cm	Raw	36.333	3.33	3	0.383	0.01	3	24.370	12.25	3	269.650	1.79	3	1000
	Treated	86.667	3.33	3	0.587	0.01	3	45.770	22.90	3	283.090	1.32	3	
	Effluent	52.667	8.33	3	0.000	0.00	3	57.213	28.64	3	335.320	2.17	3	
Cl mg/L	Raw	15.000	0.00	3	0.500	0.00	3	1.490	0.50	2	1.747	0.44	3	250
	Treated	0.000	0.00	3	0.250	0.14	3	0.740	0.25	2	1.593	0.31	3	
	Effluent	0.750	0.14	3	1.000	0.00	3	1.000	0.50	2	2.247	0.15	3	
Ca mg/L	Raw	2.000	0.08	3	3.003	1.34	3	0.200	0.04	2	0.587	0.13	3	75
	Treated	5.020	0.45	3	3.607	0.20	3	0.475	0.01	2	0.633	0.03	3	
	Effluent	2.977	0.26	3	2.153	0.62	3	0.570	0.01	2	0.960	0.08	3	
Mg mg/L	Raw	0.200	0.04	3	0.530	0.20	3	0.040	0.00	2	0.213	0.09	3	50
	Treated	0.580	0.22	3	0.393	0.04	3	0.025	0.02	2	0.500	0.25	3	
	Effluent	0.623	0.24	3	0.447	0.10	3	0.030	0.01	2	0.307	0.11	3	
SO4 mg/L	Raw	0.090	0.01	3	0.170	0.01	3	0.110	0.01	2	0.527	0.03	3	250
	Treated	0.137	0.01	3	0.160	0.05	3	0.160	0.00	2	0.693	0.04	3	



Table 8.5: (continued)

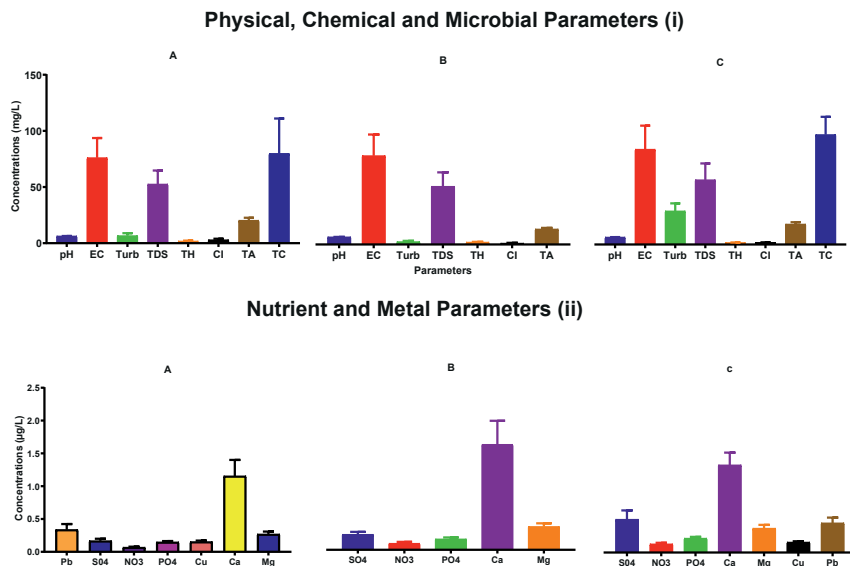
(a) Parameter	Water sample	Alausa			Akilo			Mosan			Ishasi			WHO 2011 standard		
		Mean	SEM	N	Mean	SEM	N	Mean	SEM	N	Mean	SEM	N	Mean	SEM	N
NO <sub>3</sub> mg/L	Effluent	0.250	0.03	3	0.280	0.02	3	2.300	0.10	2	1.013	0.03	3			
	Raw	0.107	0.01	3	0.107	0.01	3	0.010	0.00	2	0.143	0.03	3			50
	Treated	0.033	0.03	3	0.137	0.07	3	0.120	0.00	2	0.333	0.04	3			
PO <sub>4</sub> mg/L	Effluent	0.117	0.02	3	0.150	0.03	3	0.155	0.06	2	0.280	0.01	3			
	Raw	0.100	0.01	3	0.220	0.02	3	0.245	0.01	2	0.113	0.03	3			0.5
	Treated	0.080	0.04	3	0.290	0.02	3	0.235	0.00	2	0.133	0.05	3			
TA mg/L	Effluent	0.190	0.06	3	0.320	0.05	3	0.225	0.01	2	0.130	0.05	3			
	Raw	12.000	1.15	3	32.000	0.00	3	11.510	0.50	2	29.693	5.05	3			200
	Treated	14.000	2.00	2				17.515	4.51	2	17.680	2.91	3			
TC	Effluent	22.000	2.00	2				24.025	5.01	2	25.690	2.97	3			
	Raw	33.500	26.50	2	32.667	6.36	3									0
Cu mg/L	Treated															
	Effluent	92.500	57.50	2	135.000	15.00	2				98.333	26.19	3			
	Raw	0.127	0.02	3	0.247	0.01	3	0.140	0.00	2	0.170	0.04	3			2
Pb mg/L	Treated															
	Effluent	0.210	0.06	2	0.143	0.02	3	0.165	0.05	2	0.133	0.05	3			
	Raw	0.480	0.04	3	0.353	0.33	3	0.045	0.05	2	0.320	0.14	3			0.01
Effluent	Treated															
	Effluent	0.365	0.07	2	0.620	0.19	3	0.240	0.07	2	0.797	0.28	3			
(b) Parameter	Water sample	Otta-ikosi			Ikorodu			Iju			Adiyan			WHO 2011 standard		
		Mean	SEM	N	Mean	SEM	N	Mean	SEM	N	Mean	SEM	N	Mean	SEM	N
pH	Raw	6.930	0.29	3	5.970	0.25	3	6.320	0.30	3	6.770	0.03	3			6.5-8.5
	Treated	6.700	0.40	3	5.893	0.21	3	6.260	0.32	3	6.500	0.06	3			
	Effluent	6.813	0.29	3	5.850	0.25	3	6.610	0.30	3	6.833	0.03	3			

Table 8.5: (continued)

(b) Parameter	Water sample	Otta-ikosi			Ikorodu			Iju			Adiyan			WHO 2011 standard
		Mean	SEM	N	Mean	SEM	N	Mean	SEM	N	Mean	SEM	N	
Turbidity NTU	Raw	20.610	7.51	3	3.310	0.00	1	0.853	0.04	3	0.957	0.01	3	5
	Treated	2.455	0.41	2	1.160	1.09	2	0.407	0.01	3	0.407	0.01	3	
	Effluent	22.577	7.57	3	5.683	0.95	3	1.617	0.31	3	1.857	0.06	3	
TDS mg/L	Raw	82.667	3.71	3	23.000	7.00	2	30.000	0.00	3	40.000	0.00	3	500
	Treated	72.233	22.95	3	20.667	4.06	3	20.000	0.00	3	20.000	0.00	3	
	Effluent	87.333	9.33	3	16.667	1.76	3	25.000	0.00	3	30.000	0.00	3	
TH mg/L	Raw	1.000	0.04	3	1.035	0.35	2	1.067	0.07	3	1.133	0.07	3	
	Treated	1.120	0.07	3	1.040	0.13	3	0.867	0.03	3	0.800	0.02	3	
	Effluent	1.187	0.01	3	1.170	0.27	3	1.213	0.01	3	1.233	0.12	3	
EC $\mu$ S/cm	Raw	124.603	5.23	3	35.015	11.14	2	44.800	0.10	3	59.233	0.23	3	1000
	Treated	143.855	5.40	2	31.150	6.04	3	29.933	0.07	3	29.967	0.03	3	
	Effluent	131.713	14.18	3	25.180	2.93	3	37.100	0.10	3	44.567	0.30	3	
Cl mg/L	Raw	0.717	0.12	3	0.900	0.30	2	0.990	0.00	3	0.990	0.00	3	250
	Treated	5.247	2.16	3	0.253	0.14	3	0.297	0.15	3	0.000	0.00	3	
	Effluent	3.147	0.38	3	1.993	0.86	3	2.297	0.30	3	1.457	0.03	3	
Ca mg/L	Raw	0.757	0.11	3	0.700	0.24	2	0.760	0.00	3	0.760	0.00	3	75
	Treated	0.883	0.16	3	0.753	0.12	3	0.567	0.03	3	0.423	0.01	3	
	Effluent	0.847	0.11	3	0.780	0.10	3	0.813	0.14	3	1.103	0.03	3	
Mg mg/L	Raw	0.243	0.08	3	0.335	0.11	2	0.307	0.07	3	0.230	0.00	3	50
	Treated	0.237	0.10	3	0.287	0.04	3	0.300	0.00	3	0.377	0.01	3	
	Effluent	0.340	0.10	3	0.390	0.19	3	0.393	0.14	3	0.250	0.03	3	
SO <sub>4</sub> mg/L	Raw	0.097	0.05	3	0.160	0.02	2	0.080	0.00	3	0.080	0.00	3	250
	Treated	0.123	0.02	3	0.140	0.01	3	0.180	0.00	3	0.240	0.00	3	
	Effluent	0.130	0.06	3	0.047	0.01	3	0.400	0.00	3	0.133	0.09	3	
NO <sub>3</sub> mg/L	Raw	0.050	0.01	3	0.070	0.01	2	0.020	0.00	3	0.020	0.00	3	50
	Treated	0.073	0.03	3	0.020	0.01	3	0.040	0.02	3	0.020	0.00	3	

Table 8.5: (continued)

(b) Parameter	Water sample	Otta-ikosi			Ikorodu			Iju			Adiyan			WHO 2011 standard		
		Mean	SEM	N	Mean	SEM	N	Mean	SEM	N	Mean	SEM	N	Mean	SEM	N
PO <sub>4</sub> mg/L	Effluent	0.127	0.05	3	0.130	0.06	3	0.020	0.00	3	0.040	0.02	3			
	Raw	0.093	0.02	3	0.195	0.14	2	0.137	0.01	3	0.133	0.01	3			0.5
	Treated	0.140	0.06	3	0.330	0.00	3	0.033	0.00	3	0.040	0.00	2			
TA mg/L	Effluent	0.333	0.03	3	0.143	0.09	3	0.197	0.00	3	0.163	0.01	3			
	Raw	22.000	2.00	2	12.000	0.00	1	12.000	0.00	2						200
	Treated	12.000	0.00	2	10.000	2.00	2	10.000	2.00	2	12.000	0.00	2			
TC	Effluent	14.000	2.00	2	10.000	2.00	2	10.000	2.00	2	18.000	2.00	2			
	Raw	7.667	2.07	3	150.000	0.00	1	270.000	30.00	2						0
	Treated															
Cu mg/L	Effluent	17.083	1.93	3	120.000	0.00	2	170.000	30.00	2						
	Raw	0.095	0.08	2				0.100	0.01	2						2
	Treated															
Pb mg/L	Effluent	0.115	0.01	2	0.190	0.00	1	0.165	0.06	2	0.145	0.06	2			
	Raw	0.175	0.18	2				0.585	0.36	2						0.01
	Treated															
Effluent	0.145	0.15	2	0.580	0.00	1	0.280	0.28	2	0.300	0.02	2				



**Figure 8.1:** The concentration distribution in (i) and (ii) parameters of raw (A), treated (B) and effluent (C) water from selected water treatment plants.

0.383 and 338.80  $\mu\text{S}/\text{cm}$ . The water can be classified based on EC as type I, if the enrichment of salts are low (EC:  $<1500 \mu\text{S}/\text{cm}$ ); type II, if the enrichment of salts are medium (EC: 1500 and 3000  $\mu\text{S}/\text{cm}$ ); and type III, if the enrichment of salts are high (EC:  $>3000 \mu\text{S}/\text{cm}$ ). Hence, all the water samples in the study area fall under type I (low enrichment of salts). The recommended value of EC for drinking water purposes is 500  $\mu\text{S}/\text{cm}$ . A higher value of EC (192.30–534.00  $\mu\text{S}/\text{cm}$ ) was, however, recorded by Yusuf et al. [14]. Total dissolved solids (TDS) is a measure of the inorganic salts and small amounts of the organic matter present in water, it is related to the conductivity of the water because of the effect of dissolved ions. The levels of TDS recorded in the water samples ranged from 0.26–224.67 mg/L. There was no significant difference in TDS between the different sampling types ( $p > 0.05$ ). According to (WHO [13]), the presence of dissolved solids in water may affect its taste. Moreover, the palatability of drinking water may be classified as excellent ( $<300 \text{ mg}/\text{L}$ ), good (300–600 mg/L), fair (600–900 mg/L), poor (900–1200 mg/L) and unacceptable ( $>1200 \text{ mg}/\text{L}$ ). However, the water samples from the study area were classified excellent and within acceptable levels (1000 mg/L) for drinking purposes (WHO [10]). There was no significant change in the mean values of TH in the water samples for the different types ( $p > 0.05$ ). Average TH (as  $\text{CaCO}_3$ ) values for raw, treated and effluent water samples were 1.81, 1.96 and 1.65 mg/L, respectively, and were within the WHO limits for drinking purposes. Based on TH classification [14] all the water from the treatment plants was below 60 mg/L and can be classified as very soft water. Calcium ( $\text{Ca}^{2+}$ ) is a major cation found in water which

makes water hard. Calcium constitutes our body's bones and teeth and works as a structural element of our body. The WHO guideline value of  $\text{Ca}^{2+}$  for drinking purposes is 75 mg/L. The concentration of  $\text{Ca}^{2+}$  in the water samples ranged from 0.16–5.80 mg/L. The results showed that all samples were within the guideline value. The second most abundant inorganic ion that is present in water is magnesium with an average concentration of 0.27, 0.35 and 0.36 mg/L in the raw, treated and effluent water samples, respectively. The WHO recommended value for  $\text{Mg}^{2+}$  concentration is 50 mg/L. All samples were found within the WHO [10] permissible limits for calcium and magnesium. Total alkalinity (TA) is the amount of alkali in the form of bi-carbonates, carbonates and hydroxides present in the water. The TA varied in the water samples from 10 to 32 mg/L (as  $\text{CaCO}_3$ ). The suggested alkalinity in our drinking water is 20–200 mg/L.

Chloride ( $\text{Cl}^-$ ) concentration in the water samples ranged between 0.50 and 15.0 mg/L. Chloride concentration in the water may result from encroachment of the saline water to the freshwater zone and different anthropogenic activities. Sulphate ( $\text{SO}_4^{2-}$ ) concentration in the water samples varied between 0.03 and 2.40 mg/L. Sulphate concentration ( $\text{SO}_4^{2-}$ ) in all the experimental water samples was within the permissible limits of 250 mg/L (WHO [10]). According to World Health Organization (WHO [10]), the permissible limit of phosphate concentration in drinking water should be 0.50 mg/L. Phosphate ( $\text{PO}_4^{3-}$ ) concentration in water samples ranged from 3.0 to 40.5 mg/L. Some of the water samples exceeded the permissible limits of phosphate concentration. The presence of phosphates in water may be due to anthropogenic origin. The concentrations of nitrate ( $\text{NO}_3^-$ ) in water samples ranged from 0.01 to 0.40 mg/L and were found within the permissible limits. The source of  $\text{NO}_3^-$  may be from the high infiltration of the soil layer and anthropogenic activities.

Cadmium ( $\text{Cd}^{2+}$ ) was not found in the water samples. The concentration of copper ( $\text{Cu}^{2+}$ ) in water was found within the maximum permissible limit of 2 mg/L by the WHO [10] and ranged from 0.02 to 0.27 mg/L. The concentration of the  $\text{Pb}^{2+}$  in water samples varied from 0.0 to 1.31 mg/L. All water samples were within the acceptable guideline values of 0.01 mg/L as recommended by WHO. The TC ranged between 7.67 and 270 cfu/100 mL. The results indicated that the TC exceeded the permissible limits of zero set by (WHO [10]).

### 8.4.1 WQI analysis

Using the concentration of 14 parameters, Water quality indices (WQIs) were calculated by adopting the weighted arithmetical index method. The WQI values in Table 8.6 for this study ranged from 8.65 to 170.28 with a mean value of 39.96. The results revealed 25, 29.17 and 16.67% respectively as excellent quality for raw, treated and effluent water samples; 4.17% (treated) and 8.33% (raw and effluent) were considered good quality while 8.33% (effluent) exhibited poor quality.

**Table 8.6:** Water quality index (WQI) classification for raw (R), treated (T) and waste (W) water samples.

Sampling Point	Water sample	WQI	Water quality rating
Alausa	R1	50.39	Good water
	T1	50.20	Good water
	W1	170.28	Poor water
Akilo	R2	18.12	Excellent water
	T2	22.60	Excellent water
	W2	86.38	Good water
Mosan	R3	17.07	Excellent water
	T3	19.70	Excellent water
	W3	21.57	Excellent water
Ishasi	R4	31.40	Excellent water
	T4	23.99	Excellent water
	W4	118.89	Poor water
Otta-ikosi	R5	80.87	Good water
	T5	16.91	Excellent water
	W5	51.96	Good water
Ikorodu	R6	14.96	Excellent water
	T6	22.13	Excellent water
	W6	43.11	Excellent water
Iju	R7	14.97	Excellent water
	T7	8.65	Excellent water
	W7	18.36	Excellent water
Adiyan	R8	15.21	Excellent water
	T8	23.72	Excellent water
	W8	17.71	Excellent water
		% excellent	70.83
		% good	20.83
		% poor	8.33

### 8.4.2 Principal component analysis

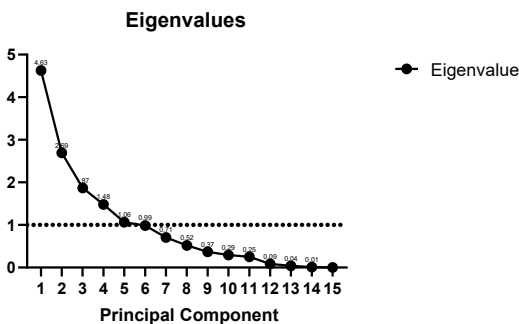
Table 8.7 summarizes the PCA results including the loadings, eigenvalues and variance given by each principal component (PCs). The PCA rendered five PCs with eigenvalues >1 explaining 89.11% of the total variance of the dataset.

The scree plot in Figure 8.2 is the way of identifying a number of useful factors, wherein a sharp break in sizes of eigenvalues which results in a change in the slope of the plot from steep to shallow could be observed. The slope of the plot changes from steep to shallow after the first two factors. The eigenvalues also drop below one, when we move factor 5 to factor 6. This suggests that a five-component solution could be the right choice which includes the total variance of 78.22%.

The loadings plot Figure 8.3 of the first two PCs (PC1 and PC2) showed the distribution of all the physicochemical parameters in the third (lower left) and fourth (lower right) quadrants. The lines joining the variables and passing through the origin in the

**Table 8.7:** Loadings of variables on principal components, eigen values and variances of the selected water treatment plants.

Principal components					
Variable	PC1	PC2	PC3	PC4	PC5
pH					-0.685
EC	0.925				
Turbidity	0.777				
TDS	0.924				
TH		0.643		0.515	
Cl			-0.817		
Ca				0.832	
Mg			0.748		
SO <sub>4</sub>					
NO <sub>3</sub>	0.842				
PO <sub>4</sub>				0.520	-0.580
TA		0.882			
TC		-0.521	0.507		
Cu		0.607	0.531		
Pb					0.705
Eigen value	4.63	2.7	1.87	1.48	1.06
Proportion %	30.8	17.96	12.46	9.86	7.09
Cumulative %	30.8	48.8	61.26	71.1	78.22

**Figure 8.2:** PAC scree plot of the eigenvalues.

plot of the factor loadings were indicative of the contribution of the variables to the samples. The proximity of lines for two variables signifies the strength of their reciprocal association [17]. Grouping of parameters (EC, TDS, Turbidity and NO<sub>3</sub>; TH, TA, TC and Cu) in the loadings plot suggests their significant mutual correlation. The score plot (PC1 and PC2) for the water samples from selected treatment plants (Figure 8.4) showed the mixed distribution of samples. Visible grouping of the majority of the samples has been observed in the upper left and lower left quadrants while loading of samples in the lower right and lower left quadrants was found to be noticeably scattered.

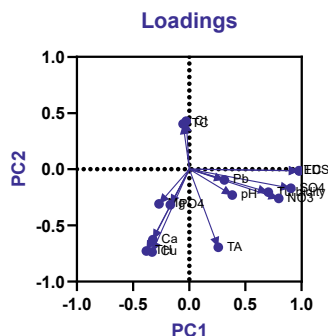


Figure 8.3: Plots of PCA loadings scores for dataset of water samples.

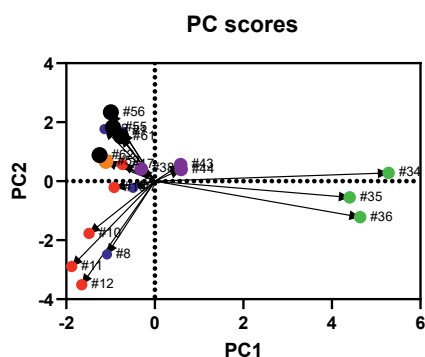


Figure 8.4: PCs score plot for dataset of water samples.

### 8.4.3 Health risk assessment

Table 8.8 showed coefficients on health risk assessment, while the non-cancer HQ values were given in Table 8.9 for both adults and children. According to the comparison of acute, sub-chronic and chronic thresholds, chronic in adult and child Pb were “high” risk in both the raw and the effluent. Oral ingestion was higher in children than in adults, making children more susceptible to heavy metals in the water. The results of this study (Table 8.9), for non-carcinogenic effects by trace metals in raw and effluent water samples, can be classified as follows:

- (i) The HQs of raw and effluent water samples (HQ) were lower than one in acute, sub-chronic and chronic adult Cu; acute and chronic child Cu ( $HQ < 0.1$ ); hence, no risk of disease for both adult and child,
- (ii) The HQs of raw and effluent water samples (HQ) were above one in sub-chronic child Cu ( $0.1 \leq HQ < 1$ ); hence, cancer risks are medium and poses health risk in child,
- (iii) The HQs of raw and effluent water samples (HQ) are above one in the chronic adult and child Pb ( $HQ \geq 4$ ); hence, cancer risks are high for both child and adult.

Finally, children are at higher risk compared with adults in the oral exposure route.



**Table 8.8:** Some coefficients about health risk assessment [1].

Parameter	RfD water oral ingestion		
	Acute	Sub-chronic	Chronic
Cd			0.0010
Cu	0.0900	0.0100	0.0370
Pb			0.0035

**Table 8.9:** Health Quotient (HQ) values for raw (a) and effluent (b) in water treatment plants.

(a) Location	Adult Cu			Child Cu			Adult Pb	Child Pb
	Acute	Sub-chronic	Chronic	Acute	Sub-chronic	Chronic	Chronic	Chronic
Alausa	0.0149	0.134	0.0362	0.088	0.795	0.215	1.415	7.946
Akilo	0.0287	0.258	0.0697	0.17	1.53	0.414	1.031	6.11
Mosan	0.016	0.144	0.0389	0.095	0.856	0.231	0.147	0.886
Ishasi	0.0194	0.175	0.0473	0.116	1.04	0.281	1.091	6.457
Otta-ikosi	0.0103	0.093	0.025	0.061	0.55	0.149	0.531	3.143
Ikorodu	0.022	0.198	0.0535	0.13	1.17	0.316	0	0
Iju	0.0114	0.103	0.0278	0.0679	0.611	0.165	1.739	10.314
Adiyan	0.0126	0.113	0.0305	0.075	0.673	0.182	1.414	8.4

(b) Location	Adult Cu			Child Cu			Adult Pb	Child Pb
	Acute	Sub-chronic	Chronic	Acute	Sub-chronic	Chronic	Chronic	Chronic
Alausa	0.024	0.217	0.0586	0.142	1.28	0.346	1.091	6.457
Akilo	0.016	0.144	0.0389	0.095	0.856	0.231	1.829	10.829
Mosan	0.0189	0.17	0.0459	0.111	1	0.27	0.709	4.2
Ishasi	0.0149	0.134	0.0362	0.088	0.795	0.215	2.357	13.971
Otta-ikosi	0.0126	0.113	0.0305	0.0748	0.673	0.182	0.443	2.629
Ikorodu	0.0219	0.197	0.0532	0.13	1.168	0.316	1.709	10.143
Iju	0.0194	0.175	0.0473	0.116	1.04	0.273	0.826	20.286
Adiyan	0.0172	0.155	0.0419	0.01019	0.917	0.248	0.884	5.229

#### 8.4.4 Correlation analysis of water quality parameters

Pearson's correlation coefficients among the parameters are presented in Tables 8.10–8.12. EC showed strong linear correlation with TDS in raw ( $r = 0.998$ ), treated ( $r = 0.995$ ) and effluent ( $r = 0.998$ ); TH correlated linearly with  $\text{Ca}^{2+}$  in raw (0.692), treated (0.993) and effluent (0.97); TA had positive correlation with  $\text{NO}_3^-$  in raw (0.613), treated (0.561) and effluent (0.594).

Correlations with one another indicate they had similar chemical characteristics.

**Table 8.10:** Correlation coefficient matrix of raw water sample.

	pH	EC	Turbidity	TDS	TH	Cl	Ca	Mg	SO <sub>4</sub>	NO <sub>3</sub>	PO <sub>4</sub>	TA	Cu	TC	Pb
pH	1														
EC	0.174	1													
Turbidity	0.283	0.148	1												
TDS	0.176	0.999**	0.134	1											
TH	-0.19	-0.368	-0.113	-0.368	1										
Cl	-0.316	0.458*	-0.062	0.449*	-0.356	1									
Ca	-0.21	-0.355	-0.037	-0.361	0.652**	-0.232	1								
Mg	0	-0.216	-0.113	-0.213	0.188	-0.392	0.358	1							
SO <sub>4</sub>	-0.103	0.822**	-0.11	0.824**	-0.055	0.393	-0.09	-0.067	1						
NO <sub>3</sub>	-0.185	0.423*	0.175	0.413	0.347	0.192	0.336	0.053	0.700**	1					
PO <sub>4</sub>	-0.286	-0.321	-0.439*	-0.311	0.259	0.039	0.205	0.145	-0.102	-0.164	1				
TA	0.097	0.392	-0.022	0.401	0.43	-0.303	0.293	0.259	0.590*	0.590*	0.194	1			
Cu	-0.510*	-0.082	-0.508*	-0.068	0.591*	0.039	0.387	0.261	0.286	0.336	0.575*	0.524			
TC	0.091	-0.134	-0.527	-0.107	-0.326	0.146	-0.319	-0.113	-0.327	-0.703**	-0.032	-0.444	-0.316	1	
Pb	0.361	-0.094	-0.109	-0.099	0.076	0.042	0.534*	0.342	-0.083	-0.056	-0.219	-0.191	-0.12	0.485	1

\*Correlation is significant at the 0.05 level (two-tailed). \*\*Correlation is significant at the 0.01 level (two-tailed).

Table 8.11: Correlation coefficient of treated water.

	pH	EC	Turb	TDS	TH	Cl	Ca	Mg	SO4	NO3	PO4	TA
pH	1											
EC	0.105	1										
Turbidity	0.263	0.467*	1									
TDS	0.040	0.995**	0.450*	1								
TH	0.606**	-0.141	0.227	-0.208	1							
Cl	-0.152	0.405*	0.136	0.338	-0.216	1						
Ca	0.592**	-0.176	0.214	-0.241	0.993**	-0.198	1					
Mg	0.283	0.171	0.069	0.135	0.403*	-0.203	0.301	1				
SO4	0.047	0.824*	0.432*	0.845**	-0.232	0.003	-0.278	0.245	1			
NO3	0.105	0.715*	0.440*	0.724**	-0.074	0.177	-0.086	0.111	0.796**	1		
PO4	-0.213	-0.158	0.187	-0.117	0.070	0.103	0.104	-0.202	-0.163	0.114	1	
TA	0.482*	0.518*	0.185	0.510*	-0.009	-0.019	0.033	-0.290	0.448*	0.561*	-0.037	1

\*\*Correlation significant at 0.01 level (one-tailed). \*Correlation significant at 0.05 level (one-tailed).

**Table 8.12:** Correlation coefficient matrix of effluent water sample.

	pH	EC	Turbidity	TDS	TH	Cl	Ca	Mg	SO4	NO3	PO4	TA	TC	Cu	Pb
pH	1														
EC	0.408*	1													
Turbidity	-0.019	0.611*	1												
TDS	0.4222*	0.998**	0.576*	1											
TH	-0.116	-0.138	0.525*	-0.196	1										
Cl	0.279	0.254	-0.264	0.279	-0.522*	1									
Ca	-0.023	-0.147	0.475	-0.203	0.970**	-0.548	1								
Mg	-0.346	-0.093	0.411	-0.132	0.613*	-0.218	0.415*	1							
SO4	-0.032	0.357	-0.006	0.363	-0.328	-0.168	-0.272	-0.396	1						
NO3	0.029	0.756**	0.645*	0.742**	0.057	-0.139	0.058	0.002	0.364	1					
PO4	0.155	-0.066	-0.148	-0.068	0.226	0.207	0.238	0.043	-0.078	-0.182	1				
TA	0.341	0.563*	0.527*	0.551*	0.173	-0.489	0.283	-0.281	0.536*	0.594*	-0.221	1			
TC	-0.337	-0.178	0.173	-0.177	0.245	-0.417	0.158	0.442*	0.145	-0.197	-0.162	-0.029	1		
Cu	-0.573	-0.260	-0.109	-0.273	0.251	-0.288	0.127	0.468*	0.005	-0.321	0.032	-0.052	0.210	1	
Pb	0.055	0.548*	0.367	0.545*	0.058	-0.201	0.021	0.125	0.015	0.434*	-0.077	0.384	0.070	0.369	1

\*\*Correlation significant at 0.01 level (one-tailed). \*Correlation significant at 0.05 level (one-tailed).

## 8.5 Conclusion

The water quality of raw, treated and effluent samples from selected treatment plants has been evaluated regarding the suitability of water for drinking purposes as well as the identification of the dominating sources of different water quality parameters. Physicochemical analysis of the samples showed high turbid water and appreciable amount of phosphate ( $\text{PO}_4^{3-}$ ). The TC concentrations in raw and effluent water samples ranged from 3.53–300 cfu 100 mL<sup>-1</sup> and 14.67–200 cfu 100 mL<sup>-1</sup>, respectively, and exceeded the WHO safe limit of 0 cfu 100 mL<sup>-1</sup>. All other parameters were within the permissible limit of WHO water quality standards. Based on TH and EC values the water samples were found to be soft. Computed WQI values revealed 70.83% of water samples ranked excellent; 20.83% exhibited good quality and the rest 8.33% were of poor-quality type (effluent). The results from the PCA analysis established that water quality parameters under PC1, PC2, PC3 and PC4 (viz., 30.8, 17.96, 12.46 and 9.86% of total variance) having strong loading (>0.75) were considered to govern the raw, treated and effluent water quality in the study area. While water quality parameters under PC5 though exhibited strong and positive loading by one parameter, was considered insignificant due to a lesser percentage of variance (i.e., 7.09%). Human health risk assessment for exposure to trace metals revealed that ingestion of the water samples poses carcinogenic risk ( $\text{CR}_{\text{ing}}$ ) in adults and children. In addition the estimated ( $\text{CR}_{\text{ing}}$ ) for Pb among children were high throughout the study. It is therefore recommended that water quality studies should be given a priority by adding it into the integrated development plans and be conducted on a regular basis to assess risks of contamination and institute mitigating measures. Water plays a major role in economic development and if this resource is not protected, the consequences are innumerable. Hence, monitoring the activities of pollutants on the quality of water samples is recommended.

**Acknowledgment:** The authors would like to thank Lagos Water Corporation (LWC) for their assistance during sampling.

**Author contributions:** K.A. Yusuf conducted the study, K.A. Yusuf, A.O. Majolagbe and S.Balogun conceptualize the manuscript and contributed immensely to the writing of the draft and final manuscript.

**Research funding:** This research received no external funding.

**Conflict of interest statement:** The authors declare no conflict of interest.

## References

1. Alver A. Evaluation of conventional drinking water treatment plant efficiency according to water quality index and health risk assessment. *Environ Sci Pollut Control Res* 2019;26:27225–238.
2. World Health Organization (WHO). Water, sanitation and hygiene programming guidance. Water Supply and Sanitation Collaborative Council and World Health Organization; 2005:84 p.

3. Akoto O, Gyamfi O, Darko G, Barnes VR. Changes in water quality in the Owabi water treatment plant in Ghana. *Appl Water Sci* 2017;7:175–86.
4. Sargaonkar A, Deshpande V. Development of an overall index of pollution for surface and water based on a general classification scheme in Indian context. *Environ Monit Assess* 2003;89:43–67.
5. Alobaidy AHMJ, Abid HS, Maulood BK. Application of water quality index for assessment of Dokan lake Ecosystem, Kurdistan region, Iraq. *J Water Resour Protect* 2010;2:792–8.
6. APHA, AWWA, WEF. Standard methods for examination of water and wastewater. 22nd ed. Washington: American Public Health Association; 2012:1360 p.
7. Ravikumar P, Somashekar RK. Principal component analysis and hydrochemical facies characterization to evaluate groundwater quality in Varahi river basin, Karnataka state, India. *J Appl Water Sci* 2017;7:745–55.
8. Howladar MF, Abdullah Al Numanbakth Md, Faruque MO. An application of Water Quality Index (WQI) and multivariate statistics to evaluate the water quality around Maddhapara Granite Mining Industrial Area, Dinajpur, Bangladesh. *Environ Syst Res* 2017;6:13.
9. Soleimani H, Nasri O, Ojaghi B, Pasalari H, Hosseini M, Hashemzadeh M, et al. Data on drinking water quality using water quality index (WQI) and assessment of groundwater quality for irrigation purposes in Qorveh & Dehgolan, Kurdistan, Iran. *Data Brief* 2018;20:375–86.
10. WHO. Guidelines for drinking-water quality. In: Health criteria and other supporting information, 4th ed. Geneva: WHO; 2011.
11. Adeniyi A, Yusuf K, Okedeyi O, Sowemimo M. Classification and health risk assessment for borehole water contaminated by metals in selected households in southwest Nigeria. *J Water Resour Protect* 2016;8:459–71.
12. EPA US. Regional screening levels (RSLs) – user’s guide. National Center for Environmental Assessment c/o – Risk Website; 2018.
13. WHO. Guidelines for drinking-water quality. 2nd ed. Geneva: World Health Organization; 1996, vol. 2: Health Criteria and Other Supporting Information.
14. Yusuf KA. Evaluation of groundwater quality characteristic in Lagos-City. *J Appl Sci* 2007;7:1780–4.
15. US Environmental Protection Agency. Guidelines for water reuse. EPA/600/R-12/618. Washington, DC: Agency for International Development; 2012.
16. United States Environmental Protection Agency (USEPA). Risk assessment guidance for superfund. Washington DC: Interim Final, Office of Emergency and Remedial Response; 1989, vol. 1: Human Health Evaluation Manual (Part A). EPA/540/1-89/002.
17. Bodrud-Doza MD, Towfiqul Islam ARM, Ahmed F, Das S, Saha N, Rahman MS. Characterization of groundwater quality using water evaluation indices, multivariate statistics and geostatistics in central Bangladesh. *Water Sci* 2016;30:19–40.



Alfred F. Attah\*, Abobarin I. Omobola, Jones O. Moody,  
Mubo A. Sonibare, Olubori M. Adebukola and  
Samuel A. Onasanwo

## 9 Detection of cysteine-rich peptides in *Tragia benthamii* Baker (Euphorbiaceae) and *in vivo* antiinflammatory effect in a chick model

**Abstract:** *Tragia benthamii* (TBM) commonly called the climbing nettle is a tropical plant claimed to have numerous anti inflammatory effects in sub Saharan African ethnomedicine which lacks scientific evidence. Aqueous extracts of TBM were further prepurified on a RP-C18 parked solid phase system to obtain 20% aqueous fraction. This fraction was enzymatically and chemically analyzed (by MALDI TOF MS and MS/MS) to contain interesting low molecular weight cysteine-rich stable peptides within the range of 2.5–3.2 KDa. The 20% aqueous fraction was further tested *in vivo* using carrageenan-induced foot edema (acute inflammation) in seven-day old chicks with diclofenac as reference drug. The cytotoxicity of this active fraction was investigated using the brine shrimp lethality assay. The brine shrimp cytotoxicity assay produced LC<sub>50</sub> above 1000 µg/mL. Pretreatment with the TBM extract (30–300 mg/kg, i.p) dose dependently ( $P < 0.01$ ) reduced foot edema with maximal inhibition of  $0.253 \pm 0.180$  (84.3%) at 300 mg/kg body weight, which was comparable to that of diclofenac with inhibition ( $P < 0.05$ ) of  $0.410 \pm 0.271$  (74.5%) at 10 mg/kg body weight. The study has therefore shown for the first time, the detection of cysteine-rich biologically active peptides in *T. benthamii* and the stable peptide extracts from this ethnomedicinal plant, which is not toxic to *Artemia salina*, exhibits anti inflammatory activity in a chick *in vivo* model. This may provide scientific evidence for its use in the treatment of inflammation and pain in traditional medicine. Further *in-depth vivo* and *in vitro* studies will be required to investigate its anti inflammatory activity including effect on HUVEC-TERT, the possible inhibition of ICAM-1 surface expression and the mechanism of the anti inflammatory effect.

**Keywords:** brine shrimp cytotoxicity; carrageenan; cysteine-rich peptides; inflammation; *Tragia benthamii*.

---

**\*Corresponding author: Alfred F. Attah**, Department of Pharmacognosy and Drug Development, Faculty of Pharmaceutical Sciences, University of Ilorin, Ilorin, Nigeria; and Department of Pharmacognosy, Faculty of Pharmacy, University of Ibadan, Ibadan, Nigeria, E-mail: attah.fau@unilorin.edu.ng

**Abobarin I. Omobola, Jones O. Moody and Mubo A. Sonibare**, Department of Pharmacognosy, Faculty of Pharmacy, University of Ibadan, Ibadan, Nigeria

**Olubori M. Adebukola and Samuel A. Onasanwo**, Department of Physiology, College of Medicine, University of Ibadan, Ibadan, Nigeria

This article has previously been published in the journal Physical Sciences Reviews. Please cite as: A.F. Attah, A. I. Omobola, J. O. Moody, M. A. Sonibare, O. M. Adebukola and S. A. Onasanwo "Detection of cysteine-rich peptides in *Tragia benthamii* Baker (Euphorbiaceae) and *in vivo* antiinflammatory effect in a chick model" *Physical Sciences Reviews* [Online] 2021, 7. DOI: 10.1515/psr-2020-0125 | <https://doi.org/10.1515/9783110710823-009>



## 9.1 Introduction

*Tragia benthamii* (TBM), Bak. (Euphorbiaceae) also known as climbing nettle or stinging nettle, is a medicinal plant widely distributed and used by traditional healers all over sub Saharan Africa where the plant appears to be endemic [1, 2]. The genus *Tragia* contains over 152 species including a newly reported species – *Tragia guayanensis* [1, 3] with only five that have received some scientific attention among which TBM remains the least investigated; others include *Tragia involucrata*, *Tragia cannabina*, *Tragia spathulata*, and *Tragia plukenetii*. Folkloric claims on the medicinal application of the plant include abortifacient activity, facilitation of child birth, treatment of venereal diseases, as an anti inflammatory remedy, and as an antibiotic. For instance, the Baule women in Ivory Coast have used TBM to induce abortion or to facilitate delivery [2, 4, 5]. Despite its adaptational irritating properties when the foliar organs are in contact with the human skin [6], there is a widespread ethnopharmacological applications among African populations; while this should attract scientific attention, only very limited investigation has been carried out on the plant with no available data on the bioactive constituents from the aqueous extracts and their possible effect on inflammation, a common denominator of several chronic diseases and initiator of different pathophysiological diseases [7–9].

*T. benthamii* is a creeping and twining tropical herbaceous plant distributed around the flood-plain thickets and flood-plain grasslands of Africa. It is commonly found in Ivory Coast, Ethiopia, Angola, Botswana, Zimbabwe, Mozambique, and Nigeria. TBM possesses stinging hairs which are covering trichome outgrowths from the surface of the leaves whose contact with the body result in local inflammation and pain lasting up to 10 min [6]. The trichome-covered leaves have leaf blade which looks more or less shallowly and cordate at the base. In Nigeria, TBM is known as *Esisi* or *Werepe* in Yoruba, *Abalagwo* in Igbo, and *Ibadidon* or *Eeghelepe* (ososo) in Edo.

A typical plant has been described as a physiological laboratory, making it a rich source of bioactive compounds with diverse structures suitable for drug design and discovery [10]. Overtime, phytomedicinal research has paid more attention to low molecular weight secondary compounds [11] while the higher molecular weight peptides have recently gained more recognition within the scientific community [11–21]. However, a major therapeutic drawback of peptides lies in their poor metabolic stability or oral bioavailability [14, 20, 22]. The cysteine-rich peptides (CRPs), particularly those containing three to six disulfide bonds have been well reported to overcome this undesirable limitation [12, 19, 23]. Of particular interest are CRPs whose molecular weights lies within the range of 2–6 kDa which are known to contain a well-defined tertiary structure arising from a uniquely coupled thiol groups resulting in a cross-linked multiple disulfide bonds (SS-bonds) that provide them with exceptional stability against thermal and enzymatic degradation [20]. Many of these plant-derived CRPs display varied interesting biological and pharmacological activities [19, 20, 24].

In the present work, we extracted the peptide-rich aqueous portion of TBM and subjected this to pre purification via solid phase extraction to yield an optimized crude peptide mixture whose biophysical properties, nature and individual masses were determined by a combination of reversed phase liquid chromatography (RP-HPLC), chemical derivatization and matrix assisted laser desorption time of flight mass spectrometry (MALDI TOF MS). Furthermore, we investigated the anti inflammatory properties of TBM using *in vivo* chick carrageenan response as a viable model for anti inflammatory response; in addition, the nauplii of *Artemia salina* were used for cellular toxicity assay using the brine shrimp cytotoxicity model. Following our new findings, we show for the first time the presence of cysteine-rich stable peptides in the aqueous extracts of TBM and also demonstrate the *in vivo* anti-inflammatory property of the peptide-rich aqueous extracts in a chick model and the safety of this extracts to cellular crustaceans.

## 9.2 Materials and method

### 9.2.1 Plant material

Shoots of *T. benthamii* Bak. (Euphorbiaceae) were collected during the raining season from the rocky areas of Egbetua land, Ososo village, and southern Nigeria in 2011. The complete plant with relevant anatomical features was identified, authenticated and a voucher specimen with the number FHI: 109853 was deposited at the Forest Herbarium Ibadan (FHI) unit of the Forest Research Institute of Nigeria (FRIN).

### 9.2.2 Extraction, SPE pre purification and preliminary MALDI TOF/TOF analysis

Dried and powdered TBM plant material was extracted with methanol: dichloromethane (1:1; v/v) for 24 h under continuous agitation at room temperature. After adding half volume of ddH<sub>2</sub>O to the extraction system and centrifuging (for 3 min at 1000 rpm), the aqueous supernatant was separated out and diluted further with solvent A (100% ddH<sub>2</sub>O, 0.05% trifluoroacetic acid) to less than 10% MeOH for C<sub>18</sub> flash pre purification. The aqueous phase was extracted on RP-C<sub>18</sub> solid-phase. Cartridges (Strata Gigatubes C<sub>18</sub>-E; 5 g, 20 mL, Phenomenex, Germany) was first preconditioned with one volume of MeOH, activated with one volume of solvent B (10% ddH<sub>2</sub>O in acetonitrile and 0.05% trifluoroacetic acid) and equilibrated with two volumes of solvent A, washed with 20% solvent B (to yield 80% aqueous fraction), eluted with 20 mL of 80% solvent B (yielding 20% aqueous fraction) and finally eluting with 100% solvent B (yielding the 0% aqueous fraction). Cryodesiccation of the eluates using the freeze drying equipment followed after pipetting out 200 µL each of the eluates for preliminary crude MALDI-TOF

MS analysis of peptide-like peaks. A volume of 0.5  $\mu\text{L}$  each of eluted fraction was mixed well with 3  $\mu\text{L}$  of matrix (alpha cyano hydroxyl cinnamic acid), spotted on the MALDI target plate and exposed to dryness away from light source. Acquired spectra were processed using the 4800 Analyzer. The freeze dried aqueous extract was kept refrigerated for RP-HPLC analysis and for bioassays [12].

### 9.2.3 RP-HPLC fractionation of C<sub>18</sub> peptide positive fraction

The dried material was reconstituted in a minimal amount of buffer A (0.05% trifluoroacetic acid prepared in distilled water). The solution was further passed through a solid phase filter (Sartorius) before purification using semi preparative RP-HPLC on Dionex Ultimate 3000 HPLC unit (Dionex, Amsterdam, the Netherlands) whose specification include 250 mm  $\times$  10 mm; 5  $\mu\text{m}$ , 100  $\text{\AA}$ , Kromasil column. Linear gradient of 0.1–1%  $\text{min}^{-1}$  solvent B at a flow rate of 3  $\text{mL min}^{-1}$ . Collected fractions were again analyzed on the MALDI TOF/TOF analyzer following the earlier described procedure. Fraction of interest was freeze dried and reconstituted in solvent A for analytical HPLC (flow rate of 1  $\text{mL min}^{-1}$ ) for hydrophobicity determination of the peptide.

### 9.2.4 Reduction/alkylation of peptides and MALDI-MS analysis

Disulphide linkages within the peptide were reduced with 2  $\mu\text{L}$  of dithiothreitol after reconstituting approximately 6 nmol of the lyophilized peptides in 20  $\mu\text{L}$  of 0.1 M ammonium bicarbonate (pH 8.2), and incubating at 65  $^{\circ}\text{C}$  for 10 min. Reduced sample was further alkylated with 4  $\mu\text{L}$  of iodoacetamide. One microlitre of TFA was used to stop the reaction. MALDI-TOF/TOF analyzer was then used to investigate the reduced and alkylated sample. Kalata B1 was used as positive control [12].

### 9.2.5 Derivatization of peptides and MALDI TOF/TOF analysis

Reduced and alkylated peptides were enzymatically digested with endoproteinase Glu-C (Sigma-Aldrich, Austria). The previous reduction and alkylation reaction was stopped by adding 1  $\mu\text{L}$  of formic acid and incubated for 10 min at 37  $^{\circ}\text{C}$ . This was followed by the addition of 2  $\mu\text{L}$  of the enzyme to the reaction mixture and further incubating for 3–14 h under mild agitation. The reaction was quenched with 1  $\mu\text{L}$  of formic acid. 0.5  $\mu\text{L}$  of the sample was mixed with 3  $\mu\text{L}$  of matrix and spotted on the MALDI target plate for MALDI TOF MS analysis. All acquired spectra were processed with the Explorer 4800 software. Digested samples were kept under minus 20 freezers for further analysis [12].

### 9.2.6 *In vivo* anti-inflammatory assay using the chick model

The carrageenan-induced edema in the footpad of chicks [25–27] was used to evaluate the anti-inflammatory activities of the extract compared to the reference drug (diclofenac). Chicks were randomly divided into six groups of six each. Chicks were then randomly selected to perform one of the following study groups: control (10 mL/kg Distilled water, i.p.); *TBM* (10, 30, 100, and 300 mg kg<sup>-1</sup>, i.p) and diclofenac (10 mg kg<sup>-1</sup>, i.p.). Foot volumes were measured by water displacement plethysmometer [28]. Edema was induced by subplantar injection of carrageenan (10 µL of a 1% carrageenan in normal saline) into the right footpad of the chicks. The control and all the drug treated groups were pretreated with the vehicle and the drugs 30 min intraperitoneal (i.p.) before carrageenan injection. Foot volumes were measured for 5 h after carrageenan injection. The foot edema was quantified by measuring the difference in foot volume before carrageenan injection and at the various time points. All drugs were freshly prepared.

### 9.2.7 Brine shrimp cytotoxicity (lethality assay)

The brine shrimp cytotoxicity assay was used to evaluate the toxicity and potential pharmacological activity of the peptide-rich extract [29, 30]. Sea water was obtained from the Lagos Lagoon, Nigeria. The sea water was poured into the hatching tank and the cysts were added to one side of the tank that has been covered with paper foil to shade the shrimp cysts from light source and were left for two days to hatch and mature.

Solutions of the plant extract were prepared at concentrations of 0, 1, 10, 100, 500, and 1000 µg/mL and filled into vials in triplicates. Furthermore, 4 mL of sea water was added to each vial and the volume in each of the vials was made up to 5 mL each. Hatched eggs of *A. salina* were counted into each vial and left for 24 h in light; after 24 h, the brine shrimp nauplii were counted and the mortality was recorded and analyzed using the Finney computer program for probit analysis to determine the LC<sub>50</sub> values and 95% confidence intervals [30].

## 9.3 Results

### 9.3.1 Extraction of cysteine-rich peptides and mass spectrometry experiment

Powdered leaves obtained from the shoot system of *T. benthamii* (TBM) was extracted using 50% (v/v) methanol in dichloromethane and the aqueous portion further extracted with half volume of double distilled water and freeze dried to yield the crude aqueous

extract. The CRP peptides in the aqueous extract were obtained by pre purification using the solid phase extraction and the peptides profiled by the matrix assisted laser desorption time of flight mass spectrometer (MALDI-TOF MS). Distinct MS profiles within a short mass window were observed (Figure 9.1), which ranged between 3000 and 3400 Da. To further characterize the peptides in the mixture as potential CRPs, the crude peptide extract was chemically derivatized via reduction and alkylation to obtain a mass shift of +348 Da (Figures 9.2 and 9.3) and enzymatically digested with trypsin and endoproteinaseGluC to result in a complete fragmentation (Figure 9.4) instead of a +18 Da observed with cysteine-rich circular peptides. The characteristic hydrophobicity of CRPs was evident in their late elution profile (25–50% acetonitrile) in RP-HLC (Figure 9.5).

### 9.3.2 Effect of extract on carrageenan-induced foot edema in chicks and brine shrimp cytotoxicity

Intradermal injection of 10  $\mu$ L of 1% carrageenan-induced a time-dependent edema response in the seven-day old chicks that peaked between 2 and 3 h post carrageenan injection (Figure 9.6a) (Roach and Sufka, 2003).

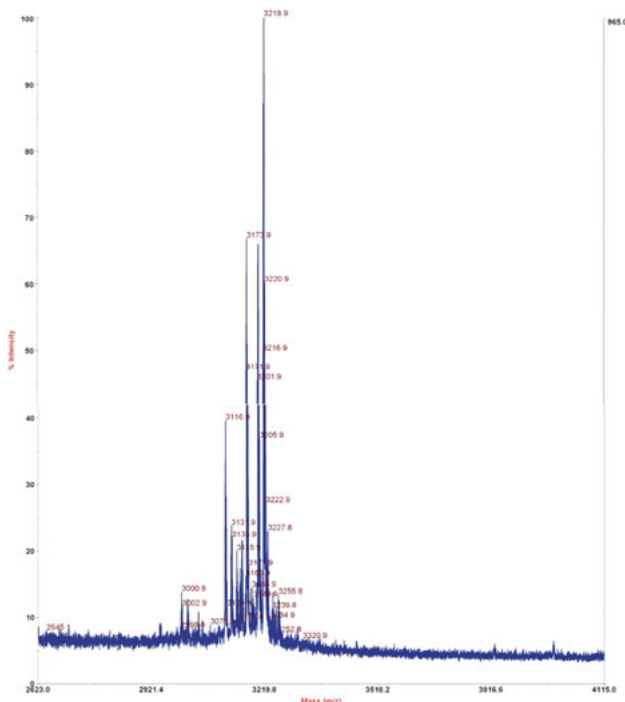


**Figure 9.1:** MS profile of peptide optimized crude extract of TBM showing peptide-like masses within the mass range of 3.0–3.4 kDa which has been obtained from the elution of bound peptides using 80% acetonitrile in solvent A.

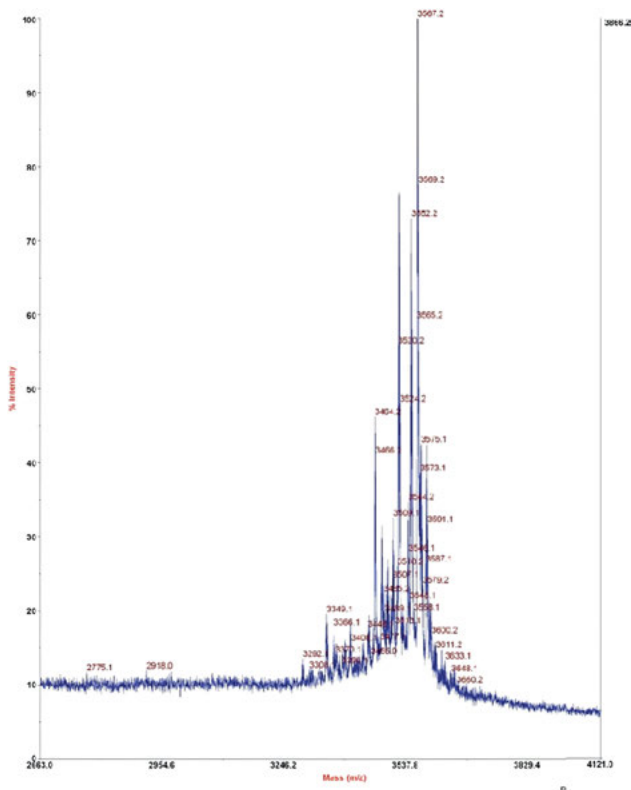


**Figure 9.2:** MS profile for the reduced and alkylated peptide enriched prepurified extracts of TBM showing a typical mass shift of +348 Da following chemical modification achieved by the incubation of peptides with dithiothreitol and iodoacetamide.

Two-way ANOVA (treatment x time) from the time-course curves and one-way ANOVA from the area under the time course curves (AUCs) (Figures 6a and b) revealed significant anti-inflammatory effects for the reference drugs and the extract. *TBM* [ $F_{5, 180} = 9.25, P < 0.0001$ ] significantly reduced total edema with maximal inhibitory effect of  $0.253 \pm 0.180$  at 300 mg/kg as shown in (Table 9.1). Diclofenac (10 mg/kg, i.p.), an NSAID, also showed significant effect on the time course [ $F_{1, 60} = 11.73, P < 0.001$ ] (Figure 9.6a); and the total edema (AUC), with maximal inhibitory effect of  $0.410 \pm 0.271$  (Figure 9.6b). Result obtained from the brine shrimp lethality assay indicates that the aqueous peptides extract of TBM is nontoxic to the nauplii of *A. salina* (Table 9.2).

## 9.4 Discussion

*T. benthamii* is an ethnomedicinal plant endemic to tropical Africa. Traditional medicinal practitioners (TMPs) and spiritual healers in Ghana were known to mix TBM

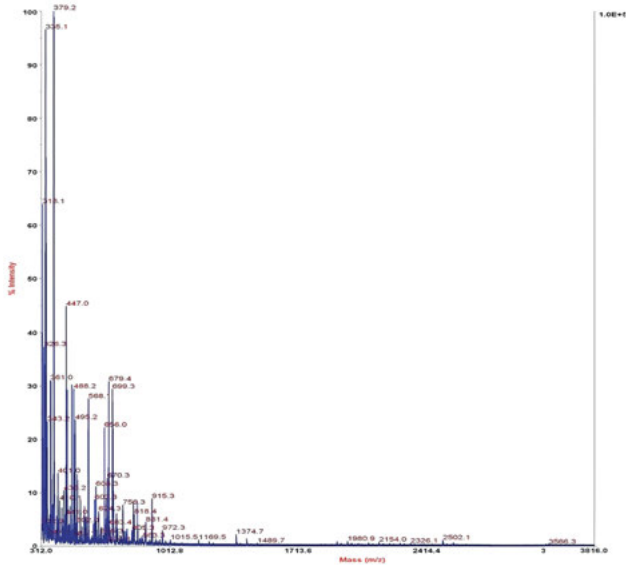


**Figure 9.3:** MS profile of digested CRPs showing heavy fragmentation of the earlier reduced and alkylated peptide masses; an addition of +18 Da was absent to confirm the linearity of the peptide or if circular, the unlikely event of the presence of more than one glutamic acid in all the digested peptides.

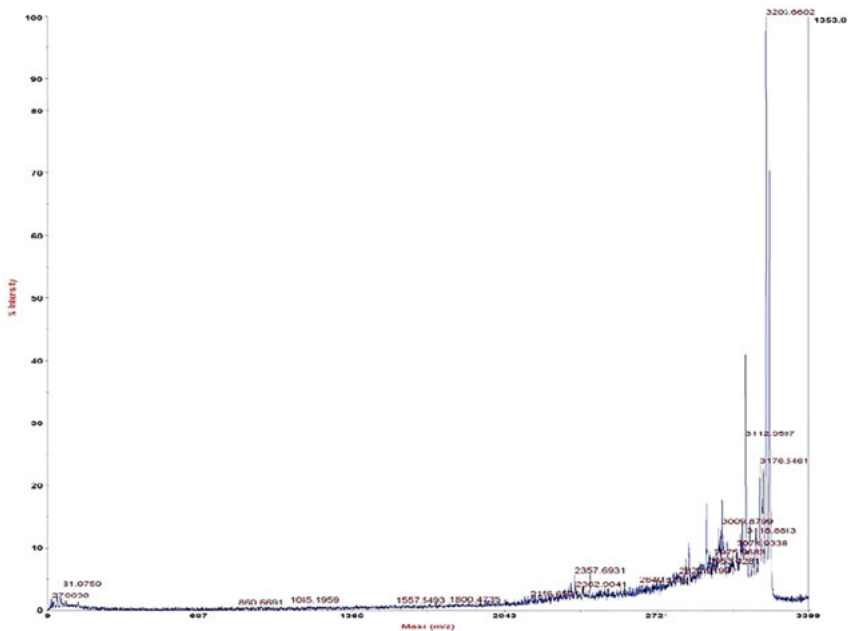


**Figure 9.4:** Very poor fragmentation pattern of the selected native mass (3218.9 Da) earlier detected in TBM following aqueous extraction and pre purification and further subjecting it to a tandem mass spectrometry experiment; this is indicative of an intact and stable peptide typical of cysteine-rich peptides particularly the knottin peptides.

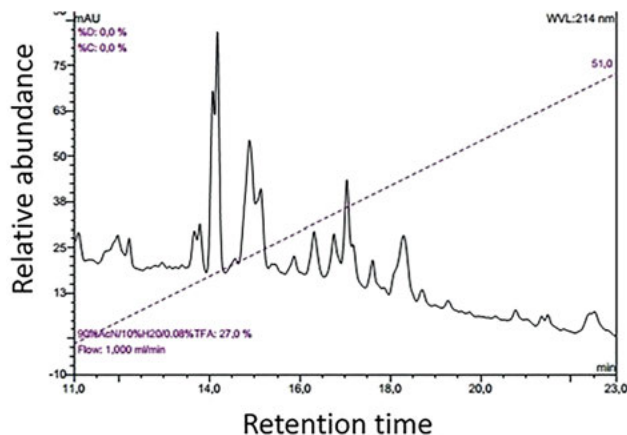


**Figure 9.5:** Analytical RP-HPLC showing the hydrophobicity behavior of the peptides and late elution profile for the 20% peptide optimized aqueous fraction obtained by solid phase extraction of  $C_{18}$ -bound peptides using a combination of 80% buffer B (10% ddH<sub>2</sub>O (v/v) in acetonitrile and 0.05% (v/v) trifluoroacetic acid) and 20% buffer A (100% ddH<sub>2</sub>O, 0.05% trifluoroacetic acid).

leaves with eggs for washing themselves while the aerial part of TBM is spread on the floor on which their sacred objects are laid. In Yoruba folklore, TBM is believed to possess some mystical powers and is thus used in proverbs and adages while in other parts of tropical Africa, TBM has commonly been used to treat pain and inflammation [2, 4]. The complete phytochemical profile of TBM has not been reported not to mention bioactive metabolites from the aqueous part of the plant. Recently, Balogun et al. [2] isolated 2, 5-dithia-3, 6-diazabicycloheptane and carried out the GC-MS analysis of the silyl group ( $R_3Si$ ) derivatized extract. Following very limited number of published articles, the genus *Tragia* is known to accumulate alkaloids, phenolic compounds, sterols, and essential oils [4, 5, 31]. For instance, the genus is well known for its stinging defense capability due to the presence of the chemotaxonomically important shellsol and calcium oxalates which are released following skin contact with the foliar organs normally surrounded by these covering trichomes and this leads to itching, inflammation, and pain [4]. However, no class of bioactive cysteine rich peptides (CRPs) has been documented for any member the genus.

Plant CRPs are emerging therapeutics whose molecular weights are lower than small-molecule metabolites. They come with additional advantages of an optimized on-target specificity and decreased off-target toxicity [11]. An interesting property of plant CRPs that has attracted further scientific attention is their high stability and their phylogenetically conserved structural configuration, which have been described as potential scaffolds that are useful for grafting bioactive peptide epitopes to increase their metabolic stability and retain efficacy [10, 20].

The MALDI TOF MS analysis of peptide optimized aqueous fraction of TBM detected peptide masses whose reduction and alkylation experiment resulted in a mass



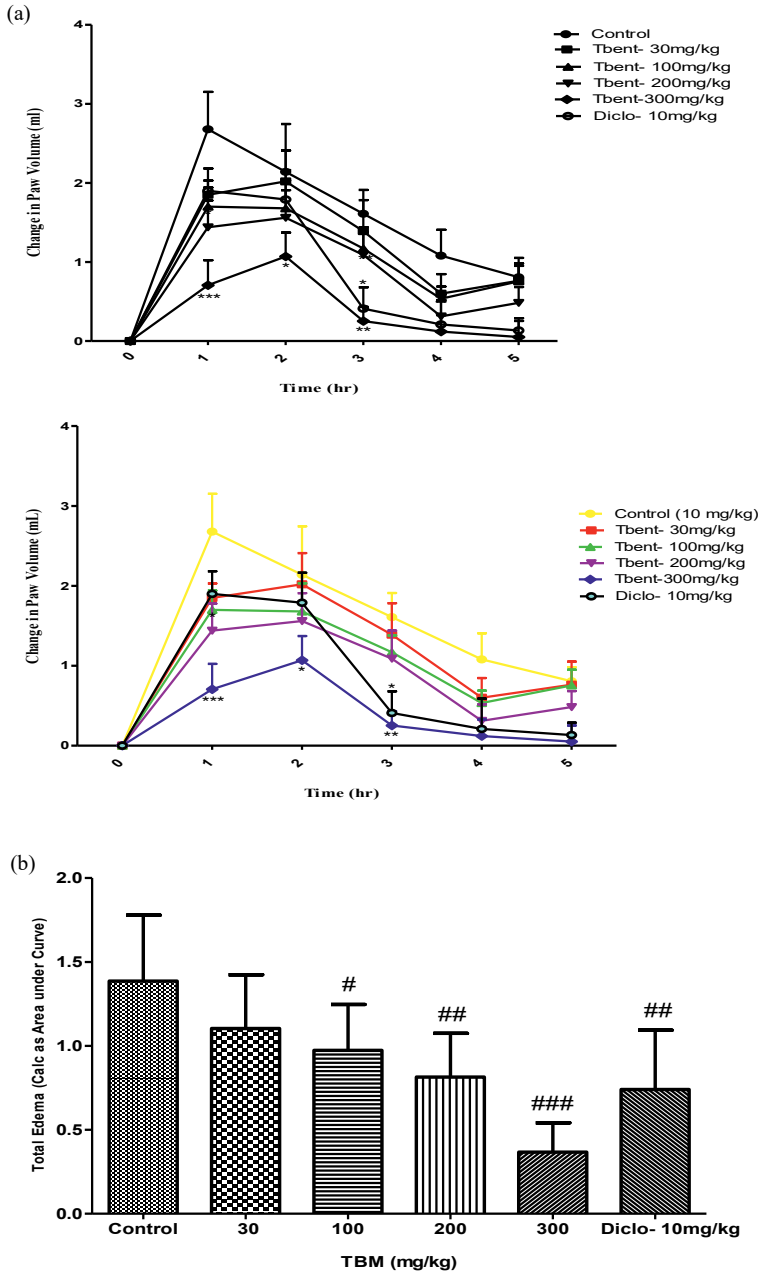


**Figure 9.6:** Effect of TBM (10–300 mg kg<sup>-1</sup>, *i.p.*), diclofenac (10 mg kg<sup>-1</sup>, *i.p.*) on time-course curves (a) and the total edema response (b) in the carrageenan-induced foot edema in chicks. Values are Mean ± S.E.M. (*n* = 6). \*\*\**P* < 0.001; \*\**P* < 0.01; \**P* < 0.05 compared to vehicle-treated group (two-way ANOVA followed by Bonferroni's *post hoc* test). ###*P* < 0.001; ##*P* < 0.01; #*P* < 0.05 compared to vehicle-treated group (one-way ANOVA followed by Newman–Keuls *post hoc* test).

**Table 9.1:** Change in the foot volume of chicks following the administration of graded doses of the cysteine-rich aqueous extracts of *Tragia benthamii*.

Treatment	1 h	2 h	3 h	4 h	5 h
Control (10 mg/kg)	2.680 ± 0.472	2.140 ± 0.606	1.610 ± 0.301	1.080 ± 0.327	0.807 ± 0.174
TBM (30 mg/kg)	1.850 ± 0.181	2.020 ± 0.391	1.390 ± 0.393	0.600 ± 0.247	0.763 ± 0.289
TBM (100 mg/kg)	1.700 ± 0.242	1.680 ± 0.352	1.170 ± 0.211	0.535 ± 0.155	0.755 ± 0.196
TBM (200 mg/kg)	1.440 ± 0.338*	1.560 ± 0.349	1.090 ± 0.350	0.312 ± 0.206	0.483 ± 0.200
TBM (300 mg/kg)	0.707 ± 0.316***	1.070 ± 0.303*	0.253 ± 0.180**	0.120 ± 0.207	0.052 ± 0.202
Diclofenac (10 mg/kg)	1.900 ± 0.283	1.790 ± 0.374	0.410 ± 0.271*	0.210 ± 0.380	0.133 ± 0.156

Values are Mean ± S.E.M. (n = 6). \*\*\*P < 0.001; \*\*P < 0.01; \*P < 0.05 compared to vehicle-treated group (two-way ANOVA followed by Bonferroni's *post hoc* test).

**Table 9.2:** Brine shrimp lethality of the peptide-rich aqueous extracts of *Tragia benthamii* Bak. (Euphorbiaceae).

Concentration of extract	Mortality/10		Total mortality/30	Percentage mortality (%)	Expected probit	Calculated probit
	Replicates <sup>a</sup>					
1000	4	3	4	11	36.67	4.68
500	4	2	1	7	23.33	4.55
100	3	3	4	10	33.33	4.23
10	0	2	1	3	10.00	3.79
1	0	0	1	1	3.33	3.34
Control	0	0	0	1	1.00	—

<sup>a</sup>An average of 10 nauplii were used for each experimental replicate. Chi squared degree of freedom = 3.4979, ED<sub>50</sub> = 6127.0890, G value = 0.3187, upper confidence limit = 1.337, 236.00%, lower confidence limit = 1073.

shift of 348 Da indicative of the presence of six cysteine residues involved in three disulphide bonds. The mass shift is a result of an addition of ~58 Da following reduction with dithiothreitol and iodoacetamide alkylation of six reduced sulfhydryl radicals [12]. Considering the detection of six cysteines involved in cystine bonds, the observed hydrophobic behavior of the peptide demonstrated by their late elution profiles and the resistance of the peptides to MALDI-TOF MS/MS fragmentation, these peptides appear to be members of the cystine knot peptides, commonly represented by knottins and hevein-like peptides which are the most reported six-cysteine CRPs having a knotted disulfide connectivity that bridges the cysteine residues I–IV, II–V, and III–VI [10, 12, 19]. However, the configuration and structure of these peptides are important for their biological function. This gives cysteine-rich short molecular weight peptides a stability advantage over other larger bioactive peptides of lower stability. The intercystine connectivity common to cysteine-rich peptides impacts additional stability to extreme conditions of heat, enzymatic and chemical attack. In this work, we applied a reversed phase system to obtain non-peptide fraction (80% ddH<sub>2</sub>O, 0.05% TFA in acetonitrile) and aqueous peptide fraction (20% ddH<sub>2</sub>O, 0.05%TFA in acetonitrile) using solid phase extraction. The MALDI TOF MS assisted characterization of the peptides showed that the mini proteins are cysteine-rich peptides. Cysteine-rich peptides identified in TBM are low molecular weight peptides rich in cysteine residues. The thiol bonds resulting from the disulphide linkages induce a folding pattern in the peptides which confers additional stability on these peptides to survive many hostile environments and several unfriendly solvent extraction steps and purification [32]. Digestion with endoproteinase Glu-C did not result in ring opening associated with +18 Da on MALDI TOF MS after reduction and alkylation. Instead, there was fragmentation of the peptide. This suggests that TBM peptides may belong to the cystine knot inhibitor (ICK) family. The ICK family of peptides is linear [33]. Gressent et al. [32], described similar class of peptides purified from *Pisum sativum*. *P. sativum* peptides were described to be bioactive, linear, containing six cysteine residues and showing high stability profiles after boiling and rigorous solvent extraction steps [32, 34].

Inflammation is a complex sequence of events initiated by the presence of foreign stimuli, infection or trauma [35, 36]. The local site of inflammation is characterized by redness, swelling, pain, warmth and often loss of functionality. Inflammation is followed by the movement of cells into the site triggered by the upregulation of adhesion molecules such as intercellular adhesion molecule 1 (ICAM-1) and E-selectin on the surface of endothelial cells, which allows leukocyte binding and subsequent migration [36]. There appear to be a big shift of interest from the less complex synthetic molecules to more complex phytochemicals mainly as a result of unavoidable side effects of synthetic drugs [37]. For instance, the commonly used drugs for the management of inflammatory diseases are the nonsteroidal anti inflammatory drugs (NSAIDs) [38]. These drugs come with undesirable side effects, especially after prolonged use such as gastric lesions, gastrointestinal damage, and kidney dysfunction [39]. Several other

diseases such as heart attacks, Alzheimer's diseases, and cancer whose underlying cause is tied to chronic inflammation have not found an efficient scientific solution. Natural compounds have been used in folklore to treat inflammatory problems. Bioactive peptides have shown great potentials as anti-inflammatory molecules of pharmaceutical relevance [40, 41]. The effect of TBM extract on carrageenan-induced foot edema in chicks has shown that the cysteine-rich peptide extracts from the ethnomedicinal plant *T. bentharii* exhibit anti-inflammatory activity in a chick model. This represents the first report on the anti-inflammatory activity of the peptide optimized aqueous fraction which has been shown in this study to be nontoxic following the brine shrimp lethality assay. The safety data appear to be in agreement with previous studies on two members (*T. plukenetii* and *T. involucrata*) of the genus which were reported to be free from acute, oral, and dermal toxicities [4, 42]. While documented data on the anti-inflammatory activity of members of the genus is still very scanty, the anti-inflammatory potentials of *T. involucrata*, a close member of the genus *Tragia* has been reported [1, 4, 43]. These findings may give some scientific credence to its use for the treatment of inflammation and pain in traditional medicine.

## 9.5 Conclusions

Indigenous knowledge on the medicinal application of plants will continue to be relevant in the study of crude drugs and the bioactive extracts or fractions derived from them. Findings from this work expand the current knowledge and library on the occurrence and distribution of cysteine-rich peptides in flowering plants and represents the first report on the identification of nature-derived CRPs with anti-inflammatory activity in a chick model from the genus *Tragia* and family Euphorbiaceae. Therefore, a further *in-depth vivo* and *in vitro* studies will be required to investigate its anti-inflammatory activity including effect on human umbilical vein endothelial cell-immortalized by telomerase reversed transcriptase (HUVEC-TERT), the possible inhibition of ICAM-1 surface expression and the mechanism of the anti-inflammatory effect.

**Acknowledgement:** Authors wish to thank Associate Professor Christian W. Gruber of the center for physiology and pharmacology, mass spectrometry facility, Medical University of Vienna, Austria for access to the mass spectrometry laboratory during the experiment.

**Author contributions:** All the authors have accepted responsibility for the entire content of this submitted manuscript and approved submission.

**Research funding:** Authors declare no funding was received for this work.

**Conflict of interest statement:** The authors declare no conflicts of interest regarding this article.

## References

1. Reddy BS, Rao NR, Vijeepallam K, Pandey V. Phytochemical, pharmacological and biological profiles of *Tragia* species (family: Euphorbiaceae). *Afr J Tradit, Complementary Altern Med* 2017;14: 105–12.
2. Balogun O, Oladosu I, Liu Z. Isolation of 2, 5-dithia-3, 6-diazabicyclo [2.2. 1] heptane and GC-MS analysis of silylated extract from *Tragia benthamii*. *IFE J Sci* 2020;22:075–80.
3. Gillespie LJ, Cardinal-McTeague WM, Wurdack KJ. *Monadelpha* (Euphorbiaceae, Plukenetieae), a new genus of Tragiinae from the Amazon rainforest of Venezuela and Brazil. *PhytoKeys* 2020;169:119.
4. Narasimhan S. Pharmacological potential of the stinging plant *Tragia* species: a review. *Phcog J* 2021;13:278–84.
5. Oladosu I, Balogun S, Ademowo G. Phytochemical screening, antimalarial and histopathological studies of *Allophylus africanus* and *Tragia benthamii*. *Chin J Nat Med* 2013;11:371–6.
6. Fred-Jaiyesimi AA, Ajibesin KK. Ethnobotanical survey of toxic plants and plant parts in Ogun State, Nigeria. *Int J Green Pharm* 2012;6:174–9.
7. Grivennikov SI, Greten FR, Karin M. Immunity, inflammation, and cancer. *Cell* 2010;140:883–99.
8. Khandia R, Munjal A. Interplay between inflammation and cancer. *Adv Protein Chem Struct Biol* 2020;119:199–245.
9. Esch T, Stefano GB, Ptacek R, Kream RM. Emerging roles of blood-borne intact and respiring mitochondria as bidirectional mediators of pro-and anti-inflammatory processes. *Med Sci Mon Int Med J Exp Clin Res* 2020;26:e924337-1.
10. Tam JP, Wang S, Wong KH, Tan WL. Antimicrobial peptides from plants. *Pharmaceuticals* 2015;8: 711–57.
11. Kumari G, Wong KH, Serra A, Shin J, Yoon HS, Sze SK, et al. Molecular diversity and function of jasmintides from *Jasminum sambac*. *BMC Plant Biol* 2018;18:1–13.
12. Koehbach J, Attah AF, Berger A, Hellinger R, Kutchan TM, Carpenter EJ, et al. Cyclotide discovery in Gentianales revisited—identification and characterization of cyclic cystine-knot peptides and their phylogenetic distribution in Rubiaceae plants. *Biopolymers* 2013;100:438–52.
13. Kini SG, Nguyen PQ, Weissbach S, Mallagaray A, Shin J, Yoon HS, et al. Studies on the chitin binding property of novel cysteine-rich peptides from *Alternanthera sessilis*. *Biochemistry* 2015; 54:6639–49.
14. Kini SG, Wong KH, Tan WL, Xiao T, Tam JP. Morintides: cargo-free chitin-binding peptides from *Moringa oleifera*. *BMC Plant Biol* 2017;17:1–13.
15. Kumari G, Serra A, Shin J, Nguyen PQ, Sze SK, Yoon HS, et al. Cysteine-rich peptide family with unusual disulfide connectivity from *Jasminum sambac*. *J Nat Prod* 2015;78:2791–9.
16. Bhardwaj G, Mulligan VK, Bahl CD, Gilmore JM, Harvey PJ, Cheneval O, et al. Accurate de novo design of hyperstable constrained peptides. *Nature* 2016;538:329–35.
17. Hellinger R, Gruber CW. Peptide-based protease inhibitors from plants. *Drug Discov Today* 2019; 24:1877–89.
18. Hellinger R, Koehbach J, Soltis DE, Carpenter EJ, Wong GK-S, Gruber CW. Peptidomics of circular cysteine-rich plant peptides: analysis of the diversity of cyclotides from *Viola tricolor* by transcriptome and proteome mining. *J Proteome Res* 2015;14:4851–62.
19. Retzl B, Hellinger R, Muratspahić E, Pinto ME, Bolzani VS, Gruber CW. Discovery of a beetroot protease inhibitor to identify and classify plant-derived cystine knot peptides. *J Nat Prod* 2020;83: 3305–14.
20. Srivastava S, Dashora K, Ameta KL, Singh NP, El-Enshasy HA, Pagano MC, et al. Cysteine-rich antimicrobial peptides from plants: the future of antimicrobial therapy. *Phytother Res* 2021;35: 256–77.

21. Pinto MEF, Chan LY, Koehbach J, Devi S, Gründemann C, Gruber CW, et al. Cyclotides from Brazilian *Palicourea sessilis* and their effects on human lymphocytes. *J Nat Prod* 2021;84:81–90.
22. Nguyen PQ, Wang S, Kumar A, Yap LJ, Luu TT, Lescar J, et al. Discovery and characterization of pseudocyclic cystine-knot  $\alpha$ -amylase inhibitors with high resistance to heat and proteolytic degradation. *FEBS J* 2014;281:4351–66.
23. Wong KH, Tan WL, Xiao T, Tam JP.  $\beta$ -ginkgotides: hyperdisulfide-constrained peptides from *Ginkgo biloba*. *Sci Rep* 2017;7:1–13.
24. Tammineni R, Gulati P, Kumar S, Mohanty A. An overview of acyclotides: past, present and future. *Phytochemistry* 2020;170:112215.
25. Ainooson G, Owusu G, Woode E, Ansah C, Annan K. *Trichilia monadelpha* bark extracts inhibit carrageenan-induced foot-oedema in the seven-day old chick and the oedema associated with adjuvant-induced arthritis in rats. *Afr J Tradit, Complementary Altern Med* 2012;9:8–16.
26. Chuku L, Chinaka N, Damilola D. Phytochemical screening and anti-inflammatory properties of Henna leaves (*Lawsonia inermis*). *Eur J Med Plants* 2020;31:23–8.
27. Mensah JK, Ibrahim A, Jibira Y. Co-extract mixture from *Strophanthus hispidus* (roots) and *Aframomum meleguta* (seeds) show phytochemical synergy in its anti-inflammatory activity. *J Pharm Pharm Sci* 2019;3:89–100.
28. Adriany A, Jéssica S, Ana O, Raimunda S, Andreanne V, Luan S, et al. Anti-inflammatory and antioxidant activity improvement of lycopene from guava on nanoemulsifying system. *J Dispersion Sci Technol* 2020;42:1–11.
29. Banti CN, Hadjikakou SK. Evaluation of toxicity with brine shrimp assay. *Bio-protocol* 2021;11:e3895-e.
30. Ogbale OO, Ndabai NC, Akinleye TE, Attah AF. Evaluation of peptide-rich root extracts of *Calliandria portoricensis* (Jacq.) Benth (Mimosaceae) for *in vitro* antimicrobial activity and brine shrimp lethality. *BMC Compl Med Ther* 2020;20:30.
31. Gobalakrishnan R, Kulandaivelu M, Bhuvaneshwari R, Kandavel D, Kannan L. Screening of wild plant species for antibacterial activity and phytochemical analysis of *Tragia involucrata* L. *J Pharmaceut Anal* 2013;3:460–5.
32. Gressent F, Da Silva P, Eyraud V, Karaki L, Royer C. Pea albumin 1 subunit b (PA1b), a promising bioinsecticide of plant origin. *Toxins* 2011;3:1502–17.
33. Reinwarth M, Nasu D, Kolmar H, Avrutina O. Chemical synthesis, backbone cyclization and oxidative folding of cystine-knot peptides—promising scaffolds for applications in drug design. *Molecules* 2012;17:12533–52.
34. Eyraud V, Karaki L, Rahioui I, Sivignon C, Da Silva P, Rahbé Y, et al. Expression and biological activity of the cystine knot bioinsecticide PA1b (Pea Albumin 1 Subunit b). *PLoS One* 2013;8:e81619.
35. Antonelli M, Kushner I. It's time to redefine inflammation. *FASEB J* 2017;31:1787–91.
36. Fereydouni Z, Fard EA, Mansouri K, Motlagh H-RM, Mostafaie A. Saponins from *Tribulus terrestris* L. extract down-regulate the expression of ICAM-1, VCAM-1 and E-selectin in human endothelial cell lines. *Int J Mol Cell Med* 2020;9:73.
37. Deepa M, Devi PR, Karur GD. In vivo evaluation of acute and chronic anti-inflammatory activity of ethanol leaf extract of *Vitex negundo* Linn. *JRJOB* 2014;9:64–9.
38. Machado GC, Abdel-Shaheed C, Underwood M, Day RO. Non-steroidal anti-inflammatory drugs (NSAIDs) for musculoskeletal pain. *BMJ* 2021;372:n104.
39. García-Rayado G, Navarro M, Lanás A. NSAID induced gastrointestinal damage and designing GI-sparing NSAIDs. *Expert Rev Clin Pharmacol* 2018;11:1031–43.
40. Guha S, Majumder K. Structural-features of food-derived bioactive peptides with anti-inflammatory activity: a brief review. *J Food Biochem* 2019;43:e12531.
41. Wang N. A promising plant defense peptide against citrus Huanglongbing disease. *Proc Natl Acad Sci* 2021;118:e2026483118.

42. Bonam SR, Manoharan SK, Pandey V, Raya AR, Nadendla RR, Jagadeesan M, et al. Phytochemical, *in vitro* antioxidant and *in vivo* safety evaluation of leaf extracts of *Tragia plukenetii*. *Phcog J* 2019;11: 338–45.
43. Pallie MS, Perera PK, Kumarasinghe N, Arawwawala M, Goonasekara CL. Ethnopharmacological use and biological activities of *Tragia involucreta* L. *Evid Base Compl Alternative Med* 2020;2020: 8848676.





Maria, Zahid Khan and Aleksey E. Kuznetsov\*

# 10 Combinatorial library design and virtual screening of cryptolepine derivatives against topoisomerase IIA by molecular docking and DFT studies

**Abstract:** Various computational approaches have received ever-growing role in the design of potential inhibitors of the topoisomerase 2 (TOP2A) for cancer treatment. TOP2A plays a key role in the deoxyribonucleic acid (DNA) replication before cell division and thus facilitates the growth of cells. This TOP2A function can be suppressed by targeting it with potential inhibitors in cancer cells to terminate the uncontrolled cell division. Among potential inhibitors, cryptolepine has higher selectivity along with the ability to intercalate into DNA, effectively blocking TOP2A and ceasing cell division in cancer cells. However, this compound has drawbacks of being nonspecific and possessing relatively low affinity. Therefore, a combinatorial library of 31,114 cryptolepine derivatives was designed and virtually screened by molecular docking to predict the molecular interactions between the cryptolepine derivatives and TOP2A using cryptolepine as a standard. All the binding poses of cryptolepine derivatives for TOP2A were investigated to calculate binding energy. The compounds with the database numbers 8618, 907, 147, 16755, and 8186 scored the highest binding energies,  $-9.88$ ,  $-9.76$ ,  $-9.75$ ,  $-9.73$ , and  $-9.72$  kcal/mol, respectively, and the highest binding affinities while the cryptolepine binding energy is  $-6.09$  kcal/mol. The strong binding interactions of these derivatives show that they can be used as potent TOP2A inhibitors and act as more effective anticancer agents than cryptolepine itself. The interactions of these derivatives with different amino acid residues were also observed and analyzed. A comprehensive understanding of the interactions of the proposed derivatives with TOP2A helped for searching more novel and potent drug-like molecules for anticancer therapy. This computational study suggests useful references to understand inhibition mechanisms that will help in the further modifications of TOP2A inhibitors. Moreover, the DFT study of the derivatives with the highest binding energies was performed, helping to further understand the binding affinities of these compounds.

---

\*Corresponding author: **Aleksey E. Kuznetsov**, Departamento de Química, Universidad Técnica Federico Santa María, Av. Santa María 6400, Vitacura, 7660251, Santiago, Chile  
E-mail: [aleksey.kuznetsov@usm.cl](mailto:aleksey.kuznetsov@usm.cl) <https://orcid.org/0000-0001-8857-3118>

**Maria and Zahid Khan**, Biochemistry Section, Institute of Chemical Sciences, University of Peshawar, Peshawar, Pakistan

This article has previously been published in the journal *Physical Sciences Reviews*. Please cite as: Maria, Z. Khan and A. E. Kuznetsov "Combinatorial library design and virtual screening of cryptolepine derivatives against topoisomerase IIA by molecular docking and DFT studies" *Physical Sciences Reviews* [Online] 2021, 7. DOI: 10.1515/psr-2020-0124 | <https://doi.org/10.1515/9783110710823-010>

**Keywords:** anticancer drugs; cryptolepine derivatives; DFT; molecular docking; topoisomerase 2; virtual screening.

## 10.1 Introduction

Cancer is considered as a second deadliest disease which causes ca. one in every seven deaths worldwide (more than acquired immune deficiency syndrome, AIDS) [1]. In the next two decades, the occurrences of cancer have been estimated to grow from 14 to 22 million, according to the report by Torre et al [2]. The total medical expenditure for cancer treatment in the US in 2013 was evaluated to be \$74.8 billion [3].

Cancerous cells are known to undergo processes of mitosis, transcription, and replication of deoxyribonucleic acid (DNA) with accelerated rate. The enzyme inhibition by various drugs is considered as one of the potent approaches to cease or slow down the uncontrolled cell growth [4]. Some specific drugs can induce conformational changes in the cancerous cell enzymes [5]. Topoisomerase II alpha enzyme (TOP2A) is known to maintain the integrity of genome by helping in DNA replication, transcription, and chromosome segregation where it participates in unwinding the double strands of DNA to further facilitate the life-maintaining process of cell growth [6]. Thus, this enzyme is considered as an effective target for cancer treatment: it can induce DNA damages in cancerous cells by complex formation with highly effective anticancer drugs, which block DNA transcription and replication by formation of numerous DNA strands breaks and thus terminate the uncontrolled division of abnormal cells subsequently undergoing apoptosis [7].

Cryptolepine is an active alkaloid and has many useful properties due to its ability to intercalate into the DNA strands, inhibit the TOP2A and further terminate the DNA synthesis [8]. This compound is a very commonly used inhibitor for studies of the apoptotic processes and its structure can be easily modified which makes it an ideal template for pro apoptotic activity [9]. Furthermore, the cryptolepine has been proven to have excellent TOP2A inhibition activity, however, due to its low specificity it cannot be successfully employed as an anticancer drug. Fortunately, this compound has a huge potential to be converted into an effective anticancer drug by derivatizing it via addition of various functional groups at various positions, which results in derivatives with modified activities [10]. Due to the fact that synthesis and screening of these numerous derivatives is a very expensive, laborious, and time-consuming procedure, the computer-assisted drug designing tools have been recently proven to be successful in preliminary screening of huge libraries of potential candidate molecules.

In the current research work, a very big combinatorial library of cryptolepine derivatives was prepared and then virtually screened versus activity towards TOP2A for predicting the derivatives with greater binding affinities, which thus can serve as better candidates for anticancer drugs. Moreover, the density function theory (DFT) study was also performed to study structures and various properties of the predicted derivatives

with the highest binding affinities. Thus, we have clearly demonstrated that from the library of millions of compounds, a set of few potentially active molecules can be predicted (with relatively low expenses) which can later be verified by *in vivo* and *in vitro* activity assays [11].

## 10.2 Computational methods

The major steps involved are as follows.

### 10.2.1 Retrieval and refinement of crystal structure

The crystal structure of the receptor TOP2A was downloaded from the protein data bank (PDB) with the accession code of 5GWK. The crystal structure was refined, and its missing part was modeled through the Modeller software. The receptor molecule was then energy-minimized using CHARMM-27 force field as implemented in the MOE software [12].

### 10.2.2 Combinatorial library designing

Combinatorial library design is a new leading field that can be used to discover a group of best substituents with enhanced potencies [13]. The combinatorial library of 31,114 molecules was designed using cryptolepine as a template (Figure 10.1) employing the Chem-T software [14].

For modification, four positions were selected in the template ligand structure as shown by the R-groups (Figure 10.1). The 2D structure of template ligand cryptolepine and the list of desired functional groups to be placed at four R-positions were drawn using the Chems sketch software and then saved in mol and smile format, respectively. The template structure and the functional groups were further uploaded in the Chem-T program, which was followed by the generation of 3D ligand library of 31,114 molecules in the mol2/sdf format. The molecules were energy-minimized using the MFF94X force field and finally visually inspected for defects through MOE [15].

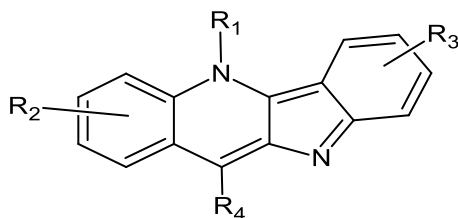


**Figure 10.1:** Structure of cryptolepine with substituents R<sub>1</sub>, R<sub>2</sub> (–CH<sub>3</sub>, –CH<sub>2</sub>CH<sub>3</sub>, –C<sub>3</sub>H<sub>5</sub>, –C<sub>6</sub>H<sub>5</sub>, –C<sub>6</sub>H<sub>4</sub>CH<sub>3</sub>, –C<sub>6</sub>H<sub>4</sub>OH, –C<sub>6</sub>H<sub>4</sub>Br), R<sub>3</sub> (–CH<sub>3</sub>, –OCH<sub>3</sub>, –Cl, –F, –I), and R<sub>4</sub> (–CH<sub>3</sub>, –C<sub>3</sub>H<sub>5</sub>, –C<sub>6</sub>H<sub>4</sub>CH<sub>3</sub>) indicating positions for the addition of various small substituents.

### 10.2.3 Docking and virtual screening

Molecular docking is used in drug discovery process to predict the lead compounds by evaluating the protein–ligand interactions details. The molecular docking process consists of two steps. (i) The protein–ligand binding affinity is estimated using force fields. (ii) The conformational space is investigated for different protein–ligand binding poses [16]. In the docking the library is screened for the prediction of lead compounds. Molecular docking scheme is shown in Figure 10.2.

Virtual screening can be used to evaluate the library containing the large number of compounds for the prediction of optimized candidate compounds using different computer-based tools. It works on the basis of protein–ligand binding interactions and scoring functions. Figure 10.3 shows the schematic binding of a ligand with a receptor. Also, the binding pocket of TOP2A for cryptolepine is presented in Figure 10.4.

### 10.2.4 Docking protocol applied by MOE

Different computer-based tools are used for molecular docking. Among them, MOE is used for the *in-silico docking* and virtual screening. This software is the most

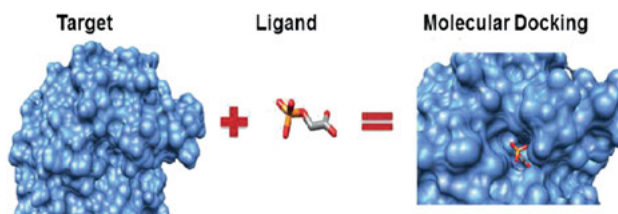


Figure 10.2: The scheme showing the concept of molecular docking.

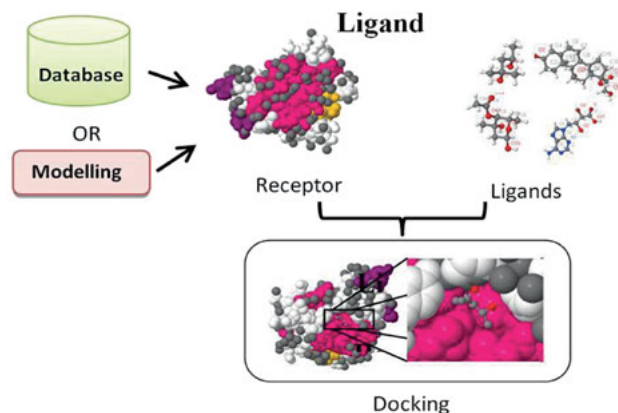
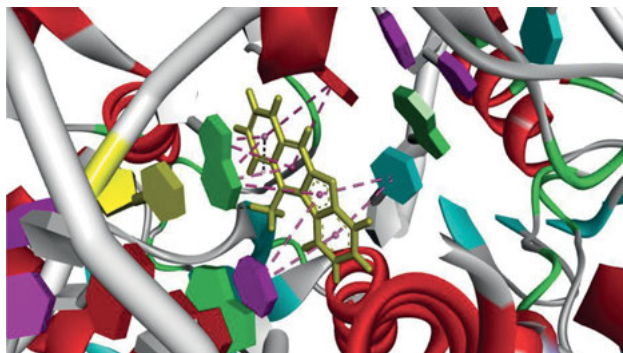


Figure 10.3: Illustration of docking of many ligands with a receptor.



**Figure 10.4:** Structure of cryptolepine within the binding pocket of TOP2A.

appropriate and reliable using accurate force field and other docking parameters for virtual screening.

The molecules were prepared for docking by the removal of water molecules and addition of hydrogen atoms from the 3D reported crystal structure of TOP2A (5GWK). The receptor macromolecule and library of around 31,114 ligand molecules were set for docking. For reproducibility and calibration of the docking software other reported inhibitors of TOP2A were also prepared in the same way and docked as well. The receptor macromolecule and the ligand molecules were then loaded in the MOE software for docking studies.

Ligand conformations were generated with the bond rotation method. These conformations were then placed in the site with the Triangular Matcher method and ranked with London dG scoring function. The retain option specifies the number of poses to pass to refinement, for energy minimization in the pocket, before rescored with GBVI/WSA dG scoring function [14].

### 10.2.5 Docking analysis

Docking simulation analysis was carried out using the Discovery Studio Visualizer software [15]. Interaction analysis, i.e., analysis of dipole–dipole interactions, electrostatic interactions, intermolecular forces, dihedral angles, hydrogen bonding, and hydrophobicity, was carried out by the Visual Molecular Dynamics (VMD) and Discovery Studio Visualizer. Among the library of the derivatives, the best-docked compounds having a greater binding affinity for enzyme were considered as lead compounds.

### 10.2.6 DFT studies

Computational studies were performed employing the Gaussian 09 [17] and Gaussian 16 [18] software packages, using as starting geometries the structures of the ligands with the

highest binding energies obtained in the combinatorial library design (see Table 10.1 below), along with the structure of cryptolepine. We optimized the ligand geometries without any symmetry restrictions and ran frequencies calculations to check if the optimized structures are the true energy minima. Because organic compounds generally exist in their singlet electronic states, we used the singlet multiplicity in our calculations. We performed all the calculations using the hybrid density functional B3LYP [19] along with the split-valence polarized basis set 6-31G\* [20–22] for C, N, Br, O, and H, and the Los Alamos effective core pseudopotential with associated double-zeta basis set for I [23–25]. These approaches are furthermore referred to as B3LYP/6-31G\* or B3LYP/Gen (for the combination of the basis sets 6-31G\* and LanL2dz). We studied the ligands with implicit solvent effects from water (dielectric constant  $\epsilon = 78.3553$ ) taken into account using the self-reliable approach IEF-PCM [26] which employs the UFF default model implemented in the Gaussian software (with electrostatic scaling factor  $\alpha = 1.0$ ). Frontier molecular orbitals (FMOs) were calculated at the B3LYP/6-31G\* or B3LYP/Gen level with the implicit water effects. Below we consider NBO charges and FMOs for all the ligands studied by DFT. Moreover, we used the values of the energies of the HOMO and LUMO, i.e., highest occupied molecular orbital and lowest unoccupied molecular orbital, respectively, and the values of the HOMO/LUMO gaps to calculate the global reactivity parameters (GRP) [27–29] (see Equations (10.1)–(10.6) below). Equations (10.1) and (10.2) were used to calculate the values of the ionization potential ( $IP$ ) and electron affinity ( $EA$ ):

$$IP = -E_{\text{HOMO}} \quad (10.1)$$

$$EA = -E_{\text{LUMO}} \quad (10.2)$$

For global hardness  $\eta$  and electronegativity  $X$  values we used Equations (10.3) and (10.4):

$$\eta = \frac{[IP - EA]}{2} = -\frac{[E_{\text{LUMO}} - E_{\text{HOMO}}]}{2} \quad (10.3)$$

$$X = \frac{[IP + EA]}{2} = -\frac{[E_{\text{LUMO}} + E_{\text{HOMO}}]}{2} \quad (10.4)$$

And global electrophilicity  $\omega$  value was calculated by Equation (10.5):

$$\omega = \frac{\mu^2}{2\eta}, \quad (10.5)$$

where  $\mu = \frac{E_{\text{HOMO}} + E_{\text{LUMO}}}{2}$  is the chemical potential of the compound studied.

Finally, the global softness  $\sigma$  value was computed with Equation (10.6):

$$\sigma = \frac{1}{2\eta} \quad (10.6)$$

The molecular electrostatic potential (MEP) was also calculated using the B3LYP/6-31G\* or B3LYP/Gen approaches with the implicit water effects. Open GL version of

Table 10.1: MOE docking score of top five derivatives for TOP2A.

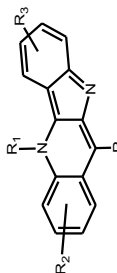
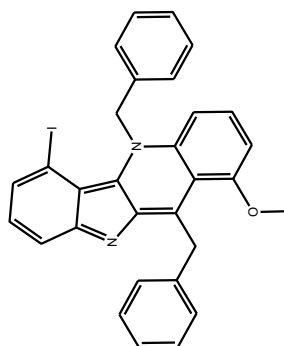
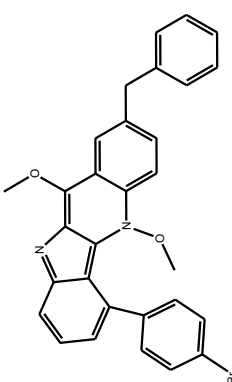
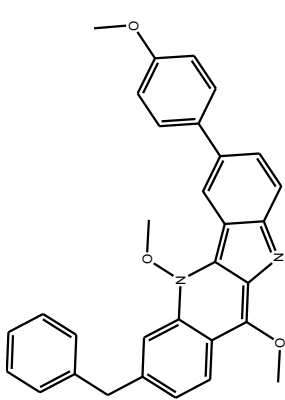
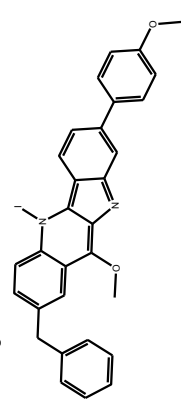
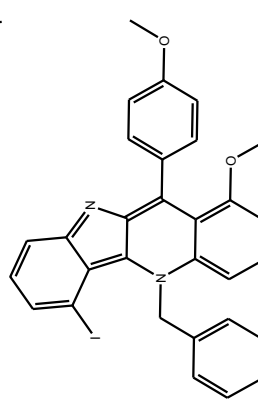
Ligand library #	Binding affinity (kcal/mol)	Structure of a ligand	R <sub>1</sub>	R <sub>2</sub>	R <sub>3</sub>	R <sub>4</sub>
5551	-6.09		-	-	-	-
8618	-9.88		Ph-CH <sub>2</sub> -	CH <sub>3</sub> O-	I-	Ph-CH <sub>2</sub> -
907	-9.76		CH <sub>3</sub> O-	Ph-CH <sub>2</sub> -	BrPh-	CH <sub>3</sub> O-



Table 10.1: (continued)

Ligand library #	Binding affinity (kcal/mol)	Structure of a ligand	R <sub>1</sub>	R <sub>2</sub>	R <sub>3</sub>	R <sub>4</sub>
147	-9.75		CH <sub>3</sub> O-	Ph-CH <sub>2</sub> -	4-CH <sub>3</sub> OPh-	CH <sub>3</sub> O-
16755	-9.73		I-	Ph-CH <sub>2</sub> -	4-CH <sub>3</sub> OPh-	4-CH <sub>3</sub> OPh-
8186	-9.72		Ph-CH <sub>2</sub> -	CH <sub>3</sub> O-	I-	4-CH <sub>3</sub> OPh-

Molden 5.8.2 visualization program was used for the visualization of the structures and FMOs of the title compounds [30], and the Avogadro software was used for the MEP map visualization [31, 32].

## 10.3 Results and discussion

### 10.3.1 Combinatorial library design and docking analysis

TOP2A (5GWK) is an effective enzyme for anticancer drug targeting. Using the MOE docking software, 31,114 cryptolepine derivatives were virtually screened to identify novel potent inhibitors of TOP2A. Among these candidates only five compounds were selected. The best binding affinity and specificity of these potent top five derivatives were predicted and calculated using the MOE software.

#### 10.3.1.1 Etoposide as cocrystallized inhibitor of TOP2A

In docking studies the cocrystallized ligand etoposide in the template structure of TOP2A (5GWK) was used to show the residues involved in the active site of TOP2A as there is no cocrystallized structure of cryptolepine with TOP2A. The amino acid residues present in the binding pocket of TOP2A include Met 1083, Gly 805, Gly 779, Arg 804, Asp 780, and Met 1079, while nucleotides involved are dA 1516, dG 1517, dG 1534, dC 1532, and dT 1533 (Figure 10.5).

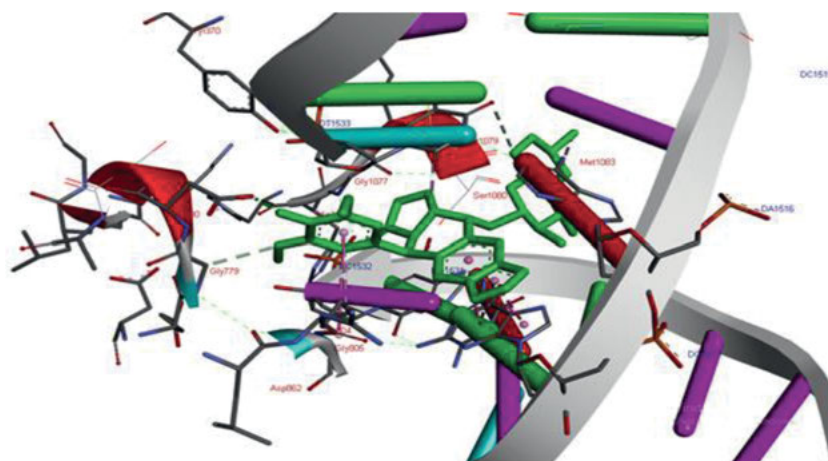


**Figure 10.5:** 3D structure showing etoposide and its interacting residues in the binding pocket of TOP2A shown by the Discovery Studio Visualizer.

The above structure (Figure 10.6) of the etoposide shows the residues interacting with the receptor and forming nonhydrophobic interactions with the protein such as hydrogen bonds, van der Waals interactions, carbon–hydrogen bonds,  $\pi$ – $\pi$  stacking interactions, amide– $\pi$  stacking interactions, alkyl and  $\pi$ –alkyl interactions.

### 10.3.1.2 Cryptolepine as parent inhibitor for TOP2A

Cryptolepine was used as a parent compound to target the unwinding property of TOP2A during replication and transcription of DNA (see Figures 10.7 and 10.8). The amino acid residues in the binding pocket of the cocrystallized TOP2A include Met 1079, Gly 805, Arg

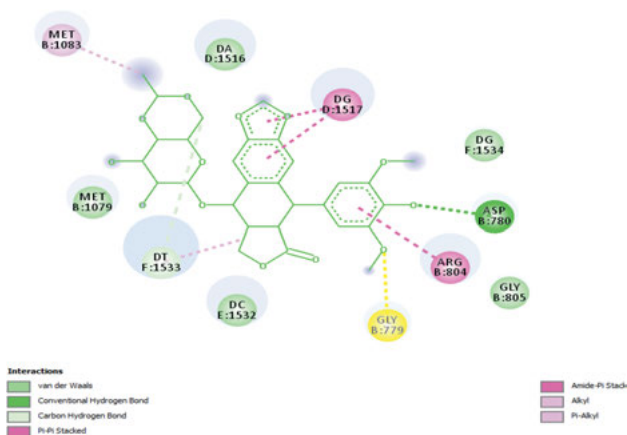


**Figure 10.6:** 2D structure of etoposide representing the residues with the interacting receptor.

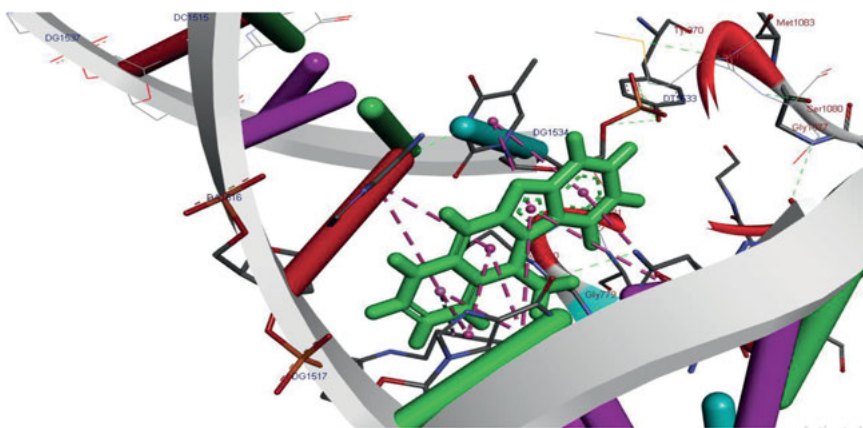


**Figure 10.7:** 3D structure showing the interaction of residues with cryptolepine in the active site of TOP2A.

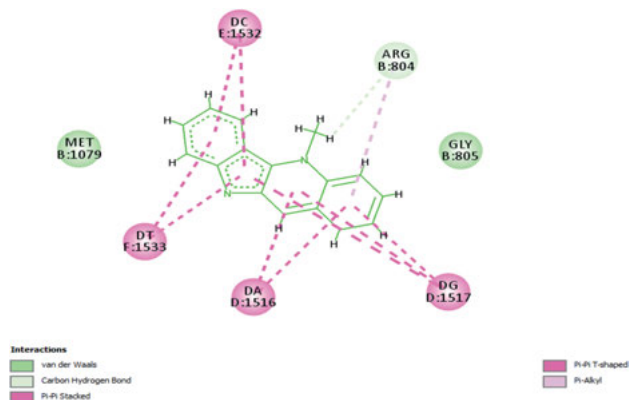


**Figure 10.8:** 2D structure of cryptolepine showing the residues interacting with TOP2A.

804, and the double stranded DNA purine–pyrimidine such as dC 1532, dT 1533, dA 1516, and dG 1517. Different functional groups attached to cryptolepine in positions  $R_1$ ,  $R_2$  are  $-\text{CH}_3$ ,  $-\text{CH}_2\text{CH}_3$ ,  $-\text{C}_3\text{H}_5$ ,  $-\text{C}_6\text{H}_5$ ,  $-\text{C}_6\text{H}_4\text{CH}_3$ ,  $-\text{C}_6\text{H}_4\text{OH}$ ,  $-\text{C}_6\text{H}_4\text{Br}$ , in position  $R_3$  are  $-\text{CH}_3$ ,  $-\text{OCH}_3$ ,  $-\text{Cl}$ ,  $-\text{F}$ ,  $-\text{I}$  and in position  $R_4$  are  $-\text{CH}_3$ ,  $-\text{C}_3\text{H}_5$ , and  $-\text{C}_6\text{H}_4\text{CH}_3$ . The positions  $R_1$ ,  $R_2$ ,  $R_3$ , and  $R_4$  are distributed over the rings as shown in Figure 10.1.

Cryptolepine interacts with the receptor TOP2A by residues such as Met 1079, Arg 804, Gly 805 and nucleotides dT 1533, dC 1532, dA 1516, and dG 1517. The residues Arg 804, Gly 805, and Met 1079 form carbon–hydrogen bonds and van der Waals interactions with the ligand, while the nucleotides dT 1533, dC 1532, dA 1516, and dG 1517 form  $\pi$ – $\pi$  stacking,  $\pi$ – $\pi$  T-shaped and  $\pi$ –alkyl interactions. All these interactions result in a total binding energy of cryptolepine with receptor of  $-6.09$  kcal/mol.

### 10.3.1.3 Virtual screening of the cryptolepine library

Virtual screening of the combinatorial library of 31,114 molecules was performed to identify potent inhibitors of TOP2A. Based on the scoring function and strong interactions with the receptor molecules five best ligands were selected. These top five molecules and their respective binding energies in kcal/mol are represented by ligand numbers 8618, 907, 145, 16755, and 8186 as shown in Table 10.1. All the top five compounds along with the standard are superimposed in the binding pocket of TOP2A as shown in Figure 10.9.

## 10.3.2 Detailed interaction analysis of the docked ligands in the binding pocket of receptor TOP2A

Top five docked derivatives of cryptolepine were selected based on their scoring function to evaluate the binding interactions and energies for the receptor TOP2A. The

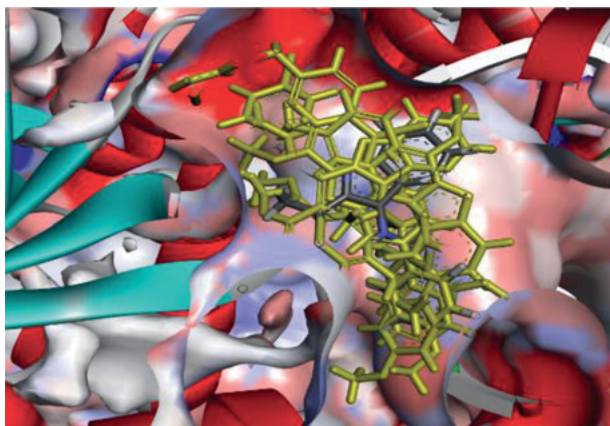


**Figure 10.9:** Docked poses of the top five selected derivatives and the standard cryptolepine all superimposed. The standard is depicted by cpk color and the five derivatives are shown as yellow-colored sticks.

details of various interactions and energy values of all the selected derivatives are provided below.

### 10.3.2.1 Derivative no. 8618

Ligand no. 8618 interacts with TOP2A by the amino acid residues Met 1079, Gly 1077, Ser 781, Tyr 370, Gly 779, Leu 803, Gly 805, Asp 780, and Arg 804 while the nucleotides involved are dG 1517, dT 1533, dC 1532 dG 1534, and dA 1516 (Figure 10.10). Ph-CH<sub>2</sub> (benzyl group) attached at position R<sub>1</sub> has  $\pi$ - $\pi$  stacking interactions with dG 1517, OCH<sub>3</sub> group in position R<sub>2</sub> forms carbon-hydrogen bond with Asp 780, van der Waals interactions with Gly 805 and  $\pi$ -alkyl interactions with Arg 804.

Iodide (I) attached at position R<sub>3</sub> has  $\pi$ -alkyl and  $\pi$ -anion interactions with dT 1533. Benzyl group attached at position R<sub>4</sub> has van der Waals interactions with amino acid residues such as Ser 781, Tyr 370, Gly 779, Leu 803, and with the nucleotide dG 1534. Due to these extra interactions formed by the ligand no. 8618 with TOP2A the binding energy is increased from -6.09 to -9.88 kcal/mol which makes the complex more stable than the complex of the cryptolepine with the TOP2A receptor (see Figure 10.11).

### 10.3.2.2 Derivative no. 907

Ligand #907 interacts with TOP2A by residues such as Ser 781, Arg 804, Asp 780, Try 370, Gly 805, Gly 779, Leu 803, Glu 778, and Asp 858 while nucleotides involved include dA 1516, dG 1534, dG 1517, dT 1533, and dC 1532 (Figure 10.12). OCH<sub>3</sub> (methoxy) group at

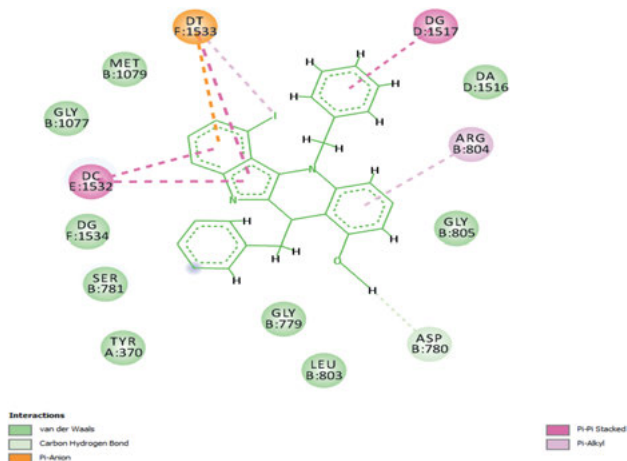


**Figure 10.10:** 2D structure of the ligand 8618 binding pocket. Green dotted line shows hydrogen bond while other lines show hydrophobic interactions.

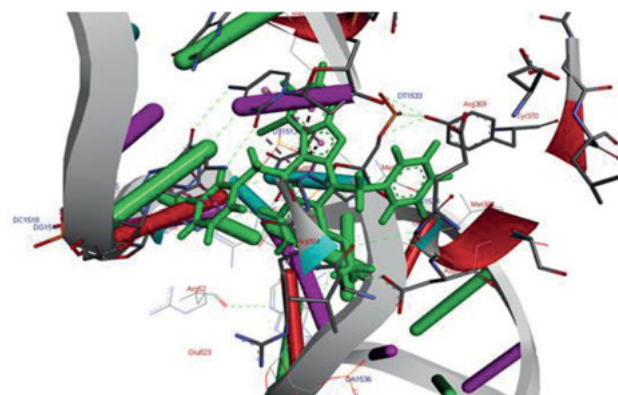


**Figure 10.11:** Residues interacting within the binding pocket of the ligand no. 8618 showing contacts with TOP2A.

position  $R_1$  forms van der Waals interactions with Gly 779 and  $\pi$ -donor hydrogen bond with the nucleotide dC 1532.  $\text{OCH}_3$  group attached at position  $R_4$  forms carbon-hydrogen bond with Asp 780. 4-Br-Ph (bromophenol) group attached at position  $R_3$  forms van der Waals interactions with amino acid Glu 778 and carbon-hydrogen bond with nucleotide dC 1532. Benzyl group in position  $R_2$  forms  $\pi$ - $\pi$  stacking,  $\pi$ - $\pi$  T-shaped, and amide- $\pi$ -stacking interactions with nucleotides dT 1533, dG 1517, and van der Waals interactions with dA 1516.

Ligand #907 can be considered as better inhibitor than cryptolepine because the number of non-bonded interactions of this ligand is greater than that of cryptolepine

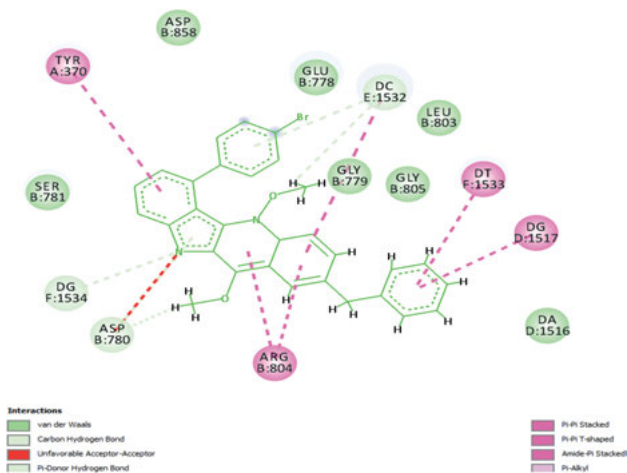


**Figure 10.12:** 2D structure of the ligand no. 907 showing dotted lines for hydrophobic contacts.

taken as a parent compound (Figure 10.13). That is why this ligand has better binding affinity for the receptor than cryptolepine itself. All the hydrophobic interactions are responsible for higher binding energy. The binding energy for this ligand is increased to  $-9.76$  kcal/mol compared to  $-6.09$  kcal/mol for the cryptolepine.

### 10.3.2.3 Derivative no. 147

Ligand no. 147 interacts with the TOP2A by amino acid residues such as Gly 1077, Met 1079, Ser 1080, Met 1083, Glu 823, Gly 805, Gly 779, Asp 780, Ser 781, Arg 804, Tyr 370,

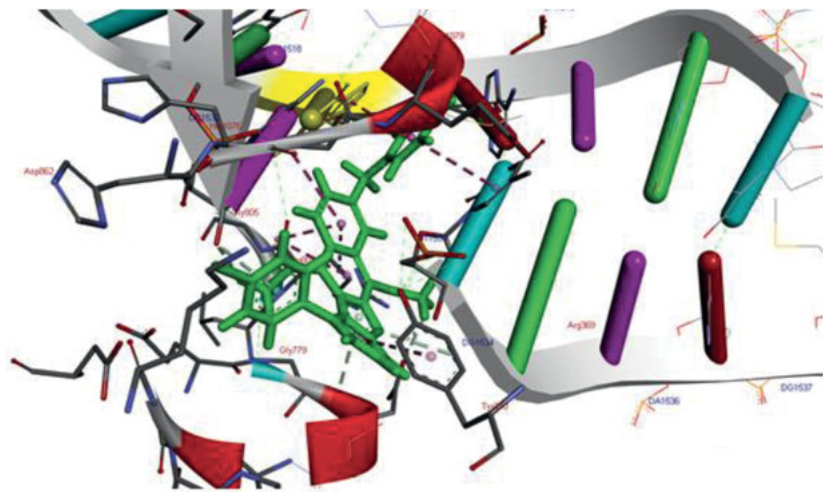


**Figure 10.13:** 3D structure showing interacting residues within the binding pocket of the ligand no. 907.



and with the double-stranded DNA such as dC 1532, dT 1533, dA 1516, dG 1531, dG 1534, and dG 1517 (Figure 10.14). OCH<sub>3</sub> group attached at position R<sub>1</sub> forms van der Waals interactions with Gly 779. Benzyl group attached at position R<sub>2</sub> forms van der Waals interactions with amino acid residues Asp 780, Ser 781, Tyr 370 and with the nucleotide dG 1534. 4-CH<sub>3</sub>OPh in position R<sub>3</sub> forms  $\pi$ -alkyl interactions with amino acid Arg 804 and  $\pi$ - $\pi$  stacking interactions with the nucleotide dG 1517. OCH<sub>3</sub> in position R<sub>4</sub> forms  $\pi$ -donor hydrogen bond with dC 1532 and van der Waals interactions with nucleotide dG 1531 and with the amino acid residues Ser 1080 and Met 1079 (Figure 10.15). These extra interactions formed by the ligand no. 147 result in stronger and more stable interactions with the receptor compared to the cryptolepine. The binding energy for the ligand no. 147 is increased to -9.75 kcal/mol due to the attachment of functional groups.

#### 10.3.2.4 Derivative no. 16755

Ligand no. 16755 interacts with the residues such as Met 1079, Gly 1077, His 1076, Lys 931, Gly 932, Ser 781, Leu 933, Ala 782, Gly 779, Asp 858, Gly 805, Arg 804, Gly 934, Glu 778, and Tyr 370 while nucleotides included are dC 1532, dT 1533, dG 1517, and dA 1516 (Figure 10.16). Benzyl group attached at position R<sub>2</sub> forms carbon-hydrogen bond with Gly 934 and van der Waals interactions with amino acid residues Ser 781, Gly 932, Tyr 370, and Gly 931. CH<sub>3</sub>OPh attached at position R<sub>3</sub> forms  $\pi$ -donor hydrogen bond and  $\pi$ - $\pi$  stacking interactions with dG 1517 and van der Waals interactions with dA 1516.

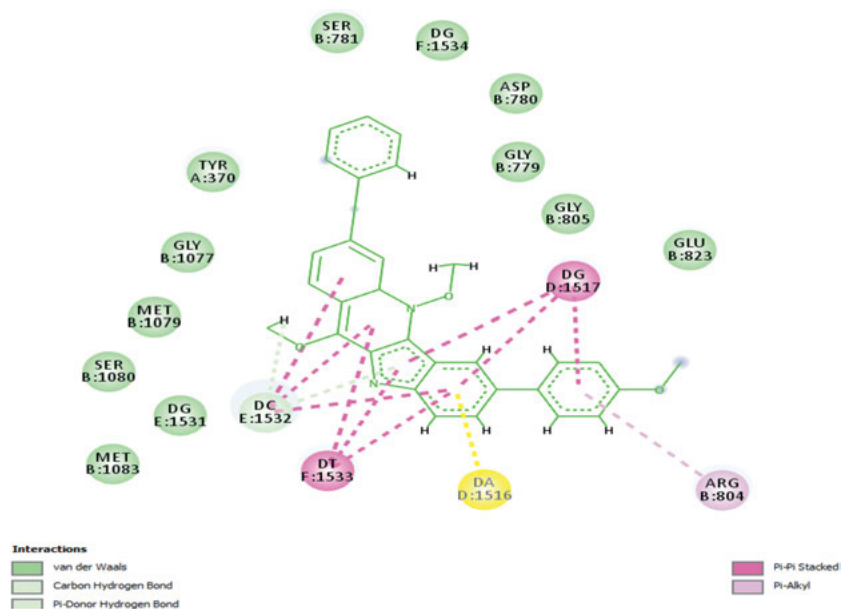


**Figure 10.14:** 2D structure of the ligand no. 147 showing the interactions by dotted lines.



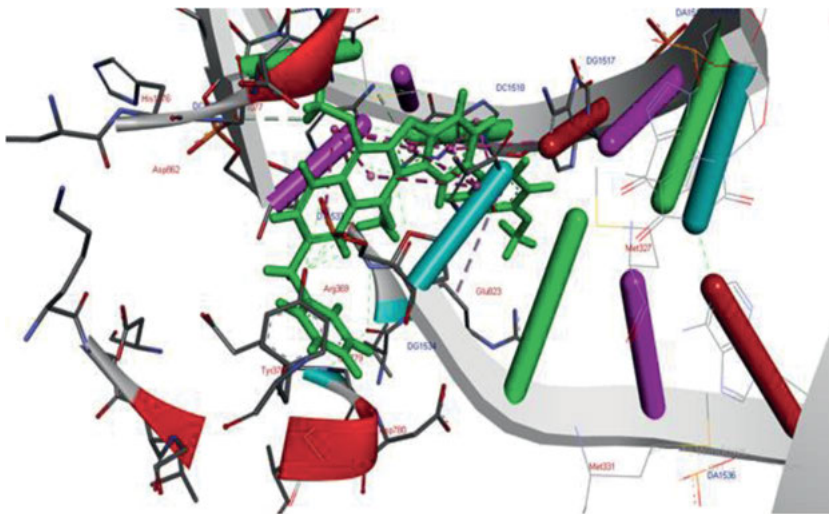


**Figure 10.15:** 3D structure shows the interacting residues within the binding pocket of the ligand no. 147 within TOP2A.

OCH<sub>3</sub> group attached at position R<sub>4</sub> forms carbon hydrogen bond with Glu 778 and van der Waals interactions with Gly 779 and Asp 858. All the interactions increase the binding energy from -6.09 kcal/mol to -9.73 kcal/mol which makes this ligand the best fit within the binding pocket (Figure 10.17).

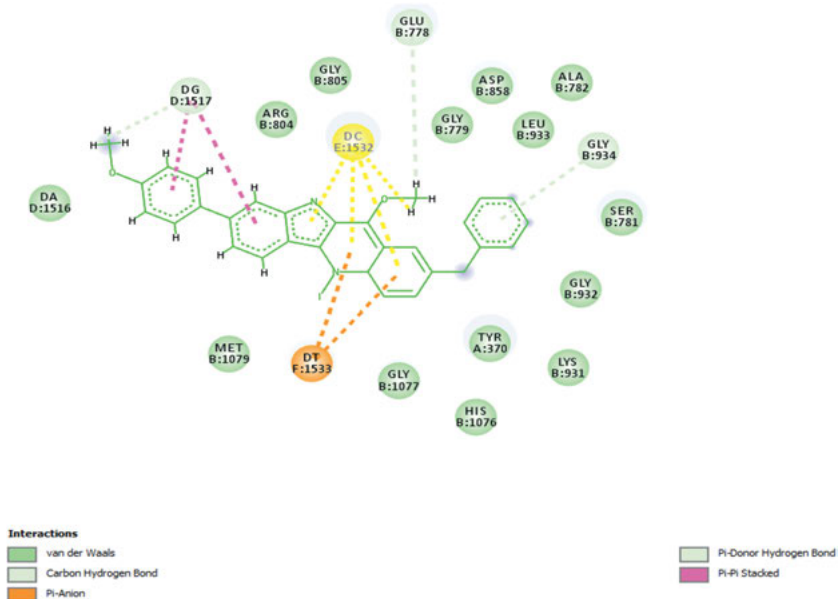


**Figure 10.16:** 2D structure of the ligand no. 16755 showing hydrophobic contacts by dotted lines.

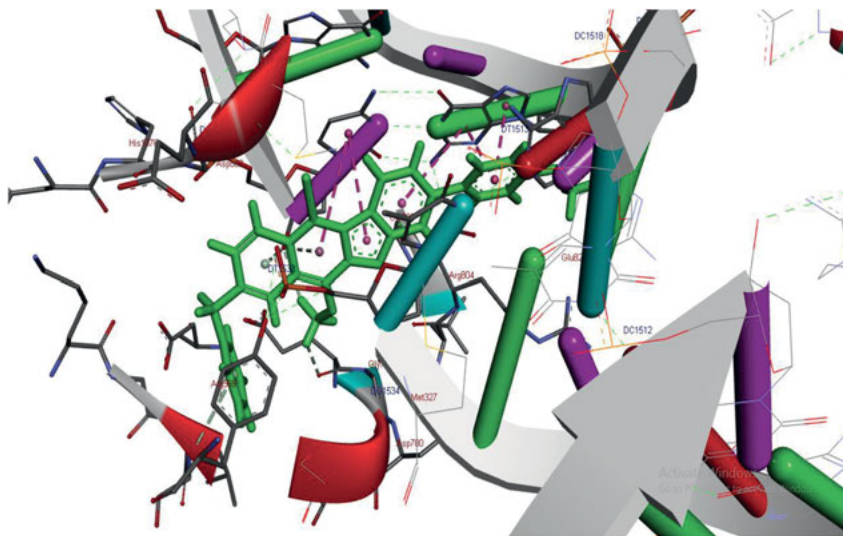


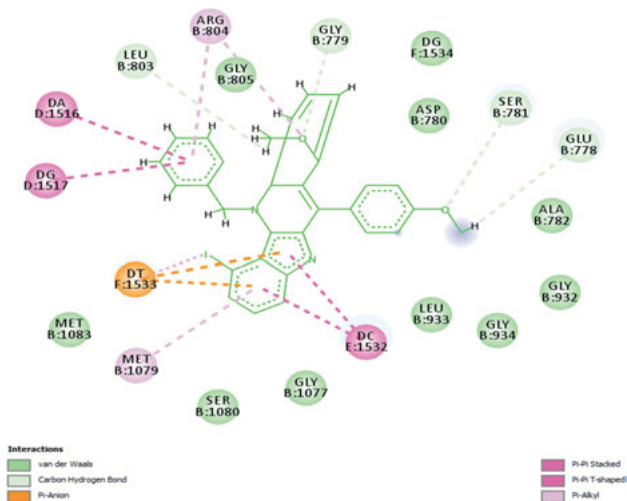
**Figure 10.17:** 3D structure representing residues interacting within the binding pocket of the ligand no. 16755.

### 10.3.2.5 Derivative no. 8186

All the interactions of the ligand no. 8186 are responsible for the best binding affinity and higher binding energy of  $-9.72$  kcal/mol. The type of residues of TOP2A with which the ligand no. 8186 interacts are Met 1083, Ser 1080, Gly 1077, Leu 933, Gly 932, Ala 782, Asp 780, Gly 805, Arg 804, Gly 779, Leu 803, Met 1079, Ser 781, and Glu 778 while nucleotides interact by dA 1516, dG 1517, dT 1533, dG 1534, and dC 1532 (Figures 10.18 and 10.19). Benzyl group in position  $R_1$  forms  $\pi$ - $\pi$  stacking and  $\pi$ - $\pi$  T-shaped interactions with dA 1516 and dG 1517 and  $\pi$ -alkyl interactions with Arg 804. Methoxy group at position  $R_2$  forms carbon-hydrogen bond with amino acid residues Leu 803 and Gly 779 and van der Waals interactions with Gly 805. Iodine attached at position  $R_3$  forms  $\pi$ -alkyl interactions with dT 1533.  $\text{CH}_3\text{OPh}$  group attached at position  $R_4$  forms carbon-hydrogen interactions with Ser 781 and Gu 778 and van der Waals interactions with Gly 932, and Ala 782. All the interactions are responsible for the best binding affinity and increased binding energy which is  $-9.72$  kcal/mol for the ligand no. 8186.

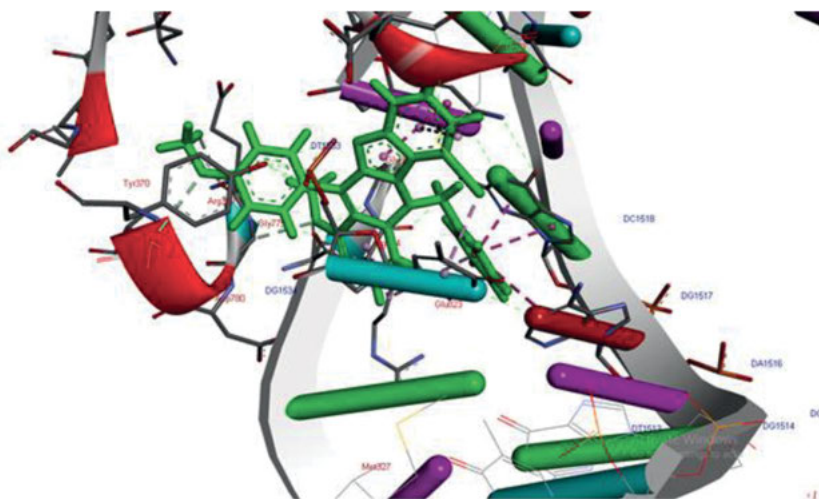
### 10.3.3 DFT studies

Table 10.2 contains the optimized structures, FMO energies, HOMO/LUMO gaps, and TDDFT gaps for cryptolepine and five ligands with the highest binding energies (cf. Table 10.1), the plots of their FMOs and MEP are provided in Table 10.3, and the global



**Figure 10.18:** 2D structure of the ligand no. 8186 representing different hydrophobic interactions.

reactivity parameters are given in Table 10.4. From Table 10.2 we can see that the HOMO/LUMO gap for the ligand #8618 is by 0.08 eV lower than this gap for the ligand #5551, but for the ligand #907 this gap is by 0.03 eV higher than for the ligand #5551, the ligand #147 has essentially the same HOMO/LUMO gap as the ligand #8618, whereas for the ligand #16755 the value of this gap drops by ca. 1 eV compared to the ligand #5551. The last ligand, #8186, has the gap lower by 0.16 eV than the ligand #5551.



**Figure 10.19:** 3D structure showing interacting residues within the binding pocket of the ligand no. 8186.

**Table 10.2:** Optimized structures, FMO energies, HOMO/LUMO gaps, and TDDFT gaps for the six ligands considered.<sup>a</sup>

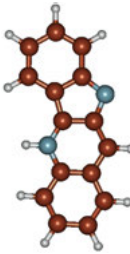
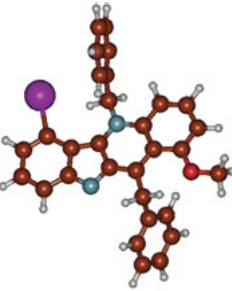
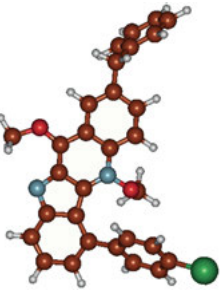
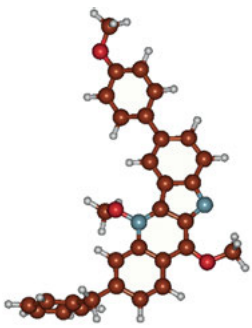
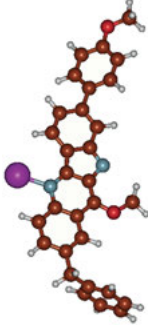
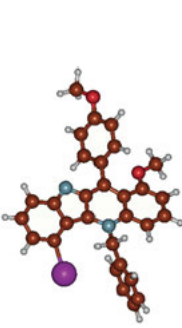
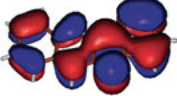
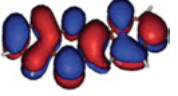
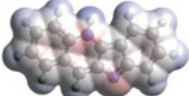
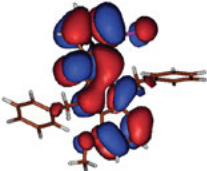
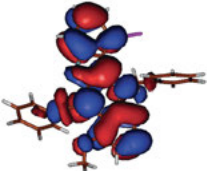
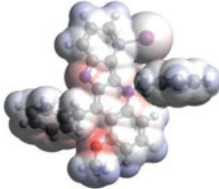
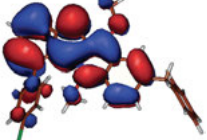
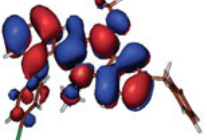
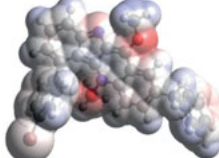
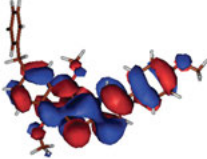
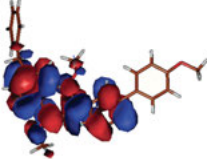
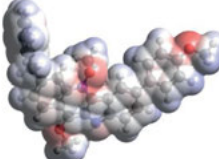
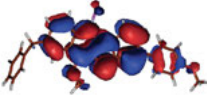
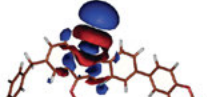
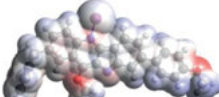
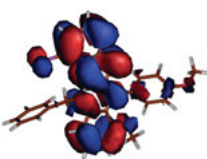
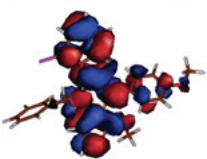
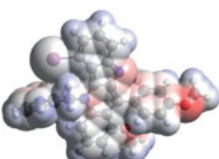
Ligand library #	Binding affinity (kcal/mol)	Structure of a ligand	E(HOMO/LUMO), A.U./eV	$\Delta E(\text{HOMO/LUMO})$ , eV	$\Delta E(\text{HOMO/LUMO})_{(\text{TDDFT})}$ , eV
5551	-6.09		-0.18664/-5.08 -0.08275/-2.25	2.83	2.24
8618	-9.88		-0.18741/-5.10 -0.08636/-2.35	2.75	2.22
907	-9.76		-0.18182/-4.95 -0.07672/-2.09	2.86	2.36

Table 10.2: (continued)

Ligand library #	Binding affinity (kcal/mol)	Structure of a ligand	E(HOMO/LUMO), A.U./eV	$\Delta E(\text{HOMO/LUMO})$ , eV	$\Delta E(\text{HOMO/LUMO})_{(\text{DOPDF})}$ , eV
147	-9.75		-0.17818/-4.85 -0.07626/-2.08	2.77	2.26
16755	-9.73		-0.18144/-4.94 -0.11375/-3.10	1.84	2.35
8186	-9.72		-0.18593/-5.06 -0.08789/-2.39	2.67	2.15

<sup>a</sup>Color coding of the structures: brown for C, light gray for H, red for O, lilac for I, light blue for N, and bright green for Br.

**Table 10.3:** HOMO/LUMO and MEP plots for the six ligands considered.

Ligand Library #	FMOs <sup>a</sup>		MEP plot
	HOMO	LUMO	
5551			
8618			
907			
147			
16755			
8186			

<sup>a</sup>Isosurface value is 0.015.

Furthermore, comparison of the MEP plots shows that the ligand #5551 has essentially only two spots where the negative electrostatic potential accumulates (as marked by red color), two N-atoms in its structure, whereas all five other ligands along with N-atoms have the accumulation of the negative electrostatic potential on the O-atoms of the  $-OCH_3$  groups. Also, the MEP plots qualitatively show for these ligands more significant accumulation of the negative electrostatic potential at specific spots in their molecules compared to the ligand #5551, which implies stronger electrostatic and

**Table 10.4:** The calculated GRPs (eV) for the six ligands considered.

Ligand	<i>IP</i>	<i>EA</i>	<i>X</i>	$\eta$	$\mu$	$\sigma$	$\omega$
5551	5.08	2.25	3.665	1.415	-3.665	0.35336	4.74637
8618	5.10	2.35	3.725	1.375	-3.725	0.36364	5.04568
907	4.95	2.09	3.52	1.415	-3.52	0.35336	4.37823
147	4.85	2.08	3.465	1.385	-3.465	0.36101	4.33438
16755	4.94	3.10	4.02	0.92	-4.02	0.54348	8.78283
8186	5.06	2.39	3.725	1.335	-3.725	0.37453	5.19686

hydrogen bonding interactions of those ligands with protein pockets. Interestingly, the FMOs of the five ligands with stronger binding energies have contributions not from the whole molecule, as in the cryptolepine case, but only from parts of their molecules. Moreover, the structures of the ligands #8186 – #8618 with the phenyl rings rotated may imply more favorite orientations of those ligands in the protein pockets and as a result stronger interactions with those.

The calculated global reactivity parameters present quite complicated picture. Thus, global hardness  $\eta$  drops noticeably from the ligand #5551 to the ligand #8618 but has the same value for both the ligand #5551 and ligand #907. Its value then again decreases for the ligand #147 and sharply drops to the ligand #16755, which has the lowest  $\eta$  value among all the ligands considered. The global softness  $\sigma$  value shows the reverse tendency, being slightly higher for the ligand #8618 and having the same value for the both the ligand #5551 and ligand #907. The ligand #16755 has the highest global softness value among all the ligands studied. It also has the highest values of the global electronegativity and electrophilicity compared to other ligands due to its unusually high electron affinity value, 3.10 eV, the highest among all the ligands considered. However, other factors, for instance, fewer number of the spots of negative MEP accumulation and not very favorable shape, might prevent it from having the highest binding energy compared to other ligands which we studied. Therefore, it should be emphasized that several various factors should be considered together as reasons for the ligand to have the highest binding affinity, such as ligand shape, presence of oxygen atoms and halogens, ligand reactivity, and number of spots for accumulation of negative electrostatic potential and degree of this accumulation, etc.

## 10.4 Conclusions

TOP2A is a key enzyme in human dividing cells and its activity is greatly enhanced in cancerous cells. Therefore, it can be considered as a good target for designing novel anticancer drugs. Computer-aided drug design and docking analysis play a key role in designing new inhibitors for particular proteins. The inhibitory effect of the drugs

towards the target protein can be determined by calculating their binding energies and can be explained by observing the ligand interactions with various amino acid residues of the binding pocket of the target protein.

In the present work we report the virtual screening of 31,114 derivatives of cryptolepine by molecular docking. Top five inhibitors of TOP2A are selected based on their best binding energies. The study reveals that the ligands #8618, 907, 147, 16755, and 8186 are the most potent ligands among the 31,114 ligands considered since they form a number of hydrophobic interactions with the target receptor which noticeably increases the predicted binding energy. The binding energies, kcal/mol, of the ligands #8618, 907, 147, 16755, and 8186 are predicted to be  $-9.88$ ,  $-9.76$ ,  $-9.73$ ,  $-9.72$ , and  $-9.72$ , respectively. All the known inhibitors of TOP2A were also docked into the binding pocket and it was observed that the selected ligands from the cryptolepine derivatives library have better binding energies and more favorable interactions with the receptor.

The DFT studies of the cryptolepine and five selected ligands with the highest binding affinities with the implicit effects from water have been performed as well. Different parameters, such as FMO shapes, energies, HOMO/LUMO gaps, molecular shapes, global reactivity parameters, and MEP maps were analyzed. It is suggested that several various factors should be considered together as reasons for the ligand to have the highest binding affinity, such as ligand shape, presence of oxygen atoms and halogens, ligand reactivity, number of spots for accumulation of negative electrostatic potential and degree of this accumulation, etc. We suppose that sum of these factors makes all the five ligands considered to have much higher binding affinities with the protein pockets compared to the cryptolepine. Moreover, the combined virtual screening study and DFT study can provide more insight in structures and properties of the ligands under investigation.

So, it is concluded that the cryptolepine can be successfully modified to generate a number of the better inhibitors to enhance the potency and lessen the side effects of existing drugs targeting the human TOP2A. We propose the set of five derivatives of the cryptolepine that were predicted to have better binding affinity towards TOP2A. All these selected ligands fit very well into the binding pocket with the minimum solvent accessible surface area (SASA). The substituents placed in various positions of cryptolepine in the selected ligands were chosen due to the fact that they can be easily incorporated into the starting compounds required for the total synthesis of cryptolepine. The total synthesis of cryptolepine has been earlier reported with different synthetic schemes [33–35].

## 10.5 Supporting information

The Supporting Information is available free of charge on PRS website.



**Acknowledgments:** Maria and Zahid Khan deeply acknowledge the financial support of the Institute of Chemical Sciences, University of Peshawar. Aleksey E. Kuznetsov deeply acknowledges the financial support of the Universidad Técnica Federica Santa Maria (USM), Santiago, Chile, along with the computational facilities of the Department of Chemistry, ITA, Brazil, and National Laboratory for High Performance Computing (NLHPC), Chile.

**Author contributions:** All the authors have accepted responsibility for the entire content of this submitted manuscript and approved submission.

**Research funding:** This study was supported by Institute of Chemical Sciences, University of Peshawa; Universidad Técnica Federica Santa Maria (USM), Santiago, Chile along with Department of Chemistry, ITA; and National Laboratory for High Performance Computing (NLHPC), Chile.

**Conflict of interest statement:** The authors declare no competing financial interests.

## References

1. Parsa N. Environmental factors inducing human cancers. *Iran J Public Health* 2012;41:1–9.
2. Torre LA, Bray F, Siegel RL, Ferlay J, Lortet-Tieulent J, Jemal A. Global cancer statistics, 2012. *CA A Cancer J Clin* 2015;65:87–108.
3. Bray F, Jemal A, Grey N, Ferlay J, Forman D. Global cancer transitions according to the Human Development Index (2008–2030): a population-based study. *Lancet Oncol* 2012;13:790–801.
4. Berti M, Cortez D, Lopes M. The plasticity of DNA replication forks in response to clinically relevant genotoxic stress. *Nat Rev Mol Cell Biol* 2020;21:633–65.
5. Bhattacharyya M, Vishveshwara S. Quantum clustering and network analysis of MD simulation trajectories to probe the conformational ensembles of protein–ligand interactions. *Mol Biosyst* 2011;7:2320–30.
6. Pommier Y, Sun Y, Huang S-YN, Nitiss JL. Roles of eukaryotic topoisomerases in transcription, replication and genomic stability. *Nat Rev Mol Cell Biol* 2016;17:703–21.
7. Sader S, Wu C. Computational analysis of amsacrine resistance in human topoisomerase II alpha mutants (R487K and E571K) using homology modeling, docking and all-atom molecular dynamics simulation in explicit solvent. *J Mol Graph Model* 2017;72:209–19.
8. Pal H, Katiyar S. Cryptolepine, a plant alkaloid, inhibits the growth of non-melanoma skin cancer cells through inhibition of topoisomerase and induction of DNA damage. *Molecules* 2016;21:1758.
9. Janockova J, Korabecny J, Plsikova J, Babkova K, Konkolova E, Kucerova D, et al. *In Vitro* investigating of anticancer activity of new 7-MEOTA-tacrine heterodimers. *J Enzym Inhib Med Chem* 2019;34:877–97.
10. Lavrado J, Reszka AP, Moreira R, Neidle S, Paulo A. C-11 diamino cryptolepine derivatives NSC748392, NSC748393, and NSC748394: anticancer profile and G-quadruplex stabilization. *Bioorg Med Chem Lett* 2010;20:7042–5.
11. Krishna S, Berridge B, Kleinstreuer N. High-throughput screening to identify chemical cardiotoxic potential. *Chem Res Toxicol* 2021;34:566–83.
12. Pradeepkiran JA, Reddy PH. Structure based design and molecular docking studies for phosphorylated tau inhibitors in Alzheimer's disease. *Cells* 2019;8:260.

13. Chen ZZ, Li SQ, Liao WL, Xie ZG, Wang MS, Cao Y, et al. Efficient method for the synthesis of fused benzimidazole-imidazoles via deprotection and cyclization reactions. *Tetrahedron* 2015;71: 8424–7.
14. Genheden S, Ryde U. The MM/PBSA and MM/GBSA methods to estimate ligand-binding affinities. *Expet Opin Drug Discov* 2015;10:449–61.
15. Rose PW, Prlić A, Bi C, Bluhm WF, Christie CH, Dutta S, et al. The RCSB protein data bank: views of structural biology for basic and applied research and education. *Nucleic Acids Res* 2014;43: 345–56.
16. Sessions Z, Sánchez-Cruz N, Prieto-Martínez FD, Alves VM, Santos HP, Muratov E, et al. Recent progress on cheminformatics approaches to epigenetic drug discovery. *Drug Discov Today* 2020; 25:2268–76.
17. Frisch MJ, Trucks GW, Schlegel HB, Scuseria GE, Robb MA, Cheeseman JR, et al. Gaussian 09, Revision B.01. Wallingford: Gaussian Inc.; 2010.
18. Gaussian 16, Revision C.01, Frisch MJ, Trucks GW, Schlegel HB, Scuseria GE, Robb MA, Cheeseman JR, et al. Wallingford CT: Gaussian, Inc.; 2016.
19. Axel DB. Density-functional thermochemistry. III. The role of exact exchange. *J Chem Phys* 1993;98: 5648–52.
20. Rassolov VA, Ratner MA, Pople JA, Redfern PC, Curtiss LA. 6-31G\* basis set for third-row atoms. *J Comput Chem* 2001;22:976–84.
21. Rassolov VA, Pople JA, Ratner MA, Windus TL. 6-31G\* basis set for atoms K through Zn. *J Chem Phys* 1998;109:1223–29.
22. Ditchfield R, Hehre WJ, Pople JA. Self-consistent molecular orbital methods. 9. Extended Gaussian-type basis for molecular-orbital studies of organic molecules. *J Chem Phys* 1971;54:724.
23. Dunning TH, Jr, Hay PJ. In: Schaefer HFIII, editor. *Modern theoretical chemistry*. New York: Plenum; 1977, vol 3:1–28 pp.
24. Hay PJ, Wadt WR. Ab initio effective core potentials for molecular calculations - potentials for K to Au including the outermost core orbitals. *J Chem Phys* 1985;82:299–310.
25. Wadt WR, Hay PJ. Ab initio effective core potentials for molecular calculations - potentials for main group elements Na to Bi. *J Chem Phys* 1985;82:284–98.
26. Tomasi J, Mennucci B, Cammi R. Quantum mechanical continuum solvation models. *Chem Rev* 2005;105:2999–3093.
27. Geerlings P, De Proft F, Langenaeker W. Conceptual density functional theory. *Chem Rev* 2003;103: 1793–874.
28. Chakraborty A, Pan S, Chattaraj PK. Biological activity and toxicity: a conceptual DFT approach. *Struct Bond* 2013;150:143–80.
29. Jorio S, Salah M, Abou El Makarim H, Tabyaoui M. Reactivity indices related to DFT theory, the electron localization function (ELF) and non-covalent interactions (NCI) calculations in the formation of the non-halogenated pyruvic esters in solution. *Mediterr J Chem* 2019;8:476–85.
30. Schaftenaar G, Noordik JH. Molden: a pre- and post-processing program for molecular and electronic structures. *J Comput Aided Mol Des* 2000;14:123–34.
31. Avogadro: an open-source molecular builder and visualization tool. Version 1.1.1. Available from: <http://avogadro.cc/>.
32. Hanwell MD, Curtis DE, Lonie DC, Vandermeersch T, Zurek E, Hutchison GR. Avogadro: an advanced semantic chemical editor, visualization, and analysis platform. *J Cheminf* 2012;4:17.
33. Radaeva M, Dong X, Cherkasov A. The use of methods of computer-aided drug discovery in the development of topoisomerase II inhibitors: applications and future directions. *J Chem Inf Model* 2020;60:3703–21.

34. Sharma M, Jha P, Verma P, Chopram M. Combined comparative molecular field analysis, comparative molecular similarity indices analysis, molecular docking and molecular dynamics studies of histone deacetylase 6 inhibitors. *Chem Biol Drug Des* 2019;93:910–25.
35. Piazza I, Beaton N, Bruderer R, Knobloch T, Barbisan C, Chandat L, et al. A machine learning-based chemoproteomic approach to identify drug targets and binding sites in complex proteomes. *Nat Commun* 2020;11:4200.

# Index

- 1,2-diaminopropane 57
- 1,3-hydroxy shift to give 4-amino-2-(1-hydroxy)quinolines 63
- 1,3-hydroxy shift 71
- 2,3-diaminopyridine 53
- 2,5-dihydroxyalkylbenzoquinones 115
- 2-alkyl-3-cyanoquinolines 62
- 2-alkyl-5,6-dihydro-4H-1,3-oxazine 61
- 2-alkylbenzimidazoles 48
- 2-alkylhezahydrobenzimidazoles 48
- 2-alkylidene-3,4,5,6-tetrahydro-2H-1,3-oxazine 61
- 2-alkylidene-4-amino-1,2-dihydro-1-hydroxyquinoline 63
- 2-alkylidene-4-amino-1,2-dihydroquinoline 63
- 2-alkylimidazolines 48
- 2-amino-4-(hydroxyalkyl)pyrimido[1,2-a]benzimidazoles 72
- 2-amino-4-phenylpyrimido[1,2-a]benzimidazoles 71
- 2-aminobenzothiazole 73
- 2-aminopyrimidine 55
- 2H-pyrimido[2,1-b]benzothiazol-2-ones 73
- 2-hydrazinopyridine 60, 70
- 2-iminopyridopyrimidines 54
- 2-phenylimidazolines 66
- 2-phenyl-3-cyanoquinoline 71
- 2-phenyl-4H-3,1-benzoxazine 71
- [3, 3] sigmatropic rearrangement 52
- 3-aminopyrazole 68
- 3-aminopyrazoles 58
- 3-H indoles 51, 52
- 3-hydroxy-2-aminopyridine 54
- 3-hydroxypropylamine 56
- 4-amino-2-(2-hydroxyphenyl)quinoline 54, 71
- 4-iminopyridopyrimidines 54
- 5-alkyl-6-cyano-2,3-dihydro-4H-1,4-thiazines 57
- 5-alkyl-7-aminopyrazolo[1,5- $\alpha$ ]-pyrimidines 58
- 5-amino-3-alkyl-1-(2-pyridyl)imidazoles 60
- 5-amino-3-phenyl-1-(2-pyridyl)pyrazole 70
- 5-Exo-Dig 51
- 5-exotrig ring closure 58
- 5-phenyl-3-aminopyrazoles 66
- 5-phenyl-7-aminopyrazolo[1,5 $\alpha$ ]pyrimidine 68
- $\alpha$ -amylase 10
- $\alpha$ -amino-acids 48
- $\alpha$ -amino-esters 48
- $\alpha$ -amino-nitriles 48
- $\alpha$ -cadinol (8) 116
- $\alpha$ -cadinol 109
- $\alpha$ -glucosidase 10
- $\alpha$ ,  $\beta$ -unsaturated carbonyl 47
- A. brasiliensis* hexane fraction 133
- A. brasiliensis* HF with ampicillin 132
- accuracy 37
- ACE inhibitors 32
- acetylenic acids 73
- acetylenic aldehydes 73
- acetylenic nitriles 77, 78
- activity 130
- agilent 1260 infinity series 33
- alcohol precipitable solids (APS) 99
- aldehydes 68
- alkylation 172
- alkynoic acids 73
- allenic nitriles 47
- allenic 77–78
- alternanthera brasiliensis* 124
- alzheimer's disease 78
- amino acid content 101
- amino furans 68
- aminobenzenethiols 66
- aminobenzimidazoles 65, 73
- aminopyridylpyrazoles 60
- ampicillin 131
- amylase 106
- amylopectin 106
- analgesic activities 6
- analysis of variation 34
- angiotensin converting enzyme 32
- angiotensin II enzyme 32
- antiarrhythmic 75
- antibacterial 2, 126
- antibacterial activity 132
- antibacterial resistance 133
- anti-convulsant 77
- antifungal 76
- antifungal activity 9
- antihistamine 76
- antihypertensive 33, 40–41
- anti-inflammatory 173
- anti-measles 77

<https://doi.org/10.1515/9783110710823-011>

- antioxidant activity 19
- antioxidants:oxidative stress diseases 8
- anti-tumour:anti-cancer 9
- antiviral 77
- aphrodisiac effects 11
- apigenin 33, 35
- aprotic solvent 73
- aqueous extract 173–174
- ascendis express column 34
- ascorbic acid 28
- aspartic acid 109
- average daily dose 150
- $\beta$ -aminoethanethiols 49
- $\beta$ -ketonitriles 48
- background correction 149
- bark 117
- baseline resolution 35
- behavioural depressor 76
- benzimidazole 46
- benzimidazoles 71
- benzothiazole 46
- benzothiazoles 58, 66
- benzoxazines 62
- benzoxazoles 70
- beta-lactam 124
- better inhibitory 132
- binding affinity 193–194, 203
- binding energy 200–201, 203
- binding pocket 195, 199, 202, 204
- binding pocket of TOP2A 190
- bioactive compounds 170
- bioassay fractionation 130
- biological 46
- biological activities 4
- biological activity 75
- bipyridines 46
- bond 199, 201
- brine shrimp 173
- brine shrimp lethality 175
- cadaba farinosa* 19
- calcium 157
- calcium oxalates 177
- calculations 192
- cancer 188
- cancer treatment 188
- candida albicans* 9
- carrageenan 173
- caryophyllene oxide 109, 116
- chemical constituents 4
- chromatogram 127
- chromatographic 34
- chromatographic plates 35
- chromatographic studies 22
- chronic thresholds 161
- clotrimazole 77
- co evaporation 86–89, 91–94
- combination of antibiotic 133
- combinatorial library design 189, 195
- compatibility 86–87, 94–95
- components expected 127
- compounds 125
- computational methods 189
- computer-aided drug design 208
- conformations 191
- coronavirus 77
- correlation 149, 160, 162
- cryptolepine 187–188, 197–199, 209
- crystal structure of TOP2A 191
- cyanquinolines 62
- cyclisation 51, 73
- cyclocondensation 73
- cysteine residues 181
- cysteine-rich peptides 170
- cystine bonds 181
- cystine knot inhibitor 181
- cytotoxicity 173
- DAD-UV/Vis 34
- decoctions 104
- degenerative diseases 20
- dehydration 57, 62, 71, 73
- dehydrogenation 62, 71
- density function theory 188
- DFT study 209
- di 129
- diabetes 10, 21, 78
- diclofenac sodium 87–89
- dihydrofurans 64, 68
- dihydrooxazines 56
- dihydrothiazine 58
- diphenoldisulphonic 149
- disease 2
- disulphide linkages 172
- docking 191
- docking analysis 195
- docking protocol 190
- dominating sources 166
- DPPH 23
- drug combination 134

- drug discovery 13
- drug resistance 135
- DSC 86–91, 93
- economical 24
- E(HOMO/LUMO) 205
- eigenvalues 150, 159
- electrical conductivity 148–149, 152
- electron affinity 192
- electrostatic potential 207
- elephantorrhiza elephantina 32
- elimination 52
- elucidation 128
- embelin 115
- enaminic nitriles 47
- enaminic proton 52
- endemic 175
- endoproteinase Glu-C 172
- enzyme 208
- essential amino acids 109
- ethanolamines 49, 70
- ethnobotanical 98
- ethnomedicinal plant 175
- ethnomedicinal uses 4
- ethnomedicine 21
- ethnomedicines 104
- ethyl acetate 28
- etoposide 195–196
- euphorbiaceae 182
- extract 23
- extracts 4
- fatty acid 129
- fatty acid and carboxylic acid 134
- FDA 36
- FICI 0.255 and 0.274 132
- flavonoid glycosides 106
- flavonoids 20, 32–36, 38, 40–42
- flow rate 35
- folin–ciocalteu 22
- folklore medicine 13
- foot edema 182
- forest herbarium ibadan, FHI 171
- formic acid 34
- fractional inhibitory concentrations 127
- free radicals 20
- furans 65
- future lead 133
- future solution 132
- GABA antagonist 76
- gallic acid 25, 106
- garden 21
- gas-chromatography-mass spectrometry 125
- gastrointestinal 111
- GC-MS 101
- GC-MS library database (NIST 08) 101
- global reactivity 203–204, 208
- glutamic acid 109
- glycoproteins 106
- gradient elution 35
- gram-negative strains 102
- gram-positive 102
- group 201, 203
- hazard quotient 150
- henyl hydrazine 51
- herbal shotgun 133
- herbarium 21
- heterocycles 46
- hexadecanoic acid 129
- hexane fraction 130
- high-throughput time-of-flight mass spectrometer (HR-GC-MS-TOF) 101
- HOMO/LUMO 207
- HOMO/LUMO gap 204
- HPLC 125
- HSQC 129
- hydrazine 50–51
- hydrogen bond 198, 199
- hydrogeological aquifers 149
- hydrophobic and lipophilicity interaction 133
- hydrophobicity 174
- hydrophobicity 172
- hydroxyacetylenic nitriles 77–78
- hydroxylamine 51, 65
- hypertension 32, 40–41
- ICH 36–38
- identification of compounds 127
- imidazolines 47
- indole 51
- indoles 52–53
- inflammation 181
- infra-red 48, 53
- infusions 104
- inhibitory activity 27
- in-silico 190
- interaction 196
- interactions 86–87, 92, 95, 191
- interaction analysis 197
- internal standards 35
- intramolecular Michael addition 48

- ionization potential 192
- isocratic elution 35
- isolated compounds 132
- isolation 125
- isoxazoles 51, 63, 67
- kaempferol 32–35, 37–38, 41
- ketones 68
- ketonic carbonyl 55
- leaf, fruit and bark samples 101
- leaves 117
- lecaniodiscus cupanioides* 2
- ligand 189, 191, 193–194, 197–201, 203–207
- limit of detection 36
- limit of quantification 36
- linear regression 36
- linearity 36
- lippia javanica 33, 42
- macromolecule 191
- magnesium stearate 87
- MALDI TOF MS 171–172
- mechanism 62
- medicinal plants 20
- MEP 207
- methanol 34
- methicillin-resistant staphylococcus aureus* 124
- Michael addition 47
- Michael adduct 51
- microcrystalline cellulose 86–88, 90, 92–93
- microdilution assays 99
- microwave irradiation 87–88
- mineral contents 11
- minimum inhibitory concentration (MIC) 5, 102–104
- minimum Inhibitory Concentration 126
- mobile phase 35
- modern medicines 24
- molecular docking 187–188, 190, 209
- molecular electrostatic potential 192
- multivariate statistical method 148
- muscle relaxing agent 76
- myricetin 33–35, 37, 40–41
- myrsinaceae family 98
- myrsinoic acids 116
- natural compound-conventional drug 133
- natural product 132
- natural products 2
- neuromodulation 111
- new antimicrobial agents 76–77
- NMR 126
- no zones of inhibitions 131
- NOESY 128
- non-hydrophobic interactions 196
- nucleophilic addition 47
- nucleophilic attack 54
- nucleotides 195
- o-aminobenzenethiols 49
- o-aminobenzylalcohol 62
- o-aminophenols 49
- o-phenylenediamine 48
- oral exposure 161
- oral ingestion 161
- organic 46
- orthodox drugs 6
- otary evaporator 22
- oxazolidine 61
- oxazolines 49–50, 60, 70
- oxidation 57
- pain 182
- peptide 172
- percentage yields 23
- pharmacological 24, 46
- pharmacological properties 2
- phenolic content 22
- phenolic glycosides 106
- phenomenex analysis kit 101
- phenylethylene diamine 48
- phenylhydrazine 51
- phenylpropynenitrile 67
- phosphorylated (metabolic) pathway 111
- phototropic rearrangement 52
- phthalate 129
- phthalates compounds 134
- physical mixture 86–89, 91–94
- phytochemical screening 19
- phytochemical variation 99
- phytochemicals:triterpenoid saponins 9
- phytochemistry 13
- plant extract 6
- plants 182
- polymerisation 60
- position 198, 201
- possess anti-MRSA activity 134
- possible solution 135
- principal Component Analysis 150
- proline 109
- protein synthesis 111
- protic solvent 72
- proton shift 57–58

- protons 128–129  
 pulmonary infections 111  
 pyrazoles 47, 50–53, 60, 70  
 pyrazolopyrimidines 68–69  
 pyrido (1, 2-a) pyrimid-4-ones 53  
 pyridopyridines 55  
 pyridopyrimidines 47, 53  
 pyridyl ketones 55, 68  
 pyrimido[1,2a] pyrimidines 55  
 pyrimidobenzimidazoles 65, 72–73  
 pyrimidobenzothiazolones 73  
 pyrimidopyrimidines 55  
 pyrolysis 61, 70–71  
 quercetin 33  
 quinolines 46  
 rapanone 115  
 reactive oxygen 20  
 recovery studies 37  
 reduction 172  
 relative standard deviation 37  
 relative weight 150  
 residue 197  
 residues 195  
 resistance 77, 124  
 retention times 38  
*R<sub>f</sub>* values 19  
 ring closure 62, 71  
 RP-HPLC 32, 33, 36–38, 41, 171  
 rutin 32–35, 37, 40–41  
 sapindaceae 2  
 saponins 106  
 SARS CoV-2 77  
 scavenge 23  
 scree plot 159  
 second Michael addition 61  
 secondary metabolites 13, 24  
 selectivity 35–36  
 serine 109  
 shellsol 177  
 sigmatropic rearrangement 53, 57  
 solid phase extraction 102, 171  
 solubility 23–24  
 South Africa 99  
 soxhlet 21  
 soxhlet extraction 117  
 (–)-spathulenol 109  
 spathulenol 116  
 spots 24  
 stacking 197  
 standard addition method 37  
 standard antibiotic 131  
 standard deviation 34  
 standardized extraction methods 41  
 steric hindrance 54  
 stinging 177  
 stinging hairs 170  
 structure 201–202, 204–206  
 sub-fraction 130  
 susceptible 161  
 Swaziland 99  
 symmetrical peak shapes 35  
 synergism 132  
 synergism between ampicillin 132  
 synergistic relationship 135  
 synthetic antioxidants 20  
 tannins 28, 106, 107  
 tautomerism 55  
 terpenes 107  
 terpenoids 24  
 tetrahydropyridines 57  
 tetrahydropyrimidines 57  
 the loadings plot 159  
 thiazoles 47  
 thiazolidine 57  
 thiazolines 49–50, 58  
 TLC 101  
 TOP2A 209  
 topoisomerase 2 (TOP2A) 187  
 topoisomerase II alpha enzyme 188  
 total alkalinity 158  
 total dissolved solid 157  
 toxicity 10  
 trace metals 161  
 traditional medicine 182  
 triterpenoid 106  
 triterpenoid saponins 9  
 triterpenoid saponins:hederagenin 12  
 trypanosomiasis 9  
 tryptone Soya Broth (TSB) 102  
 tryptophan 109  
 tuberculosis 78  
 turbidity 149, 152, 160  
 twenty-four ca 129  
 ultrasonicator 34  
 U.S Food and Drug Administration (FDA) 2  
 value 208  
 vinylic proton 65  
 virtual screening 190, 197, 209



water quality index 150

water treatment 148

wistar rats 20

world health organization 158, 166

wound 111

y-intercept 36

zingiber officinale 32

zones of inhibitions 126